MODIFICATION OF THE ROTARY MACHINING PROCESS TO IMPROVE SURFACE FORM

by

Neil Brown B.Eng. M.Sc.

A Doctoral Thesis

Submitted in the partial fulfilment of the requirements
for the award of
Doctor of Philosophy of Loughborough University

May 1999

Acknowledgements

Summary

Planing and moulding operations carried out within the woodworking industry make extensive use of rotary machining. Cuttermarks are produced on the timber surface which are generally accepted as unavoidable. More noticeable surface defects may be produced by such factors as cutterhead imbalance, and until recently most research has concentrated on removing these defects. When a high quality finish is required, a further machining operation, such as sanding, is often required to remove cuttermarks. What is required, is a modified machining process which combines a surface closer to the ideal fixed knife finish, whilst retaining the flexibility, practicality and cost effectiveness of rotary machining.

It has been theorised that the surface finish of planed and moulded timber products may be improved by oscillation of the cutterblock upon which the machining knives are mounted. This thesis concerns the progress made towards the modification of the rotary machining process to improve surface form for planed timber components. Thus, simulation of the rotary machining process is described, allowing an evaluation of the surface form quality produced by the modified machining process, and allowing a comparison to be made between the effectiveness of new machining process and conventional rotary machining. Practical experiments to validate the theory of cutterblock oscillation were also carried out.

In order to provide a system design capable of application in an industrial setting, an actuation system for cutterblock oscillation was designed using a high speed hydraulic servoactuator simulation. This servo system model was combined with the rotary machining simulation to produce a complete simulation, which represents significant progress in the field of mechatronic system modelling, and a useful device for woodworking machine tool design.

The usefulness of mechatronic simulation when applied to machine tool design, and progress is made in the fields of hydraulic servo simulation and design is confirmed. The effectiveness of cutterblock oscillation as a modified machining process is verified, which offers industry performance benefits over the conventional machining process, and gives the possibility of the removal of subsequent finishing operations, coupled with a reduced requirement for coatings. The modified machining process therefore offers significant cost, quality, and environmental benefits.

Contents

v

Nomenclature

$\overset{\Delta}{=}$	Corresponds to	-
A	single acting ram area	m^2
A_1	Ram area (principal side)	m^2
A_2	Ram area (return side)	m^2
A_E	Effective ram area	m^2
β_S	Isentropic tangent bulk modulus	$N.m^2$
β_T	Isothermal tangent bulk modulus	$N.m^2$
C	Capacitance	F
D	Dielectric displacement	m
d	Depth of cut	m
d	Strain developed / applied field	-
D_1	Duty cycle ON time for PWM	s
D_2	Duty Cycle OFF time for PWM	s
E	field	$V.m^{-1}$
ε_r	Permitivity of free space	$F.m^{-1}$
ε_o	Relative permitivity (constant stress)	-
f_m	Resonant frequency	$rad.s^{-1}$
F_d	Feedrate	$m.min^{-1}$
F_g	General feedrate	m
g	Strain developed / applied charge density	$m^2.C^{-1}$
h	Cutter wave height	m
H_i	Initial horizontal sample	-
i	valve motor current	A
$I(t)_x$	Instantaneous knife position (x)	m
$I(t)_y$	Instantaneous knife position (y)	m
k_a	Drive amplifier constant	$mA.V^{-1}$
K_g	Effective leakage coefficient	$m^3.sec^{-1}/N.m^2$
k_B	General bulk modulus	$N.m^2$
k_{LE}	Leakage coefficient	$m^3.sec^{-1}/N.m^2$
L_1	Assymetric oil column height (principal side)	m
L_2	Assymetric oil column height (return side)	m
L_t	Total internal cylinder length	m
l_e	Effective length of the trapped oil volume	m

Symbol	Description	Units
l_e	Effective length of the trapped oil volume	m
μ	Viscous friction	-
μ_L	Load friction	-
M	Ram and slideway mass	kg
N	number of cutter head knives producing surface wave.	-
n	cutter head rotational	$rev.min^{-1}$
P	Knife marking pitch	m
P	Lookup table back pressure reference point	-
p	General Pressure	$N.m^{-2}$
P_1	Assymetric cylinder pressure (principal side)	$N.m^{-2}$
P_2	Assymetric cylinder pressure (return side)	$N.m^{-2}$
P_a	Solenoid stroke force	N
P_b	Solenoid return force	N
P_{cyl}	Cylinder supply	$N.m^{-2}$
pf	Pressure required to overcome viscous friction	$N.m^{-2}$
P_g	General load pressure	$N.m^{-2}$
P_L	Load Pressure	$N.m^{-2}$
P_{LE}	Effective load Pressure	$N.m^{-2}$
P_s	Supply pressure from pump	$N.m^{-2}$
P_T	Sump pressure	$N.m^{-2}$
Q	Flow	$m^3.s^{-1}$
Q_1	Fluid flow double acting cylinder (principal side)	$m^3.s^{-1}$
Q_2	Fluid flow double acting cylinder (return side)	$m^3.s^{-1}$
Q_{c1}	Compressibility flow (principal side)	$m^3.s^{-1}$
$Q_{c2,}$	Compressibility flow (return side)	$m^3.s^{-1}$
Q_{ce}	Effective compressibility flow	$m^3.s^{-1}$
Q_{cf}	Generalised compressibility flow	$m^3.s^{-1}$
Q_{d1}	Displacement fluid flow (principal side)	$m^3.s^{-1}$
Q_{d2}	Displacement fluid flow (return side)	$m^3.s^{-1}$
Q_{de}	Effective displacement flow	$m^3.s^{-1}$
Q_g	Generalised load flow	$m^3.s^{-1}$
Q_L	Leakage flow	$m^3.s^{-1}$
Q_{L1}	Leakage flow (principal side)	$m^3.s^{-1}$
Q_{L2}	Leakage flow (return side)	$m^3.s^{-1}$
Q_{LE}	Effective Load flow	$m^3.s^{-1}$
Q_{LKE}	Effective Leakage flow	$m^3.s^{-1}$

Q_m	Energy supplied / dissipated per cycle	J
r_{ct}	Cutter tip radius	m
r_1, r_2	Potential divider resistance 1 & 2,	Ω
S	Strain	-
s	Laplace operator	-
τ	servovalve time constant	s
T	Stress	$N.m^2$
t	Time	s
T_c	PWM time period	s
v_m	Valve actuator time constant	s
V_v	Valve voltage	V
V	Single acting ram volume	m^3
V_1	Trapped oil volume (principal side)	m^3
V_2	Trapped oil volume (return side)	m^3
V_{cc}	Supply voltage	V
V_g	General ram volume	m^3
V_t	Trapped oil volume (total)	m^3
ω_{ct}	Cutterblock angular velocity	$rad.s^{-1}$
ω_v	Valve natural frequency	$rad.s^{-1}$
X_s	Valve spool displacement	m
X	Lookup table displacement reference point	-
x	Ram displacement	m
Z_m	Minimum impedance	Ω
ζ_v	Valve spool damping	-
ζ	Damping coefficient	-

1.0 Introduction

This chapter is broadly split into four sections. The first will provide some insight into why this research has been carried out, stating the chief advantages of the methods developed during this project. The next section will provide a background to the development of this area of timber machining from the first appearance of powered planing machines to the machines used in the industry at the time of writing. The next section provides a more in-depth introduction to the types of machines and tooling in use presently. The final section provides an introduction to the research undertaken, and outlines the strategy adopted to develop a method to improve the process.

1.1. Why modify the rotary machining process?

The fundamental design of the rotary planing machine was developed over 175 years ago, and has remained unchanged in its present form, apart from several design improvements with regard to tooling, for the last 30 years. The current state of the industry indicates that in it's present form, the design of rotary planing machines has broadly reached its development limit. Although the surface finish provided by modern planing machines is good, it is not defect free, so in order to further understand why the rotary machining process is to be modified, it is necessary to describe the current shortcomings of the machining method used by the present generation of machines.

Four primary advantages may arise from changing the way parts are machined. The first two apply to the machines themselves, and the second two apply to secondary benefits, and are grouped together as such.

1.1.1. Enhancement of the rotary machining process

The present generation of high speed machines utilise rotary cutters to shape the timber surface. This method suffers two main disadvantages, which can be reduced considerably through adoption of the methods described in the following chapters.

The current method of rotary machining is somewhat variable, and product quality is consequently not guaranteed. A new way of machining components is proposed which should reduce the likelihood of defectively machined components. Cuttermarks are produced on all rotary machined surfaces, a typical section being shown in figure 1.1.1.1
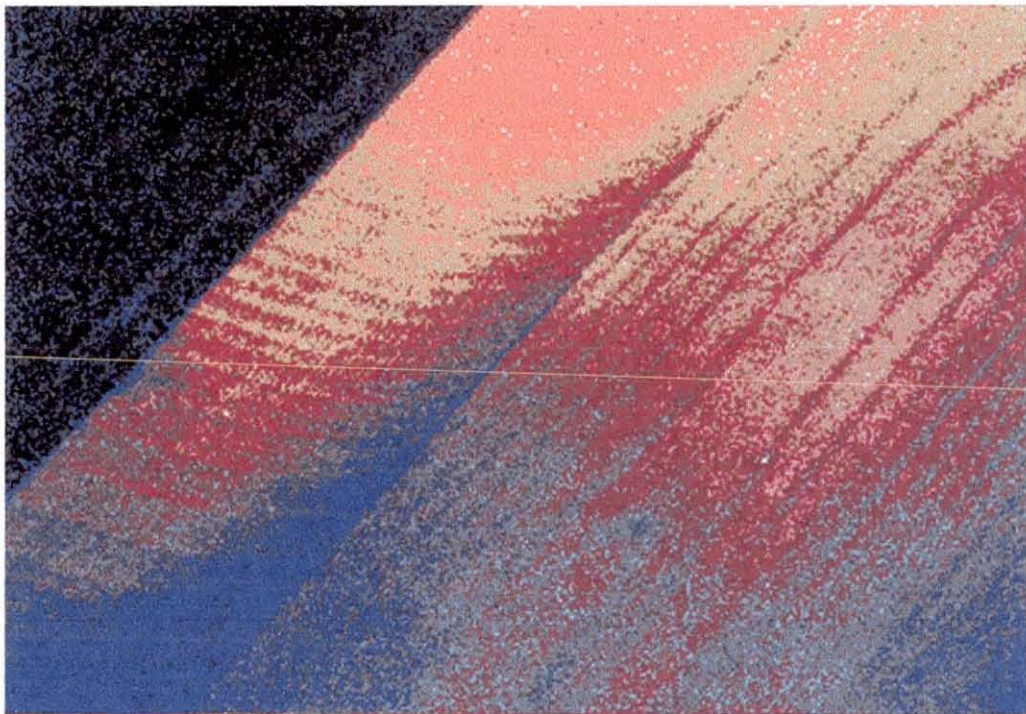

Figure 1.1.1.1 - Cuttermarks produced on machined timber surface
(Jackson, 1986)

If the size and distribution of these cuttermarks is within acceptable limits, the product is passed on to the next machining operation. Much previous research has been undertaken in order to understand the nature of the resultant surface geometry, and to detect machining faults as quickly as possible in order to keep cutter mark size within acceptable limits. A modified method of machining, as outlined later in section 2.3, could reduce the variability of this process through reducing the primary cause of the variability, the cuttermarks. There would be a resultant reduction in wastage of timber, reduced net machine power consumption for each metre of timber machined, and depending on the manufacturer's outlook, a cost saving, resulting from adopting the new process, or the opportunity to increase profit through enhanced production levels.

The second advantage is the reduction of cuttermarks. Cuttermarks are produced on all rotary machined surfaces which frequently have to be removed. Even if the machining process is working properly, these marks may be visible to the naked eye and have to be removed for critical applications such as the production of furniture. Fixed knife planing machines are available, which provide a smooth finish, but suffer from disadvantages which limit their application considerably. The new machining process offers a chance to design a machine with the output quality of a fixed knife machine, coupled with the flexibility and high throughput of a rotary machine. A reduction in tooling costs is possible as a direct effect, since a surface finish of acceptable quality could be produced with a shorter set-up time.

1.1.2. Secondary benefits

The use of a machine capable of providing a product approaching the quality of that provided by a fixed knife machine, offers a third advantage. In many cases it may now be possible to remove an entire machining process, that of sanding, which is used to finish the product after planing or moulding to a high standard. Sanding generates dust, which being finer than the chips generated by planing, can be hazardous to both machines and operators; some timber dusts, in particular mahogany, are carcinogenic. As well as making the working environment less hazardous, the reduction in the use of sanding machines has obvious cost benefits due to the smaller number of machines required, and knock on effects such as less dust extraction plant being required and reduced cost of consumables such as abrasive material.

The fourth advantage stems from a reduction in the product surface energy. After machining, timber products usually have a coating applied in order to seal the grain, and provide a protective and attractive finish. Paints and varnishes are usually used for this purpose. Several coats of finish are required for interior timber; typically a primer, to seal the wood and provide a good bonding finish, an undercoat to provide base pigment and fill-in any minor blemishes, and one or two topcoats to provide a hard wearing finish. Some paints have been developed which provide two or all three of these functions, but may be less economical or effective in use. For exterior use, many coats may be applied. In shipbuilding for instance, typically at least twelve coats of varnish are applied to exterior woodwork. The amount of finish used on timber adds significantly to the cost of the finished product. If the surface area of the product can be reduced, i.e. by providing a smoother finish, it follows that the surface area of the timber can be reduced, with resultant environmental benefits through reduced use of solvents, and cost benefits through reduced requirement of paints and varnishes.

2.0 Project background

2.1. History of woodworking machinery

2.1.1. Saw mills

Early mills utilised water power as a prime mover. Such mills, in widespread use in mainland Europe since the 1300's, though were introduced in Britain at a much later date. The primary reason for this late introduction was a fear that their use would damage the sawyers trade. These early sawmills were built around reciprocating saws, the cutting and shaping of timber by machine having only reached widespread use since the industrial revolution. Spindle moulding and shaping of timber first became practicable when rotating cutting tools were developed in the 1700's, along with the availability of readily controllable power sources.

2.1.2. The steam engine

The advent of the steam engine overcame the primary disadvantages of water power such as increased power, controllability, and the removal of the need to build factories close to the power source, as well as making available a power source which could be available all year round. The steam engine as a prime mover facilitated the industrial revolution when for the first time, the large scale production machined timber became possible.

2.1.3. Rotating cutterhead

The first true rotary machine cutting of timber came about in 1777 when Samuel Miller invented the circular saw. In 1793 the development of the rotating cutterhead by Samuel Bentham allowed the industry to realise the goal of increased throughput, with improved surface quality, where hand finishing methods had always previously dictated a trade-off between the two.

2.1.4. Fixed Knife Planers

Fixed knife planers have found limited use, their main advantage being a completely smooth finish. The design of the very first fixed knife planers was based upon those employed in the machining of metals (figure 2.1.4.1)
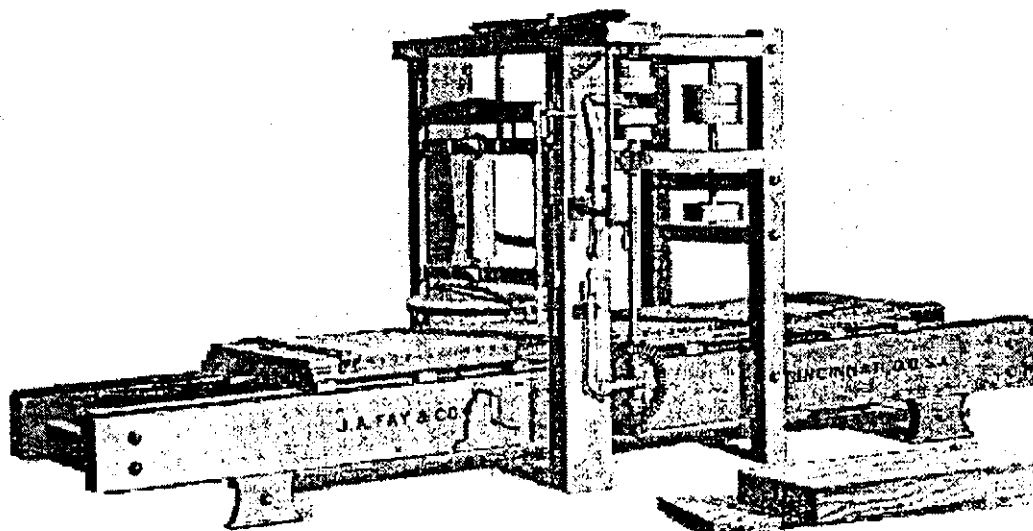
Figure 2.1.4.1. Early planing machine, analogous to metal planer.

However, although a very good finish was obtained, machining was slow. Smaller planers with a higher throughput used a rubber coated roller, placed directly above the cutter knife to grip the timber. (figure 2.1.4.2).
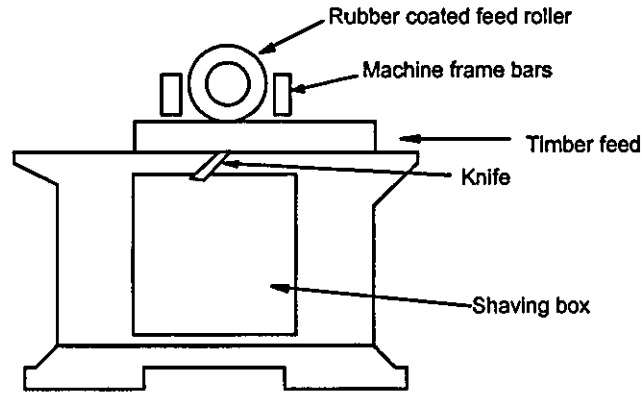
Figure 2.1.4.2. Simple fixed knife planer

A less than completely smooth finish was obtained sometimes, due to changes in cutting force. This would usually be brought about by knots, offering greater resistance, the timber would be pushed upwards against the feed roller, and depth of cut would momentarily decrease. A more sophisticated version of the fixed knife planer can be seen in figure 2.1.4.3 . Here a more positive feed is employed with multiple feed rollers which can automatically adjust to the timber thickness.
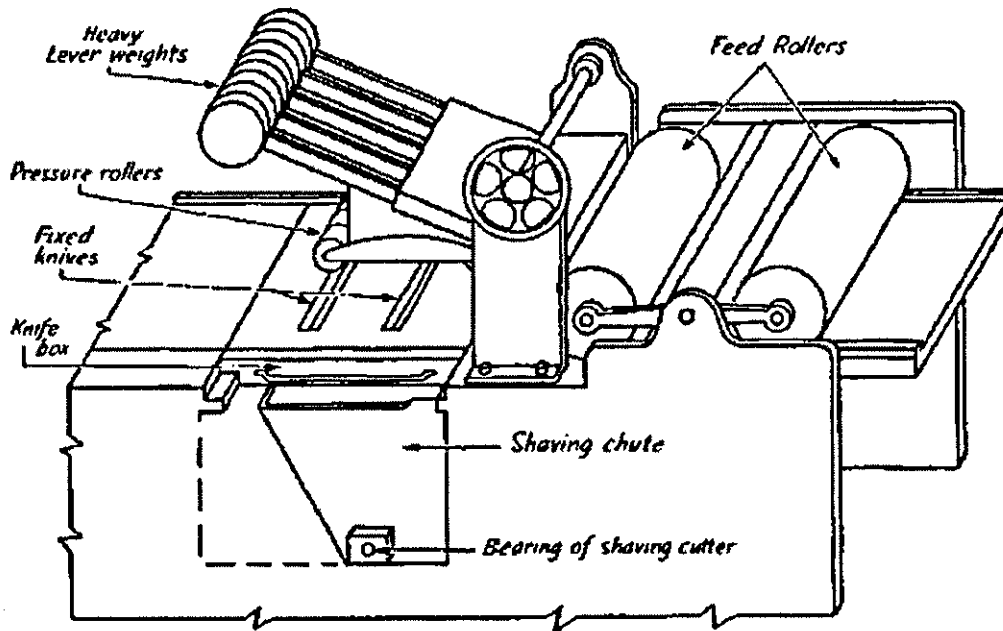
Figure 2.1.4.3. Sophisticated early fixed knife planer

12

A hogging cutter, (a cutter which provides a rough 'chopping' action), would be employed to break up the continuous shaving that would emerge at the bottom of the machine, such that it could be carried away through the plant's dust extraction system. It was found that the higher the feedrate used, the better the surface finish. Fixed knife planers often worked at very high speeds often in excess of to 150m/min. Due to this high feed speed, fixed knife planers were often referred to as 'lightning planers'. Fixed knife planers however, suffer from three main disadvantages:

1 - The wood must be practically flat before entering the machine (i.e. already rotary planed), since the maximum depth of cut available is little more than 0.2 mm. This also means that the fixed knife planing method is unsuitable for moulding.

2 - The long infeed and outfeed tables required for fixed knife planing machines mean that the machines are often prohibitively long to install in many factories (though this may also be true of modern rotary machines with long infeed and outfeed conveyors).

3 - In order to plane anything other than small stock, (usually of thickness less than 20mm and width less than 200mm), at relatively slow speeds, (the only application where fixed knife planers are still used in their original form is the planing of cigar boxes), the timber must be fed positively, usually with a serrated or toothed set of wheels. Although one surface of the timber may be of high quality, at least one of the surfaces will be marked by the feed system.

2.1.5. Rotary Planing machines

Much of the machinery invented between 1777 and 1850 paved there way for modern woodworking machines. A system of belt drives connected to pulleys mounted on long shafts called line shafts, would transmit power from the prime mover, usually a steam engine, throughout a factory. The line shaft speed would vary from about 90 to 150 rev/min; some were made of wood, others of cast-iron; the driving pulleys were made of laminated wood. From the line shaft there was a belt drive to the machine or to an intermediate countershaft.

In 1827 Malcolm Muir devised a machine from which current planers have been developed. Automatic timber feed was provided by an endless chain drive, as shown in figure 2.1.5.1. The timber first passed a rotary cutterhead mounted on a vertical spindle which machined a datum face, shown in figure 2.1.5.2 and then over three bottom knife blocks holding fixed knives, also shown in figure 2.1.5.2 for planing the underside of the timber. A tongue was then cut in the datum face by saws carried on horizontal spindles, one above the board, the other below, each cutting to a depth of the tongue. The timber then passed through two horizontal saws on vertical spindles which cut through to the saw cuts made by the vertical saws , shown in figure 2.1.5.4. This produced a sawn out tongue. On the opposite side to the datum face the board was cut to width by a saw. This saw was followed by a grooving saw which cut the horizontal groove, as shown in figure 2.1.5.3. The vertical spindles on each side of the machine (used for the tonguing and grooving operation) also carried revolving cutters which machined overlapping rebates on the top of the board which determined the board thickness. Although throughput on these machines was better than for hand feed planers, the surface finish of the products was variable and often of poor quality.
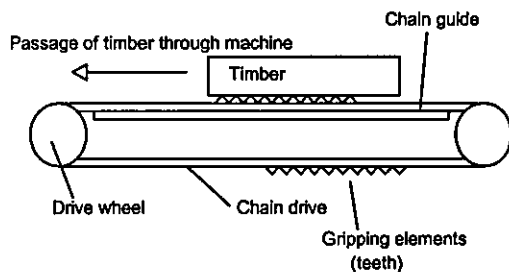
Figure 2.1.5.1. Chain feed method
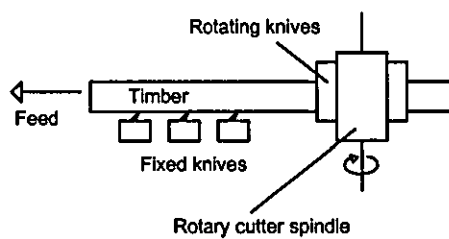
Figure 2.1.5.2 Datum face machining and surface planing

14
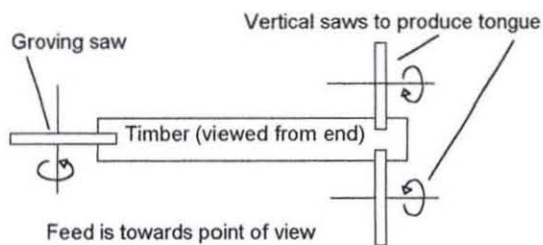
Figure 2.1.5.3. Grooving and vertical
tongue cuts
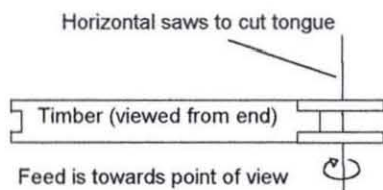
Figure 2.1.5.4. Completion of
tongue

John McDowall built machines to Malcolm Muir's designs but gradually introduced his own modifications. By 1836 when he filed his patent, his modifications had converted the original machine to the form of planers currently being manufactured, an example being shown in figure 2.1.5.5. The endless chain was replaced by feed rollers, giving a more constant feed motion. The tonguing and grooving saws were superseded by rotary cutterheads. Surface quality and material throughput was consequently bought closer to that of current machines.
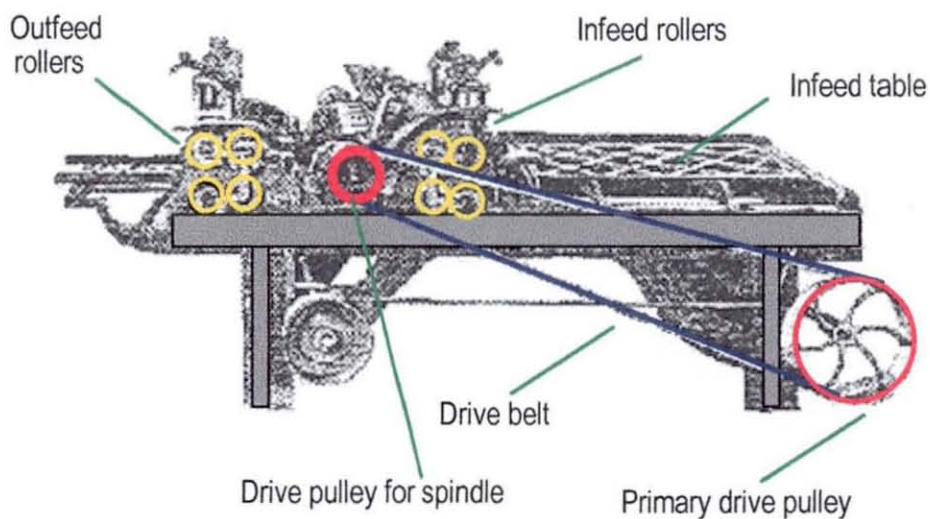
Figure 2.1.5.5 Typical early rotary planer

As late as the 20th century, some woodworking machinery manufacturers produced machinery of wood framed construction, the idea being that wood was better than iron for this purpose because it more readily absorbed the vibration of fast running machinery which would otherwise be conveyed to the products surface finish. Another theory was that it would be less easy to bruise the product if the machines were built of wood rather than metal.

2.1.6. Design Improvements

By the end of the 19th Century, progress in technology had made it possible to manufacture machinery much more accurately. The turn of the century saw many engineering developments taking place which greatly affected the quality of timber products and the rate at which they were manufactured. These included the appearance of precision ball bearings, higher spindle speeds and better tooling. The most significant example of tooling improvement was when circular cutterheads with thin knives replaced square cutterheads with thick knives. Circular blocks could accommodate higher spindle speeds, larger number of knives and therefore allow greater feed speeds for a given surface finish. The addition of feed rollers and pressure rollers permitted multiple feeding of narrow stock of differing thicknesses.

2.1.7. Electric Motors

Electric motors were first used in woodwork machinery shops as a means of breaking down complicated transmissions powered from a single prime mover. Power transmission using lineshafts, belts and pulleys dictated machine positioning. As a result, work flow through the factory was often overly complicated and inefficient. Another disadvantage was that the power losses in lineshaft systems were significant, often in the order 40 - 50 %, and downtime due to belt and bearing maintenance would often cause several machines to be unusable at once. (Mansfield J.H, 1952). The next logical progression was the implementation of electric power since woodworking machines, due to their comparatively high cutting speed requirement, readily lend themselves to being driven by a compact electric motor. Arguably the person who did the most work in modernising the timber machining industry with the introduction of the electric motor was W L Sims O.B.E (Sims W L 1985). Initially, (as may still be found in the garment industry) large

16

electric motors were used only to drive individual lineshafts. Integral electric drives were introduced later.

2.1.8. Planer and Moulder Evolution

Many refinements followed the integral drive. Cutterheads were provided with a brake to bring the spindle to rest rapidly. Belt striking was essentially a clutching operation, whereby the main machine drive belt would remain slack until shifted into position on a drive pulley mounted on the lineshaft, by a system of levers when power was required. The cumbersome, and often dangerous, belt striking gear was replaced by independent start and stop button controls which allowed only the required heads to be selected. Direction of rotation could be selected, as required, at the push of a button. It was possible to provide motors with up to six different speeds, at the turn of a switch - this eliminated the use of multi-step gearboxes. This type of machine offered much improved efficiency and flexibility, requiring one-third of the floor space of its belt driven counterpart. It eliminated the problems of belting maintenance, which was considerable on the fast machines, and there was less slowing down of spindles under load because the motor speed was relatively constant and the motors were designed to cope with sudden loads. Thus, there was no tearing of the grain due to sudden belt slippage in the cutterhead drives. As a result, product surface quality became more consistent. A self contained planing machine which typifies these design methods, as manufactured by Wadkin in the late 1940's, is shown in figure 2.1.8.1
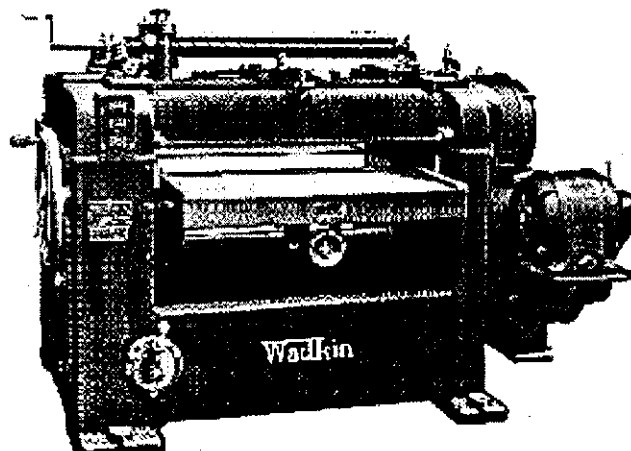
Figure 2.1.8.1. 1940's Wadkin planing machine
(Courtesy of Parry and Sons Ltd)

17

As soon as the importance of spindle rotation was recognised as a contributory factor in surface finish, a great deal of attention was given to the design of the motorised spindle unit. Ball bearing tolerances were considered and it was found that the original allowances, specified for the first electric moulders, should be reduced by one-tenth (Burnner H.E, 1929). In order to improve stability of the bearing mounted spindle, it was found that the solution to spindle design was to use a large diameter spindle with a ball bearing at either end. the cutter arbour projected beyond the main bearing at one end of the spindle and the rotor for the motor projected at the other. All of this was carried in a cylindrical frame (machined on the outside) with a flange mounting at one end to carry the motor stator frame.

Thus, the whole motorised spindle unit could be mounted in a robust sleeve on the machine. The sleeve was designed to permit lateral movement of the motorised unit together with adjustment of cutterhead position. Longitudinal movement of the whole unit, with its supporting sleeve, was also catered for. Thus the complete head was concentric and rigidly secured to a main frame, which would be of fabricated or cast construction.

2.1.10 Modern Planers and Moulders

Whereas in the past it was necessary to construct a wide range of machines, each suited to a particular planing or moulding operation, it is now far more commonplace to assemble a planer/moulder from standard components in order to build up a machine to the required number of heads. Standardised sections which are designed for a particular type of head (e.g. top, bottom, side, universal) are bolted together to produce the machine. The diagram shown in figure 2.1.10.1 shows the arrangement for a typical 4 head machine.
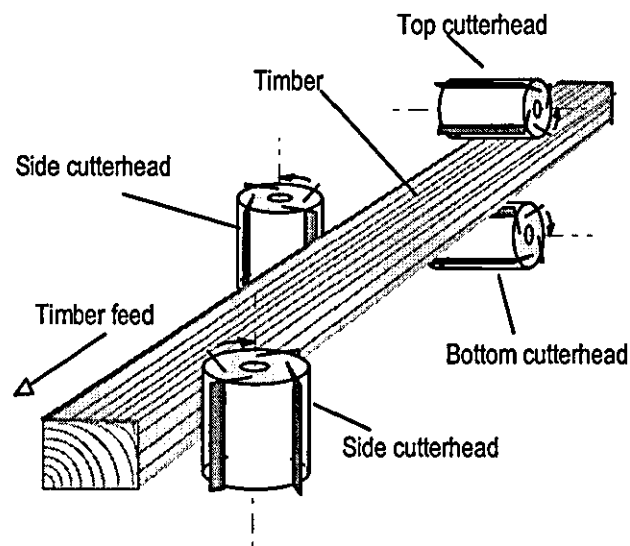
Figure 2.1.10.1 Arrangement for 4 head planing machine

Figure 2.1.10.2 shows a photograph the cutterhead arrangement for a 2 head (top and bottom) module. To the left of the picture may be seen the feed rollers. The whole assembly is enclosed during normal operation, including, for safety reasons, the transmission mechanism, whereby transmission of power to the heads may be via 'V' belts, flat belts, or a cardan shaft, whereby two universal joints are connected by a sliding splined shaft. The cardan shaft allows movement between the motor and cutterhead, for example to compensate for adjustments in cutterhead position to change depth of cut. Typical head motor sizes are in the order of 18 kW.

19
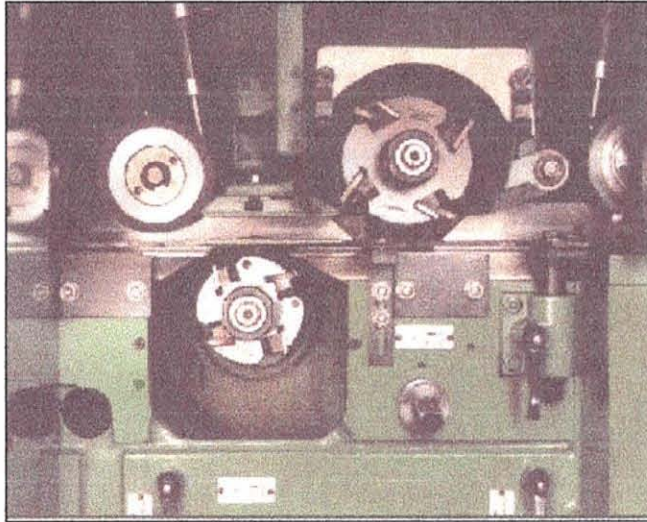
Figure 2.1.10.2. Cutterhead arrangement for modern planing machine
(Courtesy of Wadkin Ltd)

A significant development in modern planing and moulding machine design was the Router - Moulder developed at Wadkin Plc, which utilised a single point cutter running at 15 000 rev.min^{-1}, using 5kg tooling, with a material feed rate of 30 m.min^{-1}. High surface quality at moderate output was achieved (Jackson, 1986), and the design overcame problems of tooling balance and bearing life which has previously thought insoluble for machinery running at such speeds.

2.1.11 Feed methods

The feed method is also flexible, and is usually in the form of cardan shaft driven feed rollers, which are pneumatically actuated and driven either by individual motor units or from a common shaft for large machines. The cardan shaft is comprised of two universal joints connected by a sliding sleeve, to provide a shaft which transmits torque at constant velocity (figure 2.1.11.1). Infeed tables hold timber before it is pulled through the machine by the feed rollers, the outfeed table holding the finished product. These tables are usually bolted to the machine, as opposed to being comprised of a single casting as was the case in older machines.
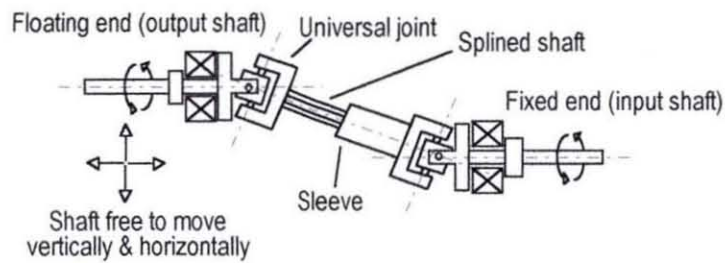
Figure 2.1.11.1 Cardan Shaft

In all but fully automated lines, timber is still initially fed into the machine by hand. A typical 4 head machine in operation is shown in figure 2.1.11.2, giving an indication of machine size and operation.
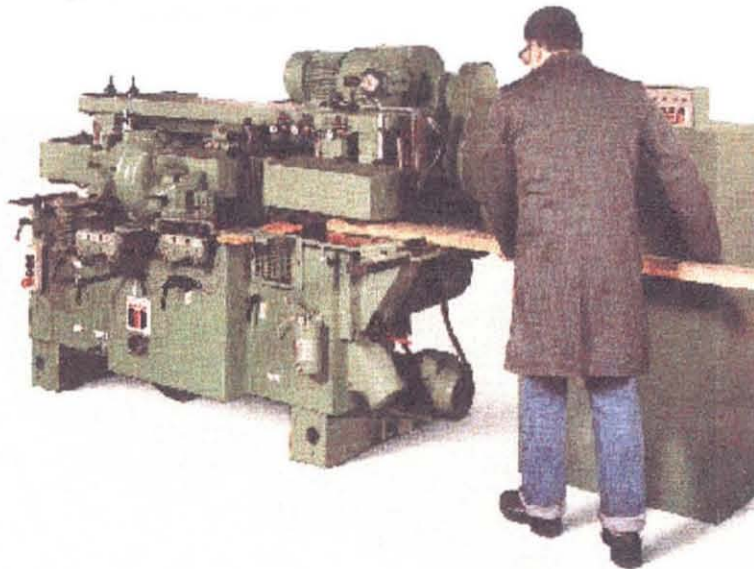
Figure 2.1.11.2. Modern planer/moulder in operation
(Courtesy of Wadkin Ltd)

21

2.1.12 Tooling

In most modern planing machines, the cutterhead runs on a spindle of typically 40mm diameter, supported by ball bearings within the spindle housing. Although the design of spindle mounting is fairly universal, the tooling for planers and moulders may take on a variety of forms. The square cutterblock has largely been superseded by round cutterblock tooling (Jackson, 1986), as illustrated in figure 2.1.12.1. High material removal rates are possible with helical cutters such as the spiramax cutterhead, though knife replacement is more costly than for straight knife tooling. Segmental cutterblocks are used for moulding. Square cutterblocks are used less, due to the substitution of more durable materials for the cutting material. Lead times for preparation of tooling are being reduced in order to reduce machine down time through an increasing application of information technology (Sansui, 1991).
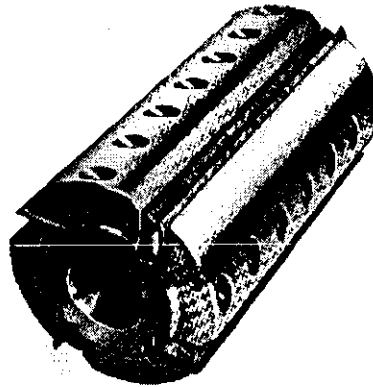
Figure 2.1.12.1 - Modern round cutterblock

Further refinements to cutterblock design include the use of replaceable tungsten carbide inserts in place of high speed steel cutter knives offering improved tool life. A typical cutterhead which uses this tooling is the Spiramax cutterhead, produced by Wadkin plc, and is shown in figure 2.1.12.2.

22
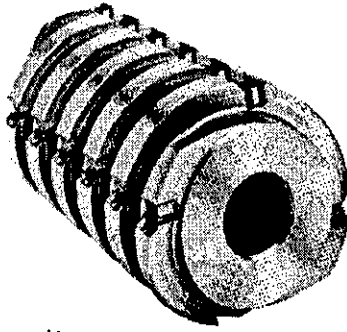
Figure 2.1.12.2. Spiramax cutterhead

High speed steel (HSS), whilst offering superior cutting quality, is not very durable and as a result is being superseded by materials such as tungsten carbide in planing and moulding operations offering vastly improved life (Mishanaevsky, 1995), (Porankiewicz et al, 1995), though stellite is sometimes used as a compromise between tungsten carbide and HSS, offering better life than HSS, but better quality than tungsten carbide. Cubic boron nitride (CBN) and polycrystalline diamond (PCD) offer even greater life than tungsten carbide (Morita et al, 1995), as a tooling material, and are now finding applications in the woodworking sector, but have yet to be applied to planing machine tooling. (Clark, Jennings, 1994), (Corinez, 1992). The primary problem with using such materials is that they are too hard to lend themselves readily to the jointing process (Lorincz, 1992), yet manufacturing tolerances are rarely better than 5 microns, which is outside the tolerance required for the conformity of knife tips to a common cutting circle in timber machining. Jointing, is a process employed to correct inaccurate knife grinding and is analogous to dressing of a grinding wheel. When the cutterhead has been bought up to speed, the knives are dressed with a carborundum stick to remove eccentric tracking and produce a new cutting edge (Figure 2.1.12.3).
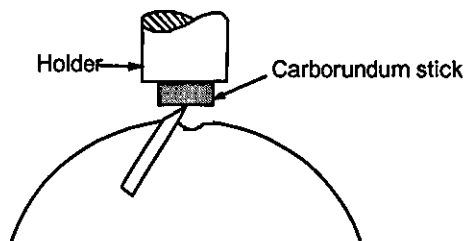
Figure 2.1.12.3. Cutter jointing

23

It can be seen therefore, that whilst tool life would be significantly greater than for high speed steel, surface quality would not be as good. In some cases, such as when machining of particle board, the diamond film coating (on faces only, not point coating) of tungsten carbide has been found to significantly reduce noise and power consumption, but at the time of writing has only been applied to small cutting tools, such as those found on saw blades.

Alternative designs of cutterblock are gradually becoming accepted within the industry. A 66% downtime saving is claimed in (Wood Machinery Manufacturers of America, 1990). where an insert knife system is used in place of conventional cutterblock knife mounting. The insert cutterblock used enables HSS or tungsten carbide knives to be changed without the adjustment of gib screws. Gib screws are essentially large grub screws with a hexagonal socket, typically some 25 x 8mm. These screws are located in the cutterblock and are used to grip the knives. A longitudinal wedge gib is used which clamps the knife uniformly along the whole cutting length by centrifugal force once the head is rotated up to speed, though the maximum operating speed and the effect on cutterhead imbalance is not given. An alternative to conventional rotary machining in the form of cone milling is proposed by (Heisel, 1995), whereby a cutter resembling a countersink is bought into contact with the timber at an angle to produce a surface largely free from rotary machining marks. However, the balancing requirement of such tooling is high, since a cutter diameter in excess of three times the size of a conventional cutterblock face would be required to perform the same function. The paper offers cone tipped milling as a basic idea and would require more development to be practicable.

Better balancing of cutterblocks by improving the mounting of the cutterblock on the spindle is achieved with hydro sleeve tooling (Jackson, 1986). A toroidial cavity along the length of the cutterblock is filled with high pressure grease after the cutterblock is mounted on the spindle, thus ensuring even clamping of the cutterblock due to slight inwards deformation of the cutterblock central bore. Knife clamping is now achieved in the same way with a cutterblock featuring small plungers in the place of gib screws. The knives are placed in position and are held by spring loaded steel balls, and when correct balancing has been achieved, pressurised grease actuates the plungers and holds the knives firmly in place. Hydro sleeve tooling was originally developed in the early 1980's. A line drawing of such a cutterblock is shown in figure 2.1.12.3. The grease nipples and channels to the central core, and knife locking plungers are clearly visible, the operation

24

of which is described more fully in the next section. Although these design improvements in tooling have greatly enhanced the surface quality of the finished timber, defects may still be present, and the surface quality features of machined timber are therefore discussed in the next section.
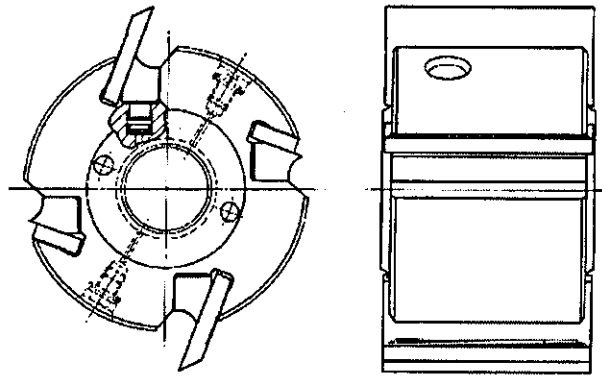
Figure 2.1.12.3. Hydro Sleeve Tooling

2.2. Surface Quality

Planed and moulded surfaces appear, when viewed closely, as a series of waves whose peaks are perpendicular to the passage of the product through the machine. Three such samples may be viewed in figure 2.2.1. Cuttermarks in this picture are visualised through illumination at an angle shallow to the horizontal (Figure 2.2.2). Cuttermarks are most easily visualised when illuminated in this way. Machining errors may exist which affect surface finish, these being error of form, and surface waviness which is the component of texture upon which the undulating knife traces are superimposed, and can result from cutterhead imbalance (the principal cause of waviness (Jackson, M.R, 1986)), flexure of the machine frame, and machine vibrations (figure 2.2.3).
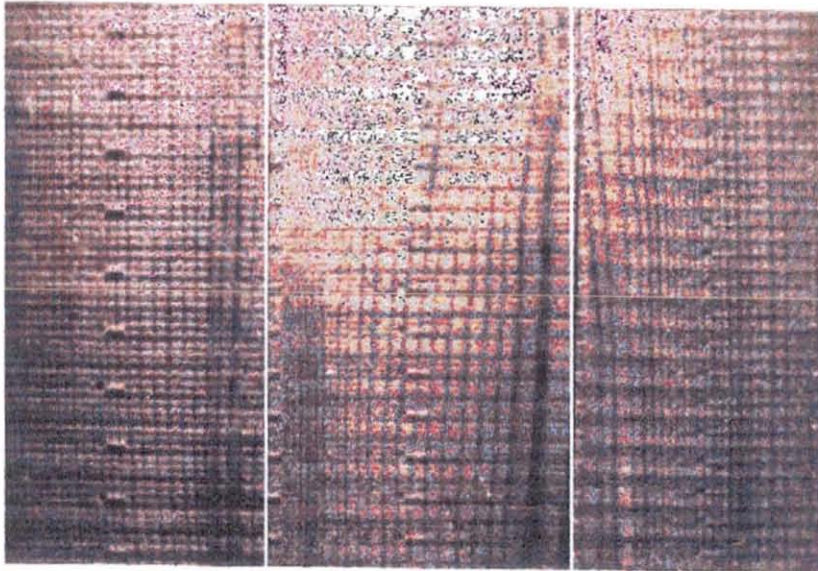
Figure 2.2.1 Cuttermarks illuminated with oblique light
(Jackson, 1986)
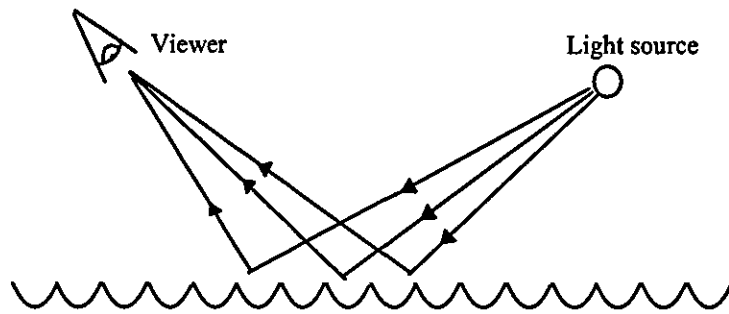
Figure 2.2.2 Viewing method
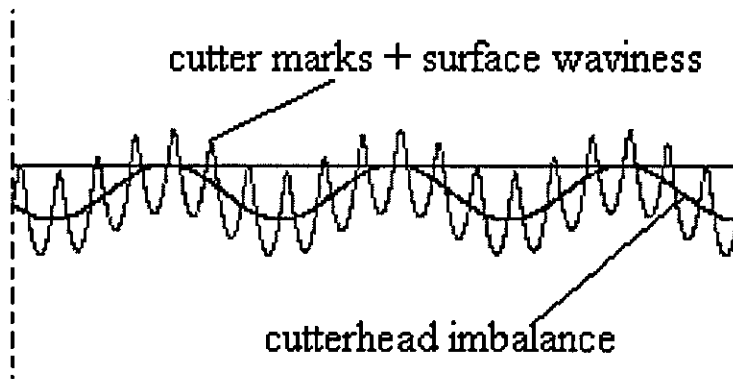
Figure 2.2.3 Timber surface defects

2.2.1. Cutter Wave Pitch and Height

Cutter wave pitch and height are given by equations 2.2.1.1 and 2.2.1.2, (Jackson, 1986), assuming a common cutting circle. Figure 2.2.1.1 is included to make these terms clear.
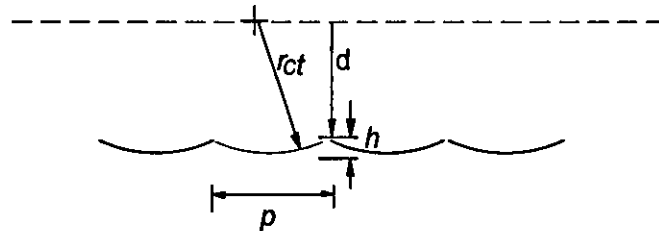
Figure 2.2.1.1 Essential features of timber surface geometry

$$pitch(P) = \left(\frac{f_d}{n.N}\right) 2\pi \qquad\qquad 2.2.1.1$$

$$Height(h) = r_{ct} - (r_{ct}^2 - P^2 / 4)^{0.5} \qquad\qquad 2.2.1.2$$

For good quality joinery, the *maximum* wave pitch allowable (Jackson. 1986) is not more than 1.8 mm.

2.2.2. Other Defects

In order to produce an acceptable surface finish yet maintain high throughput, larger numbers of cutters on each cutterblock have been employed. During ideal conditions, a large number of knives produces a smaller knife mark pitch, which gives an improved surface quality. This requires a larger cutterblock in order to accommodate the extra blades, which can exaggerate vibration problems when running the machine at high speeds. There also exists with multi - knife cutterblocks an increased likelihood that not all of the knives will follow a common cutting circle, i.e. one or more knives may stand slightly proud. These are caused by the deviation of the cutter tip locus from the ideal, not only caused by cutterhead imbalance, but sometimes caused by inaccurate knife grinding. The use of a smaller cutterblock enables a high spindle speed since vibration problems are reduced to some extent, though the smaller number of knives used will

28

reduce useful cutter life. Better balancing of cutterblocks by improving the mounting of the cutterblock on the spindle is achieved with hydro sleeve tooling (Jackson, 1986). A toroidial cavity along the length of the cutterblock is filled with high pressure grease after the cutterblock is mounted on the spindle, thus ensuring even clamping of the cutterblock due to slight inwards deformation of the cutterblock central bore.

Spindle runout is the term used to describe eccentricity due to the spindle upon which the cutterblock is mounted, not following a perfect circle of rotation within the bearings. Spindle runout will at most be around 4 microns, but on a correctly maintained machine is less than a micron.

Other defects appear as lower frequency components in the surface waveform. Defects caused by errors in machine tool slideways and flexure in the machine frame are currently harder to resolve (Dalay, 1985). Planers are of a massive construction, but flexure of the machine frame can still arise through propagation of low frequency vibrations throughout a machine fitted with two or more cutterheads. Low frequency beats will propagate through a machine frame whenever two less than perfectly balanced cutterheads are running at differing speeds. This is particularly noticeable when stock first passes through a machine, as unloaded cutterheads slow down when each begins cutting. Having outlined the defects which may apply to rotary timber machining, inherent and otherwise, a machining method is proposed in the next section with the aim of reducing the cuttermark height.

2.3. Proposed method of machining

Figures 2.3.1 , 2.3.2, 2.3.3 and 2.3.4 show how a cutterblock with two degrees of freedom may reduce cutter wave height. The cutter advances producing a clean cut (figure 2.3.1 - displacements are exaggerated for clarity). Cutter motion detail is shown in figure 2.3.2. Displacements have been further exaggerated for clarity, and only one (of 4) cutter knives on each cutterblock is shown, also for clarity. The numbered cutterblocks refer to the same cutterhead, shown in different parts of the oscillation cycle. The knife contacts the surface at the beginning of the cycle as shown by the cutter numbered 1. As the cycle progresses, the knife is advanced across the timber surface as shown by cutters 2,3 and 4. The knife is moving further away from maximum depth of cut by position 5. The cutter is then retracted. Figure 2.3.3 shows an overview of the retraction part of the cutterblock actuation cycle. Referring to figure 2.3.4, where displacements have been exaggerated further to show this part of the cycle more clearly, the cutter begins the retraction cycle with a knife cut having just been completed (position 6). Retraction is rapid, whilst the cutterblock continues to rotate, as shown by cutterblock positions 7, 8 and 9. The beginning of the next actuation cycle begins with the following cutter knife beginning to contact the timber surface, as shown in position 10. The perceived benefits are outlined in section 2.3, and typical figures for cutterblock mass, oscillation amplitude and frequency are outlined in section 4.0.
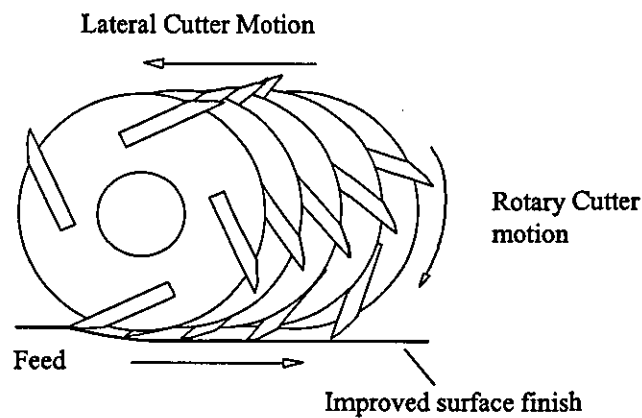
Figure 2.3.1. Cutterblock advance

30
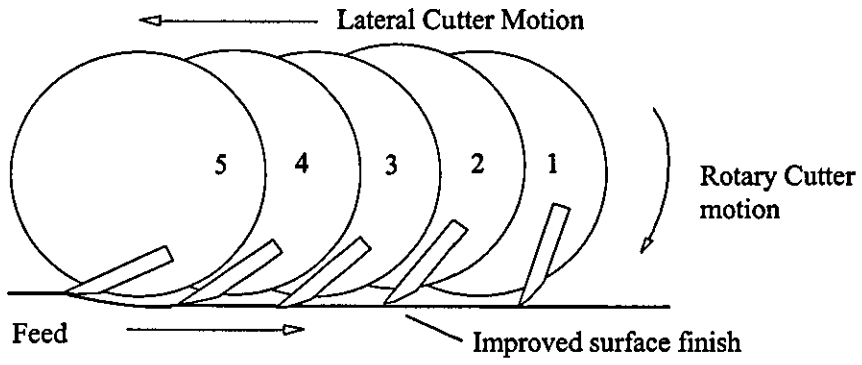
Figure 2.3.2. Detail of cutter motion during cutter advance
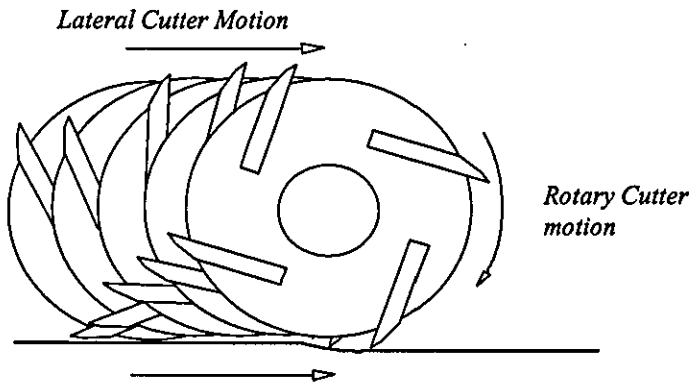
Figure 2.3.3. Cutter retract
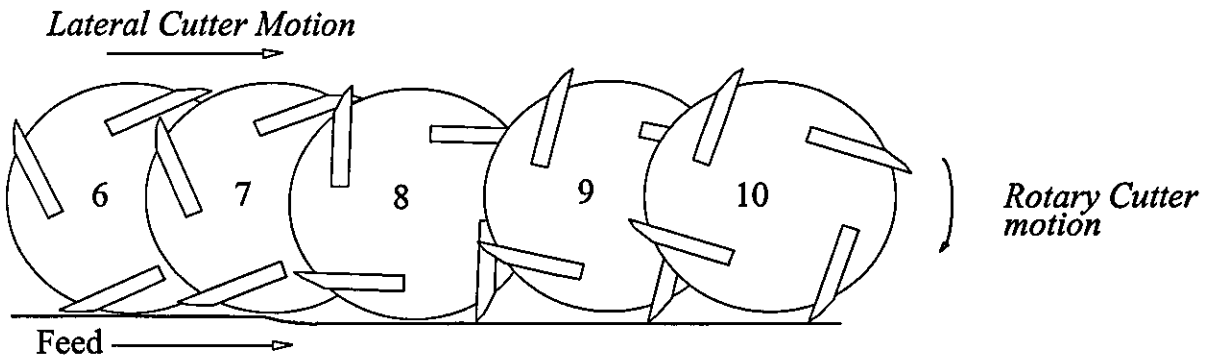
Figure 2.3.4. Detail of cuter motion during cutter retract

31

2.4. Structure of research

The project overview may be broadly visualised in the structure chart shown in figure 2.4.1. Spin offs such as experimental validation of cutterblock oscillation are carried out and described fully in this thesis. The relationship between timber surface form simulation (to identify cutter wave shape) and high speed servo simulation (to identify a method of cutterblock oscillation) becomes clear. A combined simulation is therefore produced to show the effect of cutterblock oscillation upon surface wave shape. At the same time, experimentation is carried out to check the results produced by simulations.
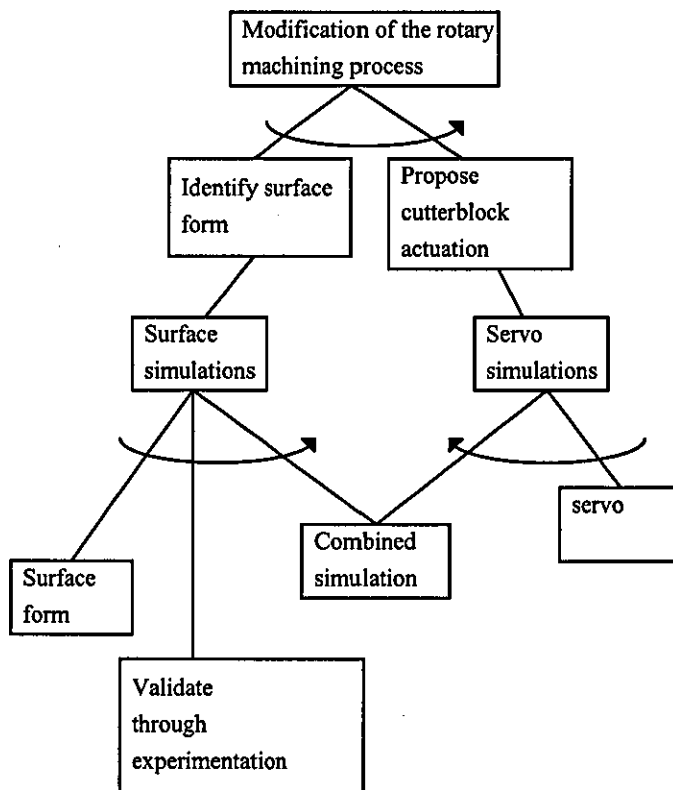
Figure 2.4.1 Structure chart for surface simulation and cutterblock oscillation procedure

2.4.1. Research Structure Outline

It can be seen that despite the developments that have taken place in both fixed knife and rotary planing, there are still inherent faults and defects within each process. In the case of fixed knife planing, pre-processing of the product is required, usually with a rotary planer, before machining. Even then, the applications for fixed knife planing are limited. Rotary planers produce a surface rippled with small cutter marks. Whilst timber which has been rotary planed, and moulded, can be of acceptable surface finish, three scenarios frequently arise:

1) When any machining errors are present, coupled with the high throughput rates in excess of 150 metres / minute, large amounts of defective timber may be produced before a fault may be detected and corrected.

2) When timber with a particularly high quality surface finish is required, further finishing of the timber is necessary, e.g. through sanding.

3) The life of HSS knives used in cutterblocks is relatively short. Because materials such as Tungsten Carbide and Cubic Boron Nitride (CBN) do not lend themselves to the jointing process, for purposes of maintaining a balanced cutterhead with a common cutting circle, high speed steel is still the preferred cutting material.

The use of the modified cutting process as outlined in section 2.3 should greatly reduce process variability through cuttermark reduction, and produce a product which requires no further finishing. Since cutter wave height will be reduced, a high quality surface may be achievable even though cutter knives may not follow a true cutting circle, such that harder materials may be used for tooling, such as CBN.

33

2.4.2 Research Declaration

It is appropriate at this point now that the background of timber machining has been covered, to reiterate and summarise the purpose of the thesis as follows:

This thesis is an account of research undertaken in the field of modification of the rotary machining process, in order to improve surface form. The research sought to demonstrate the effectiveness of modification of the cutting path to achieve this aim, and to develop a practical method of implementing it.

The research concentrates on planing operations, since the method is essentially the same as that applied to moulding, whilst simplifying the resultants surface geometry. It was felt at the outset of the project that the development of a system for cutterblock oscillation for timber planing would require the full project time span. Further projects could then refine and optimise the basic method developed in this research and make it applicable to moulding.

2.4.3. Project Management

This project had a time scale of 36 months, commencing January 1995. Appendix one illustrates the main activities anticipated. It was intended that a fully working model of the proposed system be completed by April 1997.

The first quarter (January - April 1995), concentrated on reviewing previous work relating to planing and moulding machinery, high speed actuators, and simulation before defining the main research objectives.

The detailed literature search began towards the end of the first quarter, in parallel with the beginning of the modelling and simulation process. Familiarisation with the simulation software, the writing of C code for UNIX platforms, and the use of the Sun operating system SunOS5.4 also began towards the end of this quarter. Conceptual design of a system suitable for simulation was undertaken, such that system performance using differing components could be evaluated during the conceptual design stage.

The second quarter involved a continuation of the literature search, and the initial work with the simulation software, particularly with respect to the simulation of hydraulic

servo valves. Several methods of simulation were tested in order to find the most practical model. Research into the design and implementation of high - speed actuators was conducted in parallel with the simulation work. The simulation process continued during the third quarter, such that a comprehensive model had evolved. The system model produced simulation results which were unexpected whereby simulation runs sometimes would not complete, and were eventually revealed to be caused by high pressure spikes in the hydraulic supply lines. At the time, these results led to an increase in the pace of the literature search in order to more fully understand the nature of the hydraulic parts of the system. The fourth quarter saw the computer simulation of the system produce the most complete results Consequently the design process was accelerated owing to improved knowledge of the behaviour of the proposed actuation systems. Towards the end of the fourth quarter, transfer of system component models from Saber™ to Matlab was underway. The main system component models were transferred to Matlab during the period January - late February 1996. The ongoing literature search was accelerated once again, this time looking at suitable control systems to improve the performance of the hydraulic system.

Research activities for the following period were less fragmented. Once the groundwork had been done in year one, it was possible to continue the research in several clearly defined areas which may be described more briefly. The activities for the second year focused on test rig design and construction, and the simulation and design of a suitable control system. The prototype design was refined and optimised and was fully operational in conjunction with rigorous testing towards the end of the eighth quarter.

During the final year, hypothesis verification through experimentation using the test rig, extraction of results from actuation system, and integration of the servo simulation with the timber machining simulation proceeded until the tenth quarter. Some modification of the test rig was undertaken in order to improve the quality of results, and code was written in order to post process the resultant test rig output to provide a result which could be correlated with the simulated surface finish.

3. Review Of Previous Work

Having now provided the background to the project, and having stated the projects aims, it is now appropriate to examine more closely the work which has already been carried out in areas which could be useful to the project. The literature review covers two main areas. The first section of this chapter covers precious research in the field of rotary machining with particular regard to timber machining, and the simulation of the rotary machined surface form. Material with regard to the machining of metals, as well as being more abundant, was also relevant to this project and as such, has been included where appropriate. In addition to these topics, work concerning the surface inspection of timber components has been investigated as potentially useful in the overall control of the system.

The second part of this chapter covers the appropriate aspects of high speed servo design. Two potential actuation systems were investigated due to their potential high gain, bandwidth, and ease of controllability. Pure mechanical oscillation of the cutterblock at high speeds was deemed unsatisfactory since choice of wave profile would be considerably limited. To the same end, investigation into the characteristics of pneumatic systems revealed a lack of controllability which would render them unsuitable for this application. Piezoelectric actuators were initially investigated in due to their novel application in high speed servovalves, though the final choice of servo valve design was left open ended until simulations took place, it was thought prudent to consider the use of high speed valves of novel design which are described as having performance equal to, or surpassing that of conventional servo valves such as piezo operated valves, and proportional direct driven linear motor actuated valves. The control of the hydraulic system, and other aspects surrounding the potential use of a hydraulic servo such as choice of transducers, are covered towards the end of this chapter.

3.1. Timber Surface Form

3.1.1. Detection of Surface Finish Defects

Hatzkiriakos et al (1994) describe the use of fractal dimension to characterise a wood surface by using water - sorbtion data. The primary purpose of the work was to determine the wood surface area. Of note was that the conclusion stresses the three dimensional nature of the wood surface, stating that at little more than molecular level a 2 dimensional analysis says very little about surface roughness. It becomes apparent however that for the purposes of this research that the visual effects of surface defects are considered more important often than a mean value of surface roughness. Measurement and control of surface profile off line, often begins with the use of stylus measuring devices. Contact stylus techniques are widespread for the measurement of metal and wood surface profiles (Smith, Tlusty 1990). A stylus was drawn over the surface at constant speed and it's height changes relative to a reference level was recorded. A two dimensional profile of the workpiece surface was obtained as a result. Contact based methods however, are manual and performed off line.

Non contact methods would appear to be more suitable to the timber machining process therefore, and Silven and Kauppinen (1996) stress the importance of automated wood inspection methods for looking for larger defects such as knot holes, prior to the machining process.   In fact a large amount of research in automated timber surface inspection is concentrating more on the initial quality of the timber prior to machining, as opposed to the machined surface finish. Young (1995) describes a linescan camera and DSP based wood inspection system, intended for the detection of knots, cracks in cut planks, and graining in the cut planks. It can be seen from the paper that the system developed could actually be used for surface finish evaluation with little modification. While the architecture of the image processing system was described well, surprisingly no mention was made of how effective the system actually turned out to be, no results being included in the paper.

Lampinen and Smolander (1996) show a more diligent approach, and describe the use of neural networks to identify inherent timber surface defects, stating an accuracy of defect recognition of 90% is achievable (for a colour system, monochrome efficiency is 5 - 10% less), compared with 75 - 80% for a human operator.   Unfortunately little information was gathered using this method about the actual nature of the defects, such as size and

distribution through batches of timber, which could provide useful statistical data for quality control. Hard limit neurons are utilised for an accept/reject system. The system works well, and shows the suitability of a neural network for high speed timber inspection at feedrates of between 10 and 20 m.min^{-1}. Neural networks when applied to the solution of timber machining problems could prove particularly useful, due to their ability to cope with nonlinearities (Davalo, Naim, 1992), and speed of execution (Carling, 1993). Ordinary machine vision techniques have therefore been demonstrated to perform well, but more information may be gathered about the nature of timber defects and timber classification, using spectral reflectance (Lebow et al, 1996), whereby the percentage of incident light of each wavelength reflected from the timber surface was measured. Although the system was not yet suitable for production speeds, the use of an extended colour system was proposed which could provide the necessary performance. The system was able to differentiate between loose knots and tight knots which would avoid unnecessarily rejecting suitable batches of timber.

Returning now to the subject of contact based measurement, it can be seen that optical methods could provide a superior method of inspection, since because of the high operating speeds of woodworking machinery, contact based surface form evaluation methods applicable to the milling of metals cannot be used for on line inspection. Pioneering work on non contact based surface form measurement was carried out in parallel by Devries and Lemaster in 1991, though their system was developed for monitoring of the sawing process, whereby surface waviness and surface roughness may be evaluated. Operating speed of the system was slow however, running at 0.78 in / min, due to speed limitations of the post processing software. A larger volume of work produced by Maycock (1993) shows a method suitable for determining timber surface form defects, whereby a laser based measuring system is used in conjunction with software which uses a Fast Fourier Transform (FFT) algorithm to identify surface defects such as proud knife or cutterhead imbalance.

3.1.2. Closing The Loop

Limited developments have taken place with regard to in - process monitoring and control of the timber machining process, but the results achieved so far point towards a range of methods for inspection compatible with factory conditions ((Kim, Koviro, 1994). The cross cut optimisation of boards was described by (Åstrand and Rönnqvist, 1994) whereby a machine vision system was used to inspect boards for defects prior to sawing into shorter lengths. Utilisation of timber was improved by 7 %.

The actual monitoring and correction of the wood planing process has yet to be developed, though it's importance has been noted (Altintas, Spence, 1992), (Aronson, 1994). Similar work has been carried out by Lemaster and Dornfield (1988) to use acoustic emission to monitor the circular sawing process. As with most on line monitoring of timber machining, the main problem was physically locating the transducer close enough to the cutting edge in order to reduce lags. This was overcome with a purpose built pneumatic coupling between the transducer and the saw blade. The technology developed could be applied with relative ease to the monitoring of the planing process, indeed it has already been applied to the control of router feed speed using the same method by Cyra and Tanaka (1995), although a reliable measurement of surface form may still be required in order to provide the control data. An alternative could be the monitoring of the process from the machine, for example by examining the effect of the machining process on the machine, rather than vice versa. Monitoring of cutting forces, for example, could provide useful data, and has been used to good effect. Jung and Oh (1990), monitored cutting forces in vertical face milling and controlled them in order to improve surface waviness by adjusting the feedrate using control data produced using a dynamometer. A fixed gain proportional plus integral (PI) controller was used to control cutting force. A significant reduction in surface waviness was achieved, the cutting force being controlled by varying the feedrate. Such an approach would be unfeasible for timber machining due to the continuous and non positive method of feed.

3.1.3. Timber surface simulation

Analysts predict that the use of simulation will rapidly increase during this decade. In the US alone, by the year 2000 it is expected that 40% of manufacturing engineers will be utilising simulation as a decision making tool. This compares to an estimated usage rate of 17 % in 1988. (Bergstrom, 1988). (Weidenbeck 1992) stated that in the wood products

40

industry simulation modelling was being used in research and by a few of the most innovative companies, but it had not yet been widely adopted. The large amount of references available since 1992 concerned with timber machining simulation suggest a huge increase in the use of simulation to determine the effects of machining parameters on surface finish.

With respect to surface form, the rotary wood machining process is similar in nature to the upcut milling of metals, and work carried out in the surface simulation of milled surfaces is often applicable to wood machining. Identification of effects such as inaccurate grinding of the cutter (Tarng, Shyur, 1992), may be useful when predicting dimensional accuracy in the finished product.

Effects of particular interest when simulating timber surface form such as proud knife and cutterhead imbalance are not considered as important for metal machining due to the lower machining speeds and different methods of tooling preparation. Most research on surface simulation of milled surfaces sets out to determine surface roughness and cutting forces. (Marusich, Ortiz, 1995) used a finite element method to determine the cutting forces in steels, whereby unusual cutting forces are shown to indicate excessive cutter wear and broken knife points. The face milling of metals was simulated by (Jung, Oh, 1991) in order to determine cutting forces, and therefore to implement a feedback control to vary cutting force in order to reduce surface waviness. The system was used to filter out high frequency components of the cutting force in the feed direction, and use the inverse of the low frequency signal to correct the feedrate. A significant improvement in surface waviness is claimed, initial tests giving at least a 90% reduction in L.F surface wave amplitude. (Lin, Liu, 1995), demonstrated the possibility of simulating the cutting process taking into account tool rubbing, though surface roughness prediction was the primary objective, as opposed to surface form. A good simulation model for end milling has been developed (Melkote, Thangaraj, 1992) which uses a mesh based approach similar in nature to FE, though the resultant surface geometry is not applicable to a timber machining scenario. A true FE model is proposed .(Kim et al, 1994) to predict cutting forces, and is a refinement of the work carried out by (Lee, Tryng, 1991) where a binary tool breakage predictor is realised. A simplified simulation of surface form is proposed (Kim, Chu, 1994), using a parabola as the model for scallop height, and is useful as a basic surface form predictor, but would require modification to provide a true simulation of surface form.

3.1.4. Overall simulations

Overall simulations of timber machining have shown where productivity and quality may be improved (Weidenbeck, Araman, 1995), whereby the entire production process of timber parts was simulated from debarking through rough sawing to planing and sorting, though a macroscopic view was taken, variables such as surface quality not being included in the model. (Lin et al, 1995) show that a simulation of a sawmill may be used to identify bottlenecks in production, offering refinements in the machining sequence that improve production rates by 22 % with no additional tooling required. The main requirement for simulation of the whole system is a true mechatronic simulation strategy (Bracewell, Sharpe, 1996), (Brown, Parkin, 1995), whereby mixed technology systems may be integrated on the simulation platform (Scholliers, Yili-Pietila, 1995).

3.1.5. Surface form

Jackson (1986) provided a defect specific simulation, and pointed to the need for a general surface simulation algorithm. Maycock (1993) was one of the first to design a surface simulation algorithm intended purely for the simulation of timber machining. 1024 samples were produced for each simulation run, and were produced by first describing the cutter tip locus, where:

$$I(t)_x = r_{ct} . \cos\left(\frac{F_d}{60} + \omega_{ct}\right) - r_{ct} . \cos\left(\frac{F_d}{60}\right) \qquad 3.1.5.1$$

$$I(t)_y = r_{ct} . \sin\left(\frac{F_d}{60} + \omega_{ct}\right) - r_{ct} . \sin\left(\frac{F_d}{60}\right) \qquad 3.1.5.2$$

...and then taking the lowest part of the curve (the machined surface form) with a filtering algorithm. The instantaneous knife position is represented in the following diagram, figure 3.1.5.1.
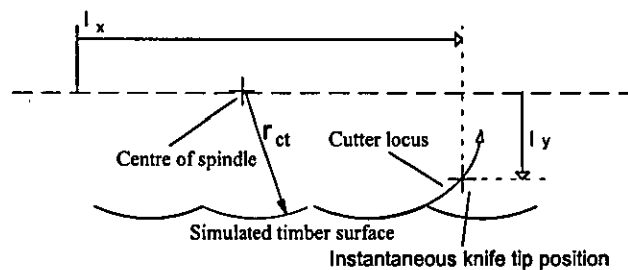
Figure 3.1.5.1 Cutter locus and simulated timber surface

Further 'cleaning up' of the image by hand was necessary since the algorithm was not completely reliable, and would include incorrect cutter tip loci points in the surface form files. These appeared as spurious samples some way above the surface waveform. Nevertheless, the speed of the simulation was good, running on an 8MHz 8 bit microcomputer, the code executes in only twice the time (per sample) than comparable current code on a 100MHz 486 PC. The generation of spurious samples in some way goes to explain the execution speed of the early software. Automatic methods of cleaning up the simulated waveform can lengthen execution time by a factor of 10.

Some previous surface simulations produced excellent surface finish results at reduced execution speed (Wang, 1995) whereby a continuous surface simulation of apparently unlimited sample points was generated. Wang stated that machine vibration would have a significant effect on the resultant surface form and as such should be included in the simulation. Unfortunately no documentation exists to describe how this was actually done, and the code produced is not portable due to video driver incompatibility with modern systems. This is a pity since screen dumps of the software suggest a particularly successful SSA. Without knowledge of the algorithms used in a simulation one cannot determine if a) the mathematical model was correct in the first instance and b) that the software was implementing the model correctly.

A simplified surface simulation algorithm has been developed by Heisel and Krondorfer (1995). It is argued that for the purpose of simulating the effects of vibration influence only the levels of cuttermarks and not their shapes. Consequently a simplified model was used whereby the cycloid shape of the groove was approximated by a circle segment of equal radius to that of the knife tip. The results produced are very clean, apparently free from discretization error. Whilst such a model is useful for analysing vibration effects, the effect of cutterblock oscillation upon surface wave shape may only be fully understood by use of a surface simulation algorithm that can extract surface data from a cycloidal cutter tip locus.

43

3.2. Actuation System components for high speed hydraulic servomechanisms

Although a hydraulic actuation system is not without limitations, it's principal advantage over a purely mechanical system is the adjustment of cut and retract cycle times and stroke lengths. Should a machine be constructed with several oscillating cutterheads, machine size need not be increased greatly when using hydraulics, due to the high power to size ratio of hydraulic rams. A purely mechanical system would require a separate oscillation motor and cam combination for each cutterhead.

The literature review has produced a wealth of information with regard to the possibilities of cutterblock actuation using a hydraulic servo. In conjunction with this, transducer considerations have been investigated, as well as novel methods of control. The tree diagram shown in figure 3.2.1 shows the relationships between the various aspects of servo design for cutterblock oscillation. A grounding in control system design such as described by (Schwarzenbach, Gill 1984), and the fundamentals of hydraulics (Viersma 1984), (Parr 1984) is assumed.
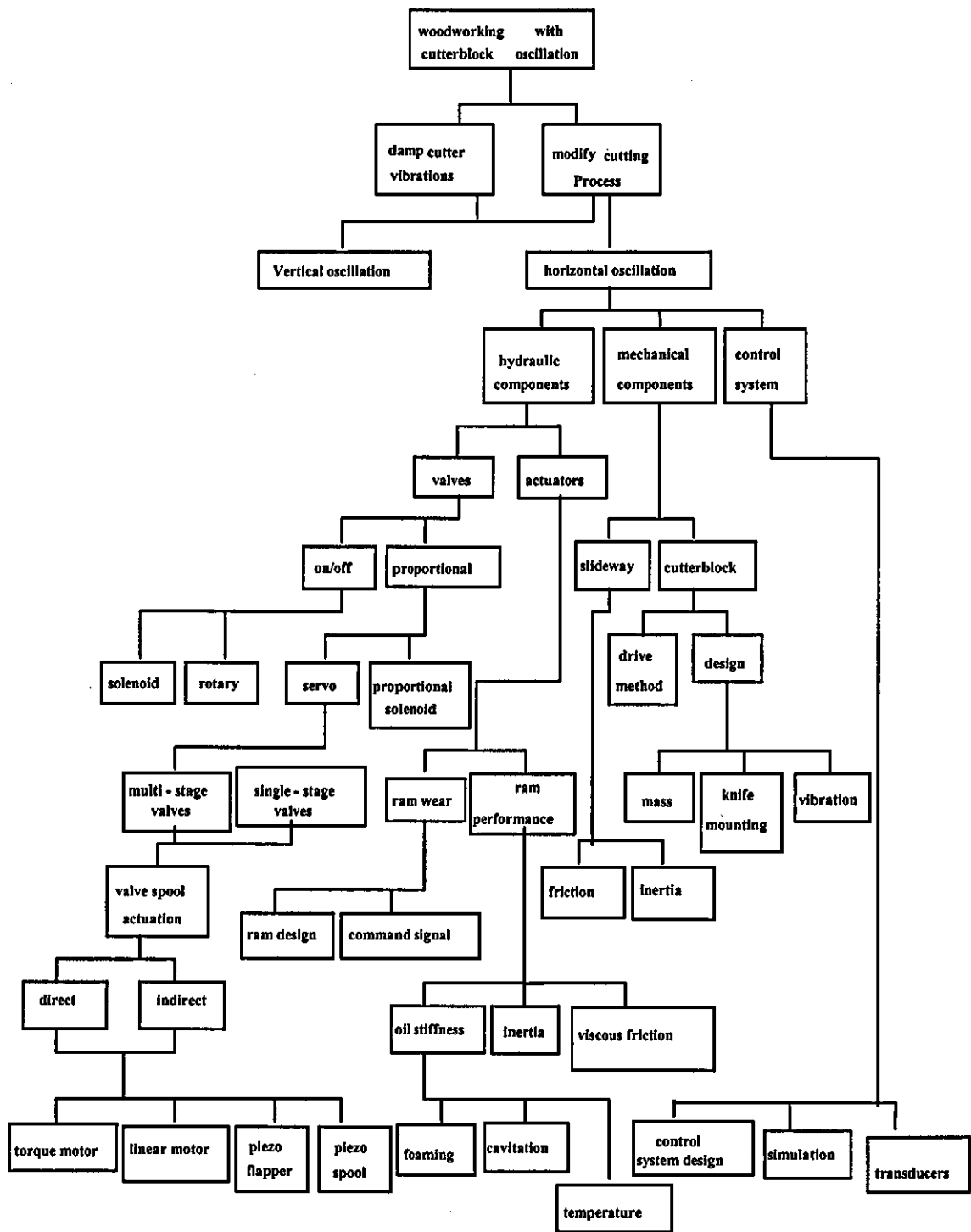
Figure 3.2.1 - The relationships between various aspects of servo design.

45

3.2.1. On/off valves

The potential need for differing rates of advance and retract, indicate that proportional control of the hydraulic valves could be favourable. PWM control of solenoid valves is possible, though specialised valves are manufactured with bandwidths intended to compete with conventional servo valves (Cullman, 1993), the technology for PWM hydraulic control is still relatively in it's infancy, but provides a cheaper alternative to torque motor valves, with easier control from digital systems (Suematsu et al, 1993). The use of poppet valves, simplifies the machining processes of a valve still further, thus driving down costs, and has found application in systems which previously required the more expensive servo valves.

The successful use of poppet valves to drive a hydraulic actuator is described (Cui, et al, 1991), and applied (Stewart, 1991), where servo poppet valves (SPV's) are used in the design of a high frequency hydraulic powered vibrator seismic source (VSS) used for seismic profiling, using   Although the VSS may sweep to a maximum frequency of 500 Hz. The decrease in available ram amplitude with increasing frequency was highlighted. The SPV rating is 1200 l/min decreasing 20 dB as frequency increases from 50 Hz to 300 Hz, with a further 17 dB decrease as the frequency increases from 300 Hz to 500 Hz. The maximum amplitude of the system is in the order of 0.2 mm, which is not large enough for horizontal cutterblock oscillation.

Following these developments, A further development of poppet valve application was published very quickly. Conventional PWM was used to drive the high speed electro - hydraulic valve described (Yokota, Akutu, 1991), where multi layer piezoelectric actuators are used to operate on-off type poppet valves. These poppet valves in turn operate a spool valve. Feed forward control was utilised such that response to within 100 microseconds of the switching speed is achieved. The valve design was ascertained by experiment to respond and follow a 2kHz rectangular wave input. It can be seen that while using such a valve is not yet commercially available, actuator response speed would only be limited by the maximum flow rate of the valve spool, and the possibility of high pressure spikes along supply lines due to the sudden nature of the fluid metering.

46

3.2.2. Rotary Valves

A rotary valve is proposed (Halstead, 1995) whereby a rotating spool meters flow of hydraulic fluid to the hydraulic ram. Response time of the system would then only be limited by the effects of pressure transients in the hydraulic lines, and the maximum system operating pressure. The solution proposed is both simple, and effective, though control of the ram position would be more difficult than with, say, a conventional servo valve. An advanced control system would be required however which would ensure that the ram is kept operating over the same portion of it's stroke, as any fluctuation in cutterblock load, hydraulic supply pressure or the speed of the valve spool drive motor, would cause rapid drift of the ram with potentially destructive results.

3.2.3. Solenoid Valves

Frequencies of up to 20 Hz have been successfully achieved (Hwang,Lan, 1994), whereby differential PWM was used to control a hydraulic actuator operated by two 3 way solenoid valves, though the details of the actuator ram and slideway mass are unclear. The operating characteristic of the differential PWM actuator is represented by the duty difference:

$$\Delta D = (D_1 - D_2) \qquad\qquad 3.2.3.1$$

versus the time average of the pressure difference for driving the actuator:

$\overline{\Delta p}$ (which is the mean value of $\Delta p = (p_a - p_b)$ over the time interval T_c).

The system is shown to have good stability and step response which exceeds that of conventional PWM, and the method of control applicable to the 3 way valves shows that such a system would be suitable for use with an assymetric hydraulic cylinder, though naturally the speed of response of the system when oscillating a cutterblock of typical mass in the order 25 - 30 kg, would have to be ascertained through simulation. Permanent magnet DC linear motors are beginning to replace solenoids in some critical applications, but are more suitable as replacements for torque motors in servo valves (Moog, 1995), (Bangert, 1992). Solenoids with a linear force/stroke relationship are now available (Parmeko, 1995) which would be more straightforward to control than conventional solenoids.

3.2.4. Servo Valves

Generally, Servo Valves are positioned by an electrical control signal, usually the process control standard current loop signal of 4 to 20 mA. Appendix 2a section 2.0 figure 3.2.4.1 shows a cross section of a typical direct drive servo valve. Single - stage valves have a low flow capacity (limited because of the force required to move the spool at higher flows). Where higher flow rates are required two stage or multi-stage pilot operated valves are used.
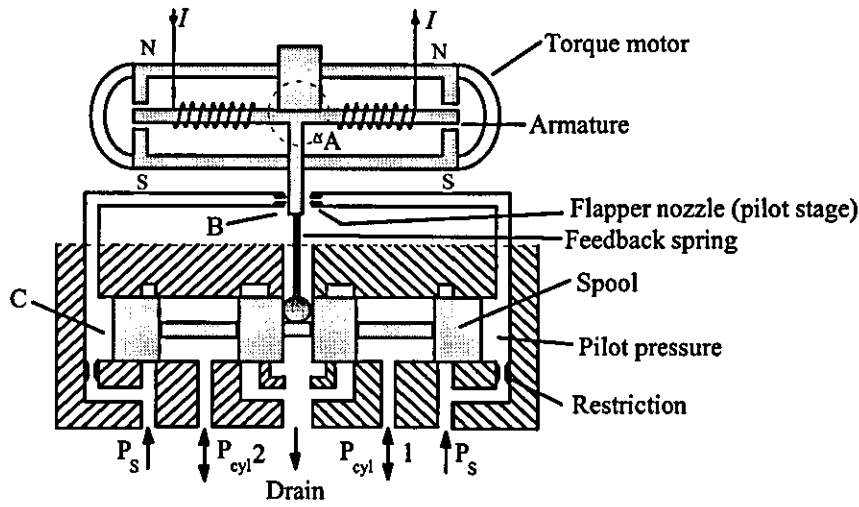
Figure 3.2.4.1. Torque motor actuated servo valve

Operation of the servo valve can be summarised as follows. Should an output flow from $P_{cyl}1$ be required, (and corresponding input flow to $P_{cyl}2$) in order to shift cylinder ram position, an input current is applied to the torque motor coil in order to rotate it clockwise. The output flow from the servo valve should be proportional to the input current flow to the coil (Compton, 1986). The valve flapper hangs between two orifices, through a very small hydraulic flow passes, which is then vented to the drain. A clockwise rotation of the armature will move the valve flapper closer to orifice B. This will bring about an increase in pressure in the left hand side of the valve, acting on face C of the valve spool. The spool will consequently move to the right. When the force returned to the flapper through the feedback spring is equal in moment to the torque generated in the motor armature, flow will remain proportional to the current through the motor. Thus the small force generated by the torque motor is amplified by the ambient hydraulic pressure in order to provide a rapid change in spool position. When current is

48

returned to zero, the pressure acting on each end of the spool is equalised and the spool returns to the central position.

Hydraulic servo valves have been used in high speed applications before with good results. (Wilson et al, 1992) Describes the use of servo valve to control an active valve train, with a hydraulically actuated valve lift in the order 1 - 2mm. - This provides a flexible method of controlling the lift and timing of an engine valve, thereby replacing the camshaft in a conventional engine. Although the system was found to perform well at frequencies less than $\approx$ 60 Hz, performance at greater frequencies is estimated by extrapolation - consequently extended results are only accurate within a limited range. One reference suggests that large flow rates could be applicable to high speed servos, whereby a high power application is described by (Allan, 1962), whereby a hydrofoil test-rig uses a hydraulic servo system to oscillate a mass of approximately 100 kg. The maximum frequency of oscillation was relatively slow at 20 Hz. However, 90mm diameter actuators are necessary, and the stroke was 13mm. Consequently reducing the stroke and the ram diameter should mean that with the same servo valve maximum flow rates, a hydraulic circuit of the same design could operate in excess of 20 Hz.

3.2.5. Proportional Solenoid Valves

Electrohydraulic proportional control valves now match or exceed the performance of older industrial grade servo valves (Cullman, 1993), (Hitchcox, (a) 1993). The fundamental design of proportional valves has changed little in recent years, though interesting developments have taken place with regard to the control circuitry, whereby digital controllers have begun to superseed analogue, (Virvalo, Puusarri, 1992), (Smith et al, 1991), often built around inexpensive PLC's (Hitchcox, (b) 1993), and frequently abandoning classical control methods in favour of fuzzy logic, (Lee et al, 1994), or artificial neural systems (Mathworks, 1993) where ANN's may be used for simulation, after which the inverse of the plant model is built into the control loop (Burton et al, 1994). It is widely agreed that newer control methods offer significant advantages in terms of reliability and performance (Cheng, DeMoor, 1994), (Rabie, 1994), (Tunay, Kaynak, 1993) (Shih, Sheu, 1991) A basic proportional control valve uses a proportional solenoid to position a spool which, in turn, meters flow to the actuator. The spools have machined metering notches that act as variable orifices when the spool traverses within the valve body. Spool position was typically monitored by an LVDT (Linear Variable

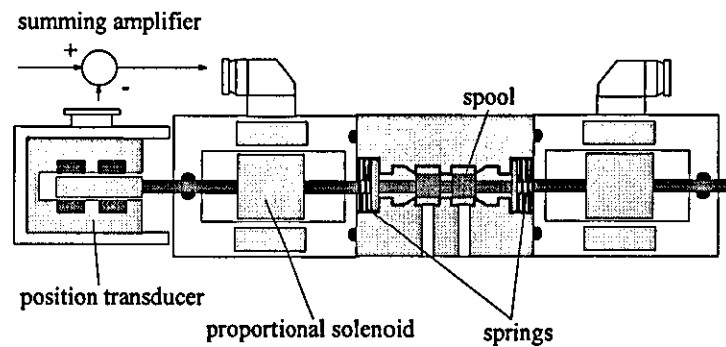Displacement Transducer) . Figure 3.2.1 shows a cross section of a typical proportional solenoid valve.

Figure 3.2.5.1 Proportional solenoid valve

The electronic drivers for proportional valves have improved in design in recent years: For example, the electronics will momentarily overdrive the solenoid to reduce the effects of inductance, and current recirculating techniques quickly remove stored energy from the coils. Both actions increase frequency response (Bolton, 1980), (Moog, 1995). Good electrical feedback of spool position is required to provide solenoid control, and temperature compensation is employed in some valves for the spool position monitoring LVDT to limit null shift effects over a wide range of temperatures. Vibration and shock resistance for proportional valves can exceed that of servo valves, some models now being available which can withstand a 150g shock load (Cullman, 1993).

3.2.6. Hydraulic Ram

Wear of the hydraulic ram poses an interesting problem, since the actuator is required to operate over a great many cycles, over a short stroke of 3 - 4 mm. Seal wear is critical , and high performance seals or double seals must be used in the design (Allan, 1962).

Static friction of the valve spool is usually avoided by applying a high frequency (≈2kHz) dither signal in order to keep the valve spool constantly in motion. Since the cylinder will constantly be in motion, it could be argued that static friction should be less of a problem than for a conventional hydraulic positioning system (Robotics World, 1993). However, static friction may cause problems such as overrunning and pressure spikes when the system is started up, and this was taken into account in the simulation and design of the system.

Asymmetric cylinders are lower in cost than symmetric cylinders (Parr, 1991), (Bosch, (a) 1997), but would require a more sophisticated control system. For example, if a square wave is used to control an asymmetric cylinder, then the mark/space ratio must be very carefully controlled such that more fluid is fed to the side of the cylinder with the largest area, per unit time. Thus displacements for piston advance and retract would be equal (Taylor, 1992). Findings in (Martin, 1970) show that stability and step response of asymmetric cylinder exceeds that of an equal volume system containing the same total volume of oil. Damping is also enhanced.

A short stroke hydraulic actuator has been developed by (Tran, DeBra, 1994) suitable for toolpost actuation, for spindle motion error correction and non circular cutting. The actuator has a throw of 180 μm at 2 MPa. The dynamic response is limited by the hydraulic resonance (around 20 000 rad s^{-1}. The choice of servovalve and feedback design govern the dynamic response. Even then, the actuator proposed, shows rise times of better than 25 ms.

3.2.7. Hydraulic Ram Performance - Fluid Properties

The preferred working fluid in most applications is mineral oil (Watton, 1989), although in certain applications there is a requirement for water-based fluids. Water based fluids and high water based fluids provide fire resistance at a lower cost and have the advantage of relative ease of oil storage and fluid disposal (Bosch, (b), 1997). One possible advantage in this application over mineral oil is reduced fluid compressibility. The main groups of hydraulic fluids are as follows (Viersma, 1980).

1) Dilute emulsions, i.e. oil-in-water emulsions, typically with 95% water content.

2) Invert emulsions, i.e. water-in-oil emulsions, typically with 40% water content.

3) Aqueous glycols, i.e. solutions of glycols and polyglycols in water, typically with 40% water content.

4) Synthetic fluids containing no water, such as silicones and silicone esters.

Bulk modulus is a measure of the compressibility of a fluid and is inevitably required to calculate the undamped natural frequencies in a system. It is perhaps the one fluid parameter that causes most concern in it's numerical evaluation due to other effects which modify it. (Martin, McLoy, 1979), (Martin, 1970), (Bobrow, 1995). At this point, it is appropriate therefore to provide a definition of bulk modulus. The basic definition of fluid bulk modulus arises by considering the compression of a fluid initially at atmospheric pressure and volume V_0 to a new value V at pressure P. Tangent bulk modulus is then defined by one of the following expressions:

Isothermal tangent bulk modulus: $\beta_T = -V\left(\dfrac{\delta P}{\delta V}\right)_T$ 3.2.7.1

Isentropic tangent bulk modulus: $\beta_S = -V\left(\dfrac{\delta P}{\delta V}\right)_S$ 3.2.7.2

where T, s refer to conditions of constant temperature and entropy respectively.

3.3. Piezoelectric Actuators

3.3.1. Background

Piezoelectric materials posses certain properties which make them useful as sensors or control elements. The first is that they strain when an electrical field is applied across them. This property makes them well suited as actuators for control systems (where the control signal is typically an applied voltage). The second is that they produce a voltage under strain. This property makes them well suited as sensors. In general, piezoelectrics have the ability to transform electrical energy to mechanical energy and vice versa.

Multilayer piezoelectric actuators consist of thin sheets of tape cast ceramic. (Park, 1991, Jun et al, 1991) bonded together. (figure 3.2.1). Electrodes are then applied to the sheets which are then stacked and fired. Actuation forces are large - figure 3.2.2 gives force generated vs. displacement for Morgan Matroc piezo-stacks. Displacement versus input voltage, and the hysteresis inherent to piezo actuators may be clearly seen in figure 3.2.3 Referring to figures 3.2.2 and 3.2.3 the plots are represented by codes 7111/03031/030, and 7111/05051/030. These are manufacturers codes used to represent piezoelectric actuators with differing stack heights (Morgan Matroc, (a), 1996).
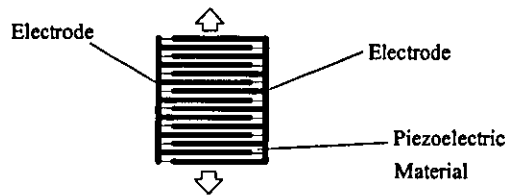
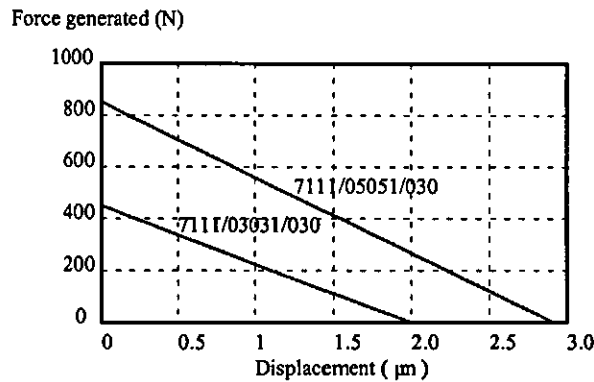

Figure 3.2.1: Piezo stack construction

Figure 3.2.2: Force vs. displacement characteristics for piezoelectric actuator
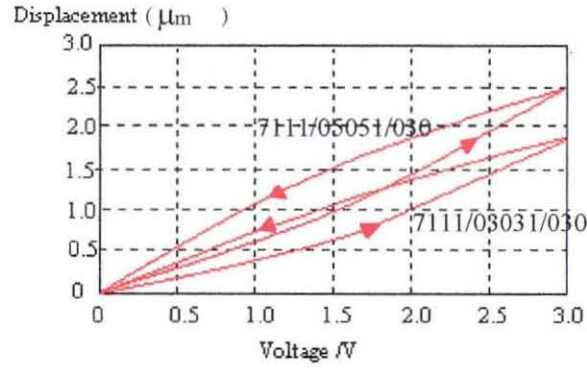
53

Displacement (μm)

Figure 3.2.3: Displacement vs. voltage characteristics for piezoelectric actuator.

Piezoelectric bimorphs are constructed in a similar manner to the bimetallic strips used in thermostats. Displacements available are much larger, but output forces are low, being in the order of around 5N typically for a bimorph of 4mm displacement..

Both multilayer and bimorph piezoelectric actuators are relatively straightforward to drive, indeed, a standard audio amplifier can often be utilised in order to make the actuator perform as required. Several design considerations must be taken into account when considering piezoelectric actuators as a prime mover (Morgan Matroc (a), (b), 1996), principally, the avoidance of delamination. A low speed motor is proposed by (Funakubo et al, 1995) which could provide similar amplitudes to a hydraulic system, but is severly limited in terms of output force.:

3.3.2 Environmental considerations

Several environmental aspects concerning the use of piezoelectric actuators should be taken into account. Handling of piezo actuators should be carried out with care. Piezoelectric actuators are made of ceramic and may be damaged if subjected to sudden physical or thermal shock Either D.C or A.C voltage can be used to drive the actuators, though a bias voltage must be added to an A.C signal in order to prevent reverse polarity voltages exceeding 20v. As voltages up to 150 V (d.c) may be employed, it is necessary to ensure that the actuators do not come into direct contact with moisture. The devices are best attached with an epoxy resin adhesive that cures at temperatures below 75°C. To obtain maximum stiffness and displacement, the bond should be as thin as possible. No shear or tensile stresses must be placed on the actuator, in order to avoid delamination.

3.3.3 Applications

One application of particular interest using bimorphs is suggested by (Ikebe, Nakada, T, 1974) where a piezoelectric bimorph is used as the flapper in a hydraulic servovalve. Such an application offers advantages of improved response to a step input for small displacements, whereas hydraulic torque motors exhibit a better response for a large step input, and the bimorph occupies a smaller space than a torque motor.

Whilst piezoelectric bimorphs can find applications as components of a hydraulic servo system, forces available from such devices are not sufficient for their consideration as a means of modifying the cutting circle in a planing machine. Multilayer actuators offer more potential, offering a far greater actuation force, albeit with a reduced maximum displacement. Frequency response is excellent, and is relatively flat from d.c. to around 10 kHz with no load.

Piezoelectric multilayer actuators are finding applications many areas, including the active and passive control of vibrations within structures (Hagood et al, 1990), whereby a charge generated by a piezoelectric stack fixed between two vibrating or flexing connecting elements is transferred by a cable to another part of the structure, where another piezoelectric stack is positioned so as to absorb vibrations set up within the structure. Although this method has been applied with some success to relatively large structures such as roof supports, it can be seen that correct positioning of piezo elements within a planing machine frame could possibly be used to 'mop up' extraneous low frequency components passing through the machine and consequently improve surface waviness.

Of particular note with respect to rotary timber machining, especially the damping of cutterblock vibration, are two papers which describe the use of piezoelectric actuators to damp tool vibrations in the machining of metals. The cutting process has been improved in turning by using a cutting force feedback system to regulate the position of the turning tool (Dunn 1994), where a multilayer piezoelectric actuator is used to regulate cutting force. A similar application for milling of metals is described by. In both cases the cutting speeds and tool vibration frequencies to be controlled are correspondent with the machining of metals. The high bandwidth of piezoelectric actuators (Jung, Oh, 1991), of around 0.3Hz - 20 kHz should allow the design of a system capable of damping the higher frequencies of vibration associated with timber machining.

Piezoelectric actuators are also finding favour because of their lack of magnetic components, and their small size has led to applications in micro machinery (Smits, 1992) where a piezoelectric bimorph is used as the prime mover. The only major problem with the use of piezoelectric actuators is their relatively small displacement (Uchiki et al, 1991), (Ishida et al, 1992). Whilst actuation forces are high at minimal displacement (figure 3.2.2), it can be seen that available actuation force rapidly tails off towards full extension of the actuator. A stack of devices would offer improved performance (Molianen et al, 1994), but it is uncertain whether the available forces would be great enough to compensate for large amounts of cutterhead imbalance, and performance data and references describing similar applications are still relatively scarce . Modelling of the piezoelectric actuator would provide further insight into it's capabilities, and would need to be developed further (Avellaneda, 1994).

Modelling of piezoelectric actuator dynamics has been carried out by (Sosa, Pourki, 1993), though a more comprehensive model was previously developed by (Hagood et al, 1990). Both models largely concentrate on the electrical properties of the actuators. State space models are derived in both cases for a multilayer actuator in the first instance, and a bimorph - like actuator in the second. since the main areas of interest are hysteresis and the force/stroke relationship, as opposed to how the actuator affects driving circuitry, it would be more useful to create a new model from scratch using manufacturer's data (Morgan Matroc, (a), 1996). The literature reviewed thus far therefore, suggests that piezoelectrics could find limited application in timber machining control, though more information has been found to suggest the suitability of a hydraulic system. Because of the excellent bandwidth of piezoelectrics, and the high power gain offered by hydraulics, it could be necessary to consider a hybrid system.

3.4. Hybrid Piezohydraulic systems

Hydraulic systems using piezoelectric actuators are of particular interest with respect to active vibration control, and whilst widely used in gas turbine construction (Tang, et al, 1994), it can be seen that such a method may be applicable to the balancing of rotating cutterblocks in timber machines. The main argument for a piezohydraulic system is that piezoelectric actuators are not robust enough to mount within an aero engine, where a temperature range of at least -40F to 400F is required. Clearly at these extremes of temperate piezoelectric actuators would de laminate either due to brittling of epoxy resin at the lower temperatures or a severe drop in elastic modulus due to high temperatures. Of interest to this research is the potential for amplifying the available displacement, and the mechanical protection of the piezo stacks from sudden shock loads. It can be seen that the improved bandwidth resulting from the use of piezoelectric actuators could provide the performance necessary should a conventional servovalve driven hydraulic servo prove too slow. Unfortunately, the current useful life of such actuators is short, and they are used in devices rating performance over longevity, mainly by the ESA and NASA for control systems in expendable rockets.

(Tsao, T-C. Tomizuka, M., 1994) Propose a hybrid system whereby a membrane is operated by a piezoelectric stack to move the hydraulic fluid, in theory eliminating problems associated with seal wear exaggerated by the short stroke. (Ulbritch, 1991) conducted research on a similar hydraulic actuator system and demonstrated that this configuration could be prone to accumulate bubbles reducing the effectiveness of the actuator, may fail from high cycle fatigue, and may reduce output stroke due to secondary deformation of the membrane. (Montague et al, 1991) also detected leakage and fatigue problems in their membrane type hydraulic actuator experiments. The main problem with such hybrid actuators is apparently the trade-off between having a thin enough membrane to provide the desired bandwidth and efficiency, yet providing the strength necessary to withstand the large transient forces and hydraulic pressure surges inherent to such applications.

3.5. Control System

3.5.1. Control system design

The literature search produced some interesting material with regard to the control of hydraulic servo systems. Good results for positional control are achieved in (Rabie, 1994), where a pseudo derivative feedback (PDF) controller is utilised. A detailed non-linear mathematical model is developed for the servo, and the coefficients of the transfer function of the model are used to find a first estimate for the parameters of the PDF controller. The reduction in settling time and improvement in bandwidth are notable, though performance of such a system at high frequencies and high gains should still be determined by time domain simulation as opposed to a purely frequency domain based approach. All literature studied acknowledges the difficulty of controlling hydraulic servo systems by conventional methods due to their inherent nonlinearities (Krus et al, 1994) and time variant characteristics, (Hodgson, Raine, 1992), in particular the variability of the hydraulic fluid (Lallement, 1989), (Martin, 1972).

Adaptive controllers similar to that described by (Yun, Cho, 1991) have been used with some success. Improvements in the design of such controllers have taken place (Bobrow, Lum, 1995), where fluid compressibility is monitored with an on - line identification scheme. A four fold improvement in bandwidth is claimed when compared to a conventional fixed gain proportional controller.

Where system plant characteristics are better known, it has been argued that neural network based controllers may offer improved performance (Lee, Wang, Tan, 1994), (Taylor, 1993). In such controllers the inverse of the plant is built into the neural networks, which are then used in the control loop (Simpson, 1990). AI methods are also useful in predicting compliance problems due to varying bulk modulus (Sepehri et al, 1994), and in the overall design and placement of hydraulic servo components, using a knowledge based system. (Sharpe, (a) 1995), (Sharpe, (b), 1995), which takes further the more general work carried out by (Takata, 1993).

It has been argued that a fuzzy logic controller would provide a more rapid solution to the control problem (Zhao, Virvalo, 1993),(Wang, Tan, 1994), because of the slow convergence of the neural networks. A fuzzy controller allows the implementation of "rule of thumb" experiences, intuition and heuristics which do not require a complex

mathematical model of the plant (Wang, Tan, 1994). The characteristics of various transducers are also worth considering, since eventually a commercial prototype machine could be built, and the effect of transducer variances could have a significant effect upon the system controllability. To this end, transducers are researched in the next section.

3.6. Transducers

A transducer is basically defined as a device which produces a signal (e.g. electrical, pneumatic, optical) which is dependent on the physical property it is designed to measure. Response time of the transducers to be used in the system is particularly important, since the high gains involved in conjunction with transducers with a large lag would be a major source of instability.

3.6.1 Transducer types

The primary objective of the literature survey with regard to transducers was to establish which types of transducer would be most suitable for use with the actuation system. Figure 3.7.1 shows the primary design considerations with regard to transducers which emerged from the literature review.
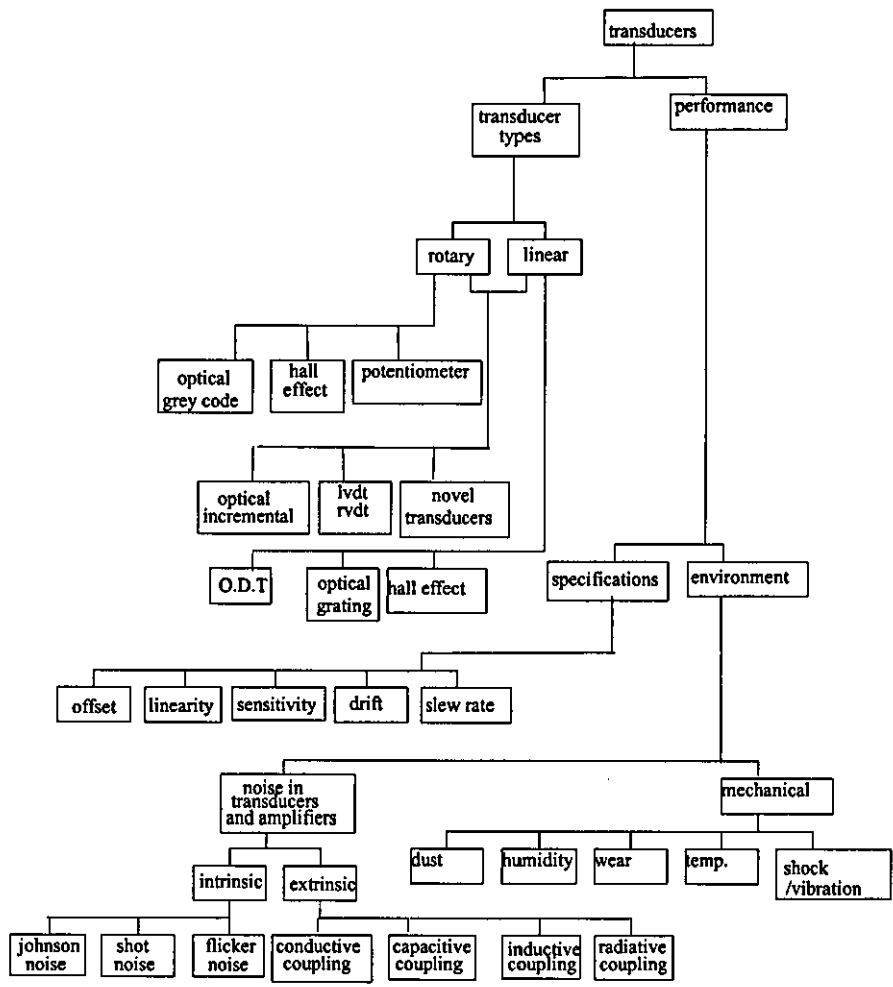
Figure 3.7.1 Transducer considerations

The principal types of transducer which emerged from the survey are as follows:

Rotary	Rotary + Linear	Linear
	optical incremental	Optical Displacement Transducer (O.D.T)
hall effect	LVDT, RVDT	optical grating
potentiometer	novel transducers	hall effect

60

Familiarity is assumed with most of the types of transducer mentioned above, with the possible exception of the O.D.T. The optical displacement transducer measures the gap between the transducer head and a reflective surface. Light is shone on the surface from an optical fibre and the proportion of light reflected into an adjacent fibre is used to measure the gap. This type of transducer requires no contact with the target, is electrically passive, and can have an extremely good frequency response. The simplest technique used to make the transducer insensitive to ambient light is to modulate the light transmitted at a constant high frequency. This needs to be well above the maximum displacement signal frequency. Typically 10 kHz is chosen as this is well below the maximum frequency which op amps can handle. The reflected light signal is therefore also modulated at this frequency whereas (it is assumed) no other components are. A band pass filter (e.g. Butterworth), typically of order 4 - 6 is therefore also used to only select the reflected signal with this frequency and the amplitude of the output of this filter is used to evaluate the gap. Since the output of such transducers is highly non-linear, the relationship between the output signal and the gap is often calibrated and then paremeterised by fitting to an equation using a least squares technique.

Novel transducers have been developed using magneto strictive sensors, primarily for the measurement and control of angular position and rotational speed for the automotive industry. The transducers are able to withstand high shock and vibration, and the presence of foreign matter such as wood shavings or oil. Magnetic sensors generally meet these requirements better than optical devices. Having identified the principal system characteristics through the literature survey, the next step is the design of an actuation system for cutterblock oscillation.

4.0 Servo design

The development of the simulation of the hydraulic servo forms five clearly definable stages.

Firstly, a transfer function based model simulation was undertaken. This was primarily carried out to provide a general check as to the suitability of a hydraulic servo for such high speed operation. Also, the transfer function provided a useful method of testing the simulation software. The transfer function based simulation was of use later in the project for a straightforward method of providing an overall simulation of the hydraulic servo and the action of the cutter upon the timber surface.

An early component level model then followed, modelled using Saber™ software. This simulation provided an insight into the difficulties of modelling a hydraulic servo, particularly when the servo is meant to be run at high frequencies. Although it was not expected that the first component level model should form the final design, it was useful to construct the model at this stage. Problems encountered with simulations appeared to be stemming from some aspect of the hydraulic servo valve and ram models employed by Saber™, though the actual cause was uncertain. The component level method of modelling the hydraulic servo was returned to later in the project, in order to produce a final design.

A low level model of the system was then developed, whereby system variables such as feedback pressure to the servo valve could be monitored and checked after each simulation run. Here the cause of frequent non-runs and simulation problems was identified as a variable changing too rapidly for the simulation algorithm. This variable was the fluid pressure in hydraulic supply lines, which corresponds to shock waves travelling through hydraulic lines in a physical system. The detailed low level model allowed the viewing of system variables which could not be seen before, such as feedback pressure to the hydraulic valve. This made it possible to pin point the cause of error reports which were produced by Saber™ during aborted simulations. The rapid change in hydraulic pressure throughout the simulated system when the servo valve first opened, revealed itself as the cause of the problem. The low level model thus revealed the nature of high pressure transients, or shock waves within the system. Having identified the cause of the problem, a high level model was then returned to, and two methods of filtering out the high pressure shock waves were employed. One was to provide a slight leakage to

63

the supply lines in order to vent excess pressure. The other was to experiment with hydraulic accumulators of varying sizes and charging pressures throughput the circuit. Effectively placed accumulators were found to solve the problem, and simulations thus ran successfully. This method has been used to good effect with servosystems working at lower speeds, primarily to reduce power consumption (Lallement, 1989), and in novel systems to provide a flow / pressure trade-off (Scheidl et al, 1996).

Since the double acting model was now functioning properly, the use of the accumulator raised an interesting point. The accumulator was being used to soak excess surges of energy, which would then be returned to the system, and it was thought that a likelihood might exist of being able to store energy during each cycle of the actuator, such that a single acting ram could be used. An accumulator was tested, and a model of a simple coil spring. Since no cutting occurs on the return stroke, the velocity profile of the cutterblock is irrelevant (Brown, Parkin, 1996), as long as it is correctly positioned in order to begin the next cycle on time. A coil spring provided a simple yet effective solution.

4.1. Hydraulic circuit simulation

4.1.1. Hydraulic servo valve transfer function

A transfer function is often used for the analysis of performance of hydraulic servovalves, particularly when looking the valve 'in context' i.e. the effect of the valve dynamics upon the performance of a larger system. Such a representation is, at best, only an approximation of actual servovalve performance. However, the usefulness of linear transfer functions for approximating servovalve response in analytical work is well established (Viersma, 1980), (Thayler, 1962). The trouble with assuming an explicit transfer function for electrohydraulic servovalves is that many design factors and unpredictable variables (e.g. loss of stiffness in hydraulic fluid due to air ingress) produce significant differences in the actual dynamic response.

Considering the variables of the valve design, It is known that internal valve parameters (e.g., nozzle and orifice sizes, spring rates, spool diameter, spool displacement) may be adjusted to produce large variations in dynamic response, though once a servovalve is built, the actual dynamic response will vary somewhat with operating conditions such as

64

supply pressure, input signal level, hydraulic fluid temperature, ambient temperature, valve loading, and so forth. These effects are insignificant for small variations about design values, but should be considered where wide excursions are anticipated. It is important to appreciate and control these and other operational variables when performing measurements of servovalve dynamics. If such precautions are not taken, misleading and inaccurate results may be obtained (Thayler, 1962).

Another difficulty in assigning simplified, linear transfer functions to represent servovalve response is that these valves are highly complex devices that exhibit high-order, nonlinear responses. If a first, second, or even third-order transfer function is selected to represent servovalve dynamics, an approximation to actual response is still only possible. Fortunately, for cutterblock oscillation, the servovalve is not the primary dynamic element, so it is only necessary to represent valve response throughout a relatively low frequency spectrum. These approximations to servovalve response have resulted in such expressions as "the equivalent time constant of the servovalve is x seconds" or "the apparent natural frequency of the servovalve is x radians/second."

If a representation of servovalve response throughout the frequency range to about 315 rad.s^{-1} is sufficient, then a first-order expression is usually adequate. Figure 4.1.1.1 shows a typical valve dynamic response, together with the response of a first-order transfer function shown in equation 4.1.1.1. Referring to equation 4.1.1.2, in this case τ is obtained from manufacturers experimental data (Thayler 1962), the same bulletin being the source for equations 4.1.1.1 and 4.1.1.2.

$$\frac{Q}{i}(s) = \frac{k}{1 + \tau s} \qquad\qquad 4.1.1.1$$

where:

$$\tau = \frac{1}{2\pi.120} = 0.0013 \text{ sec} \qquad\qquad 4.1.1.2$$

The first-order approximation is seen to be quite good throughout the lower frequency region. The time constant for the first-order transfer function (i.e., the equivalent servovalve time constant) is best established by curve fitting techniques. Phase lag representation above 40 rad/sec can be seen to be trailing away from the actual valve

65

response as the higher order dynamic effects contribute low frequency phase lag in the servovalve response, while not detracting appreciably from the amplitude ratio.
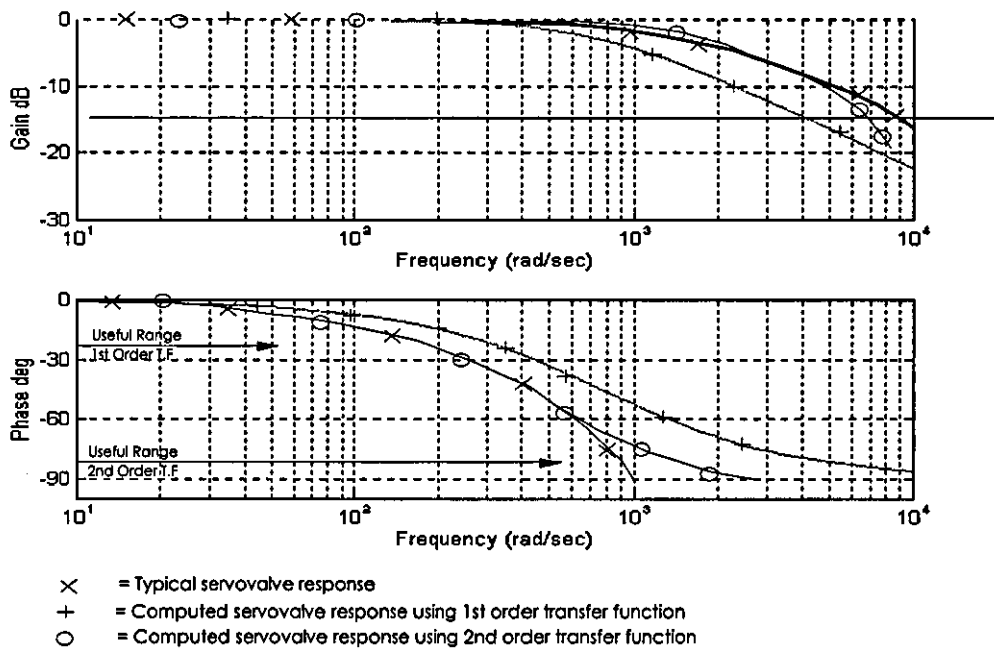

X   = Typical servovalve response
+   = Computed servovalve response using 1st order transfer function
O   = Computed servovalve response using 2nd order transfer function

Figure 4.1.1.1 Actual and computed frequency response for Moog 'D' Series Servovalve

If servovalve response to frequencies up to 90, phase lag point is of interest, then a second-order response should be used. (Thayler, 1965) In a positional servomechanism, a second-order representation of the servovalve response is usually sufficient, as the actuator contributes an additional 90, phase lag from the inherent integration. Figure 4.1.1.1 also shows a second-order approximation to the servovalve dynamics:

$$\frac{Q}{i}(s) = \frac{k}{\left(\dfrac{s}{\omega_v}\right)^2 + \left(\dfrac{2\zeta}{\omega_v}\right)s + 1}$$
                    4.1.1.3

where:

$\omega_v = 2\pi.185 = 1160 \; rad/sec$

$\zeta = 0.7$

66

Here, the natural frequency is best associated with the 90° phase point, and the damping ratio with the amplitude characteristic. Other factors will often weigh more heavily in the choice of an approximate natural frequency and damping ratio. For example, it may be desirable to approximate the low frequency phase characteristic accurately and, to do so, a second order transfer fiction which does not correlate with the 90, phase point may be used. A good deal of judgement must, therefore, be exercised to select the most appropriate transfer function approximation (Viersma, 1980) .

4.1.2. Servovalve Transfer Functions

Whilst most manufacturers publish only frequency response curves for servovalves, appropriate transfer functions for standard Moog servovalves have been published, although a limited number of transfer functions for other makes of servovalve can be found in standard texts (Viersma, 1980). In all cases it must be borne in mind that these expressions are linear, empirical relationships which approximate the response of actual servovalves when operating without saturation. The time constants, natural frequencies, and damping ratios cited are representative. However, it is rightly stressed in the manufacturers literature that the response of individual servovalve designs may vary quite widely from those listed (Moog (a), 1995), (Moog (c), 1995). Nevertheless, these representations are very useful for analytical studies and can reasonably form the basis for detailed system design.

4.1.3. Flow Control Servovalves

This basic servovalve is one in which the control flow at constant load is proportional to the electrical input current. Flow from these servovalves will be influenced in varying degrees by changing load pressures. For null stability considerations, it is argued that only the region of this plot about the origin need be considered (Thayler, 1966). Here, the influence of the load on flow gain of the servovalve can be considered negligible.

In order to improve the accuracy of the model, a lookup table based system of representing spool dynamics has been developed in C code, in ANSI standard C (a good example of ANSI standard C programming may be found in Harrison, 1995), and graphical iteration methods which are a further development of the one dimensional iterative methods described by (Stroud, 1987). Another linearity assumption which is often made is that servovalve flow gain is constant through null (Burrows et al, 1991).

67

This is theoretically true for an ideal "zero lap" null cut of the valve spool; however, the actual lap condition will vary with production tolerances. If the spool becomes overlapped, the servovalve flow gain is reduced at null. Likewise, an underlap produces higher-than-normal servovalve gain. Normal production tolerances maintained at Moog hold the spool lap within ! 0.0001 inch for all four null edges (Moog, (b) , 1995). This close control gives a very small range of possible nonlinear flow control through null (about ± 3% for an "axis" null cut); but within this range, flow gain may be from 50% to 200% of nominal. The change in servovalve flow gain at null may sometimes cause system instability; or, in other cases, poor positioning accuracy, or poor dynamic response of the actuator at low-amplitude input signals. This situation can be varied one way or the other by holding a nominal overlap or underlap, as appropriate.

The dynamic response of most flow control servovalves can be approximated in the frequency range to about 50 Hz by the first order expression shown in equation 4.1.1.1. For simulation of servovalves up to around 250 Hz, a second order approximation should provide adequate performance. For frequencies in excess of 250 Hz, higher order approximations may prove necessary.

4.1.4. Development of ram - slideway transfer function

In order to derive the ram - slideway transfer function, a single acting hydraulic ram is considered as shown in figure 4.1.4.1 . The piston cross sectional area is taken as A, the input fluid flow to the ram is given by q(t), p(t) is the fluid pressure and the ram position is given by x(t).
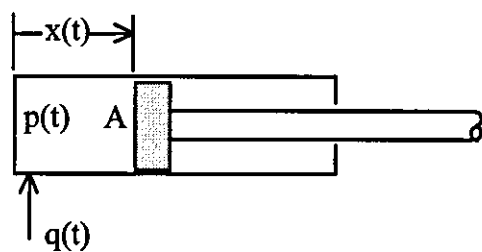

Figure 4.1.4.1: Hydraulic ram

In order to provide a comprehensive model, it is necessary to consider the mass moved, (i.e. ram, slideway and cutterblock), any leakage which may exist between ram and cylinder wall, effects of viscous friction, and the compressibility of the fluid, i.e. the fluid bulk modulus.

The governing equation for a simple ram is given by:

$$Q(t) = A\frac{dx(t)}{dt} \qquad 4.1.4.1$$

Taking into account leakage, where a leakage flow of $k_{LE}p(t)$ exists, the flow continuity equation then becomes:

$$A\frac{dx(t)}{dt} + k_{LE}p(t) \qquad 4.1.4.2$$

Calculation of $p(t)$ due to inertia is achievable through applying Newton's Second Law, i.e. *Force = Mass x Acceleration.*

$$p(t)A = M\frac{d^2x(t)}{dt^2} \qquad 4.1.4.3$$

The ram is subject to a viscous load, whereby the coefficient of viscous friction μ affects the force available from the ram. The pressure $p_f(t)$ required to overcome this frictional loss is therefore:

$$p_f(t) = \mu\frac{dx(t)}{dt} \qquad 4.1.4.4$$

It is then necessary to consider the effects of fluid compressibility. Bulk modulus may be defined as change in fluid pressure divided by change in volume per unit volume (Various, 1968), i.e.

$$k_B = \frac{\Delta p}{\Delta V/V} \qquad 4.1.4.5$$

$$\therefore \frac{dv}{dt} = \frac{V}{k_B}\frac{dp}{dt} \qquad 4.1.4.6$$

69

The complete flow continuity equation is therefore:

$$q_{in} = q_{vel} + q_{leakage} + q_{compressibility} \qquad 4.1.4.7$$

$$\therefore Q(t) = A\frac{dx(t)}{dt} + k_{LE}\,p(t) + \left(\frac{V}{k_B}\cdot\frac{dp(t)}{dt}\right) \qquad 4.1.4.8$$

Viscous friction and inertia are used to calculate the pressure required to move the ram:

$$p(t)A - \mu\frac{dx(t)}{dt} = M\frac{d^2x(t)}{dt^2} \qquad 4.1.4.9$$

$$\therefore Q(t) = A\frac{dx(t)}{dt} + k_{LE}\left(\frac{M}{A}\frac{d^2x(t)}{dt^2} + \frac{\mu}{A}\frac{dx(t)}{dt}\right) + \frac{V}{k_B}\left(\frac{M}{A}\frac{d^3x(t)}{dt^3} + \frac{\mu}{A}\frac{d^2x(t)}{dt^2}\right) \qquad 4.1.4.10$$

$$\therefore Q(t) = \frac{VM}{k_B A}\frac{d^3x(t)}{dt^3} + \left(\frac{k_{LE}M}{A} + \frac{\mu V}{k_B A}\right)\frac{d^2x(t)}{dt^2} + \left(\frac{k_{LE}\mu}{A} + A\right)\frac{dx(t)}{dt} \qquad 4.1.4.11$$

Taking Laplace transforms for zero initial conditions gives the ram - slideway transfer function:

$$\frac{x(s)}{Q(s)} = \frac{1}{\dfrac{MV}{k_B A}s^3 + \left(\dfrac{k_{LE}M}{A} + \dfrac{\mu V}{k_B A}\right)s^2 + \left(\dfrac{k_{LE}\mu}{A} + A\right)s} \qquad 4.1.4.12$$

4.2 Early component level model

Initial experiments indicated that the early transfer function based model could form a sound basis of a hydraulic servo simulation, and so it was decided that a component level model could be constructed, using the Saber™ standard template library, in order to attempt to simulate the hydraulic servo. This was seen as a straightforward way to model the friction in the system, which is nonlinear due to static friction. Also the ram size required could be determined, and various values of fluid bulk modulus could be tested, to simulate the effects of temperature, and the reduction in bulk modulus which would occur due to air ingress as the ram cycles. The diagram in figure 4.2.1 shows the early component level servo model.
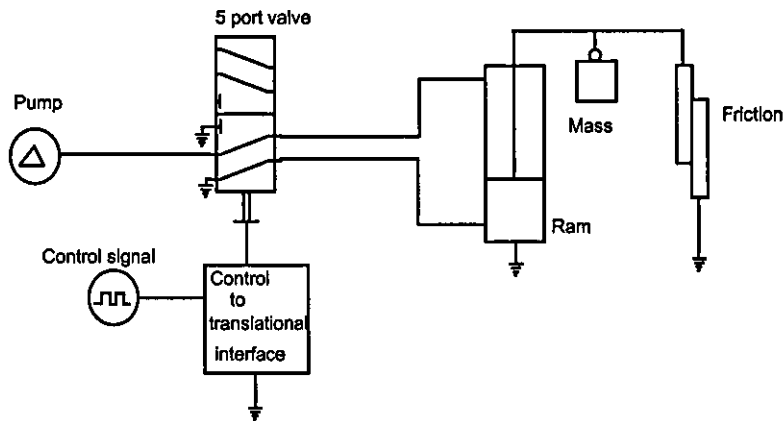
Figure 4.2.1 Early component level model

The simulation was found to be unstable, with typically only 0.05s of transient analysis being produced before the simulation algorithm would halt. It was found that by reducing the mass to zero and the friction to a bare minimum, i.e. $\mu_1 = 0.01$, the simulation could be made to work. Of course in a real system this would prove impossible, but the results produced thus far were useful since it suggested that the simulation fault could be due to a problem with fluid pressure. In order to ascertain exactly the cause of the simulation crashes, it was necessary to construct a lower level model of the hydraulic servo. Thus individual parts of the system could be examined in more detail and the fault could be found and corrected.

71

4.3. Development of detailed mathematical model of hydraulic servo

The detailed mathematical model is based upon an asymmetric double acting hydraulic cylinder, as would be found in a conventional servo system. Transient pressure surges, and the differing flow rates between one side of the cylinder and the other, should all be visible during a simulation of this model.

Through and across variables are used in many simulation packages such that two related variables are able to be transmitted along the same track, or wire. This offers a different environment to a simple block diagram based model where only one variable is passed between blocks. The upshot is that high level systems may be modelled very rapidly using through and across variables. Typical pairs of through and across variables may be listed as follows in order to explain the concept:

Variable for transfer	Through variable	Across variable
Electrical	Current (A)	Voltage (V)
Thermal	Heat energy (J)	Temperature (°k)
Mechanical (linear)	Displacement (m)	Force (N)
Mechanical (rotary)	Angle (rad)	Torque (N.m)
Hydraulic	Flow (m^3)	Pressure $(N.m^{-2})$

The simulation algorithms within Saber™ have proven more stable when dealing with a simple block diagram model, with no through and across variables, since variables such as, for example, flow and pressure may be separated and thus plotted at the end of each simulation run. When through and across variables are combined, one of the variables is masked, preventing examination.

The definition for load is normally considered as:

$$P_l = P_1 - P_2 \qquad\qquad\qquad 4.3.1$$

and where no external leakage occurs then load flow is given by:

$$Q_g = Q_1 (= Q_2)$$ 4.3.2

Although these expressions can be used for symmetric hydraulic cylinders, they cannot be applied conveniently to assymetric cylinders. This is, of course, because of the limiting effect of the cylinder rod upon one side of the hydraulic ram surface area. Considering the assymetric hydraulic ram shown in figure 4.3.1:
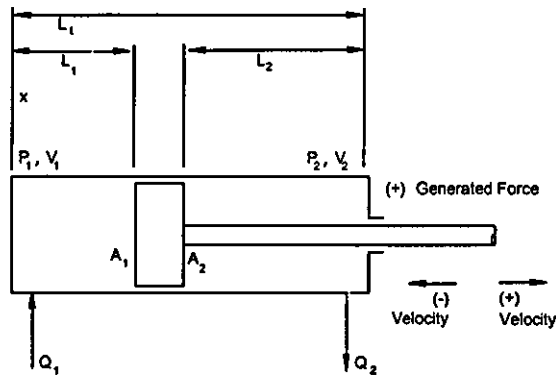

Figure 4.3.1 Assymetric hydraulic cylinder

A secondary flow now exists for the double acting cylinder, such that Q_1 and Q_2 can be thought of as having three components; a displacement flow, a compressibility flow and a leakage flow.

$$Q_1 = Q_{d1} + Q_{c1} + Q_{L1}$$ 4.3.3 $$Q_2 = Q_{d2} + Q_{c2} + Q_{L2}$$ 4.3.4

where

$$Q_{d1} = Velocity \times A_1$$ 4.3.5 $$Q_{d2} = Velocity \times A_2$$ 4.3.6

and

$$Q_{c1} = \frac{sP_1.V_1}{k_B}$$ 4.3.7 $$Q_{c2} = \frac{sP_2.V_2}{k_B}$$ 4.3.8

The leakage component here is equal on both sides of the cylinder, assuming the rod seal has no leakage. Therefore the leakage flow may now be referred to as Q_L where:

$$Q_L = Q_{L1} = Q_{L2} \qquad\qquad 4.3.9$$

The applications of generalised definitions of load flow Q_g and load pressure P_g must satisfy the following constraints:

Power = (effective load pressure) × (effective load flow)
$$= \text{(force)} \times \text{(velocity)} \qquad\qquad 4.3.10$$

Force = (effective load pressure) × (effective area) $\qquad\qquad$ 4.3.11

Velocity = (effective load flow) ÷ (effective area) $\qquad\qquad$ 4.3.12

Effective load flow = (effective displacement flow) + (effective compressibility flow)
$$+ \text{(effective leakage flow)} \qquad\qquad 4.3.13$$

By proposing the following definitions it can be seen that all constraints are satisfied bar that for effective load flow.

$$P_g = \frac{P_1 A_1 - P_2 A_2}{\sqrt{(A_1 A_2)}} \qquad 4.3.14 \qquad\qquad Q_g = (signQ_1)\sqrt{Q_1 Q_2} \qquad 4.3.15$$

$$A_e = \sqrt{(A_1 A_2)} \qquad 4.3.16 \qquad\qquad Q_{DE} = (sign\ Q_{d1})\sqrt{Q_{d1} Q_{d2}} \qquad 4.3.17$$

$$Q_{cf} = (sign\ Q_{c1})\sqrt{Q_{c1} Q_{c2}} \qquad 4.3.18 \qquad\qquad Q_{LKE} = (sign\ Q_{L1})\sqrt{Q_{L1} Q_{L2}} \qquad 4.3.19$$

Using the Q_g definition above we get:

$$Q_g = \sqrt{(Q_{d1} + Q_{c1} + Q_L)(Q_{d2} + Q_{c2} + Q_L)} \qquad\qquad 4.3.20$$

It can be shown that only 4.3.13 and 4.3.20 equate if $Q_{d1} = Q_{d2}$ and $Q_{c1} = Q_{c2}$. It must be borne in mind that for an assymetric cylinder, $Q_{d1} \neq Q_{d2}$ at all times. A different set of definitions as follows overcomes this.

$$P_{LE} \triangleq \frac{P_1 A_1 - P_2 A_2}{A_e} \qquad 4.3.21$$

$$Q_g \triangleq \frac{Q_1 + Q_2}{2} \qquad 4.3.22$$

$$A_e \triangleq \frac{A_1 + A_2}{2} \qquad 4.3.23$$

$$Q_{DE} \triangleq \frac{Q_{d1} + Q_{d2}}{2} \qquad 4.3.24$$

$$Q_{ce} \triangleq \frac{Q_{c1} + Q_{c2}}{2} \qquad 4.3.25$$

$$Q_{LKE} \triangleq \frac{Q_{L1} + Q_{L2}}{2} \qquad 4.3.26$$

Consequently constraints 4.3.11 and 4.3.12 can now be seen to apply.

$$\text{Force} = P_g . A_e = P_1 A_1 - P_2 A_2 \qquad 4.3.27$$

$$\text{Velocity} = \frac{Q_g}{A_e} = \frac{Q_1 + Q_2}{2} . \frac{2}{A_1 + A_2} = \frac{Q_2\left(\frac{A_1}{A_2} + 1\right)}{A_1 + A_2} = \frac{Q_2}{A_2} \qquad 4.3.28$$

$$\text{Power} = P_g . Q_g = \left(\frac{P_1 A_1 - P_2 A_2}{A_e}\right) . Q_g \qquad 4.3.29$$

In addition, constraint 4.3.13 applies for all values of Q_{c1}, Q_{c2}, Q_{d1} and Q_{d2}:

$$\frac{Q_1 + Q_2}{2} = \frac{Q_{d1} + Q_{d2}}{2} + \frac{Q_{c1} + Q_{c2}}{2} + Q_L \qquad 4.3.30$$

Since a hypothetical design is considered, leakage is of secondary interest at present. The effective leakage coefficient K_g is determined using a leakage coefficient based upon manufacturers' data and previous experimentation (Viersma, 1980), (Martin, 1979).

A simpler definition of the total trapped oil volume can be used, for the purposes of simulation, since ram position feedback can be used to determine the trapped oil volume as part of a block diagram based simulation using Saber™ software. The complete derivation for total trapped oil volume is useful for determining compressibility flow, and is discussed later in this chapter.

The effective trapped oil volume V_t can be described as:

$$V_t = (A_1 L_1 - A_2 L_2) - (L_t A_1 - (L_1 + L_2)A_1)$$

<div align="right">4.3.31</div>

V_g can be defined as the ram volume not counting the cylinder rod, which detracts from the total empty cylinder volume. This is calculated before the simulation commences, as is such that equation 4.3.31 may be re written as:

$$V_t = (A_1 L_1 - A_2 (L_e - L_1)) - V_g$$

<div align="right">4.3.32</div>

where: l_e is the effective length of the trapped oil volume, i.e. $L_e = L_t - (L_1 + L_2)$

Recalling that the load flow consists of displacement, leakage and compressibility flows thus:

$$Q_{LE} = Q_{ce} + Q_{DE} + Q_L$$

<div align="right">4.3.33</div>

$$\therefore \delta Q_{LE} = \delta Q_{ce} + \delta Q_{DE} + \delta Q_L$$

<div align="right">4.3.34</div>

$$Q_{DE} = A_E + sx$$

<div align="right">4.3.35</div>

$$\therefore \delta Q_{DE} = A_E + s\delta x$$

<div align="right">4.3.36</div>

$$Q_L = K_L (P_1 - P_2)$$

<div align="right">4.3.37</div>

$$\therefore \delta Q_L = K_L (\delta P_1 - \delta P_2)$$

<div align="right">4.3.38</div>

compressibility:

$$\delta Q_{C1} = \frac{sV_1 \delta P_1}{k_B}$$

<div align="right">4.3.39</div>

$$\delta Q_{C2} = \frac{-sV_2 \delta P_2}{k_B}$$

<div align="right">4.3.40</div>

Assuming linear valve spool dynamics and negligible cross port leakage, a linearised relationship between input ram pressure and output ram pressure is possible, as suggested by (Leaney 1986). Since valve spool dynamics may be included elsewhere in the model, e.g. in the form of a look up table, the simplified relationship becomes:

$$\delta P_1 = -\left(\frac{A_1}{A_2}\right)^2 \delta P_2 \qquad\qquad 4.3.41$$

Equation 4.3.40 becomes:

$$\delta Q_{C2} = \frac{sV_2}{k_B}\cdot\left(\frac{A_1}{A_2}\right)^2 \delta P_1 \qquad\qquad 4.3.42$$

Recalling equation 4.3.28, δQ_{ce} may be alternatively defined by substituting equation 4.3.32 :

$$\delta Q_{ce} = \frac{s\delta P_1}{2k_B}\left(V_1 + \left(\frac{A_2}{A_1}\right)^2 V_2\right) \qquad\qquad 4.3.43$$

Considering the generalised definition of load pressure , 4.3.21, it can be seen that:

$$\delta P_{LE} = \frac{\left(\delta P_1 A_1 - \delta P_2 A_2\right)}{A_E} \qquad\qquad 4.3.44$$

Which in conjunction with equation 4.3.41 becomes:

$$\delta P_1 = \frac{A_E}{A_1}\left(\frac{1}{1+\left(A_2/A_1\right)^3}\right)\delta P_{LE} \qquad\qquad 4.3.45$$

$$\delta P_2 = \frac{-A_E}{A_2}\left(\frac{1}{1+\left(A_1/A_2\right)^3}\right)\delta P_{LE} \qquad\qquad 4.3.46$$

77

so that 4.58 may be re written thus:

$$\delta Q_{LE} = \frac{s\delta P_1}{2k_B} \cdot \frac{-A_E}{A_2} \left(\frac{1}{1 + \left(A_1 / A_2 \right)^3} \right) \cdot \left(V_1 + \left(\frac{A_2}{A_1} \right)^2 V_2 \right)$$ 　　　4.3.47

which simplifies to: $\partial Q_{ce} = \dfrac{s\partial P_{LE} \cdot V_t}{4k_B}$ 　　　4.3.48

Recalling 4.3.48, bulk modulus may be considered constant, and V_{TE} is constant for any given cylinder position, so:

$$P_{LE} = \frac{4k_B}{sV_t} \cdot Q_{ce}$$ 　　　4.3.49

The net volume flowrate, or compressibility flow, is given by :

compressibility flow = valve flow demand - ram flow feedback - leakage flow

$$Q_{ce} = Q_{LE} - Q_{DE} - Q_{KE}$$ 　　　4.3.50

and $Q_{DE} = A_E + sx$ 　　　4.3.51

The force exerted on the actuated mass by the cylinder is of course, pressure x area:

$$F = P_{LE} \cdot A_E$$ 　　　4.3.52

The penultimate model for the asymmetric cylinder with load is shown in figure 4.3.2. A simpler model could be made ignoring pressure feedback (Viersma, 1980) - however such a model would bear little resemblance to the real-life system. The large transients caused by rapid changes in flow would not be represented, and the simulated power gain of the servoactuator system would be misleading. The inclusion of velocity and pressure dependent friction and actuated mass produces the following block diagram model of the system:

78
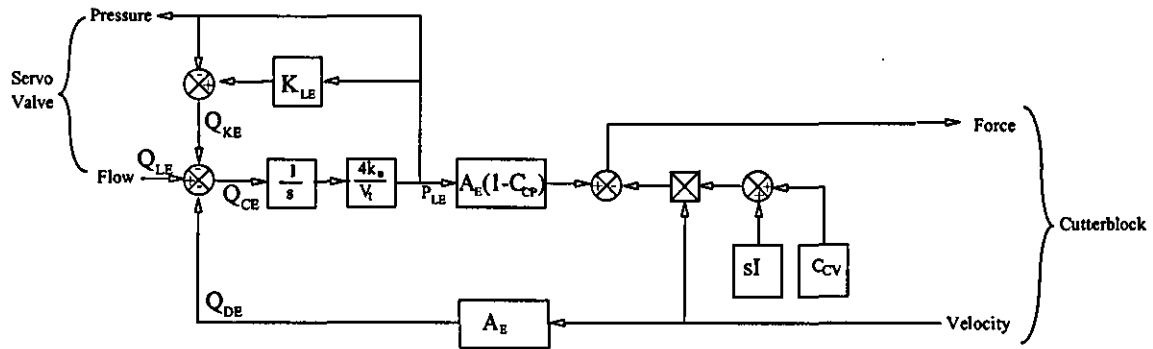
Figure 4.3.2 Low level hydraulic servo model

Oil column stiffness is at a minimum when $L_1 = L_2$ (Martin, 1970). Many previous models have assumed a "worst case scenario" (Burrows et al, 1990), (Leaney, 1986), whereby $L_1 = L_2$. Consequently a ram-valve combination may be dismissed which could fit performance criteria in the final design. Ram position has therefore been used in the model to modify oil column stiffness accordingly:
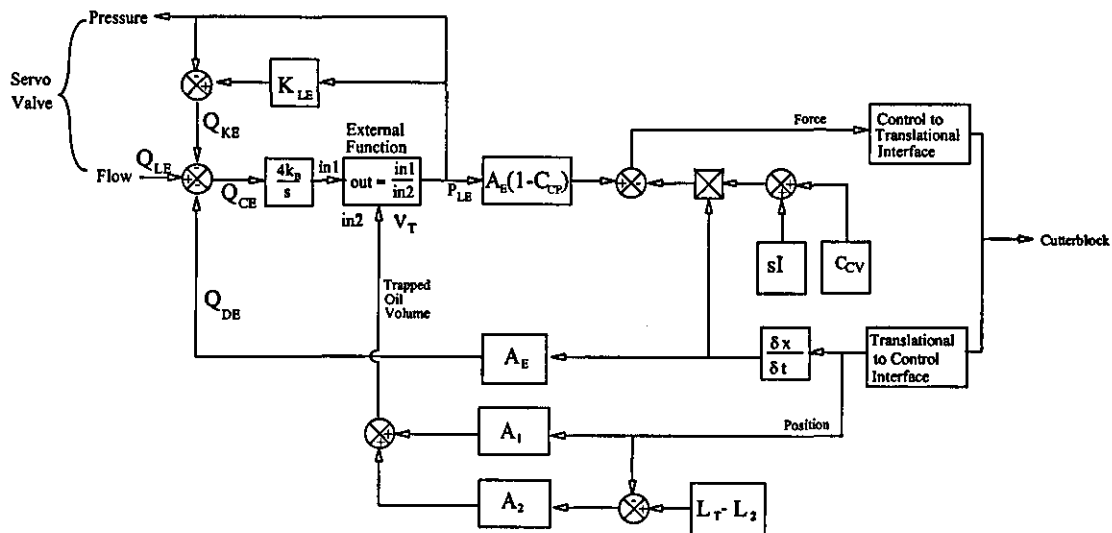
Figure 4.3.3 Low level model with oil column stiffness

The cause of algorithm instability was found to be high pressure transients in the hydraulic supply lines, which are present when the system power up. The time required for these transients to settle is small, in the order of 4 - 5 mS for a servo oscillating at 100hz, and pressures are no more than 40% greater than peak running pressures. What does cause a problem however, is the rate of change of hydraulic fluid pressure. The graph shown in figure 4.3.4 shows a typical output response for the hydraulic servo model described in this section, running at 100Hz.

79
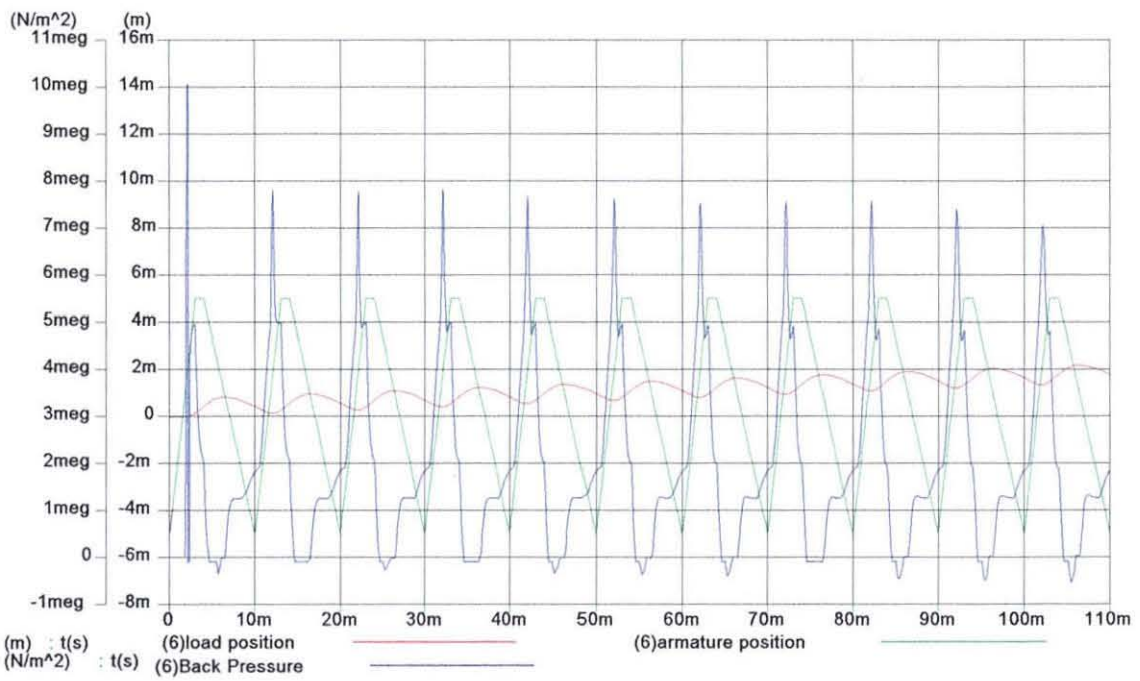
Figure 4.3.4 Saber™ simulation of transient response of low level model with oil column stiffness

4.4 Higher level model of the hydraulic servo

Early simulations carried out in Saber™ would frequently produce erratic results, and it was necessary therefore to re check the simulation in greater detail. When this part of the research began it was not apparent if these erratic results were the fault of the model, or of the simulation code itself. The Saber™ simulator will abort when algorithm oscillation is detected, which is useful for simple models. However, when a simulation has been carried out with algorithm oscillation, it is relatively straightforward to detect the presence of such oscillation. The low level simulations described in section 4.3 showed that high pressure transients present in the hydraulic supply lines were the cause of these results. Since hydraulic servos are generally not made to operate at speeds of around 200Hz continuously, manufacturers data concerning such operation is scarce. Three courses of action were seen to be necessary:

1) To reduce the effect of these transients by building in accumulators within the system.

2) To produce a more accurate model of the valve spool than had been used in previous research (Viersima, 1980), (Leaney, 1986) in order to produce a high level simulation which would be an accurate representation of the servo, enabling the selection of component level model parts to produce a workable design.

3) To provide a complete model of the timber surface simulation, in conjunction with a hydraulic servo model to produce an oscillation waveform.

Simulink, does not warn the user of algorithm oscillation, which is not always clearly visible on the resultant output wave forms from a transient simulation . In order to avoid algorithm oscillation, the size of the integration step should be chosen carefully. The basic Euler method suggests that the integration step size should be around 60 times the bandwidth. This figure was found to work well for the Euler algorithm within Saber™. Simulink however uses a more basic algorithm, which whilst executing more quickly, requires greater care in setting up. A step size of minimum 100 times the bandwidth was found to work well.

Simulation results from the Matlab based hydraulic servo model are discussed in full in section 8. The next logical step was to simulate a hypothetical servo design based on standard components. Component models are called templates. An extensive template

81

library already exists for modelling mixed technology systems, though custom templates have been written in order to describe extra components. Templates are written in Mast - the Saber™ modelling language. Functions describing complex component behaviour have been developed in C, which are then interfaced with Saber™ as foreign subroutines (Analogy Inc., 1995), (Figure 4.4.1). Short routines for this project were written in MAST, and longer code is developed on PC's running DOS in ANSI standard C. This code is then fully compatible with the sun OS5.1 compiler used on the Sun Sparcstation running Saber™. The C code is developed as standalone functions, offering independent testing to the simulation platform, allowing greater ease of error checking through a simplification of the overall data flow (Brown, 1994).

```
                    ┌─────────┐
        - - - - - - │ DSSYM   │      Create Template Symbol
       ¦            └─────────┘
       ¦
       v
  ┌─────────┐      ┌─────────┐
  │ Symbol  │──┐   │ DStar   │      Graphical System Design
  └─────────┘  └─► └─────────┘
  ┌─────────┐      ┌─────────┐
  │ MAST    │──┐   │ Netlister│     Connect components
  │ Code    │  │   └─────────┘
  └─────────┘  │
       ¦       │
       ¦       │
  ┌─────────┐  │   ┌─────────┐
  │ External│──┘──►│ Saber   │      Simulation
  │ Code    │      └─────────┘
  └─────────┘      ┌─────────┐
                   │ PLTool  │      View Results
                   └─────────┘
```
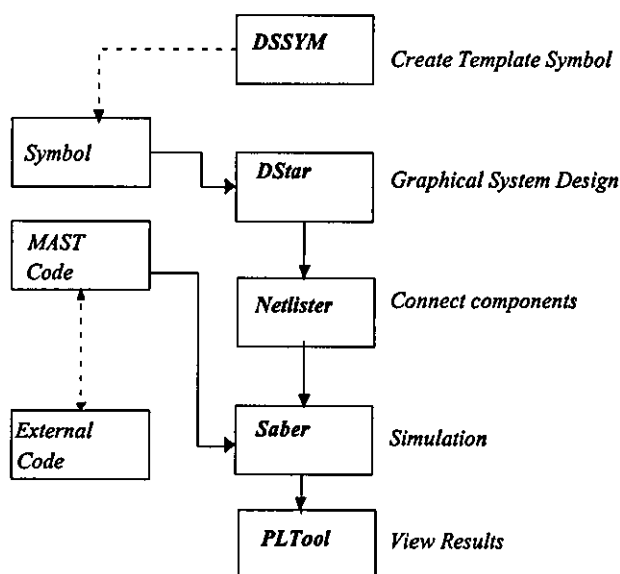
Figure 4.4.1: Simulation process using Saber™

4.4.1 Valve Spool Lookup Table

Previous servo valve simulations (Leaney, 1986) relied upon a best straight line to represent the relationship between output flow, pressure feedback, and valve spool displacement. Early simulations by these authors ignored pressure feedback altogether. Whilst this approach could be deemed entirely appropriate if transient response of the servo is the primary consideration and internal pressure transients and system power consumption are not, the simulation developed as part of this research needed to show more clearly what was happening within the hydraulic servo, particularly with regard to pressure transients.

Consider a three dimensional mesh as shown in figure 4.4.1.1, which represents the behaviour of a hydraulic servo valve spool. Axes represent flow(Q), pressure feedback (P), and displacement (X). In order to rapidly model these characteristics, the use of a lookup table was the most effective method since manufacturer's data could be entered directly into the C code used for modelling this part of the system.
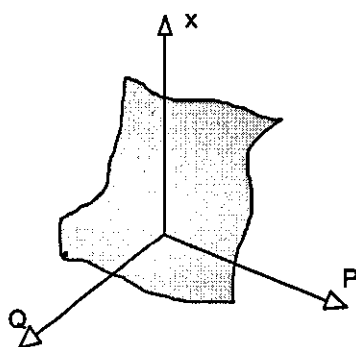
Figure 4.4.1.1 Servo valve variables

A two point interpolation is used primarily for reasons of speed of simulation execution. It was found that taking a three dimensional curve fit of manufacturers data, whilst taking almost 4 times as long to perform as entering manufacturers data into a lookup table, and using the resultant polynomials in a simulation proved unwieldy as a simulation tool. Implementation in C of a lookup table based system proved more computationally effective. Some changes needed to be made to the basic lookup table concept however, in order to provide a smoother output curve from this routine. To explain this point further, it must be stated that any lookup table used will suffer from quantisation, whereby the output flow value will not be smooth, rounding to the nearest point. Whilst the

83

simulation is being used to simulate the oscillation of the ram, quantisation has no noticeable effect on the output waveform of the ram, the quantisation is visible as steps in the output flow from the simulated valve. It was decided that since one of the primary simulation concerns was the behaviour of the hydraulic fluid as a mass spring damper system, producing unforeseen pressure transients, for a more effective simulation the quantisation should be reduced as far as possible, in order to reduce the effect of unknown variables (i.e. the possible effect of quantisation upon pressure transients).

The solution is to interpolate between lookup table points, which effectively removes the jarring effect on the overall hydraulic simulation of sudden small changes in output flow from the servo valve simulation. In addition, the process was found to execute effectively within Saber™, as a foreign function written in C. The pseudo code used to develop the lookup table based spool simulation is as follows:

1. Get absolute spool position
2. Get absolute back pressure
3. Quantise floor (position) to find nearest lookup table point for X
4. Quantise floor (pressure) to find nearest lookup table point for P
5. Iterate between pressure point taken, and the preceding point, find out how far along this line the absolute pressure imported from the Saber™ simulation falls. This becomes ΔP (actual) - Integer P (integer), the two values added together correspond to the input pressure. (Back pressure to the servo valve).
6. Iterate between spool command point taken, and the preceding point, find out how far along this line the absolute spool command position imported from the Saber™ simulation falls. This becomes ΔX (actual) - Integer X (integer), the two values added together correspond to the input spool displacement.
7. Take the equation of a straight line (y = mx +c) along the lines ΔX and ΔP, to find the vector Q, representing output flow.

Pressure and displacement points are evenly spaced, the points corresponding to A and B representing one standard unit in displacement, and A and D representing one standard unit in pressure.
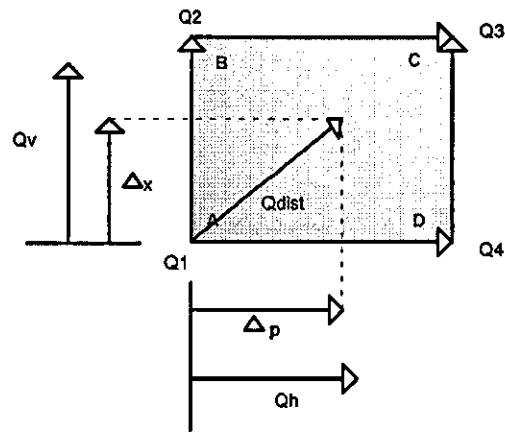
Figure 4.4.1.2. Lookup table elements.

Since the slope of the lookup table is such that Q will increase from A to B, B to C, and A to D and D to C, the vector Qdist is resolved horizontally and vertically from the corresponding vectors Δp and Δx. This is then checked against the flow differences Qv and Qh This gives a point represented by the vector Qdist in the area ABCD (figure 4.4.2), where A, B C and D represent table entries, with corresponding flow values assigned to these table entries, Q1,2,3,4 respectively. The output flow Q, is thus computed with simple geometry.

4.4.2 Valve Controller

Unlike Matlab and Simulink, the Saber™ waveform generators may not have their parameters altered during run time. Discrete component parameters may be varied however, such that when a large number of simulations are carried out, a way can be found to alter the driving frequency of the hydraulic servo without having to exit Saber™, enter Designstar (the Saber™ design tool), and change model parameters. The Saber™ netlist may be edited directly, but this is no more user friendly, and no less time consuming than editing the graphical model. When loops are set up to vary model parameters within the Saber™ netlist and thus produce a range of simulations, only the first parameter in each model description in the netlist may be changed. For example, a sine wave generator may be amplitude variable from loop to loop, but frequency will remain unalterable. Figure 4.4.2.1 shows the potential divider simulation which is used to achieve a variable voltage. The value of r_1 is varied, r_2 is fixed.
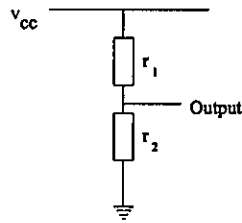
Figure 4.4.2.1 Potential divider

This circuit is used to drive the waveform generator shown in figure 4.4.2.2
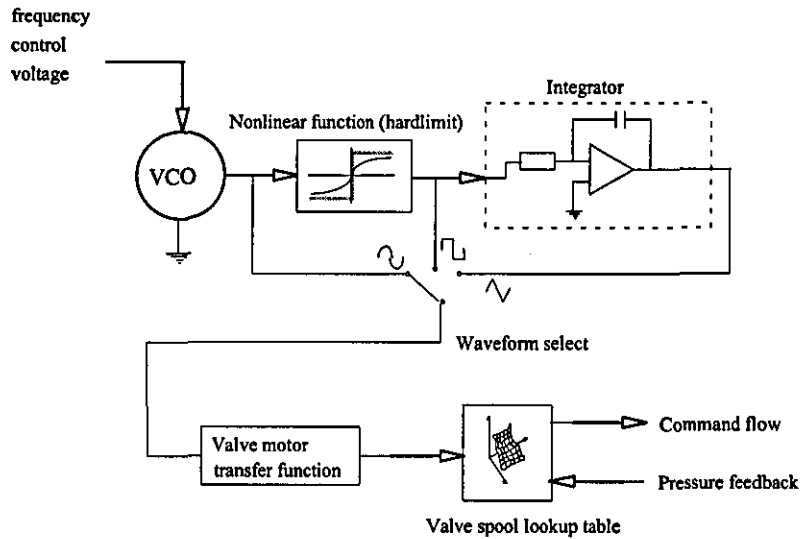
Figure 4.4.2.2 Waveform generator

4.4.3 High level double acting model

The double acting Saber™ simulation of the hydraulic servo is shown in figure 4.4.3.1. This model uses an accumulator in the hydraulic supply line to reduce pump ripple, and to absorb pressure spikes in the supply lines when the system is powered up. The simulation was found to run well up to frequencies of 200Hz using a square wave actuation control signal.
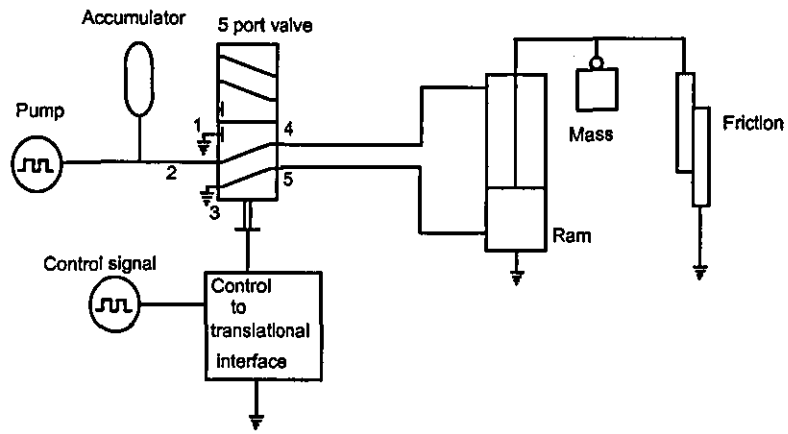
Figure 4.4.3.1 High level simulation of servo with double acting ram

Specifications: Double acting model

Pump: max. flow = 10cc/sec,

max. pressure = 7MPa (running pressure <6MPa)

Ripple: 1Mpa at 50Hz

Accumulator: vmax = 1 litre

pcharge = 3MPa,

pvmax = 13MPa

Valve: spool positions: open1 & 2 = 6mm

close 1 & 4, 2 & 5 = 1mm

open 2 & 4 , 3 & 5 = -3mm

max. area: 5mm^2

Ram: 50mm diameter maximum,

100mm stroke, symmetric

Cutterblock mass = 20kg maximum for 1.8mm oscillation at 100 Hz.

4.4.4 Single acting model

Many standard parts from the Saber™ hydraulic template library have been introduced, and it has been found that actuator performance requirements can be closely approached with a single acting cylinder combined with a return spring. Simulations were initially based on an approximation to a sawtooth wave. This type of wave would produce the best next possible finish with rapid acceleration for the cut stroke to a square wave. The spring returns the ram and cutterblock on the return stroke whilst the accumulator is charged.

The system shown in figure 4.4.5.1 is capable of providing oscillation of 1.85mm peak - peak at 100Hz, though with increased pump flow capacity amplitude increase is virtually linear with respect to available flow up to 150Hz.. Higher amplitudes are possible with any fixed flow capacity, of course at the expense of frequency response. A 1.85 mm peak - peak maximum amplitude is more than adequate for a prototype machine, or production machine with relatively low feedrates or spindle speeds. For good quality joinery, the *maximum* wave allowable (Jackson, 1986) is 1.8 mm, which is within the capabilities of the system. Higher amplitudes have been reached on subsequent simulations, though power consumption becomes excessive (>8kW for 4.5 mm peak-peak at 100Hz).

4.4.5 Specifications: Actuator System.

Pump: max. flow =   10cc/sec,
             max. pressure =   7MPa (running pressure <6MPa)

Check valve: amax =   1mm²
             pcrack = 10MPa
             stroke = 1mm
             pfull =   12MPa

Accumulator: vmax =   1 litre
             pcharge = 3MPa,
             pvmax =   13MPa

Valve: spool positions: open1 & 2 = 6mm
                                close 1 & 2 = 1mm
                                open 2 & 4 = -3mm
             max. area: 5mm²

Ram: 50mm diameter maximum,
             100mm stroke,

             spring rates: fmax = 3k
                            fmin = 2k

Damper: = 10 N/m/s - used for stabilisation during early simulation runs only.

Cutterblock mass = 20kg maximum for 1.8mm oscillation at 100 Hz.

Figure 4.4.5.1 Single acting ram based simulation of hydraulic servo

4.4.6 Hydraulic system power consumption

It was important to know the amount of power which would be required to oscillate the hydraulic ram and slideway - obviously the system would not be viable if power consumption was found to be excessive, and if consumption may be reduced the purchase and running costs of the system will follow suit. To this end, Matlab code (appendix 1, section 12.13) was written to calculate the system power consumption for varying actuator wave forms. The results are shown below in figure 4.4.6.1 The addition of an accumulator reduces the amount of ripple on the pump supply considerably, allowing the use of a smaller hydraulic power pack.
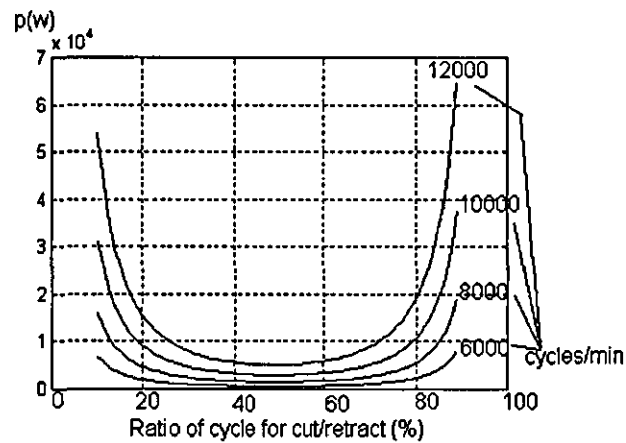
Figure 4.4.6.1   Hydraulic system power consumption

Applying the code shown in section 12.13, it is possible to gain an understanding of the size of the forces involved, and power consumption.   For example, oscillating a 10kg cutterblock over a distance of 2mm at 100 Hz, requires an acceleration (and deceleration) force of 2.44 kN.   Peak power consumption would be 2.88 kW.   These figures are by no means excessive for timber machinery power consumption, and a modest hydraulic servo such as that described in section 4.4.5 is capable of producing the required output. Having found a suitable method of oscillating the cutterblock, it was then necessary to determine the effect of using the hydraulic servo simulation to drive a timber surface form simulation, on the final output.   The development of the timber surface form generation software is described in the next chapter.

91

5.0 Modelling of rotary machining process

5.1 Mathematical background

Taking an initial horizontal sample, H_i upon which to base the simulation, we can choose to determine knife tip position based upon time with an external clock overseeing the simulation, or by putting H_i equal to the instantaneous position of the spindle centre, assuming zero runout. This allows a simplification of the model from the beginning which makes it more straightforward to add a signal for cutterblock oscillation. Since the cutterblock oscillation waveform is likely to be complex, it would be difficult to model. A more straight forward approach is to keep the cutterblock model open to this waveform. The following diagram, figure 5.1.1, is a development of figure 2.2.1.1 and shows the principal variables used in the equations used in this section.
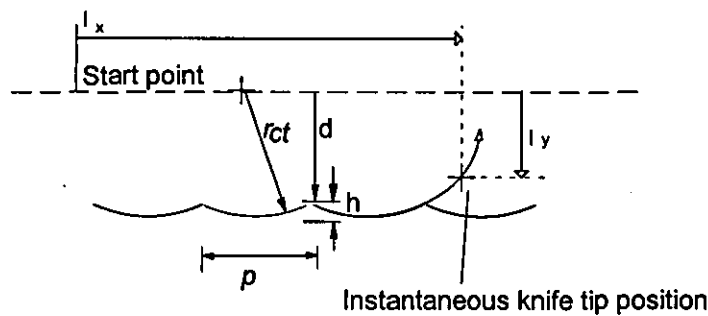
Figure 5.1.1 Surface geometry variables

Two output arrays are therefore produced, taking unit cutterblock diameter since the wave shape is of primary interest. For multi knife cutterblocks, a suffix is used to represent the knife number, (for example instantaneous position of knife is number three is $I_{x\_3(t)}$).

For a single knife cutter, instantaneous knife tip position is given by:

$$I_{x(t)} = cos(2\pi H_i) + F_g H_i \qquad 5.1.1 \qquad\qquad I_{y(t)} = \sin(2\pi H_i) \qquad 5.1.2$$

For a 2 knife cutterblock:

$$I_{x\_1(t)} = cos(2\pi H_i) + F_g H_i \qquad 5.1.3 \qquad\qquad I_{y\_1(t)} = \sin(2\pi H_i) \qquad 5.1.4$$

$$I_{x\_2(t)} = cos((2\pi H_i) + \pi) + F_g H_i \qquad 5.1.5 \qquad\qquad I_{y\_2(t)} = \sin((2\pi H_i) + \pi) \qquad 5.1.6$$

93

And for a 4 knife cutterblock:

$$I_{x\_1(i)} = \cos(2\pi H_i) + F_g H_i \qquad 5.1.7$$

$$I_{y\_1(i)} = \sin(2\pi H_i) \qquad 5.1.8$$

$$I_{x\_2(i)} = \cos\left((2\pi H_i) + \frac{\pi}{2}\right) + F_g H_i \qquad 5.1.9$$

$$I_{y\_2(i)} = \sin\left((2\pi H_i) + \frac{\pi}{2}\right) \qquad 5.1.10$$

$$I_{x\_3(i)} = \cos((2\pi H_i) + \pi) + F_g H_i \qquad 5.1.11$$

$$I_{y\_3(i)} = \sin((2\pi H_i) + \pi) \qquad 5.1.12$$

$$I_{x\_4(i)} = \cos\left((2\pi H_i) + \frac{3\pi}{2}\right) + F_g H_i \qquad 5.1.13$$

$$I_{y\_4(i)} = \sin\left((2\pi H_i) + \frac{3\pi}{2}\right) \qquad 5.1.14$$

The pitch of the knife markings can be found using equation 2.2.1.1.

94

5.2 Surface simulation software

Equations odd numbered 5.1.1 to 5.1.13 show that the cutter tip loci will posses an irregular horizontal spacing when taking the spindle centre as a datum. Whilst this is to be expected, it consequently becomes difficult to extract and process the simulated timber surface data. What is required, and is the basis of previous surface simulation algorithms, is an array containing surface data as vertical co-ordinates with the array spacing representing regular physical points. At all times it must be borne in mind that the cutter tip locus can be one or more arrays containing irregularly spaced both vertical and horizontal components.

It is not satisfactory to merely trim off the cutter loci above predicted surface wave height as generated by equation 5.18, since deviations from the ideal would produce crossed over or clipped sample points. However, intense mathematical modelling of the modified cutting process also presents problems, for example: When an actuation waveform is applied to the cutterblock generated by a hydraulic ram, either as a simulation or in the physical world, the actuation signal would be complex and the effect upon the surface waveform difficult, if not impossible to predict with trigonometry. (Maycock, 1991), (Wang 1993) stated that in addition, machine vibration has a significant effect upon surface quality, and whilst not included in the model developed herein, could be added as a subroutine with ease..

The model thus becomes complex unless machine vibration is taken as either a pure sine wave, or a combination of sine waves. Nonlinearities, due for example to machine chatter, are perhaps best included in the model as pre-prepared waveforms, but fortunately, numerical methods readily lend themselves to software based simulation of a system where not all of the waveforms are known. Simple changes to x and y knife displacement due to machine vibration and cutter oscillation may be included, and the more complex waveforms such as that output by a hydraulic servo, may be included later in the overall model for a complete system simulation.

Previous surface simulation algorithms have taken a horizontal sample from the knife tip loci. (Maycock, 1991) developed a surface simulation algorithm which plotted the knife tip loci and then extracted the surface information by horizontally scanning the loci. Since the horizontal loci points are frequently not conveniently near to the scanning line, spurious sample points are picked up as can be seen in figure 5.2.1.

95
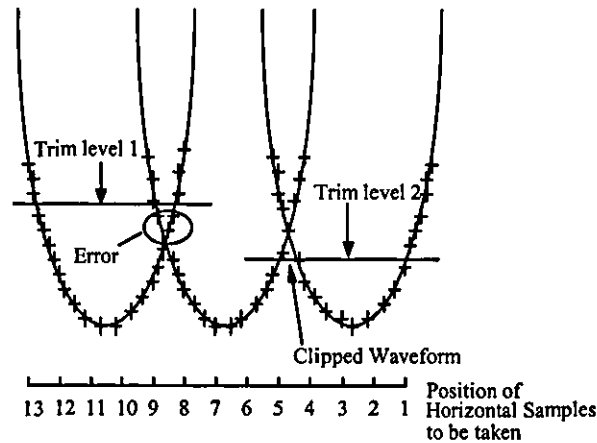
Figure 5.2.1 Spurious samples resulting from an arbitrary trim level.

5.2.1 Surface simulation software detail

Taking a model of the cutter tip locus and extracting the surface data has been a proven method of predicting surface form, albeit with limitations of speed, and slight inaccuracies due to horizontal quantisation. The waveform cannot be predicted for multiple wave forms using a straightforward mathematical model, because complex results are produced for inverse sines and cosines which cannot be further integrated into the model. Figure (5.2.1.1) shows that data flows for the surface simulation software which has been developed in Matlab.

The preliminary surface waveform generator describes the cutter tip loci for either a 1, 2, 4 or 6 knife cutter. Feedrate, cutter speed, number of knives and the knife tip radius are input to the software through the routine **loci**.

Vertical and horizontal vibration components are added separately, data being extracted for spindle runout, proud knife, and machine vibration for output as a horizontal vibration component to the preliminary surface waveform generator function, and as a vertical component for the final addition of waveform components. The high speed filter is a routine developed in Matlab to extract the surface waveform from the cutter tip locus.

96
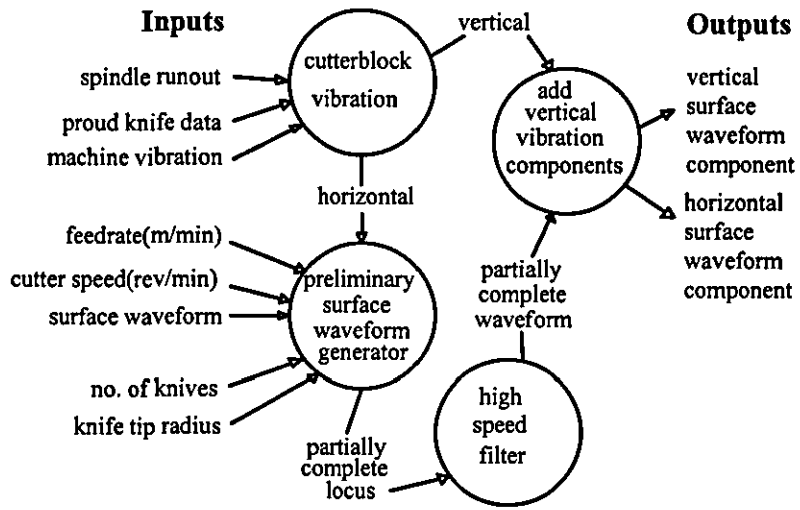
Figure 5.2.1.1 Data flows within simulation software

The high speed filter was designed to give the software developed in Matlab equivalent performance to software previously developed in C. The cutter tip locus is scanned to produce the waveform as shown in figure 5.2.1.2.
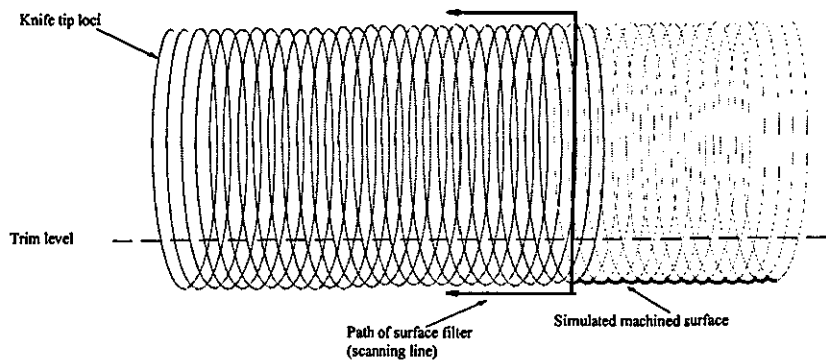
Figure 5.2.1.2 - Extraction of surface data from cutter tip loci.

97

The trim level shown in figure 5.2.1.2 is reached through using a sorting algorithm . The vertical components of the entire locus are sorted in ascending order, with a separate array storing the locations of the corresponding horizontal components. The lowest 20% of the vertical components are then extracted, and the corresponding horizontal components are stored in a similar output array. The order of these components is not important since the sorting algorithm will still scan through the vertical components within a fragmented equivalent of a 2 dimensional variable space (i.e. not every location in the variable space is filled).

Figure 5.2.1.3 shows the effect of using a fixed sampling period to produce a waveform with regular horizontal steps. In practice such a method generates a particularly messy output waveform, often with spurious samples having vertical components from the upper curves of the cutter tip locus. The use of a large number of loci points appears to overcome this problem in part, but the appearance of spurious samples is of course not completely overcome, and the large arrays used to hold the cutter loci are too unwieldy for computation. An array of around one Mb in length for the cutter loci was found to be capable of producing a 1000 point regularly spaced horizontal sample with around 50 spurious samples. The time spent processing this data would be inordinate, unless manual cleaning up of the results was deemed acceptable.

Figure 5.2.1.3 - Spurious data produced by uneven horizontal loci.

98

The main control loop of the filtering software initially specifies which output sample is to be taken. A scan is then made of which loci points are above the sample point. A small tolerance is built in such that a specified number of sample points which come nearest to the vertical sampling line are taken only. A high speed bubble sort algorithm is used to sort the surrounding area in order of distance from the sample line. A fixed number of the lowest sample points in the list are taken.

This list is then sorted using the same algorithm in order of vertical height. Ideally, the first sample point in the list would always be the lowest loci component, and therefore the appropriate point to be stored in the horizontal sample array. Unfortunately the same loci sample may be shared by one or more inputs to the horizontal sample, so it is necessary to successively pull in the spread of loci samples until it is clear that the lowest loci sample nearest to the sample line has been found.

For example, referring to figure 5.2.1.4, it is clear that sample point v1 is the closest, and therefore most appropriate sample to take in terms of accuracy at the vertical line marked by sample 5. Vertically spurious samples are easily produced by exiting software: a simpler algorithm may pick up the loci point closest to the sample line, which in this case would be v6, which would clearly be a spurious sample, giving an incorrect picture of the surface waveform. Horizontally spurious samples must be avoided by taking successively smaller pictures of the surrounding area to the sample line, e.g. in the first wave of sampling, in general all v samples as well as w1 -7, and in particular samples w8 - 10 would be produced as candidates for the lowest sample point. The code contained in the while loop in the filtering software is able to home in on the sample point V1 in order to alleviate this. The final iteration may produce samples v1, v2, v6 and v7. It is then very straightforward to pick the lowest of these samples. The listing for the Matlab surface simulation is shown in appendix 1, section 12.3.

The while loop contains the body of the filtration code, which works by counting down the number of points taken near to the sample line with each loop. Code then re sorts the nearest loci points to the sample line and checks the lowest value against that found in the preceding loop. When the value of the vertical loci component of the lowest perceived loci sample starts to rise in the following loop, it is clear that a minimum vertical loci point has been found with no 'smearing' of the results from one fixed horizontal point to the next. Consequently the sampling method is completely robust, and changes in the spacing of the loci points will not affect the performance of the sampling code, which

adjusts automatically. The complete code for the filter, whilst taking much design, is very compact at less than 30 lines of code. Processing of a 10 000 sample point loci to produce a 1024 sample point output waveform takes around 40 seconds on an 80 MHz 486 PC.
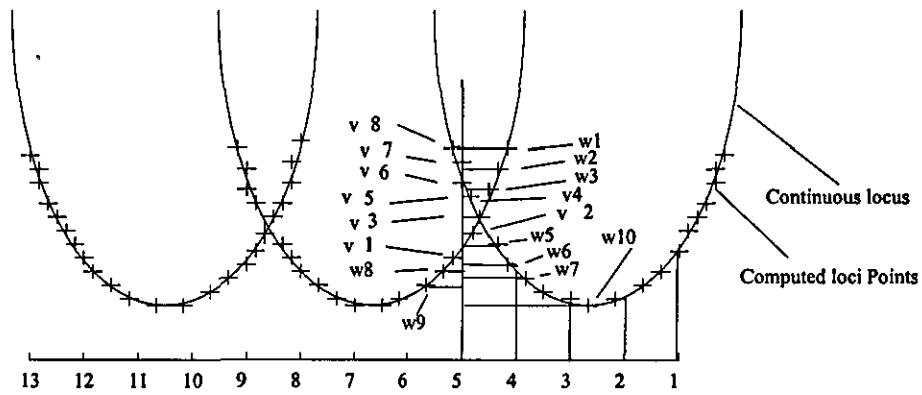
Figure 5.2.1.4 Modified sampling method

6.0 Overall Simulation

In order to simulate the entire system, the hydraulic and cutterblock simulations were translated into Simulink, the simulation environment for Matlab, which became available at the beginning of month 23 of the project. There followed a transition from the use of a combination of Saber^{TM} and Matlab to simulate the hydraulic servo and timber surface, to an overall simulation developed solely in Simulink. The overall simulation was developed in stages, the hydraulic simulation being exported to the Simulink environment and rigorously tested. A simplified version of the timber surface simulation was implemented, which produces an unevenly horizontally spaced surface plot. The surface processing is then carried out off line using the filtering software described in section 4.0. This split method of producing a plot was carried out for three reasons.

Firstly, conventional PC hardware available at the time was unable to cope with time based simulations in conjunction with the surface simulation algorithm. Matlab variables may be packed in memory in order to reduce space occupied, but only from the Matlab command window.

Secondly, memory limitations resulting from inefficiencies in the Windows memory manager, and in the Student edition of Matlab used, necessitated a two stage approach. the array size available in the version of Matlab used is equal to 655355 16 bit floating point numbers, though the memory management of the Windows 95 environment is such that software reliability is greatly enhanced if array size is limited to 10000. Even with swap space in excess of 50Mbytes and 64Mbytes of RAM, it is difficult for the operating system to handle a single contiguous block of data over 10Mbytes in length. It was thought that a memory management system could be developed for Matlab which would automatically take sections of large arrays and store them on disk as compressed binary files, to be retrieved for processing when necessary. However, time limitations dictated that this coding be abandoned. Also, since currently available environments such as Professional Matlab have memory management code that allows infinite array length, it was thought that the writing of a memory manager would contribute little to the knowledge base.

Thirdly, it was found that when Simulink is not required to interface with external code which requires a lot of processor time, it is more stable, and is able to carry out several simulations at once. The result is that the running of 5 or more simulations each producing 10000 point surface samples is possible, allowing for rapid experimentation and tuning of the system.

6.1 Simulated timber surface generator with Simulink

The simplified cutter locus generator works in a very similar way to the one produced using Matlab code which outputs horizontal and vertical cutter locus data to the SSA. Since a time input is possible however, it is now possible to run the simulation with realistic feedrates, e.g. feed / min instead of feed / rev, and speed variable effects such as power consumption due to cutter windage may be included in future research in order to provide a further insight into machine operation.

In order to devise a complete a model of the cutterblock oscillation system in conjunction with the hydraulic servo it was necessary to reconstruct the entire simulation within an environment which was capable of modelling the hydraulic servo and providing a graphical output to represent the timber surface. Simulink provides a graphical front end to Matlab software, and also features at Adams and Runge Kutta variable time step algorithms for transfer function based, and non linear system simulation. A library of standard simulation component is included with Simulink. Other components may be described either in transfer function form, or may be modelled using Matlab software. An example of a Simulink model for timber surface simulation is shown in figure 6.2.1.
Referring to this diagram, it is possible to see how the stationary vertical and horizontal cutter tip loci are produced by a sine and cosine wave. The cosine wave which is used to produce a horizontal cutter tip locus, is added to a variable which increases with time which represents the feed per revolution. In order to produce the vertical cutter tip locus, a sine wave is used. A dead band function is then used to extract the part of the sine wave which represents the timber surface.

103

6.2 Effect of cutterblock oscillation upon surface finish under perfect conditions

The simulation shown in figure 6.2.1 was created in order to clearly demonstrate the effectiveness of (simulated) cutterblock oscillation. The driver circuit for the cutterblock oscillator is represented by gain 7, saturation 2 and gain 4. This takes the horizontal cutter tip locus and generates a square wave (figure 8.2.4.5) to activate the cutterblock when the cutter reaches a predetermined position. Firstly a sine wave is amplified to infinity, and consequently driven to saturation. The gain of the resultant square wave is controlled to produce an output square wave of equivalent amplitude to the input sine wave.
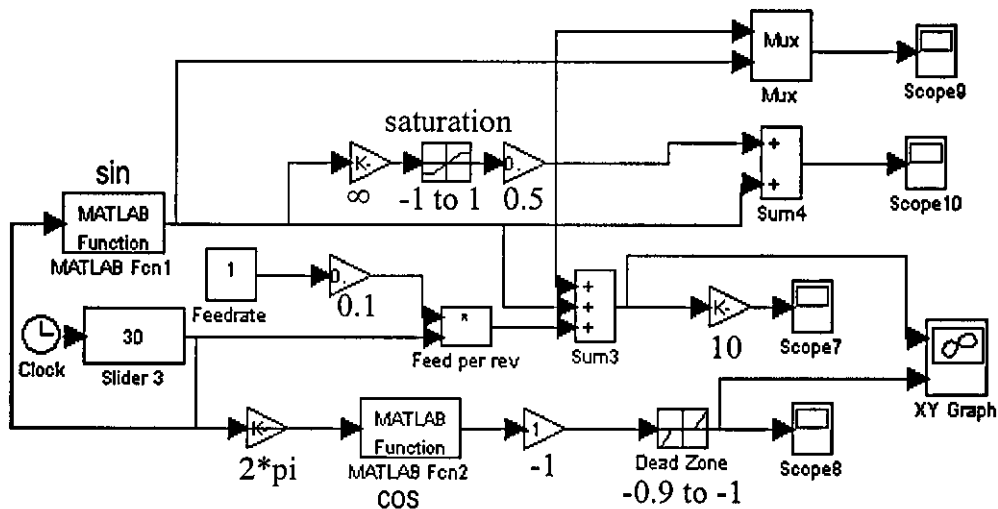
Figure 6.2.1 Timber surface simulation in Simulink with cutterblock oscillation

6.2.1 Varying degrees of cutterblock oscillation

A parallel implementation of the model shown in figure 6.2.1 is shown below. This provides varying degrees of cutterblock oscillation both for pure sine oscillation (as utilised in the test rig) and an actuation wave closer to the ideal (a square wave). The model may be switched between the two. 'Base' and 'step' select the amplitude spacing of 5 oscillation wave forms. The base figure gives the start point for the stepped amplitudes, and the step variable sets the increments, where for both cases,

104

$$(0 \rightarrow 1) \overset{\Delta}{=} (10\% \rightarrow 100\%)$$

For example, a base of zero, and step 1 gives oscillation amplitudes of 0, 25%, 50%, 75% and 100%. A base of 0.1 and step 0.2 would give steps of 10%, 15%, 20%, 25% and 30%.

6.3 Hydraulic servo lag

The lag inherent to the hydraulic servo can have a significant effect upon surface finish. The simulation shown in figure 6.3.1, is a simple transfer function based simulation developed in order to predict the lags which will be present in the system for an open loop servo. The model for the servo valve is a state space model, based upon the servo model for a Moog 'D' Series servo valve, as described in section 4.4.1, which takes the form:

$$A = \begin{bmatrix} -1580 & -775000 \\ 1 & 0 \end{bmatrix} \quad 6.3.1 \qquad B = \begin{bmatrix} 1 \\ 0 \end{bmatrix} \quad 6.3.2$$

$$C = \begin{bmatrix} 0 & 775000 \end{bmatrix} \quad 6.3.3 \qquad D = \begin{bmatrix} 0 \end{bmatrix} \quad 6.3.4$$

The ram and slideway model uses the specifications given in section 4.4.5, and is translated into state space from the transfer function based model described in section 4.1.4. The model takes the form:

$$A = \begin{bmatrix} -1.5e-6 & -1.256637e7 \\ 1 & 0 \end{bmatrix} \quad 6.3.5 \qquad B = \begin{bmatrix} 1 \\ 0 \end{bmatrix} \quad 6.3.6$$

$$C = \begin{bmatrix} 0 & 2.5e18 \end{bmatrix} \quad 6.3.7 \qquad D = \begin{bmatrix} 0 \end{bmatrix} \quad 6.3.8$$

All servo valve models and hydraulic ram and slideway models described from sections 6.3 to 6.5 use the state space models shown above in equations 6.3.1 to 6.3.8.
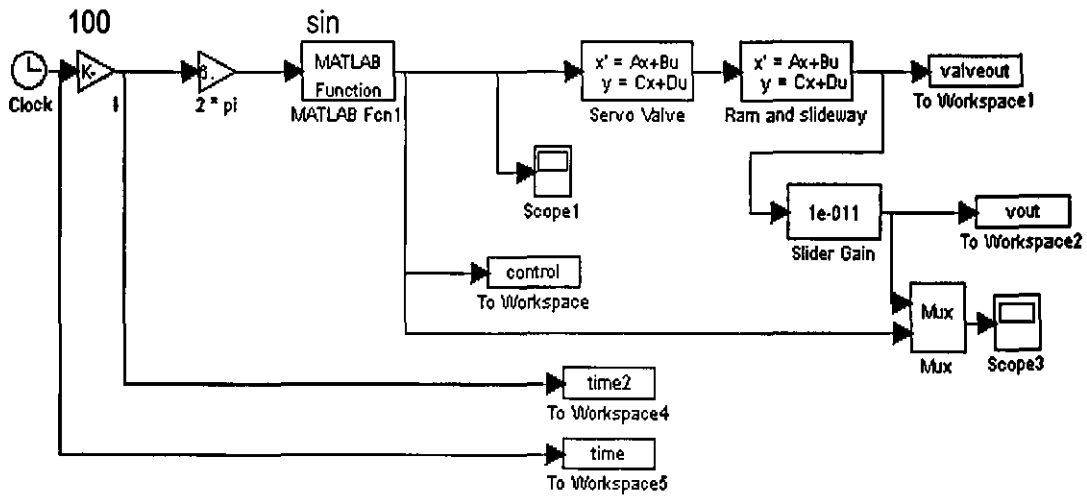
Figure 6.3.1 Transfer function based servo model

Figure 8.1.1.1 shows the hydraulic servo response for a sinusoidal control waveform of 100Hz. Amplitude of the output is arbitrary in this instance since servo gain is in the order of 1.0e10.

A reduction of output gain has been included merely such that the time lag can be effectively visualised on the same graph. Simulations included in chapter 8 using the comprehensive model in Saber™, bear out this model, and are used to give more information about the available actuation amplitude. It becomes clear that oscillations in the order of around 20mm are theoretically possible, but limiting oscillation amplitude to between 2 and 5 mm greatly improves system stability and reduces drift, largely due to the reduction of the nonlinear effect of cavitation. A 100 Hz actuation waveform for a single knife cutter computes to a spindle speed of 6000 rev/min. Naturally the real system would be balanced, i.e. 2 or more cutters, such that for a 2 cutter system running with this actuation signal, spindle speed of 3000 rev/min could be achieved. Servo lag in this instance is 2ms. Control of the system could therefore be achieved by building in a fixed time delay, with a variable additional time delay used for fine tuning. Experiments carried out to see the effect of altering fluid bulk modulus, which would occur as fluid warms, are described later in this chapter. It becomes clear that a degree of drift in servo response must be taken into account and compensated for. Figure 6.3.2 shows a typically lagging servo response to a sinusoidal control signal. Full results showing servo lag may be seen in chapter 8.
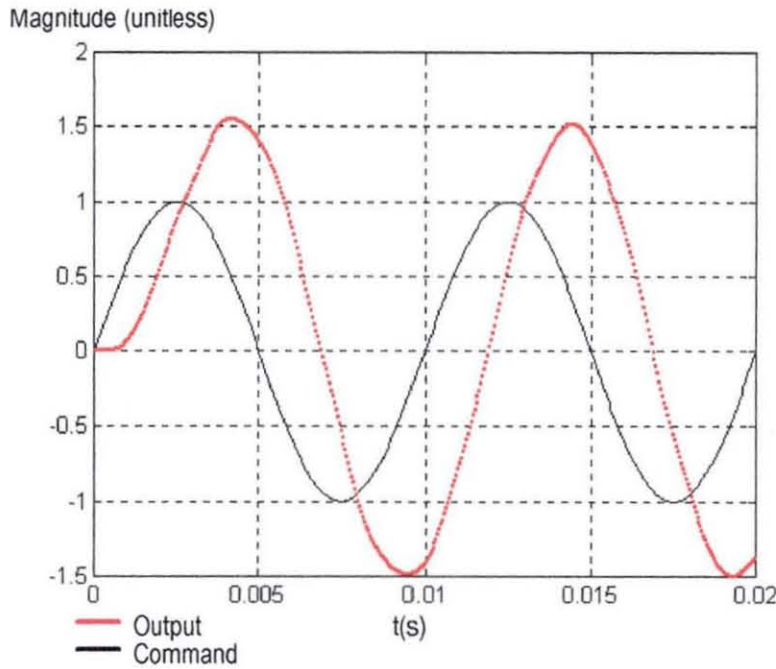
Figure 6.3.2. Typical hydraulic servo lag

6.3.2 Lag compensator

In order to provide an output in phase with the input, bearing in mind that the open loop system is stable, it is possible to connect an additional lag to the input of hydraulic servo as shown in figure 6.3.2.1. A typical result is shown for input and output waveforms is shown in figure 6.3.2.2. Although at the design stage the servo model can be fitted with a suitable controller to improve tracking, the principal aim of this research has been to prove the effectiveness of cutterblock oscillation in a general sense. Although inroads were made into the design of a suitable PID controller for the hydraulic servo, time constraints dictated that the research concentrated on the overall system with controller design to form a further refinement, and possibly the basis for future research. Also, transducer lags in an actual system, which at the time of writing were unknown, would necessitate the re design of the controller in any case. It therefore seemed prudent to postpone controller design. To this end, a simple lag compensator in the form of a fixed time delay is used in front of the hydraulic servo.

107
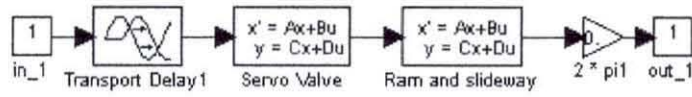
Figure 6.3.2.1 Lag compensation with pure time delay
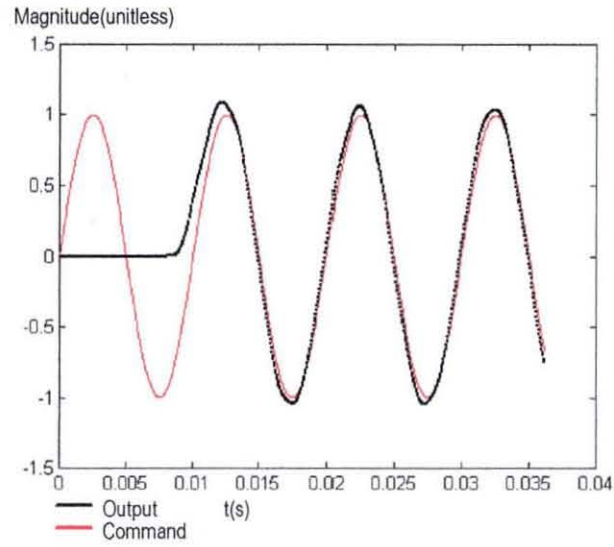
Figure 6.3.2.2 Effect of lag compensator

108

6.5 Effect of hydraulic servo lag upon surface finish

The simulation shown in figure 6.4.1 is a Simulink simulation written in order to ascertain the effects of lags between control signal and hydraulic servo response upon timber surface finish. The purpose of this simulation is to provide a system with direct control over simulated servo lag, such that a tolerance can be defined whereby as long as the hydraulic servo is working within certain limits, it may be ascertained whether or not hydraulic oscillation of the cutterblock is practicable at certain speeds. It must be borne in mind that certain lags may actually make the cuttermarks larger than for an un-oscillated system, and the results of simulations showing the effects of a range of lag values are shown in chapter 8.0.
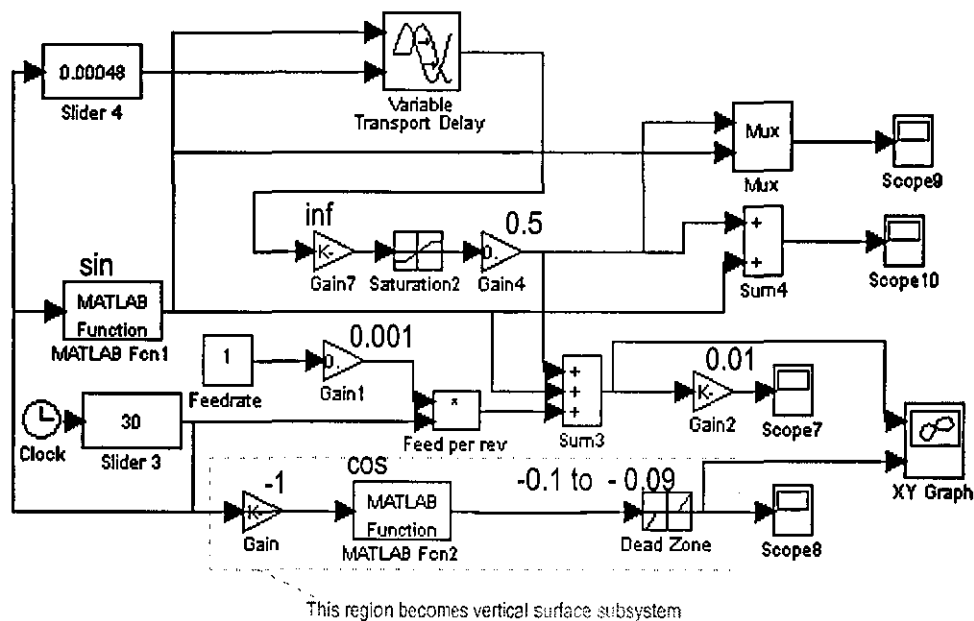
Figure 6.4.1 Basic simulation to determine the effect of oscillation signal phase lag upon surface finish.

The system shown in figure 6.4.1 was used primarily for development of the model. The parallel implementation of the system shown in 6..4.1 is shown in figure 6.4.2. This system is basically 4 simulations connected in parallel.

109
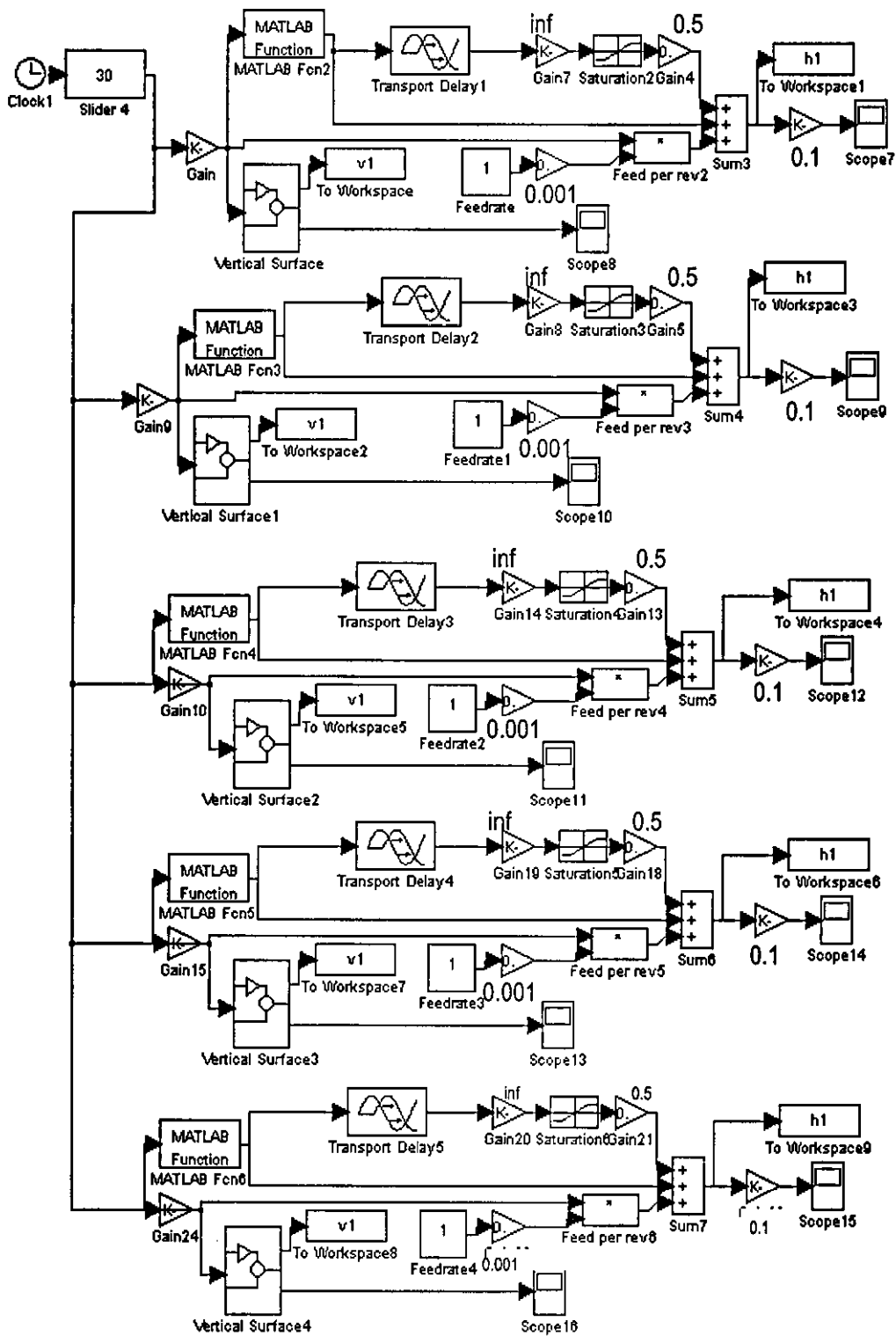
Figure 6.4.2 Parallel implementation of Simulink model to determine effect of oscillation
signal lag upon surface finish.

110

6.5 Parallel implementation of overall system simulation

6.5.1 Top level overall system model

Once the Simulink based cutterblock oscillation and hydraulic servo models had been developed and tested, there remained the simulation of the overall system. The simulation consists of five overall system simulations connected in parallel. The amount of cutterblock oscillation used was varied throughout the model, to produce a block of five results in each case. Frequency of the oscillation signal with respect to cutterblock rotary speed may also be varied. The top level model of the overall system simulation is shown below in figure 6.5.1.1.
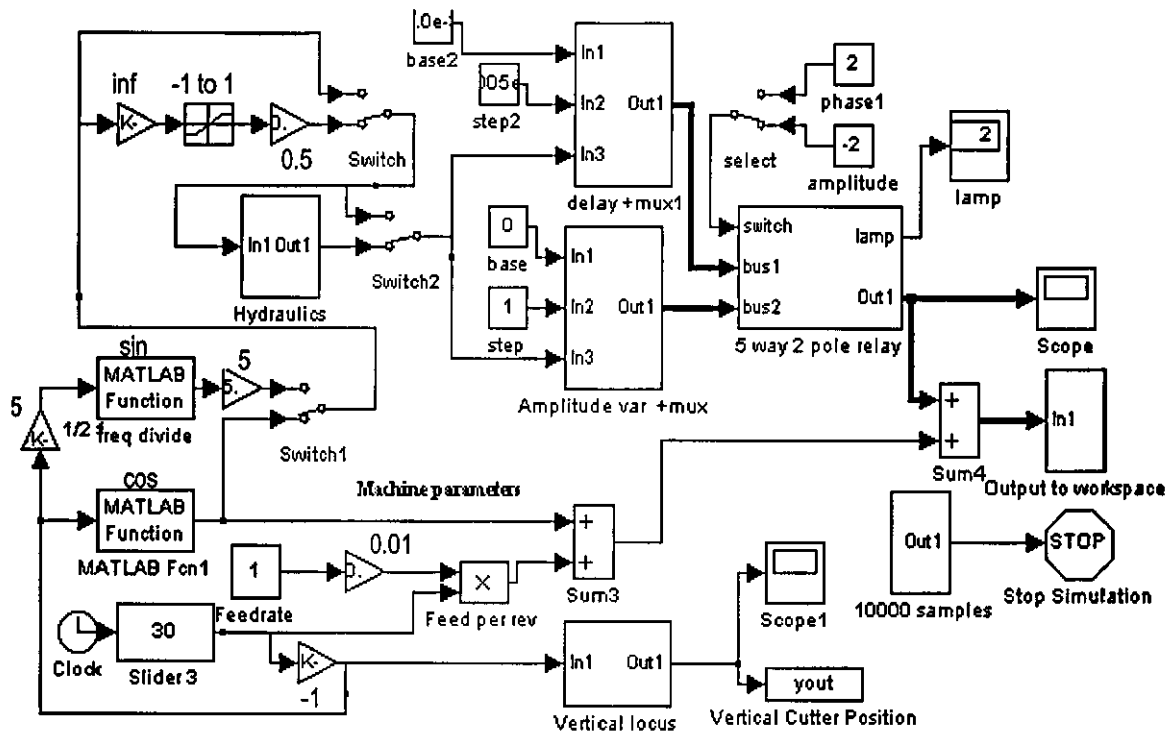
Figure 6.5.1.1 Parallel implementation of simulation of actuation system and timber surface

111

The previous diagram shows the top layer of the overall simulation. Simulation sub circuits have been designed to take care of some of the simulation system functions. The following structure chart shown in figure 6.5.1.2 shows the overall simulation and subsystems. In practice the top level of the hierarchy (the Simulink environment), being a common platform for all simulations, has been left in only for the sake of completeness, and may be ignored when examining the simulation structure from the standpoint of system modelling.
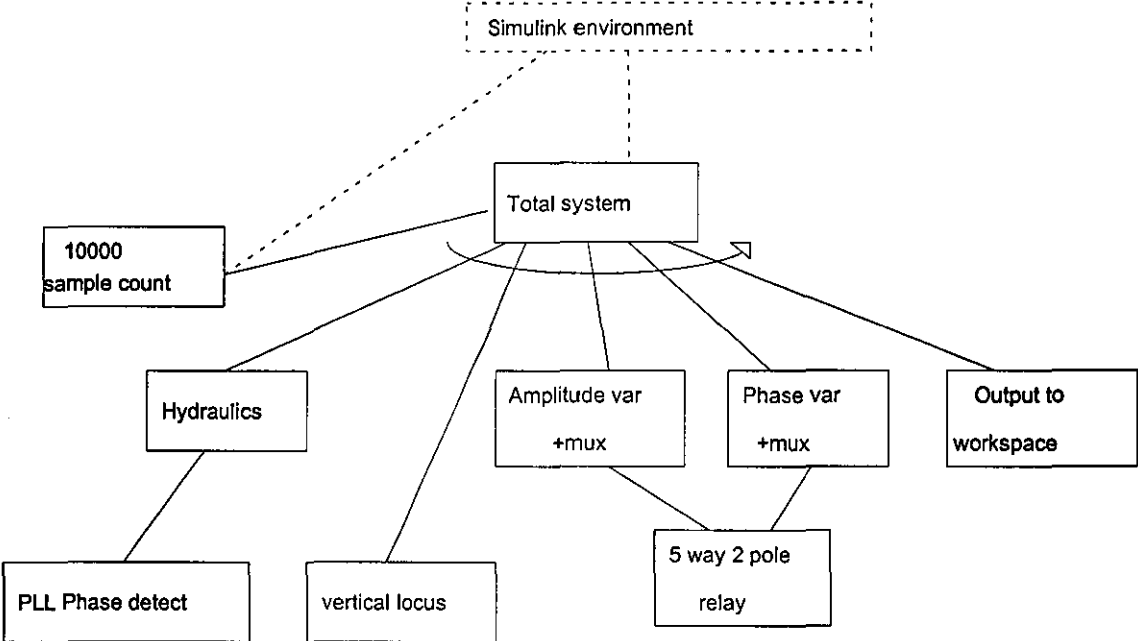
Figure 6.5.1.2 Simulation structure

6.5.2 Overall system simulation – subsystems

The subsystems outlined in the boxes shown in figure 6.5.1.2 are shown in this section.

The hydraulic subsystem is based upon the hydraulic simulation developed using Saber™, and eventually Simulink, as described in chapter 4. The kernel is a state space implementation of the transfer function based model developed previously. Since hydraulic circuit design is less of an issue at this point than hydraulic circuit performance, and the transfer function based model exhibits very similar transient characteristics to the detailed model at 100 Hz, this model was used in order to produce a viable model with respect to reducing the amount of required processor time.
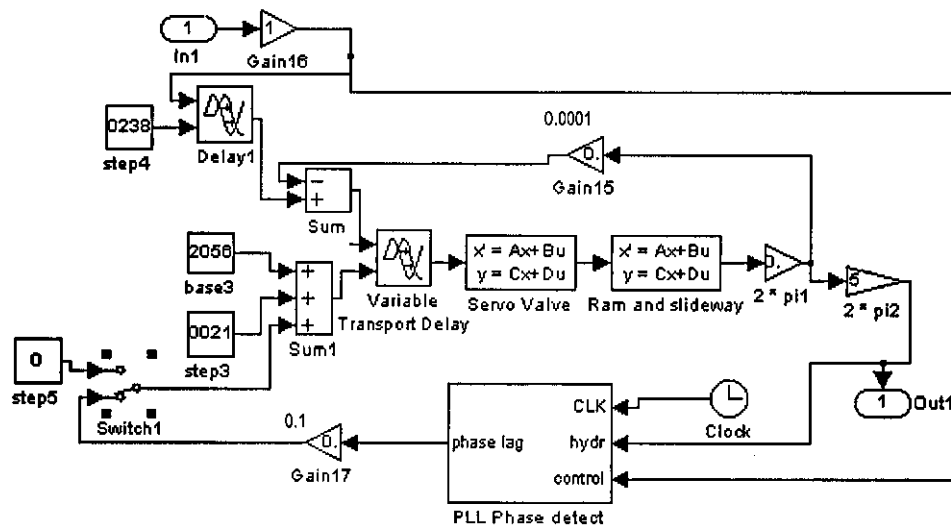
Figure 6.5.2.1 Hydraulic subsystem.

In order to allow for drift within the hydraulic system and save on set up time when altering actuation waveforms, a kind of phase locked loop has been devised (Figure 6.5.2.2) which alters the control signal lag in order to compensate for any phase discrepancies between the control signal and the hydraulic servo output. The phase detector is based on two zero crossing detectors sensing the phase of input and output signals. Following these functions are flip flops which trigger only on the positive going cycle for each signal. The following switching arrangement captures time from the simulations internal clock, crossing point times are subtracted to find the phase lag. This

113

is then ported to a variable transport delay back in the next level up (the hydraulic subsystem) in order to provide phase compensation.
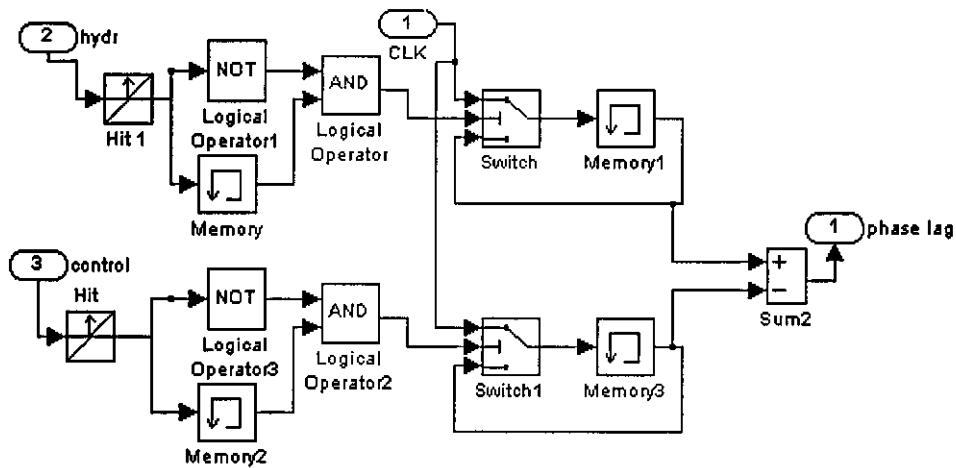
Figure 6.5.2.2 Phase detect and lag determination for Phase Locked Loop.

The cutterblock vertical locus is basically a cosine function followed by a cut-off which restricts the vertical part of the cutterblock waveform roughly to the region of interest, i.e. the timber surface. The vertical locus subsystem is shown in figure 6.5.2.3.
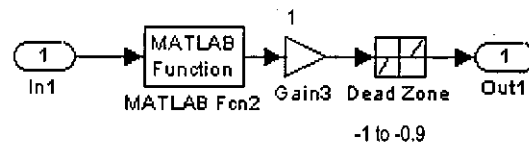
Figure 6.5.2.3 Vertical locus subsystem.

Figure 6.5.2.4 shows the subsystem for generating 5 degrees of cutterblock oscillation phase lag. This subsystem was used in determining the effect of cutterblock oscillation phase lag upon the timber surface. The base delay is settable from input 1, which then rises in increments set on input 2. The output is multiplexed for further processing. Input three carries the cutterblock oscillation waveform from the hydraulic servo model.
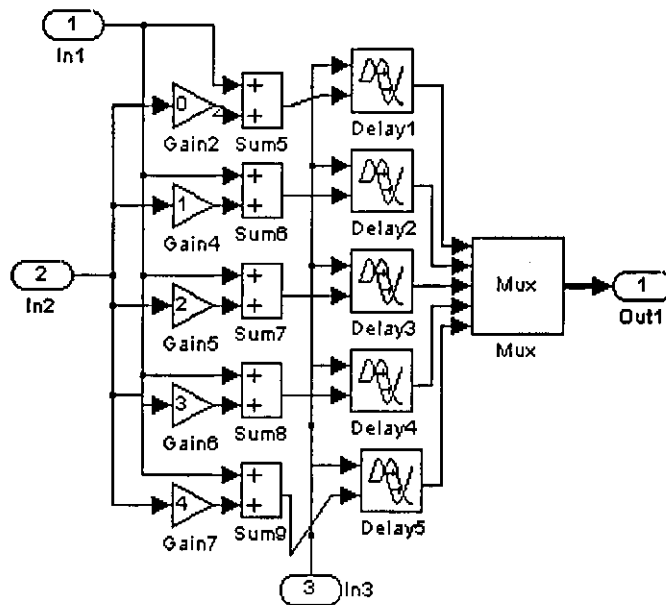
Figure 6.5.2.4 Subsystem for generating
differing degrees of cutterblock oscillation phase lag

115

Figure 6.5.2.5 shows the subsystem for generating 5 degrees of cutterblock oscillation amplitude. This subsystem was used in determining the effect of differing amounts of cutterblock oscillation upon the timber surface. The base amplitude is settable from input 1, which then rises in increments set on input 2. The output is multiplexed for further processing. Input three carries the cutterblock oscillation waveform from the hydraulic servo model.
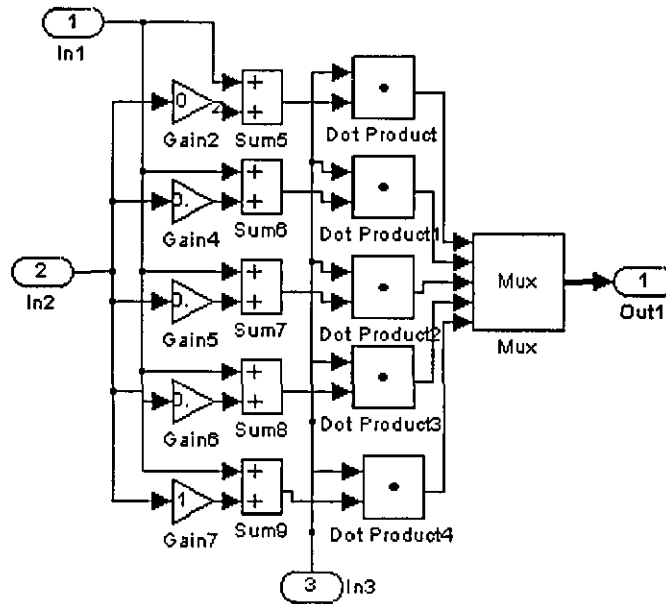
Figure 6.5.2.5 Subsystem for generating
varying amounts of cutterblock oscillation amplitude.

The 5 way 2 pole relay subsystem shown below in figure 6.5.2.6 enables switching between multiplexed lines. This is a problem which can often crop up during modelling within environments like Simulink. The solution is often untidy and makes for clutter in the model, making debugging difficult. The solution proposed here neatly encapsulates a multiway switching system in a single block.
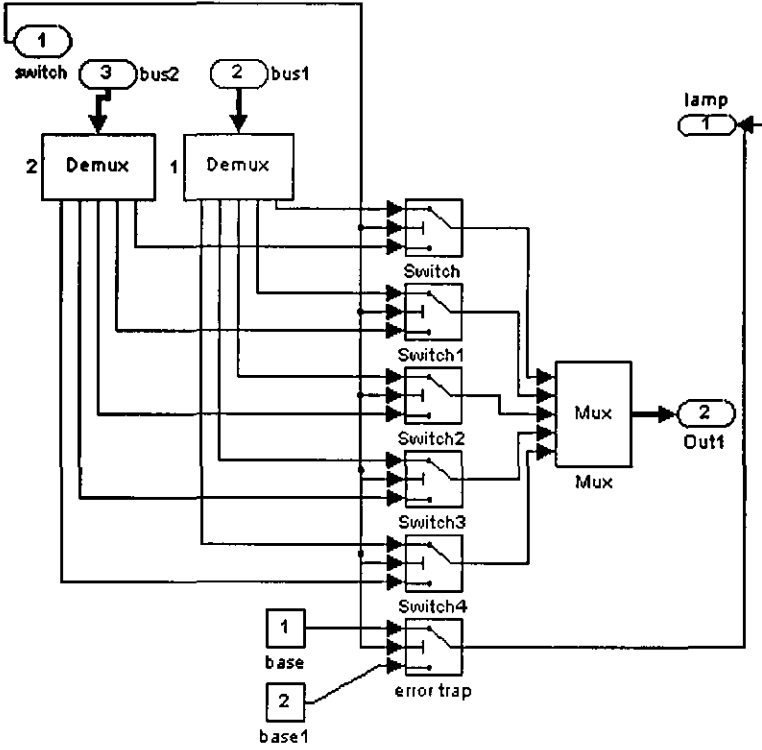
Figure 6.5.2.6   5 way 2 pole relay model

After adding feedrate to the multiplexed cutterblock oscillation lines, the results are ported back to the Matlab environment for examination. To this end, a demultiplexer is used to provide separate arrays, offering simplified data handling through providing 5 10000 element arrays, whereas a multiplexed output would produce a single 5 x 10000 contiguous block of data. Such a large 2D array would be far more likely to cause a machine crash than individual arrays. The demultiplexer is shown in figure 6.5.2.6
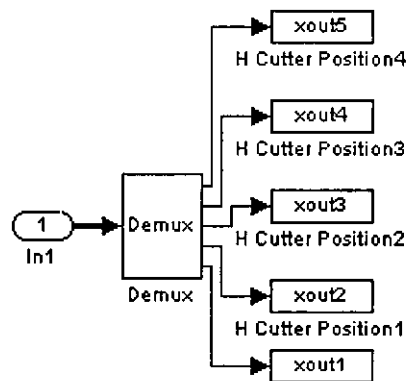
Figure 6.5.2.6 Demultiplexer

The simulation results are based upon the number of samples taken, since a variable time step algorithm within the simulation code means that were the simulation results plotted using a system based on time, arrays of variable length would be produced. The sample counter still allows a variable time step to be used, enhancing simulation performance over a fixed time step simulation, but outputs 5 arrays of fixed size, enabling them to be plotted together. The simulation is made to stop when the sample limit has been reached. The sample counter is shown in figure 6.5.2.7
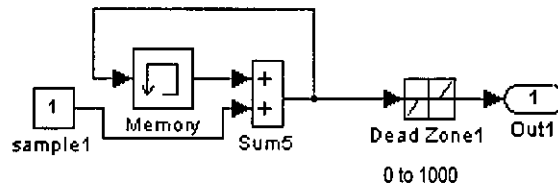
Figure 6.5.2.7 Simulation controller based on sample counts.

7.0 Cutterblock Oscillation test rig

7.1 Description of machine elements

The cutterblock oscillation test rig was built in order to verify the results produced by simulation of cutterblock oscillation in Matlab. An overview of the rig is shown in figure 7.1.1. The cutter tip locus is plotted on paper which is drawn through the machine on a rail mounted table. All principal parameters are adjustable, such as feed rate, number of plotter pens (representing cutter knives), and the degree of cutterblock oscillation. The angle of phase between cutter (pen) position and the oscillation waveform is adjustable also. The machine uses bronze bearings throughout, excepting areas of high load where ball bearings are used. Gearing design is such that backlash is minimal. The structure is braced in critical areas to ensure maximum rigidity.
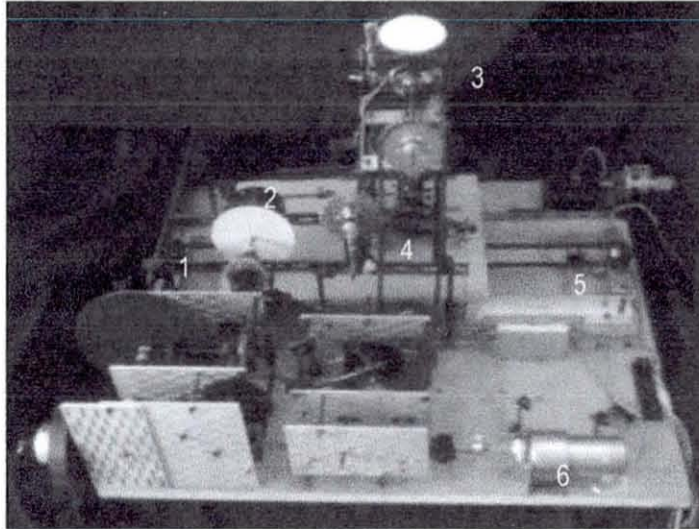
1 - Drive sprocket for variable feed
2 - Oscillation crank
3 - Plotter head position indicator
4 - Plotter head mechanism
5 - Chain drive for plot table
6 - Drive motor
7 - Flywheel

● Power transmission path
● Cutterblock oscillation gearing
● Plotter head rotation transmission
● Variable feed speed drive
● Main driveshaft and gearboxes
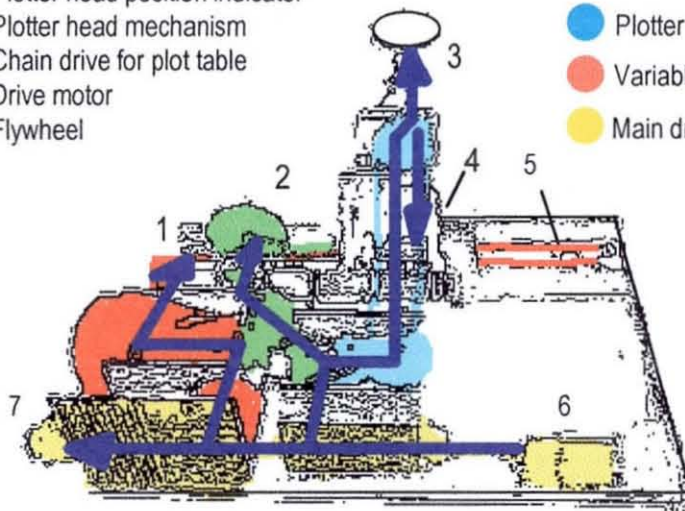
Figure 7.1.1 Test rig overview

The arrangement for the variable speed drive is shown in figure 7.1.2. Drive is initially transmitted into the variable speed drive from the primary drive shaft to a set of helical gears (5). These gears are set at 90 degrees, and the 45 degree helix angle imparts considerable force on the driven shaft. Normally this would present a design problem, but the choice of these gears is deliberate. The net effect of the reaction from these gears is to increase the grip of the drive wheel (2) with applied torque. As the torque through the drive increases, so the grip increases. The vertical parting forces between the gears is compensated for by the adjustment mechanism (6), which applies a lightly sprung pre load to the gears in order to maintain contact. The drive disk (1) consists of a mild steel disk with a 0.8mm thick layer of fabric reinforced rubber bonded to it. Drive is thus transmitted to the output shaft to the rear of the picture.
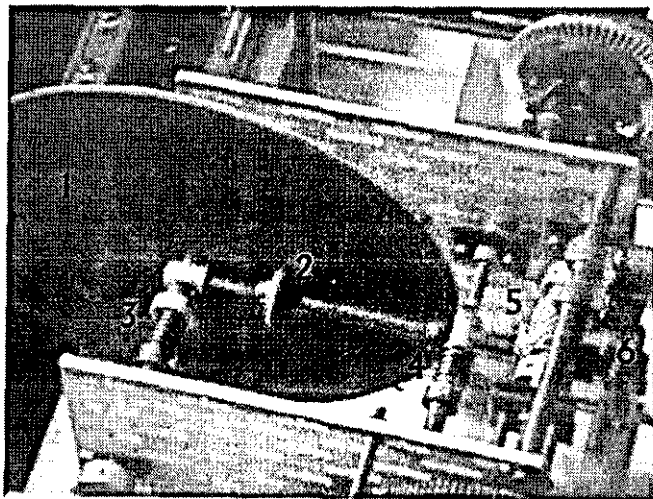
Figure 7.1.2 Variable speed drive

Figure 7.1.3 shows the plotter table and associated parts. The table (1) is driven by a chain, with automatic tensioning on the trailing end of the chain (4) in order to keep the drive stiff. The table runs on steel wheels on aluminium rails (2, 3) which are through bolted to the base plate and is kept aligned in a horizontal plane with ball bearing mounted pre tensioned rubber pressure rollers. The plotter head (5) is self adjusting such that gravity holds the pen in contact with the paper. The horizontal gantry (6) carries the guide rails for the bearing mounts which hold the spindle upon which the plotter head is mounted. This makes the plotter head free to oscillate as the material passes through the machine. The oscillation of a plotter head poses drive problems. A combination of two universal joints would provide constant velocity, but would require that part of the drive train be free to move vertically as the lower set of bearings moves. This is overcome by use of a cardan shaft (7) where two shafts are spaced 20mm apart and allowed to float in sliding bearings (8) around a floating central spindle. This allows longitudinal expansion and contraction of the shaft as a whole, whilst transmitting torque. The sliding bearing block is connected to an aluminium disk (9)via a sliding rod which is brought out through a slot in the main horizontal gantry (6). This allows a dial gauge to be connected to the machine in order to accurately measure the amount of cutterblock oscillation imparted to the plotter head.
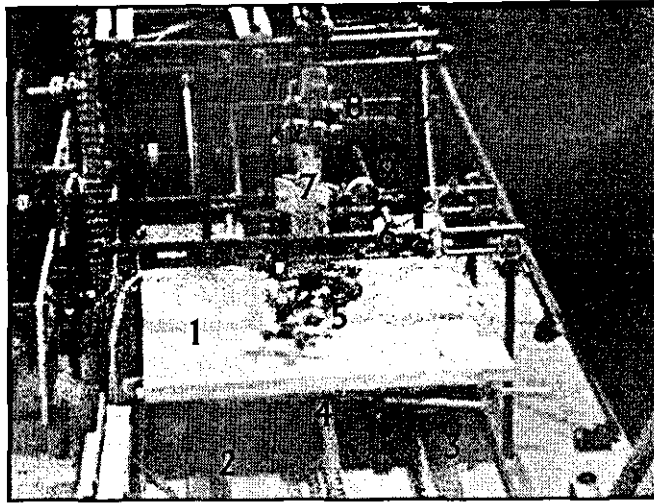
Figure 7.1.3 Plotter table arrangement

The top section of the machine is shown in figure 7.1.4. The chain drive sprocket (1) rides in bronze bearings, driving a small pinion (2). All bearings are adjustable so as to apply a degree of pre load on the gears in order to minimise backlash. The rotary indictor (3) is used to adjust the angle of phase lag between the plotter head and the oscillation crank. This indicator is mounted onto the flat face of a spur gear, and locating wedge shown towards the rear of the wheel, is used to lock the wheel for alignment purposes. The universal joint mounted at the top of the cardan shaft can be seen towards the bottom of the picture (4)
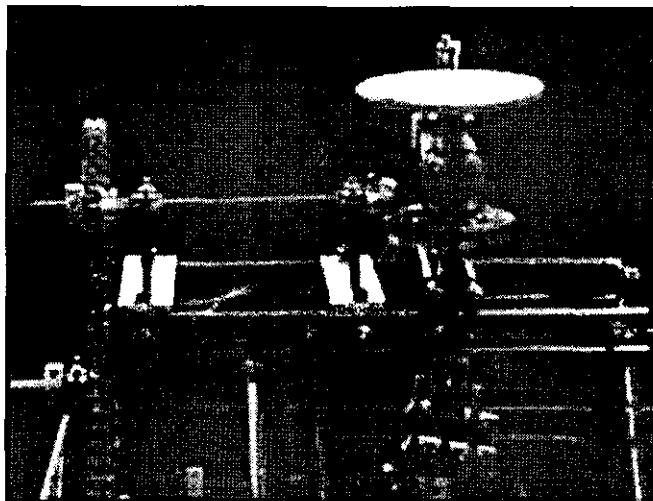
Figure 7.1.4 Top section of machine

125

The feedrate is monitored using the device shown in figure 7.1.5. A micrometer screw (3) adjusts the distance between a contact (1), and earthing contact (2) attached to the table.

A voltmeter is connected to the motor power supply positive terminal. The machine frame is connected to the negative power supply terminal. The negative terminal of the voltmeter is connected to contact 1.

When the table is bought to the start position, current flows through the terminals and the voltmeter will register accordingly. The drive is then engaged and the plotter head is rotated for one full turn. When the plotter head is reached exactly 360 degrees, it is possible to engage the sliding wedge into the top indicator wheel, as described in the previous paragraph. The contacts will be broken at this point and the meter will register 0v. The micrometer is adjusted until the contacts close gain and the amount of feed per revolution may be read from the micrometer scale.
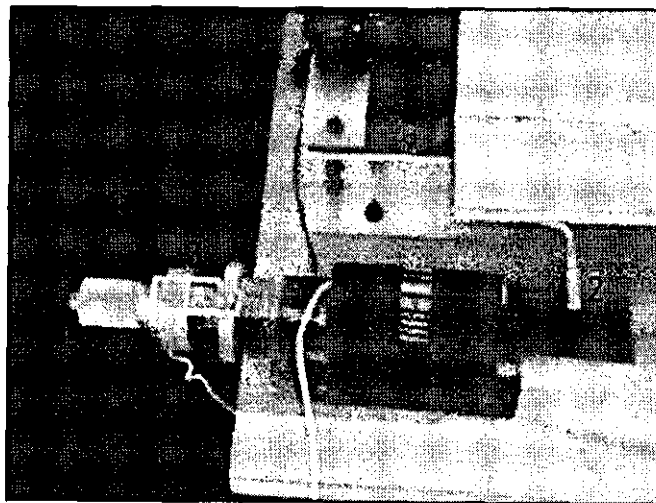
Figure 7.1.5 Feed per revolution measurement

The primary drive for the plotter head runs from the motor via a wormwheel (behind the plate shown in (1), through the Norton gearbox shown in figure 7.1.6. Gears are carried

126

on two shafts, (2), and (4). Provision has been made for future research using multi knife plotter heads, through the use of gear ratios allowing one oscillation of the sine crank for each single revolution of the cutterhead, and 2, 4, and 6 oscillation cycles per revolution, allowing the simulation of single, 2,4, and 6 knife cutterheads. The idler gear (3) is mounted on sliding rails (2) to provide compensation when using driving gears of varying sizes. The idler gear may be lifted to break the connection between the cutterhead and the sine crank in order to adjust the angle of lag. The output to the sine crank runs through the leftward bevel gear (5), and the output to the plotter head runs through the chain drive sprocket shown to the right (6).
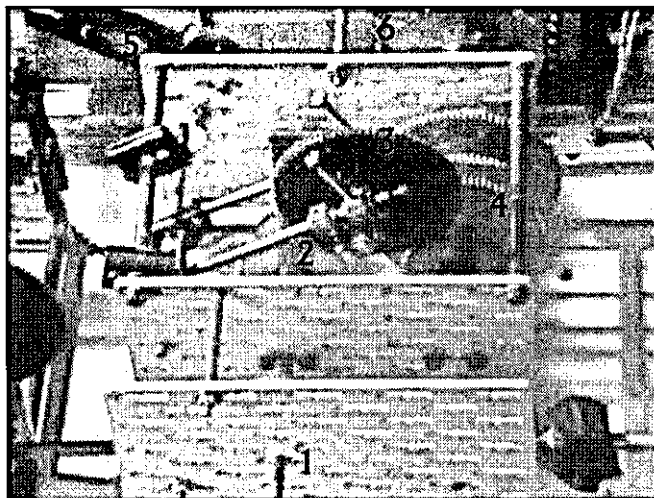
Figure 7.1.6 Primary gearbox

127

The sine crank shown in figure 7.1.7 is used to provide the cutterblock oscillation waveform. The sine crank is adjusted by a screw (1) against a tension spring in order to adjust the radial position of the crank (2). This adjustment will change the degree of plotter head oscillation, representing the degree of cutterblock oscillation used in an actual system. This crank works a connecting rod (3) which in turn drives the sliding element containing the plotter head lower bearings (4). A graduated indicator, marked in degrees (5) is used in the adjustment of phase lag between the plotter head and the sine crank

In order to check the degree of plotter head oscillation used, a dial gauge is mounted on the rail (5) which connects with the sliding element via an aluminium disc (6).
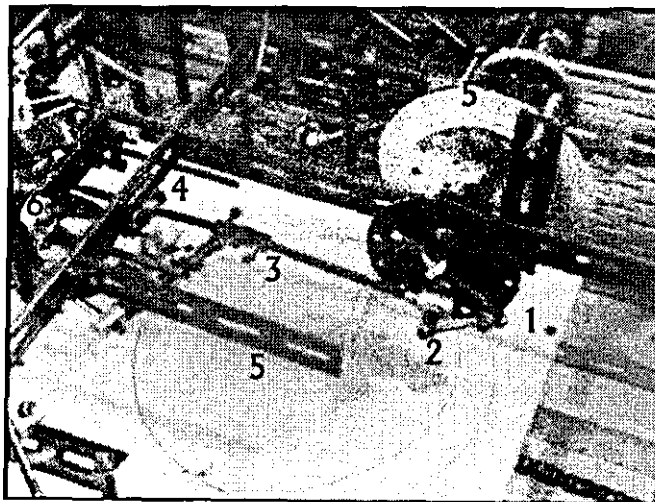
Figure 7.1.7 Cutterblock oscillation mechanism

7.2 Machine modifications

The set of results shown in chapter 8.1 shows the results of early machine operations. The output was relatively noisy due to mechanical faults in the machine, and it was decided that a degree of machine redesign was necessary in order to produce a good set of results.

The main bearing for the plotting head was initially a plain bearing. Performance was poor with a degree of play in the bearing. This bearing was replaced by two vertically spaced ball bearings, 30mm apart. This virtually eliminated any slackness and chatter in this part of the machine which had been noticeable as backlash on plots produced with cutterblock oscillation.

Several drive methods were tried, the original cardan shaft drive from the motor to the gearbox being a temporary solution. The use of a section of flexible PVC pipe provided a coupling low in vibration.

The transmission of power from the motor to the variable speed drive and the plotting head gearbox was proving unreliable. This had originally been carried out using two separate gearboxes linked with an idler gear. A more direct approach was to use a main drive shaft, with power being transmitted to each section of the machine using wormwheels, combined with simple further reduction gearing if required. The shaft on which the wormwheels now terminates in a relatively heavy (500g) flywheel, which runs at full motor speed. Drive to the cutting head is now consequently smoother and virtually backlash free.

The mounting method for the frictional element in the variable speed drive has been changed. Originally, drive was transmitted from the frictional drive to the output shaft to the drive chain by 3 equally spaced ball bearings sitting in small recesses in the frictional backing disk to a flat faced gear. The torque was limited by a holding spring, which also held the drive wheel against the frictional disk. Unfortunately as the drive wheel was adjusted it was necessary to clamp the frictional disk to the flat faced gear in order to prevent loss of the ball bearings. This soon became a nuisance and the frictional disk was simply glued to the flat faced gear. Setting up of this machine now had to be more precise, since the disk positioning mechanism was no longer self compensating. The improvement in ease of machine running however, more than made up for this.

7.3 Data capture

After plotting, the cutter loci plots were originally scanned as TIFF (Tagged Image Format File) images using a scanner resolution of 39 pixels / mm. The advantage of TIFF images is that the processing software used could operate directly on these images without having to convert the files, saving processor time. The TIFF images were converted into raw images using Paint shop Pro software, and then imported into Matlab for re-scanning. In this way it is possible to adjust for any inaccuracies in positioning of plots on the scanner. Since the results were now stored in Matlab, it was possible to provide a direct comparison between simulated effect of cutterblock oscillation, and the experimentally obtained results on the same plots. The first sets of results called for an improvement in image resolution however.

7.4 Post processing

Hardware limitations (the machine available for scanning was a 386 PC of limited processing power and storage) meant that the TIFF images were unduly large to store, and port to the machine used for post processing. Instead, images were stored in GIF format, which utilises a degree of image compression. A serial RS232 link was employed for data transfer of image files. Since the images were purely black and white, no appreciable loss of quality resulted from the image compression. Thus in the same file size it was now possible to handle images of 60 pixel /mm resolution. The images were then converted into raw file format on the processing machine.

Images were backed up on the local Sun network, allowing rapid conversion of backed up copies of plots produced by all simulations, timber surface and hydraulic servo, into PC readable format (GIF).

Figure 7.4.1 shows the method of data management used during this stage of the project.
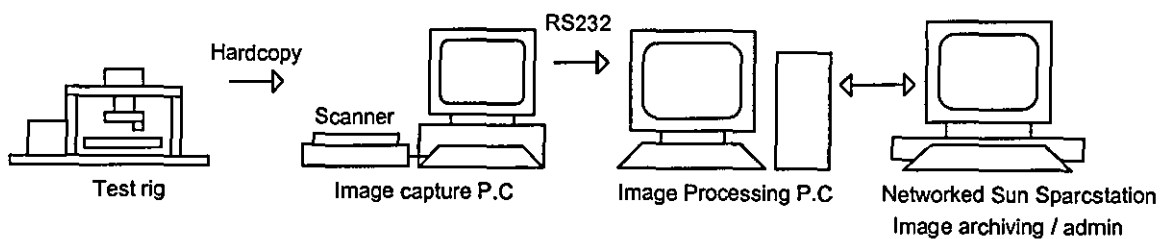
Figure 7.4.1 - Flow of data during experimentation

7.5 Data Extraction

Data is extracted to produce a regularly spaced histogram using straightforward Matlab looping software. Scanning the raw image, which corresponds to 255 grey scale levels. Bearing in mind that only a Bi-Tone image (Pure black and white) has been ported to Matlab as a raw image file, the software has to pick between the values 255 (white), and 0 (Black) only. The type of image which is ported to Matlab for processing is shown in figure 7.5.1, showing an image of a cutter plot taken with a low feedrate, and figure 7.5.2, showing an image of a cutter plot taken with a high feedrate.

232 pixels

3068 pixels
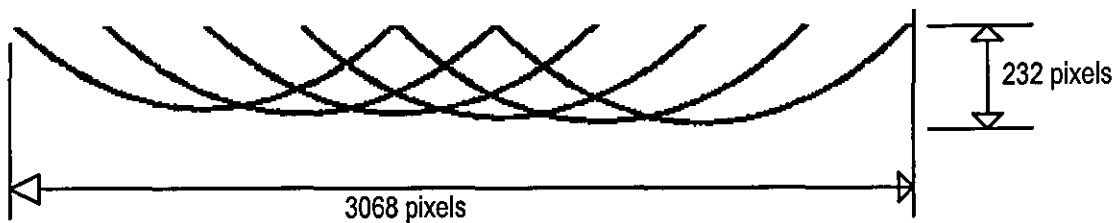
Figure 7.5.1 Image of a cutter plot taken with a low feedrate, 60 pixels/mm

232 pixels

3068 pixels
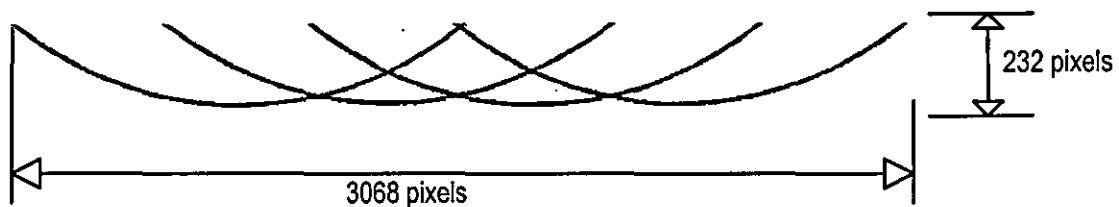
Figure 7.5.2 Image of a cutter plot taken with a high feedrate, 60 pixels/mm

A nested loop is used to produce a histogram of regular horizontal spacing. The top surface of the histogram is plotted to show the experimentally obtained surface finish. The software used to perform this operation is listed in appendix 1.

133

8.0 Results

8.1 Hydraulic servo simulations

Hydraulic servo simulations were carried out with several aims.

To begin with, after checking the robustness of the model and debugging of simulation code, simulations of the hydraulic servo under ideal conditions were carried out. These tests were carried out in order to check that the simulation was reliable enough to port the actuation wave produced by these simulations to the timber surface generator software.

Servo phase lag could adversely affect the quality of the timber surface form, so a further batch of simulations was run in order to define the operating boundaries at typical actuation frequencies.

Secondary effects are briefly examined, these simulations show interesting characteristics of the hydraulic simulation and reveal second and third order effects which must be taken into account when running the overall simulation.

8.1.1 Servo under ideal conditions
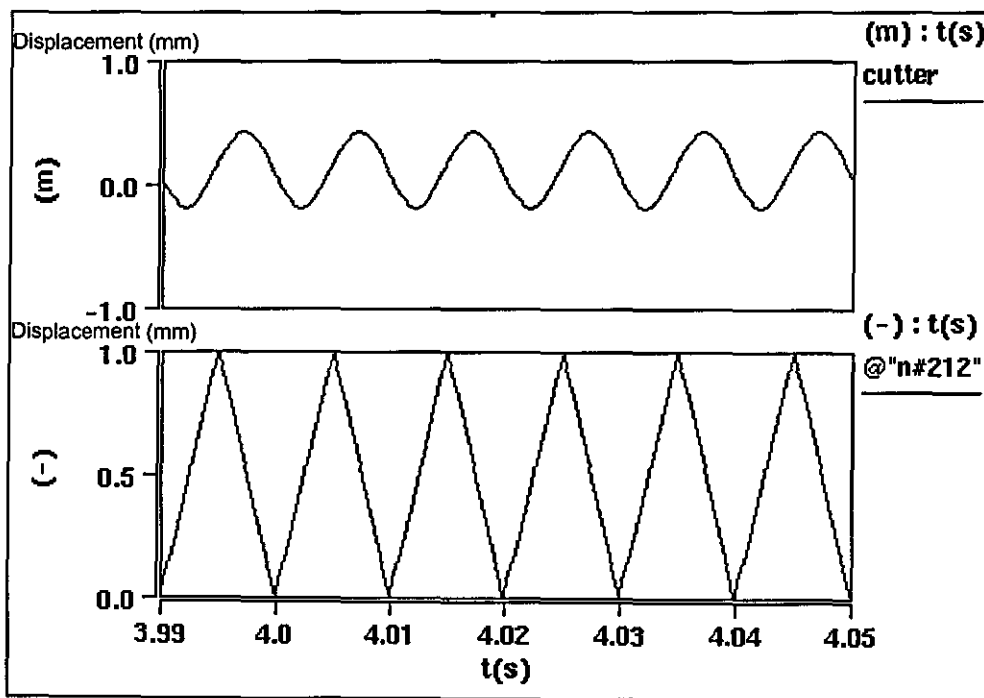
Figure 8.1.1.1 Servo under ideal conditions, triangular wave control signal - 1
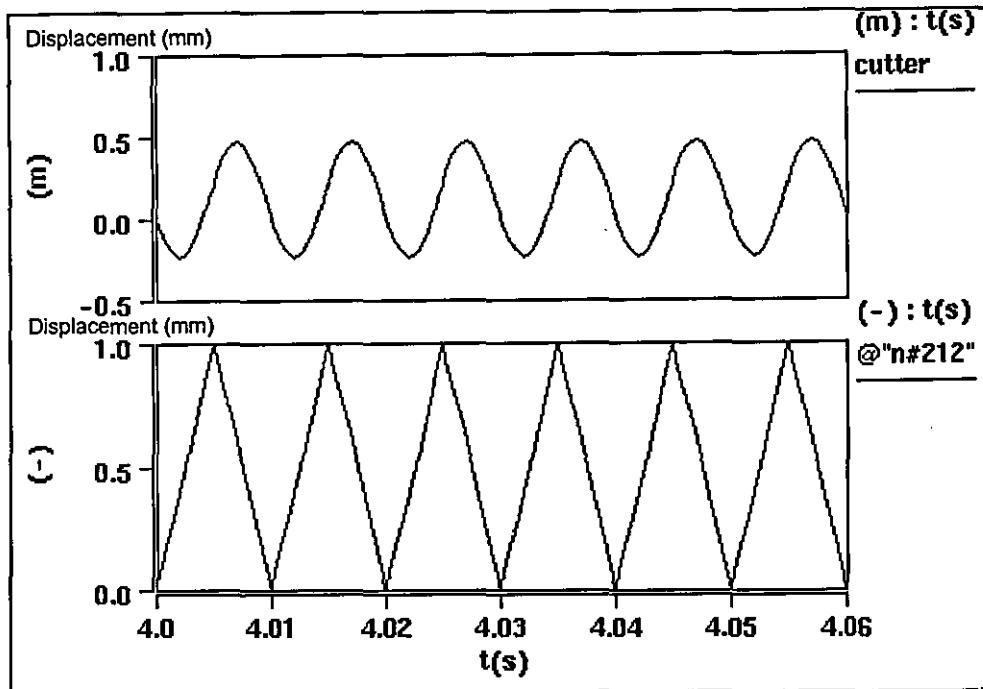
Figure 8.1.1.2 Servo under ideal conditions, triangular wave control signal - 2
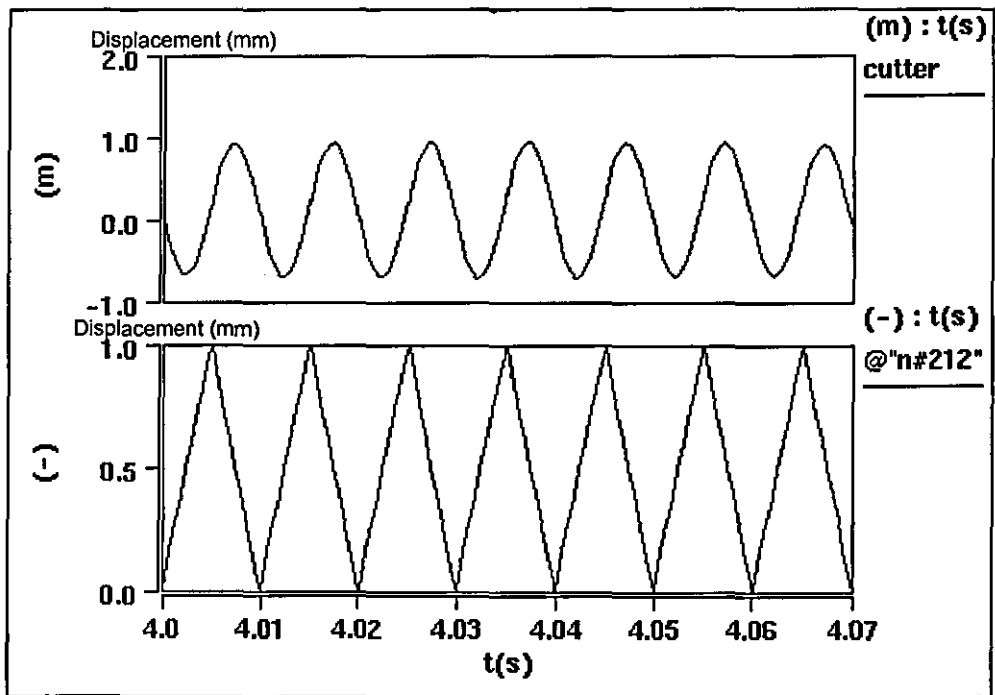
Figure 8.1.1.3 Servo under ideal conditions, triangular wave control signal - 3

136
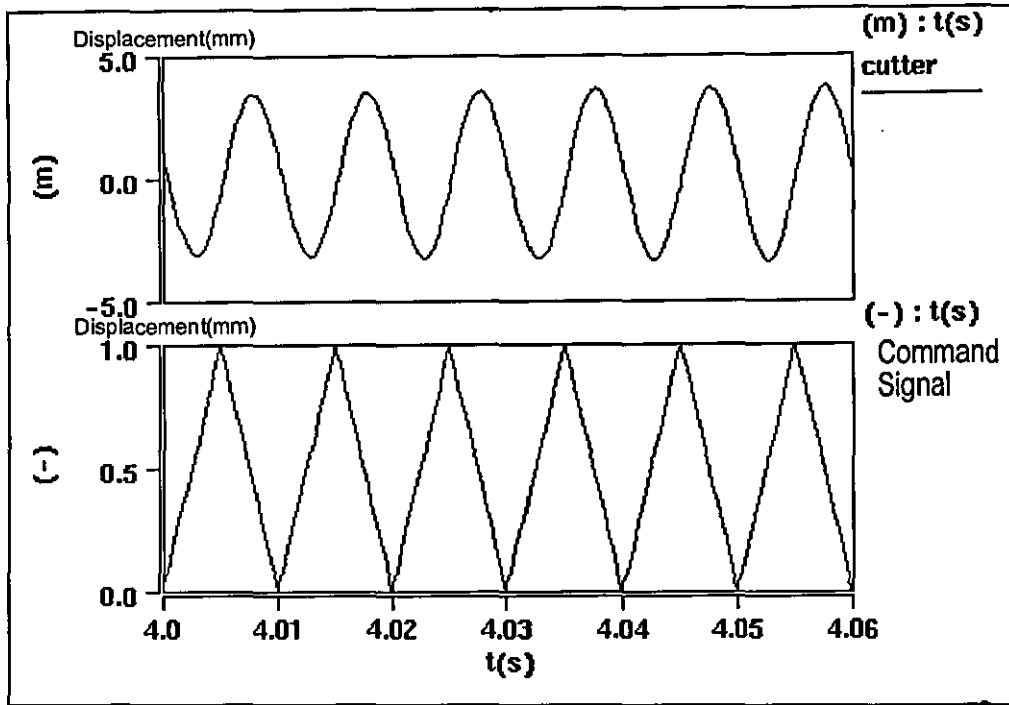
Figure 8.1.1.4 Servo under ideal conditions, triangular wave control signal - 4
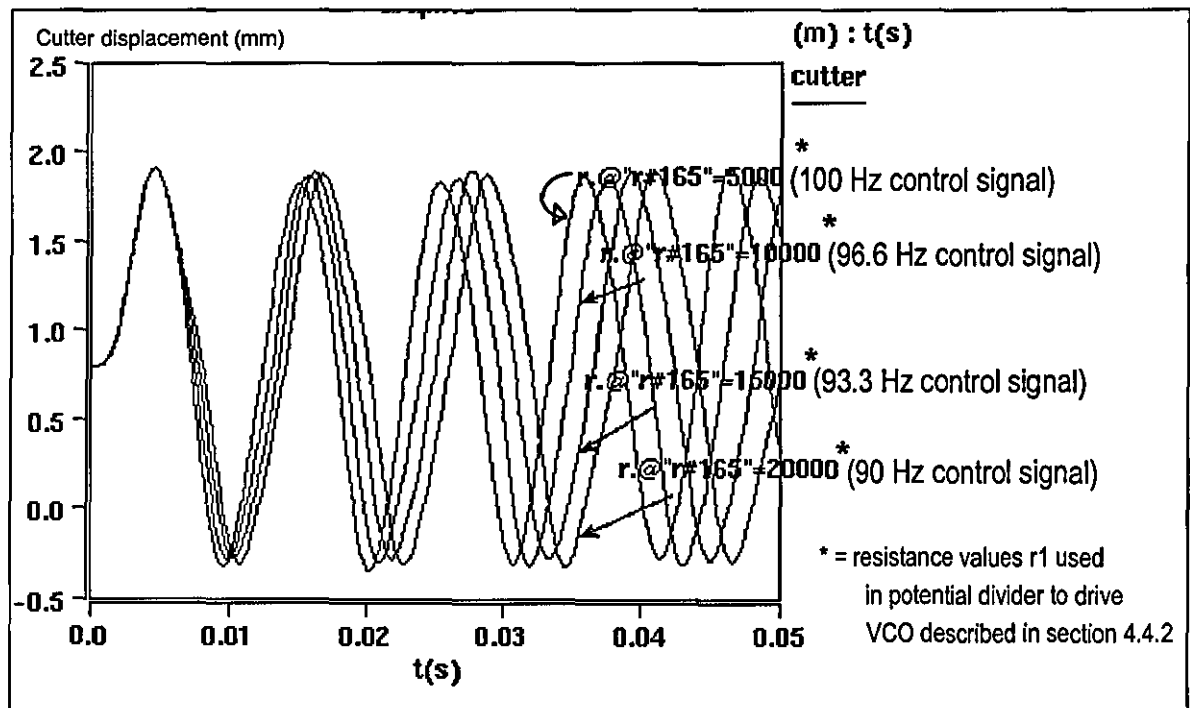
Figure 8.1.1.5 Output signals at start-up for varying frequencies
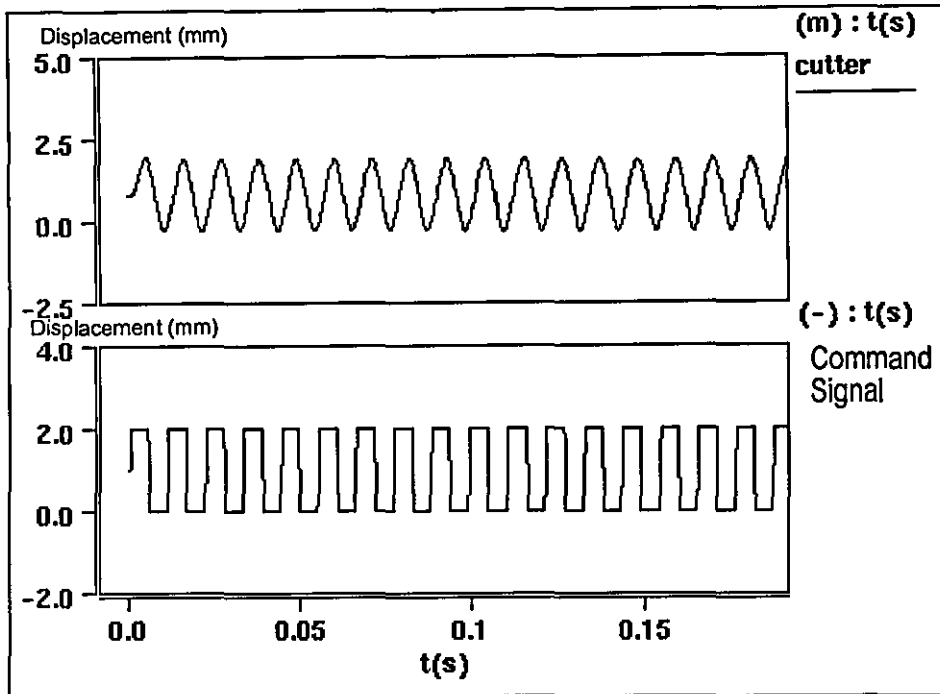
Figure 8.1.1.6 Square wave response

8.1.2 Servo lag for high level system developed using Saber™

Frequency of excitation was 100Hz to produce the plots shown in figures 8.1.2.1 to 8.1.2.3, the highlighted points shown on the plots were part of an automatic peak finder, featured within the Saber™ simulation viewer, and were used to compute servo phase lag.

Figure 8.1.2.1 Servo lag 1 - Saber™ model

138
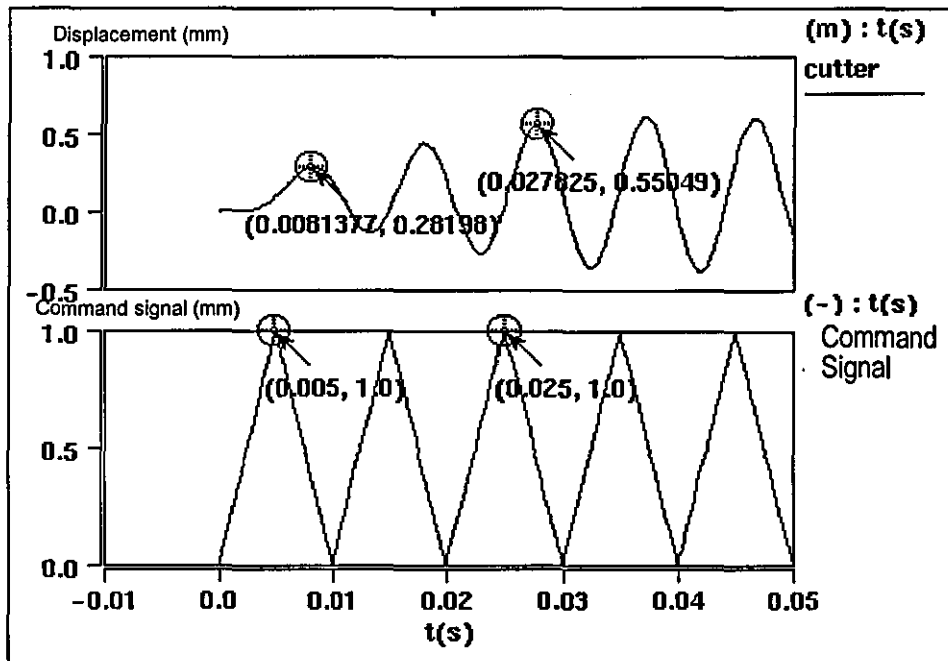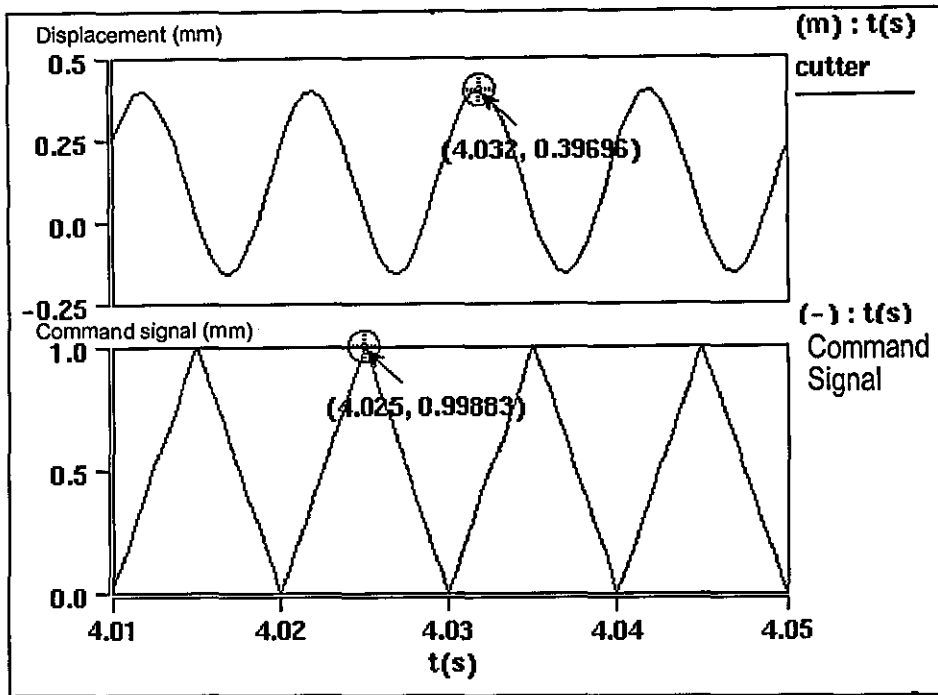
Figure 8.1.2.2 Servo lag 2 - Saber™ model
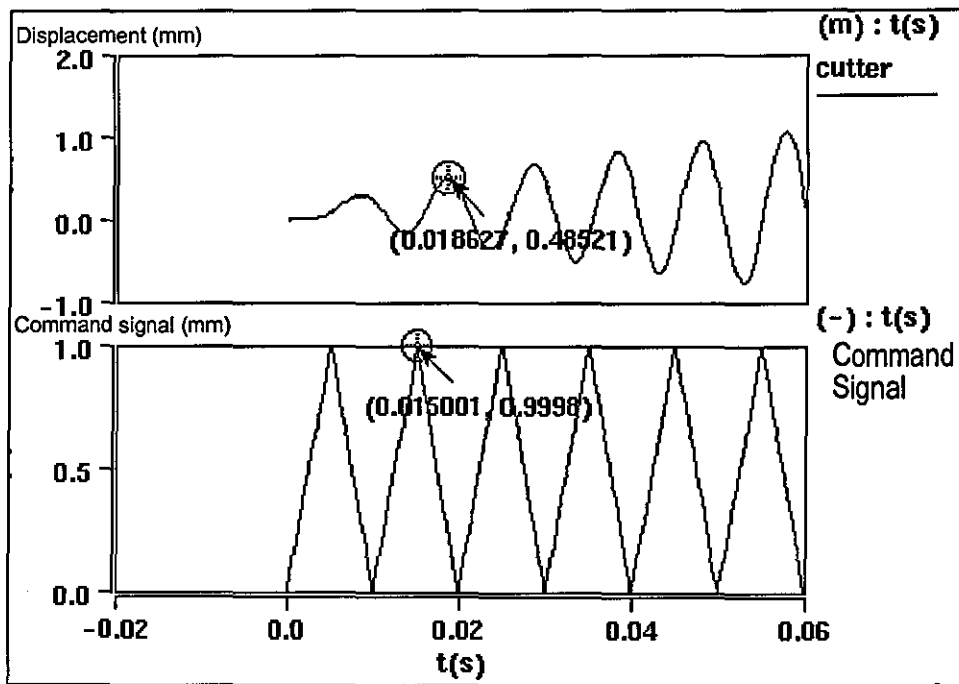
Figure 8.1.2.3 Servo lag 3 - Saber™ model

139

8.1.3 Servo lags for Simulink based model

The Simulink based model was able to be more easily swept over a range of frequencies, and produced the plots shown in figures 8.3.1.1 to 8.3.1.7 which were used to compute servo phase lag for the Simulink based model.
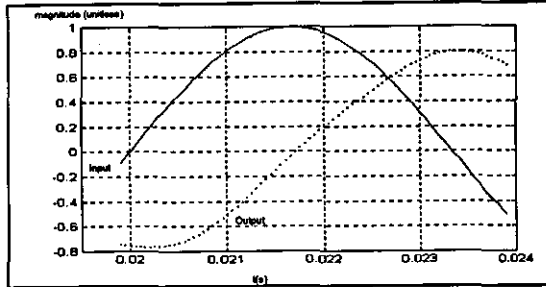
Figure 8.1.3.1: 150Hz, 0.00175s delay
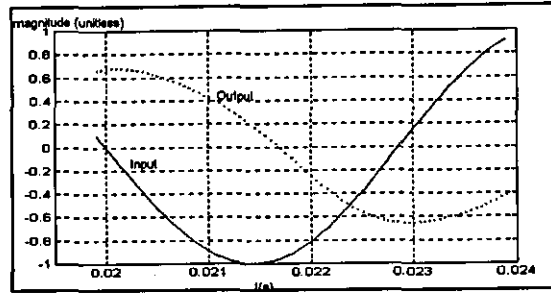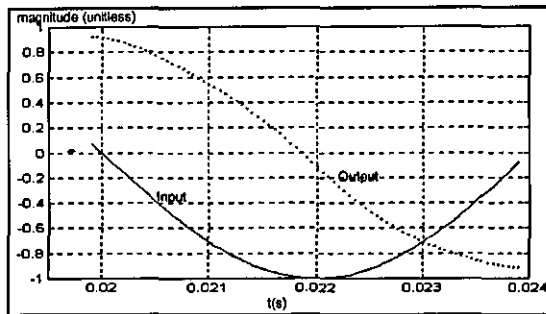

Figure 8.1.3.2: 160Hz, 0.00175s delay

Figure 8.1.3.3: 170 Hz, 0.0018s delay
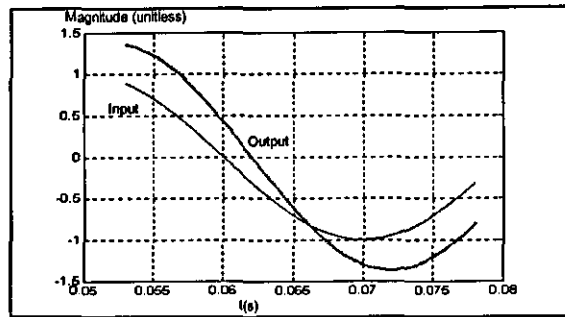
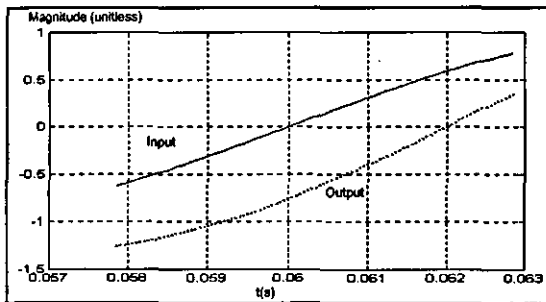Figure 8.1.3.4: 180 Hz lag = 0.002s delay

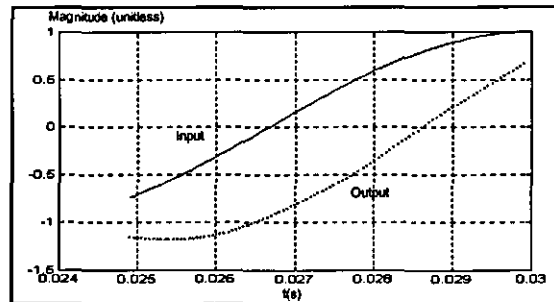Figure 8.1.3.5: 190Hz, 0.002s delay
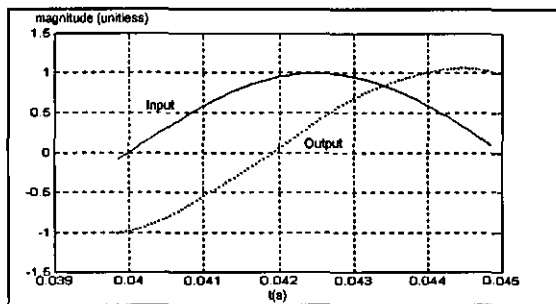

Figure 8.1.3.6: 200 Hz, 0.002s delay

Figure 8.1.3.7: 210 Hz 0.00225s delay

140

8.1.4 Secondary effects

This section shows the results obtained from high level Saber™ simulations, and show interesting second and third order effects typical of a hydraulic servo, particularly in the form of low frequency superposition.
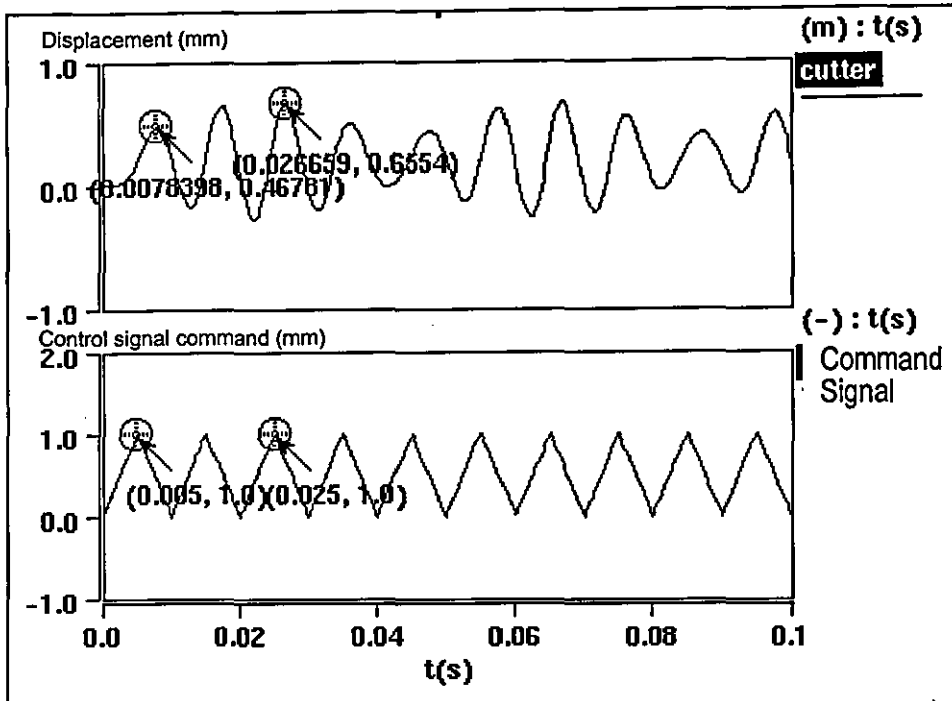

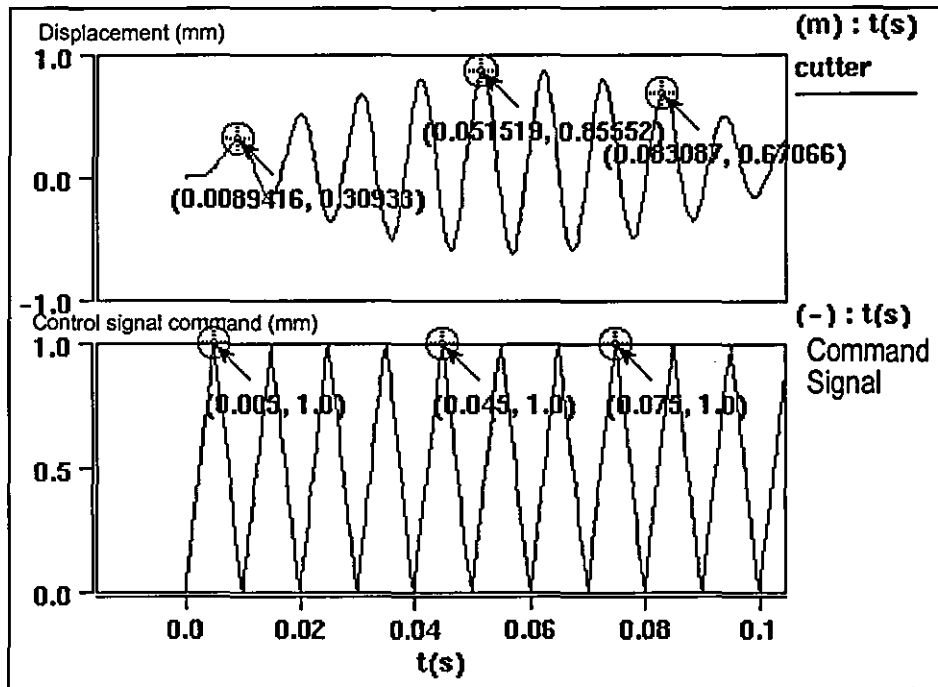Figure 8.1.4.1 Low frequency superposition - 1

Figure 8.1.4.2 Low frequency superposition - 2

141

8.1.5 Operating near to the resonant peak

The bode plot shown in figure 8.1.5.1 shows the frequency response of the hydraulic servo model, and suggests resonant behaviour in the region $1.25e5$ rad.s^{-1}
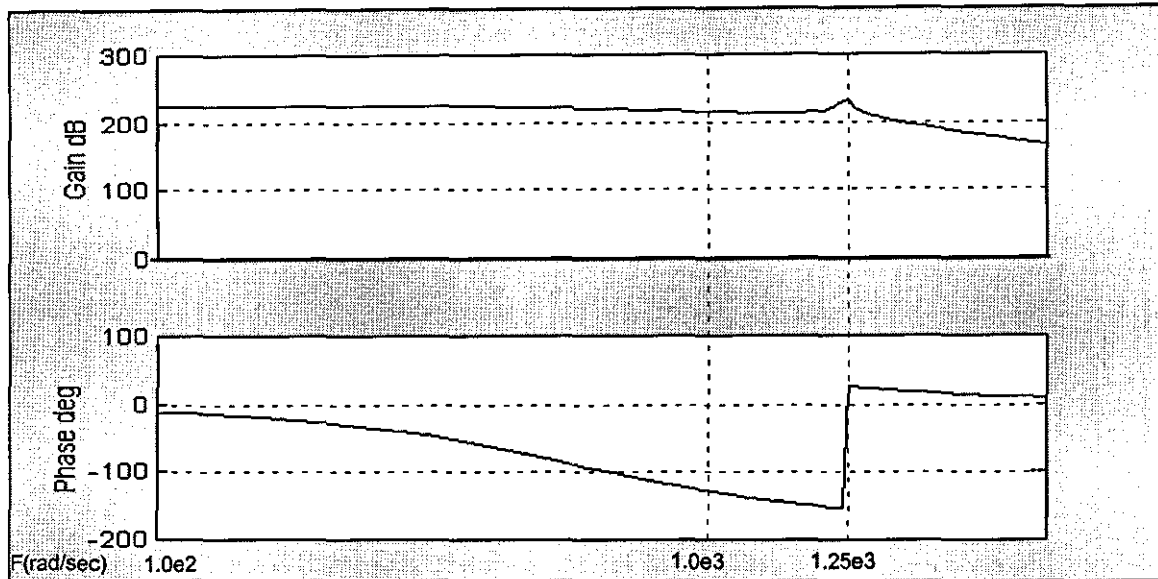

Figure 8.1.5.1 Bode plot for servovalve and servo

The following two plots, figure 8.1.5.1 and 8.1.5.2 are the results of transient simulations where the actuation command signals were varied in a region close to resonance. 5 simulations are shown in each figure.
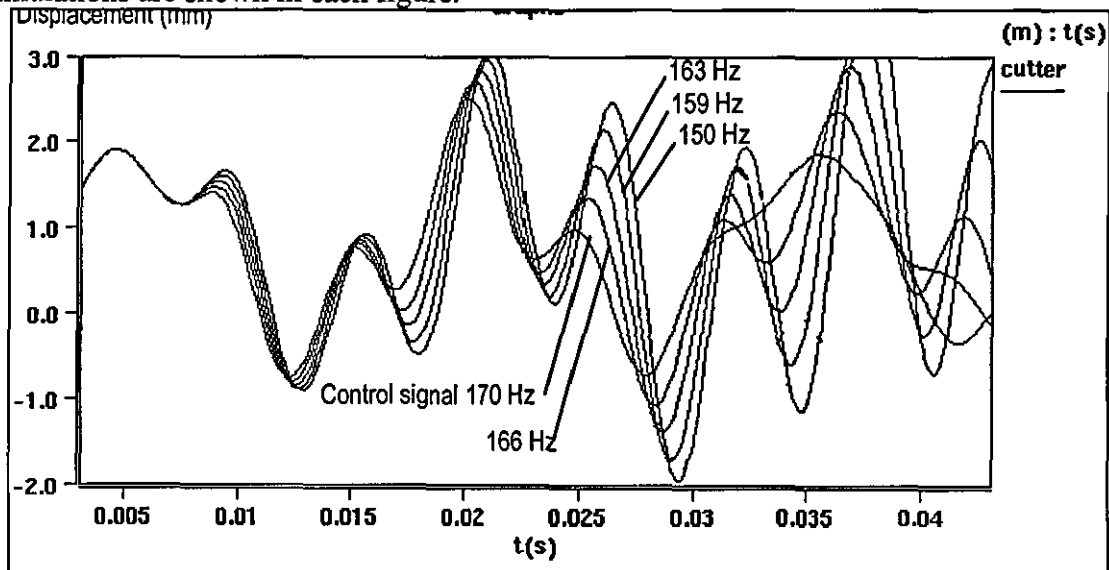

Figure 8.1.5.2 System operating near resonance - 1
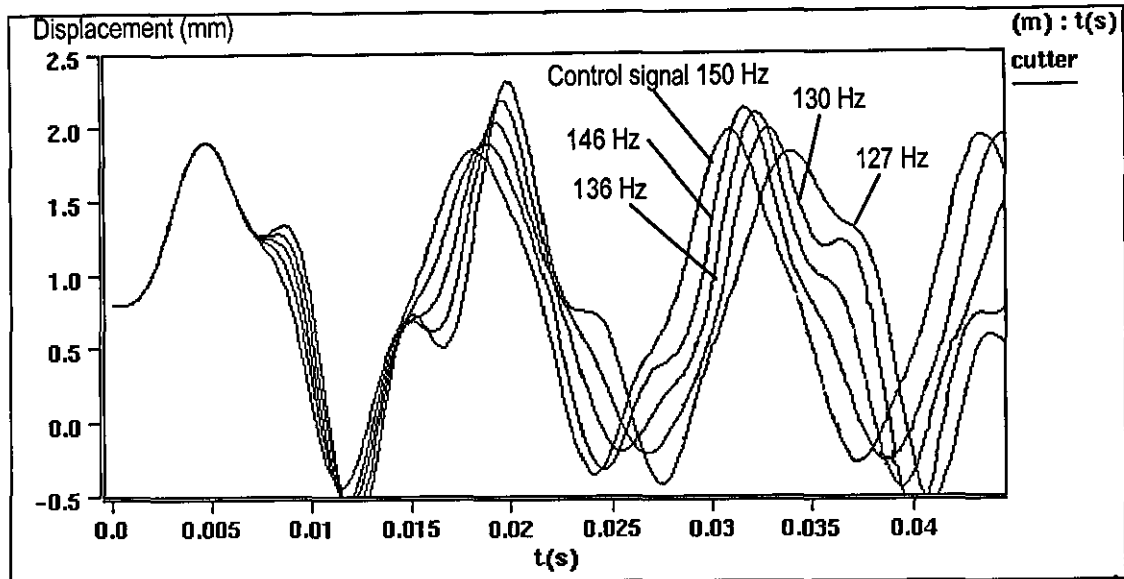
Figure 8.1.5.3 System operating near resonant peak - 2

8.1.6 Effect of square wave odd harmonics on reduced stiffness system

Bulk modulus was reduced by 30% for the plots shown in figures 8.1.6.1 and 8.1.6.2, the actuation signal for the simulation which produced the plot shown in figure 8.1.6.1 was a square wave.
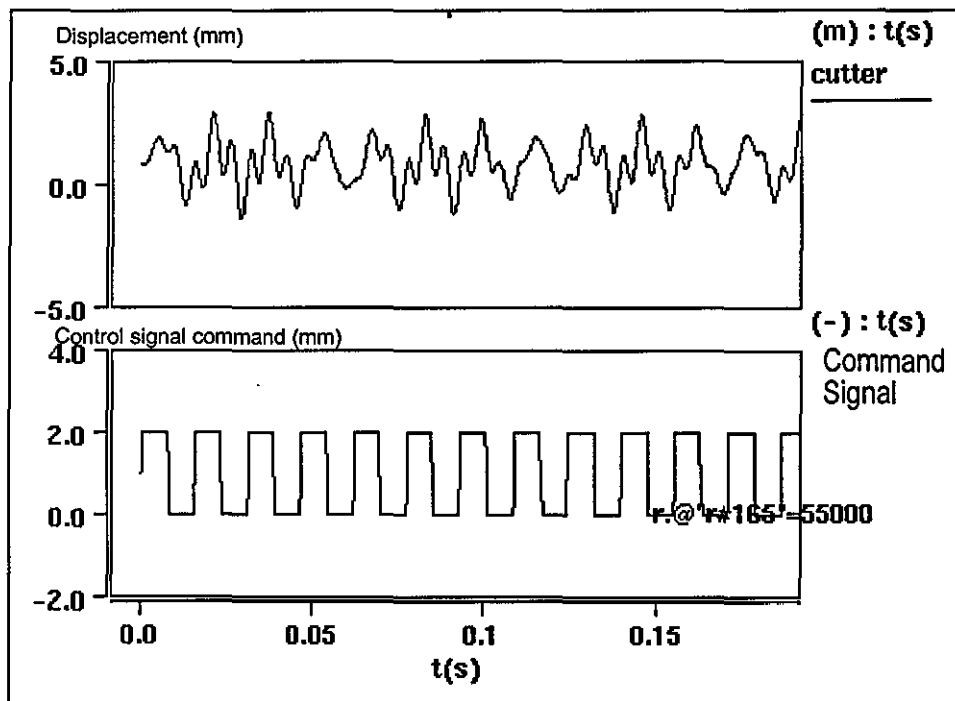
Figure 8.1.6.1 Low stiffness system with square wave actuation

143

8.1.7 Effect of triangular wave upon reduced stiffness system

Generally the same machine parameters were applied as those which produced the plot shown in figure 8.1.6.1, in order to produce the following plot, shown in figure 8.1.7. The only exception was the different actuation signal, since this simulation used a triangular wave.

Figure 8.1.7.1 Low stiffness system with triangular wave actuation

144

8.2 Timber surface simulations

The colour loci plots included in section 8 show the cutter tip loci at the timber surface, and include the results of 5 simulations on each image. In order to interpret these images it is necessary to know the colour progression which is employed.
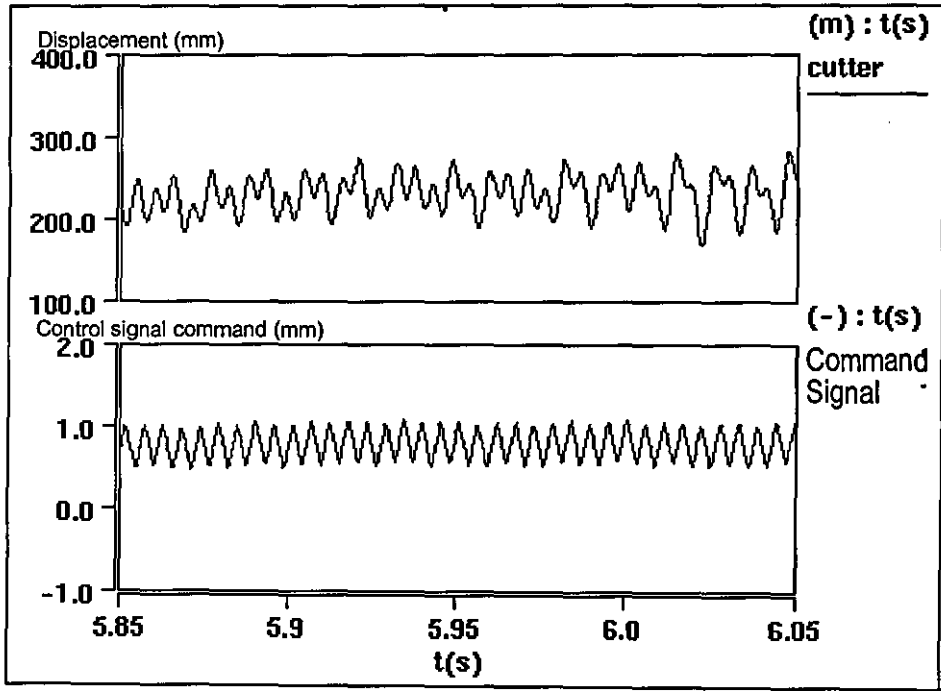
The colour progression is:

1 - Purple   2 - Cyan   3 - Red   4 - Green   5 - Blue

Consider figure 8.2.1. This is a close up of a group of simulations using cutterblock oscillation where 100% = 0.5 of feed/rev. This means that the *maximum* amount of cutterblock oscillation employed is half of the material feed per cutterblock revolution. These amounts are unitless, i.e. the model is transparent to tooling dimensions. For example, if the feedrate were to be 4mm per revolution, the oscillation amplitude would be 2mm, 20mm feed per revolution would produce a corresponding oscillation of 10mm.

Considering figure 8.2.1, oscillation amplitude is in steps from 0 to 100%, 25% steps, pure sine wave oscillation. This means that the spacing of the steps is 25%, minimum amplitude is 0% (i.e. conventional tooling path), and the maximum amplitude is 100% where 100% equals half of the feed per revolution as stated above. This information may then be combined with the colour progression in order to produce the table below. When other parameters are altered, phase lag for example, the colour progression is the same, and plots may be interpreted in the same way.

1 - Purple	0	x Feed per revolution
2 - Cyan	0.125	x Feed per revolution
3 - Red	0.25	x Feed per revolution
4 - Green	0.375	x Feed per revolution
5 - Blue	0.5	x Feed per revolution

The axes on the loci plots are also unitless, and represent a knife tip radius of 0.1, which may be scaled to represent a cutterblock of any size. The centre of the cutterblock exists therefore at cartesian coordinate $Y = 0$, and the knife tips *lowest* point is -0.1.
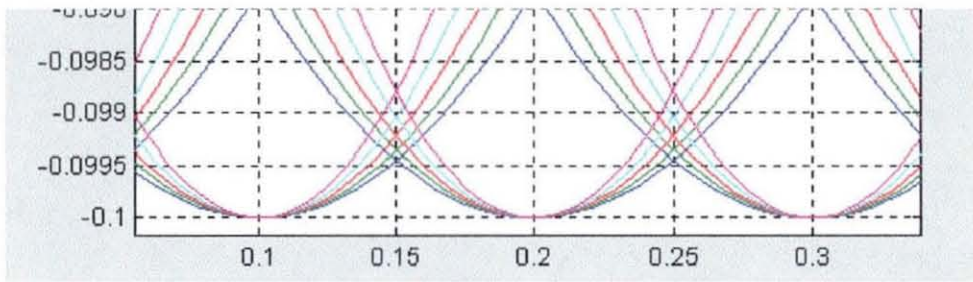
Figure 8.2.1 - Example cutter loci plot.

145

8.2.1 Pure sine wave

Pure sine wave oscillation simulations are first shown using the Matlab surface simulation algorithm. For comparison, these results are then produced using the Simulink model, to show the portability and repeatability of the model.

Figure 8.2.1.1 No oscillation

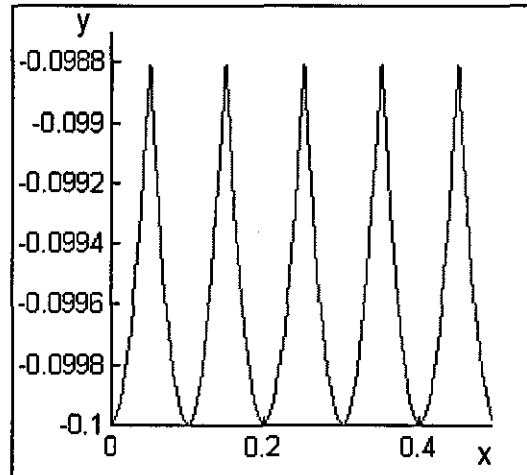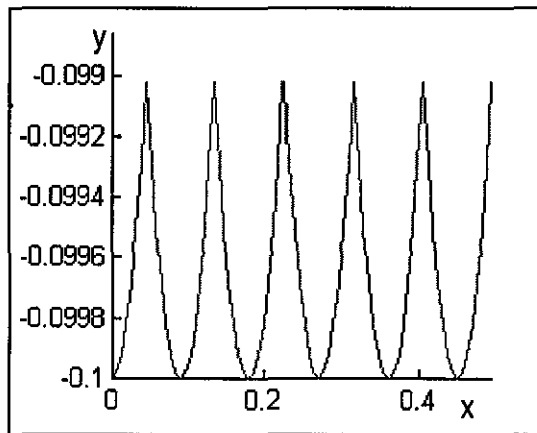Figure 8.2.1.2 Pure sine oscillation, 10% of feed/rev
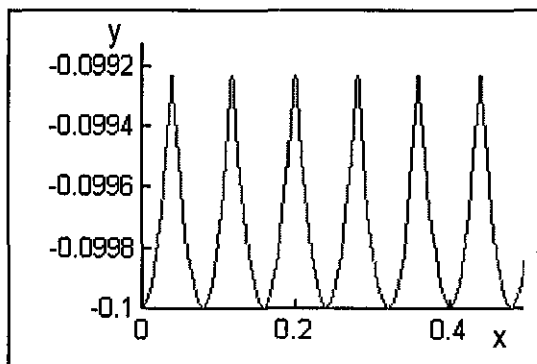
Figure 8.2.1.3 20% of feed/rev pure sine oscillation

146

Figure 8.2.1.4 30% of feed/rev pure sine oscillation

Figure 8.2.1.5 40% of feed/rev pure sine oscillation

Figure 8.2.1.6 50% of feed/rev pure sine oscillation

Figure 8.2.1.7 60% of feed/rev pure sine oscillation

Figure 8.2.1.8 70% of feed/rev pure sine oscillation

147

Figure 8.2.1.9 80% of feed/rev pure sine oscillation

Figure 8.2.1.10 90% of feed/rev pure sine oscillation
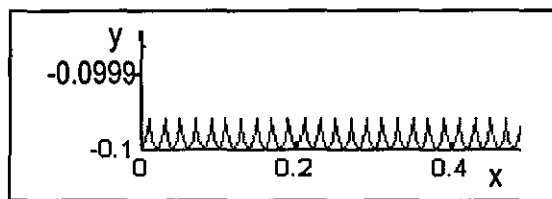
Figure 8.2.1.11 100% of feed/rev pure sine oscillation

The Simulink timber surface model was developed in order to produce a complete simulation of the timber surface and hydraulic servo. This also provided a means of checking the performance of the surface simulations against each other. Timber surface simulations under ideal conditions using the Simulink model and a sine wave cutterblock actuation waveform are shown in the following three plots.

Shown below is figure 8.2.1.12, oscillation 100% = 0.5 of feed/rev. steps from 0 to 100%, 25% steps, pure sine wave oscillation
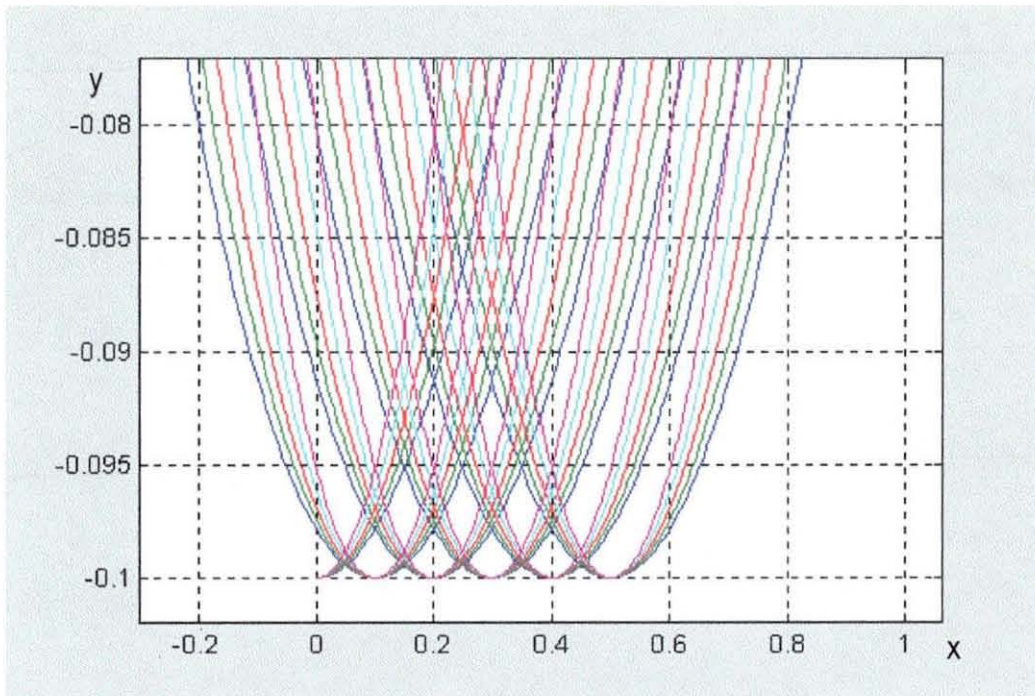
Figure 8.2.1.12 Simulink model using pure sine wave oscillation

Figure 8.2.1.13 shown below, is a zoom in on the above figure 8.2.1.12
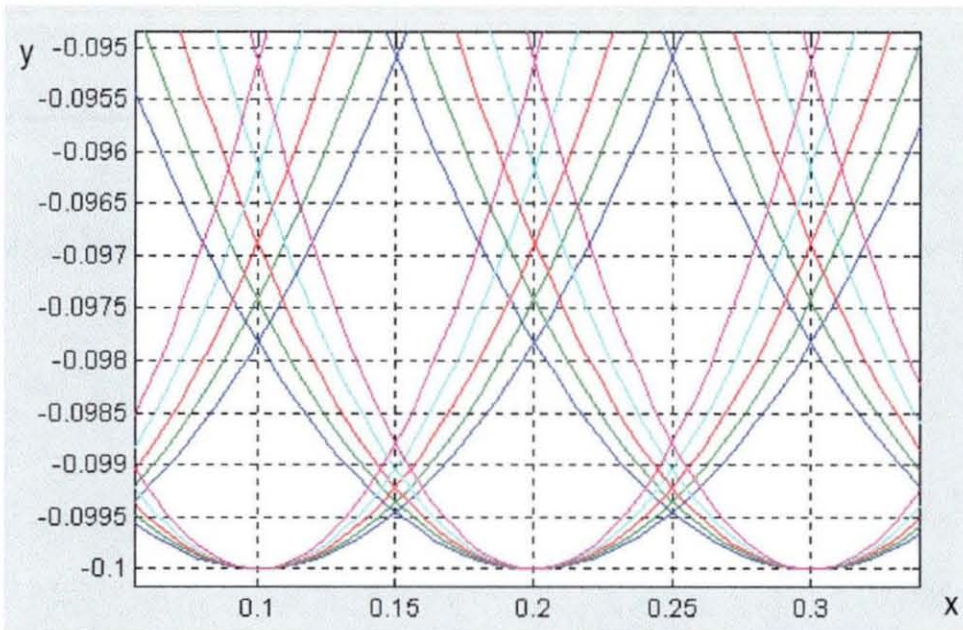
Figure 8.2.1.13   Zoom in of timber surface shown in figure 8.1.1.12

In figure 8.2.1.14 shown below is simulation plot zoom in 25% steps from 0 to 100% showing effect on cutter wave height where 100% = 100% of feed per revolution
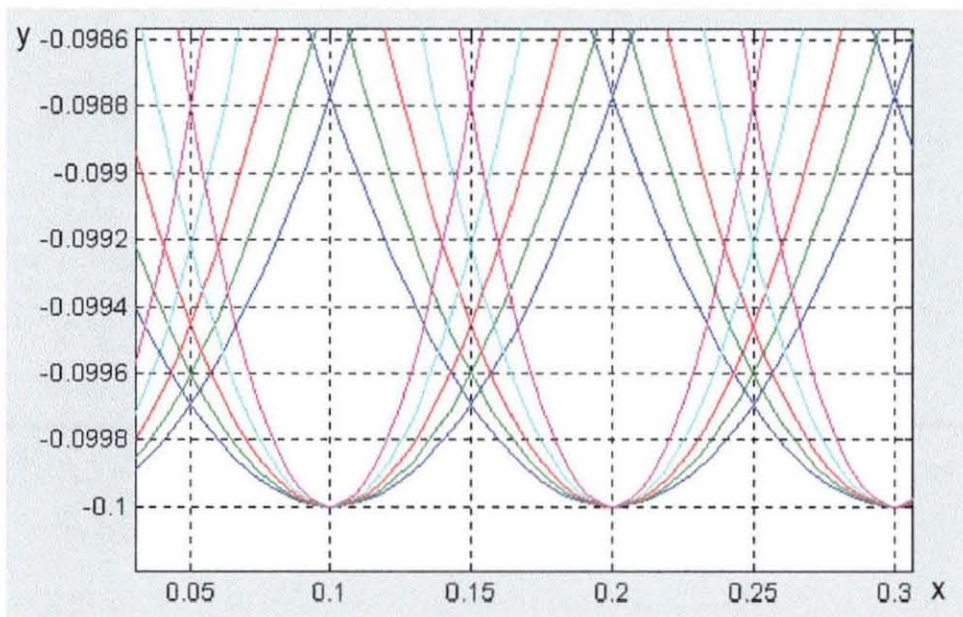
Figure 8.2.1.14. surfaces produced using Simulink model using sine oscillation.

150

8.2.2 Pure square wave

Square wave oscillation of the cutterblock in the amplitude range 0.1 - 1.0x feed/rev, was used for all of the simulations shown here in section 8.2.2.
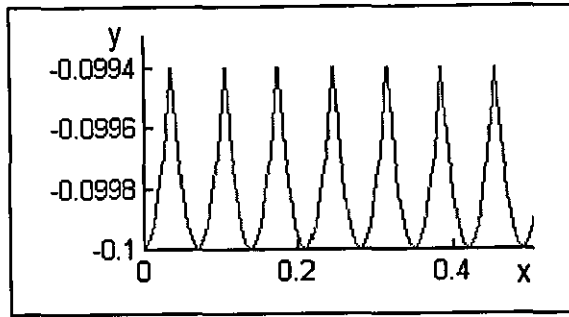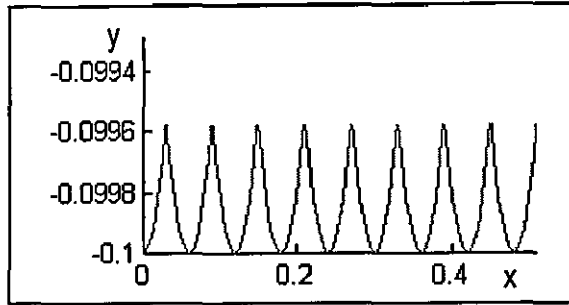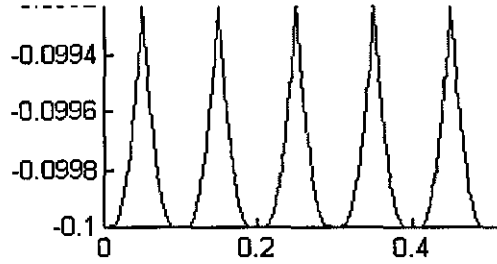

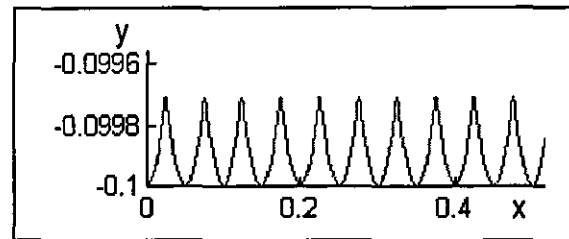Figure 8.2.2.1 0% of feed/rev pure square oscillation
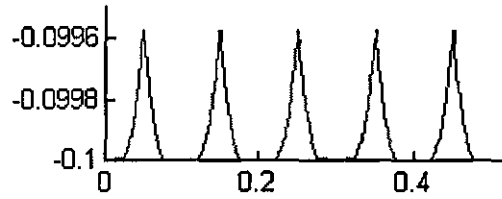
Figure 8.2.2.2 25% of feed/rev pure square oscillation
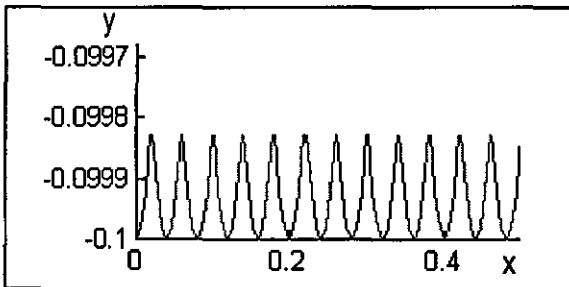

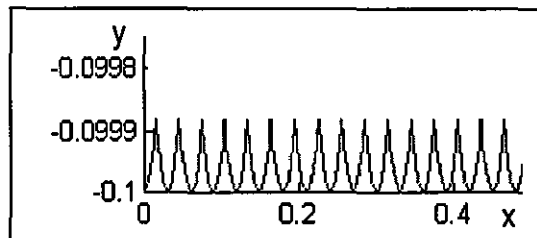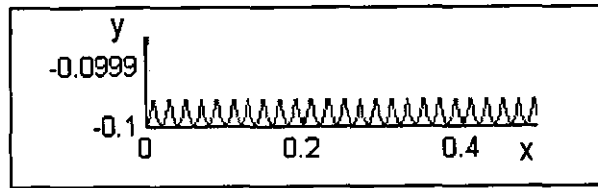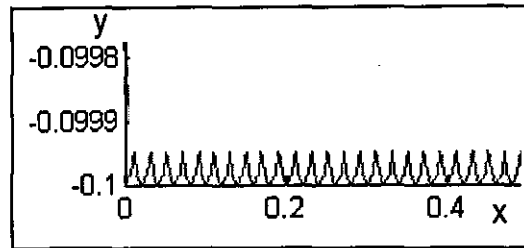Figure 8.2.2.3 50% of feed/rev pure square oscillation

Figure 8.2.2.4 75% of feed/rev pure square oscillation

151
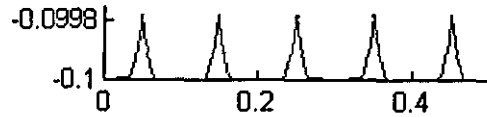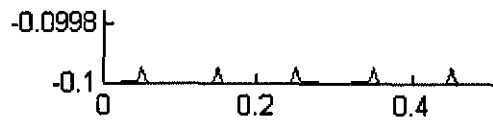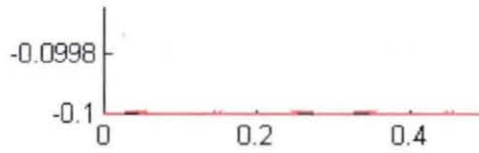
Figure 8.2.2.5   98% of feed/rev pure square oscillation

As described in the previous section, the validation of the Simulink model of the timber surface generator was carried out by producing results correspondent to those produced by the Matlab surface simulation code. The figure below (figure 8.2.2.6) shows a cutterblock oscillation simulation under ideal conditions using a square wave actuation waveform. Oscillation amplitude ranges from 0 to 100% in 25% steps.
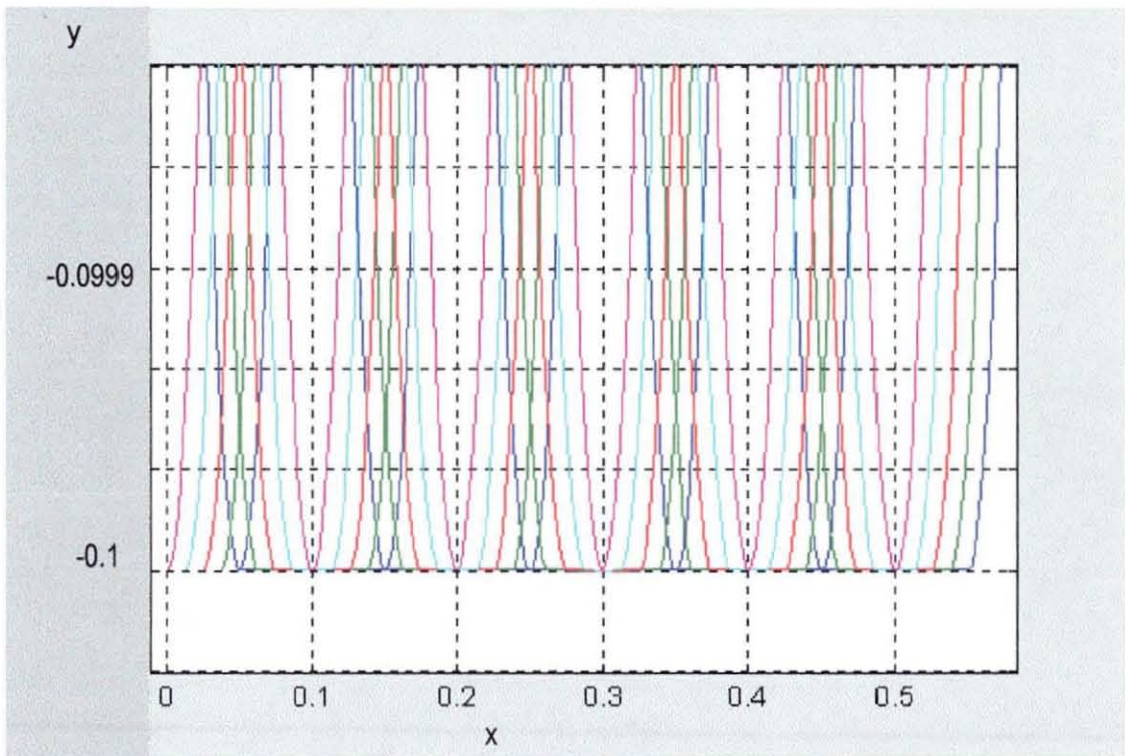
Figure 8.2.2.6 Simulink model of surface produced with pure square wave oscillation

Shown in figure 8.2.2.7 is a zooming in of the above figure showing the change in land width for each successive increment in oscillation amplitude.

152
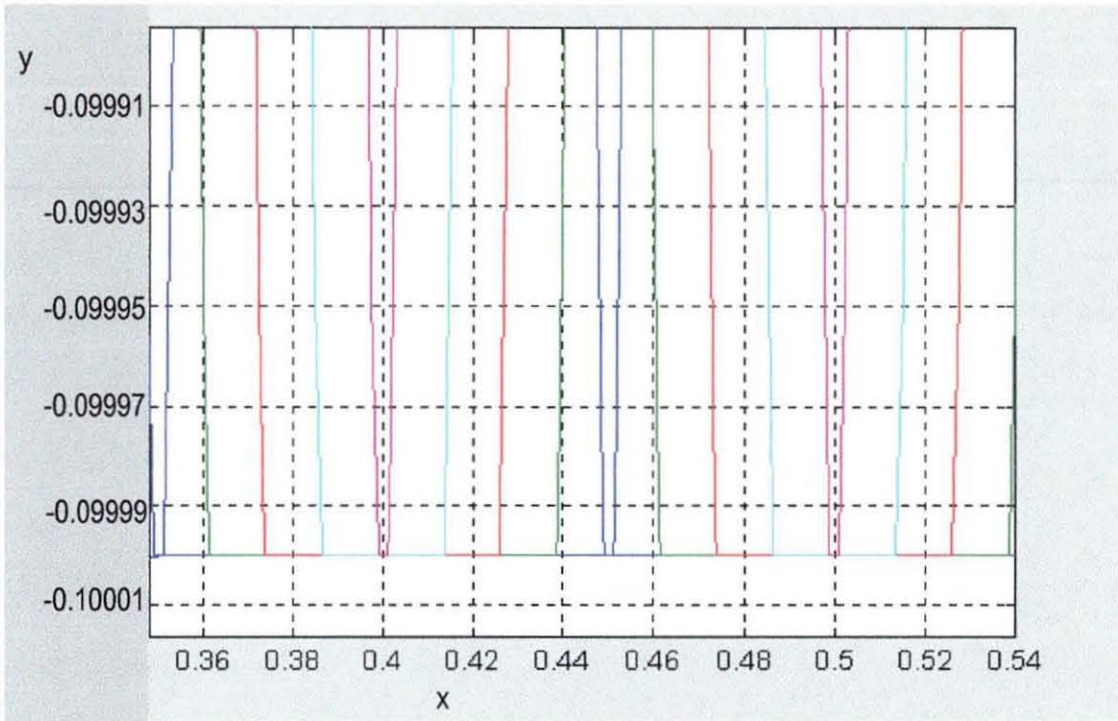
Figure 8.2.2.7 Pure square wave oscillation using Simulink model: zoom in on timber surface

8.2.3 Effect of phase shift

The following figure, 8.2.3.1, shows the actuation wave used to oscillate the cutterblock for the results shown in figures 8.2.3.2 to 8.2.3.9.
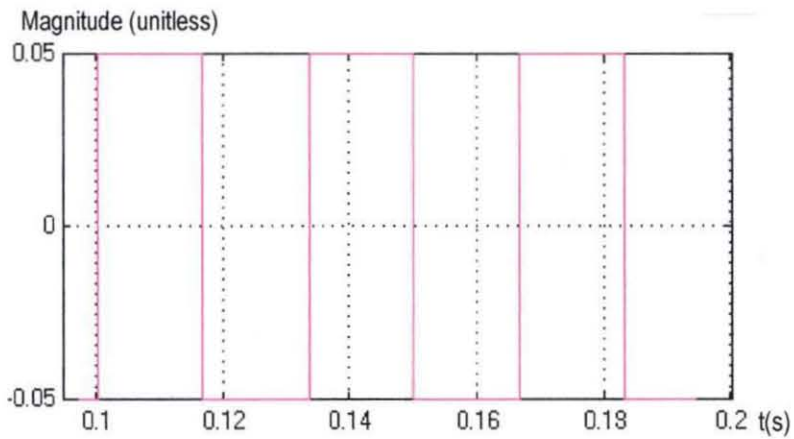
Figure 8.2.3.1 Square wave used to generate cutterblock oscillation

The surface form plots 8.2.3.2 to 8.2.3.9 are shown below, whereby 5 simulations are combined in each figure. The figure captions describe the amount of oscillation phase lag which was applied to the cutterblock oscillation model.
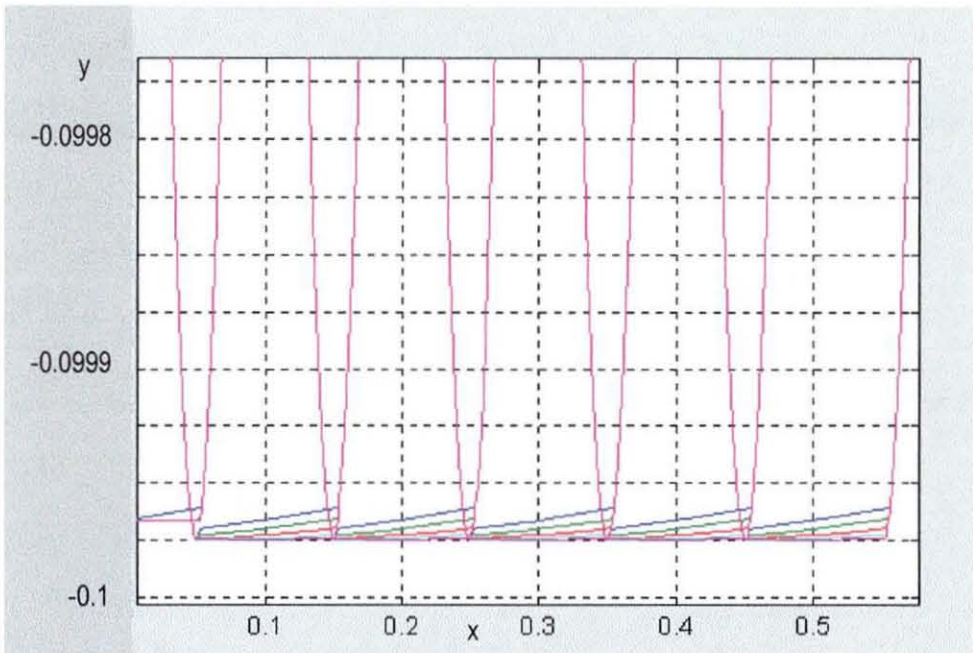
Figure 8.2.3.2   oscillation phase lag with varying time step from 0 to 0.020ms in 0.005ms steps
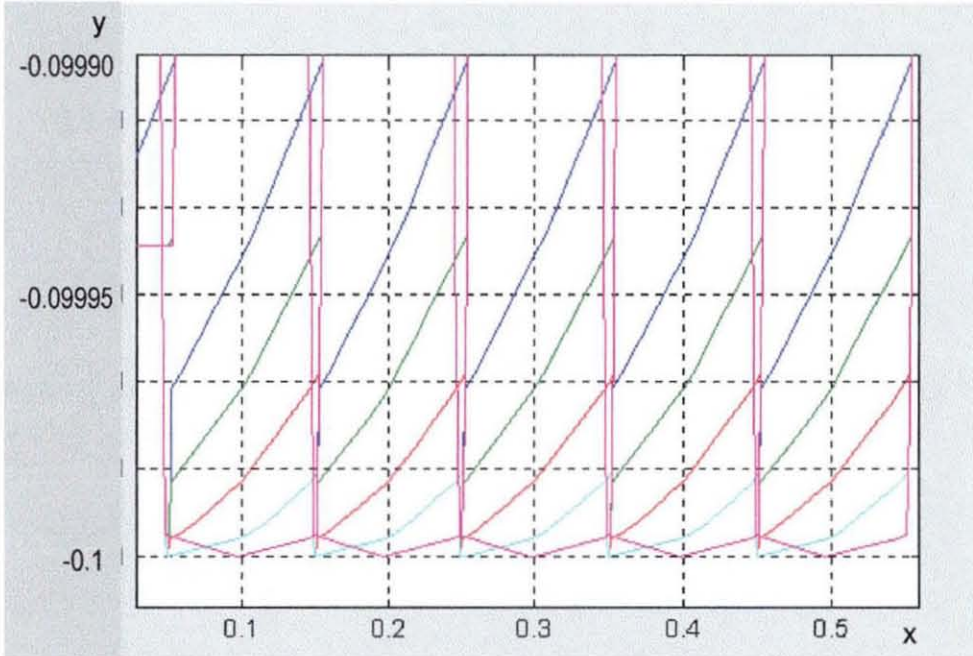
Figure 8.2.3.3   Zoom in using same parameters as 8.2.3.2
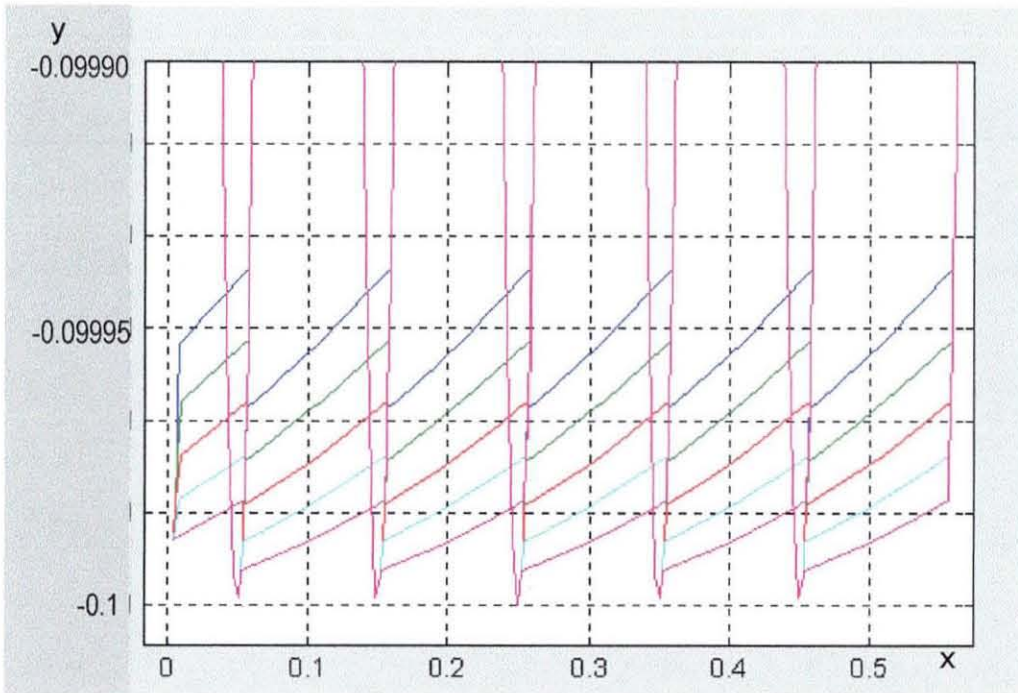
Figure 8.2.3.5 Zoom in using same parameters figure 8.2.3.4
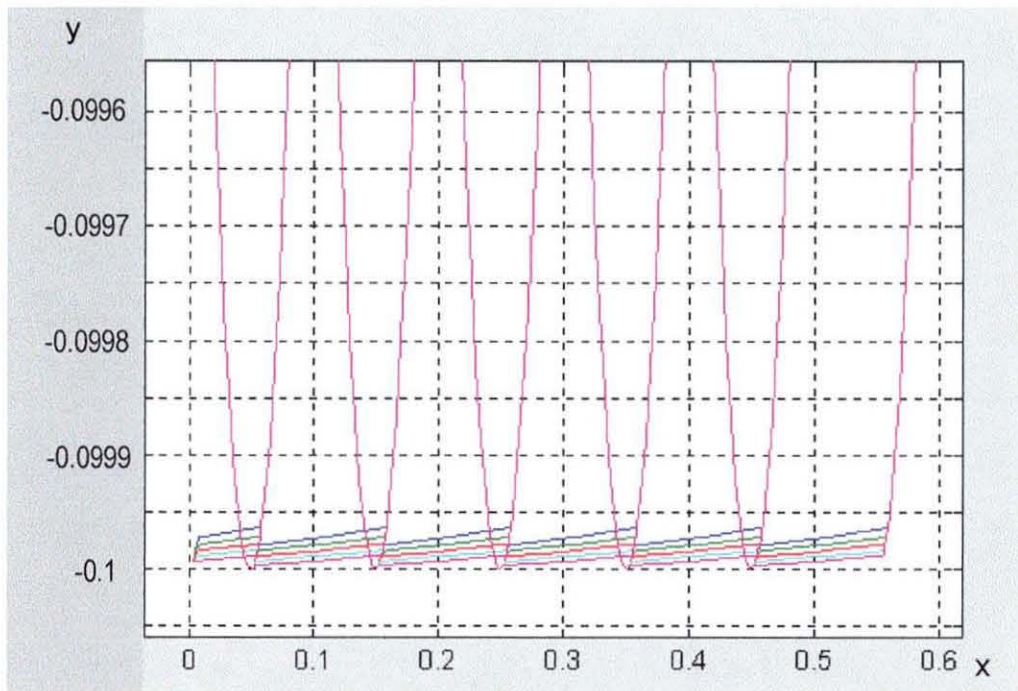
Figure 8.2.3.4 Oscillation phase lag from 0.020ms up, stepping at 0.005ms for 4
additional steps

155
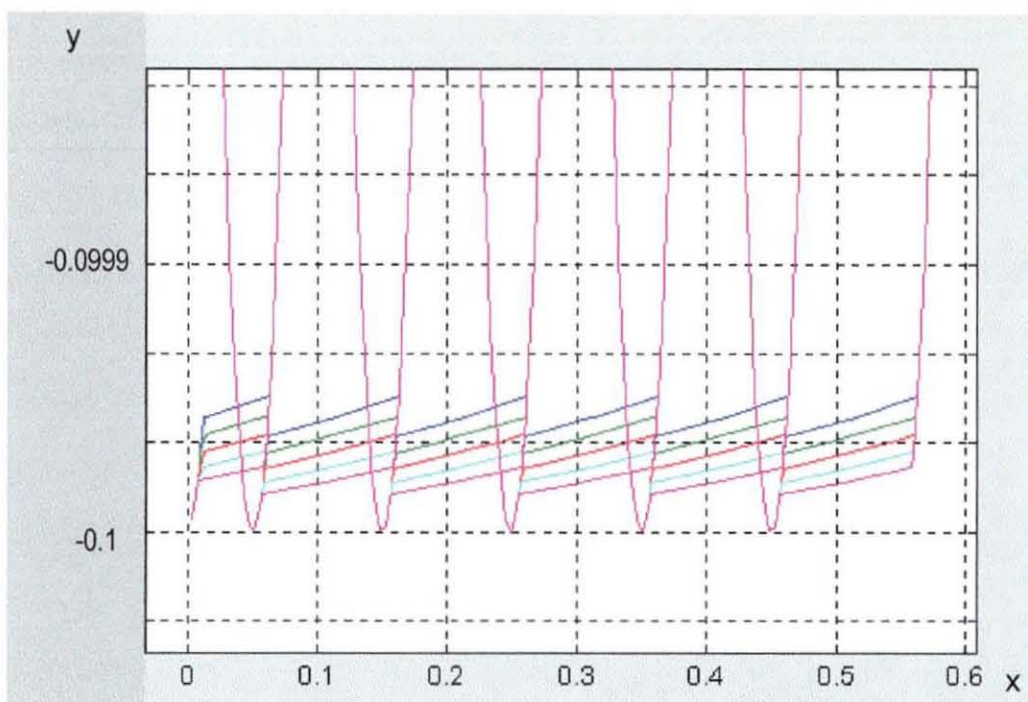
Figure 8.2.3.6 Lag from 0.04ms stepping up for 0.005ms
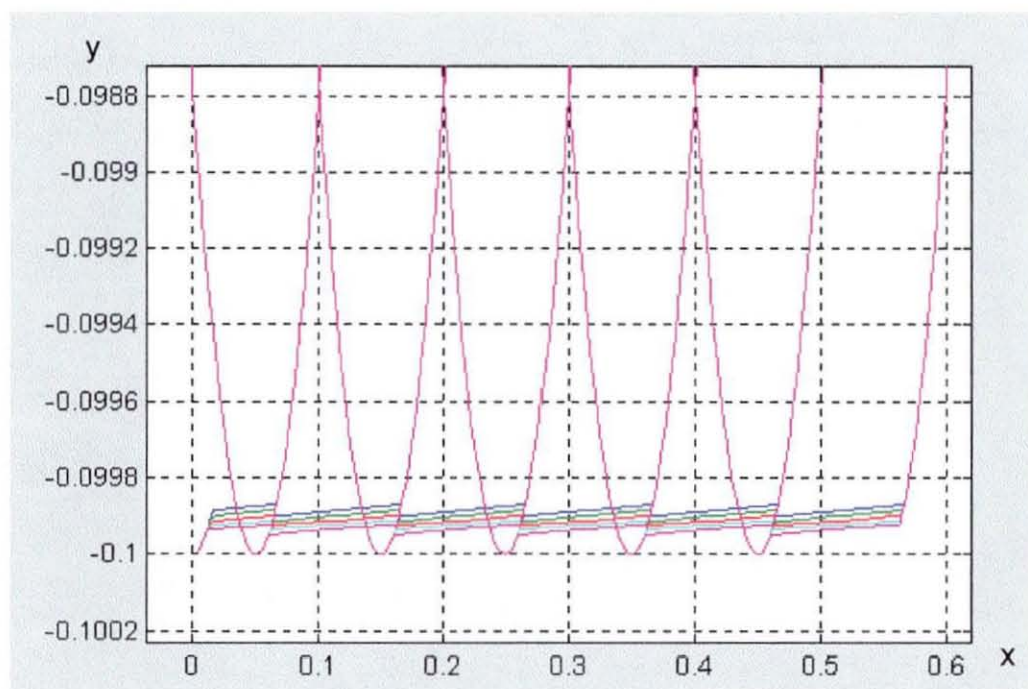
Figure 8.2.3.7 Same parameters as 8.2.3.6, except base = 0.06ms

156
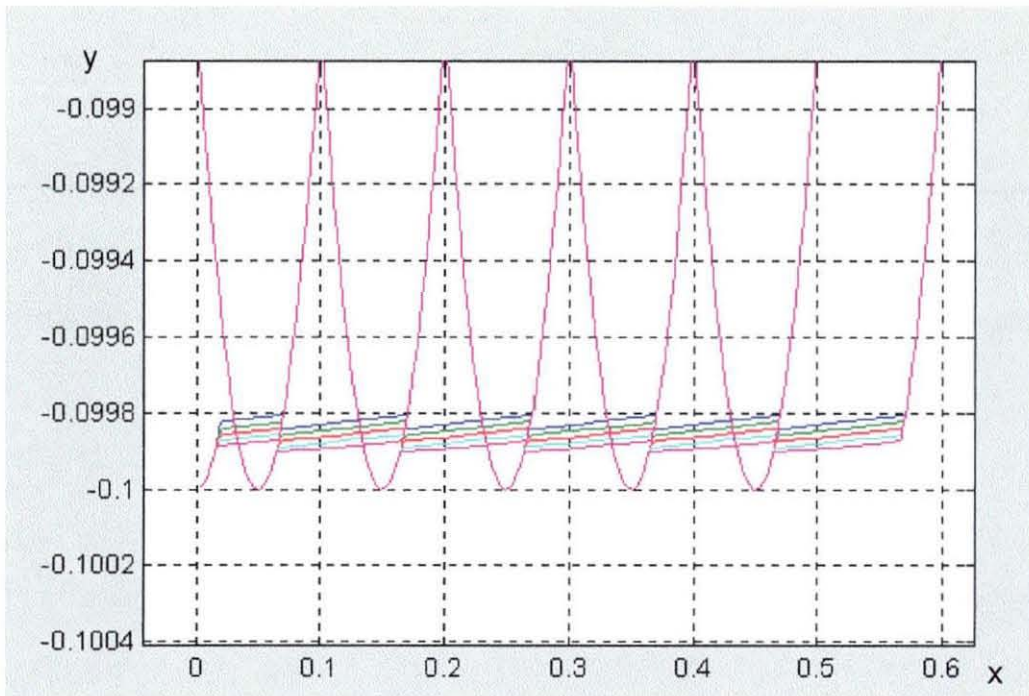
Figure 8.2.3.8 Same parameters as 8.2.3.7, except base = 0.08ms
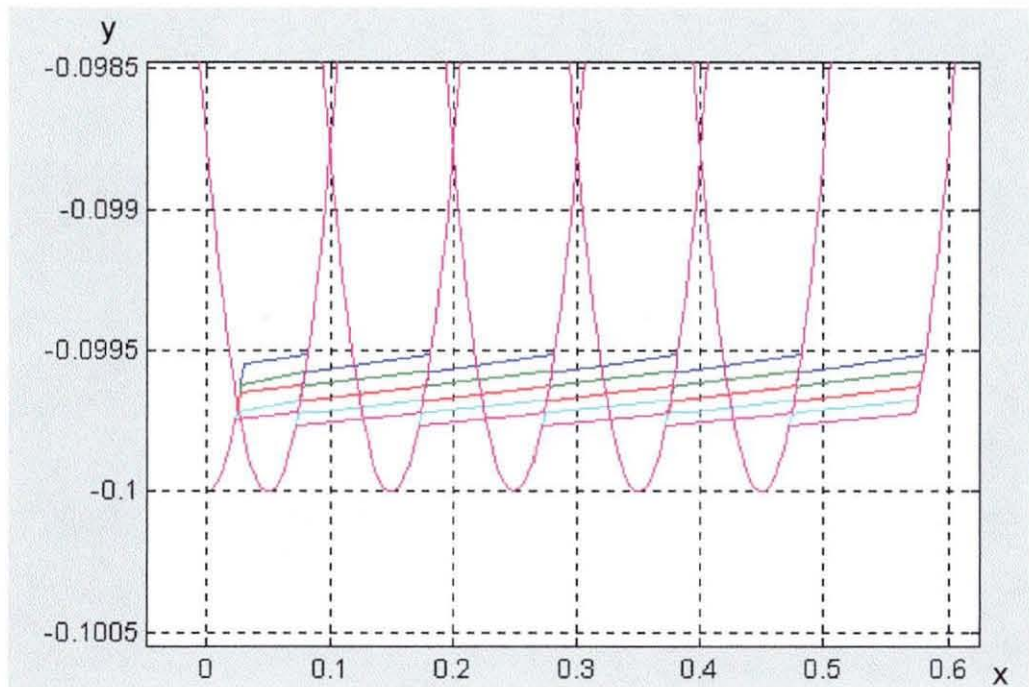
Figure 8.2.3.9 Same parameters as 8.2.3.8, except base = 0.1ms

157

8.2.4 Overall simulation of hydraulic system and timber surface form

Ideal servo conditions (specifications as for actuator system described in section 4.4.4), using a square wave generated as shown in figure 6.5.1.1, produce successive reductions in cutter wave height as shown in figure 8.2.4.1. 5 simulations are shown here, the oscillation amplitude is stepping in 5 steps from 0 to 100%, ranging from blue (0%) through green (25%) , red (50%) , grey (75%), purple (100%). This colour progression uses the standard Matlab colourmap and subsequent plots may be assumed to follow the same progression.
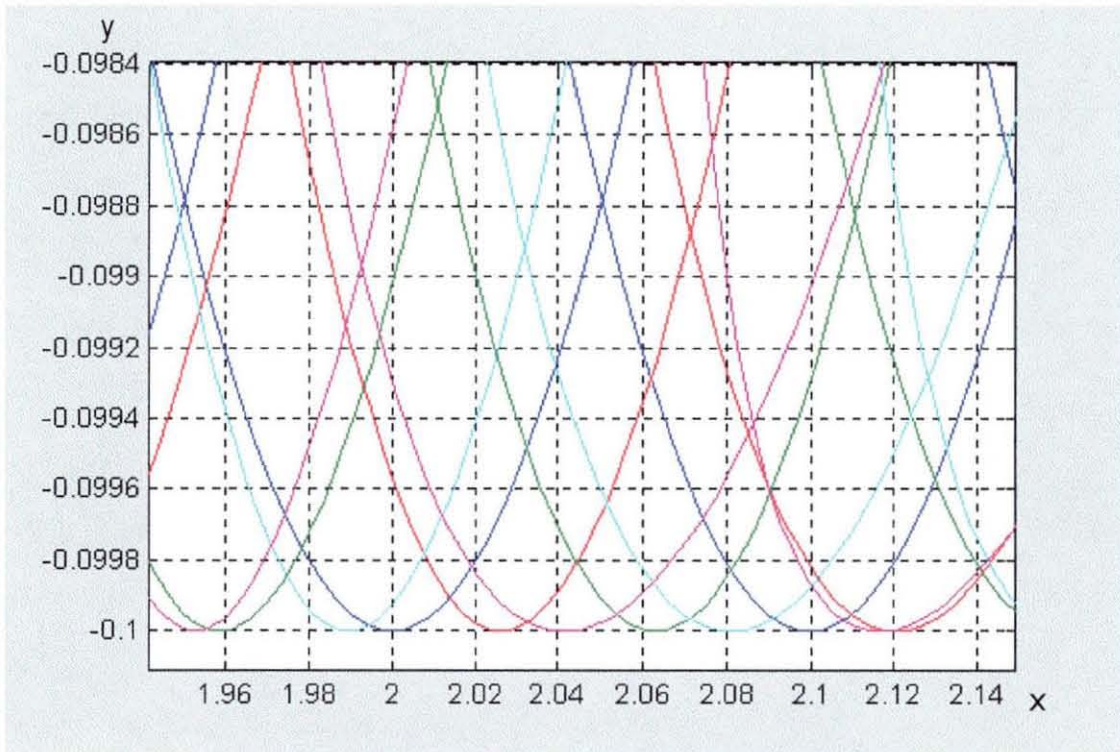
Figure 8.2.4.1 Overall system simulation.

Figure 8.2.4.2 shown below shows an output from a tuned system, using standard actuation wave to control a hydraulic servoactuator. Overshoot is employed in order to improve the quality of the actuator output signal at the point of zero crossing. The system is not optimised as yet with regards to hydraulic servo phase lag adjustment, as can be seen from the crossed over points of loci where loci utilising cutterblock oscillations of dissimilar amplitudes reach a common point sooner an would normally be expected, but as can be seen, an improvement of 60% between the un actuated system (blue) and the actuated system (purple).

158
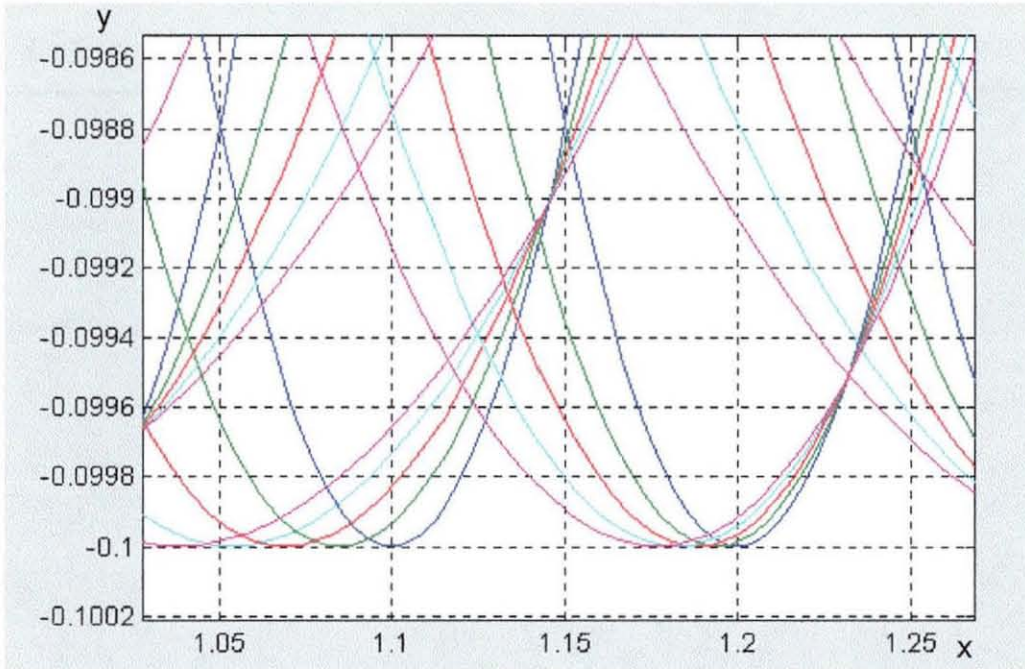
Figure 8.2.4.2 Timber surface form produced with from tuned hydraulic system.

Figure 8.2.4.3 shown below shows an output from a system with enhanced lag compensation in the form of the phase locked loop simulation described in figure 6.5.2.2. The blue locus represents the knife generating the surface finish for an oscillated system. The blue locus is for a conventional cutterblock.. The surface wave height reduction is 89%.
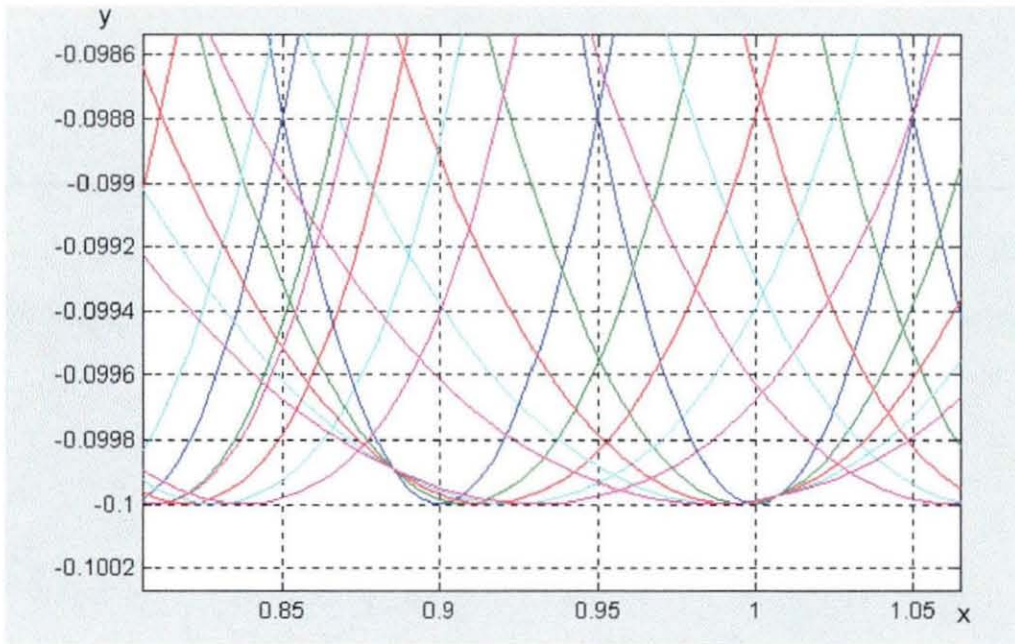
Figure 8.2.4.3 Simulation using PLL hydraulic control

In order to improve the stability of the hydraulic servo, and thereby reduce the low frequency drift which may be seen in previous plots, the time delay was kept tuned, but feedback delay was reduced slightly. The figure below (Figure 8.2.4.4) shows result of using a tuned time delay in the feedforward section of the hydraulic controller. The hydraulic servo lags by 0.02375s less than a full revolution. The feedback delay compensator in the hydraulic servo is operating with reduced gain of 0.05, in order to improve the stability of the hydraulic servo, with a small decrease in rise time.

160
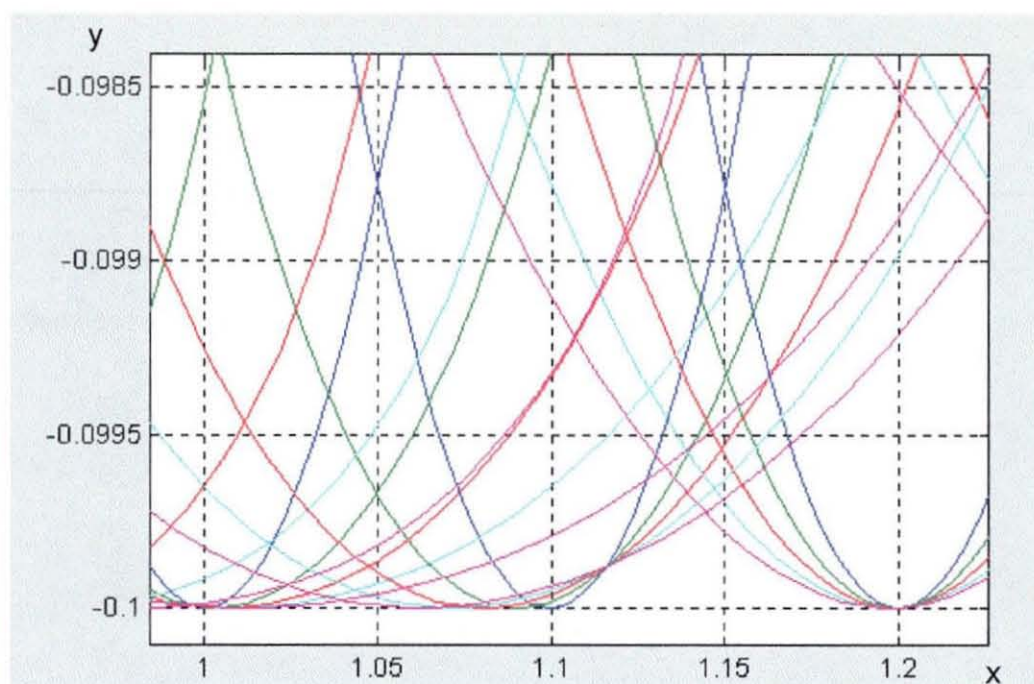
Figure 8.2.4.4 Timber surface produced from further experimentation with hydraulic
servo controller.

The figure 8.2.4.5 shown below shows current tracking performance of hydraulic servo
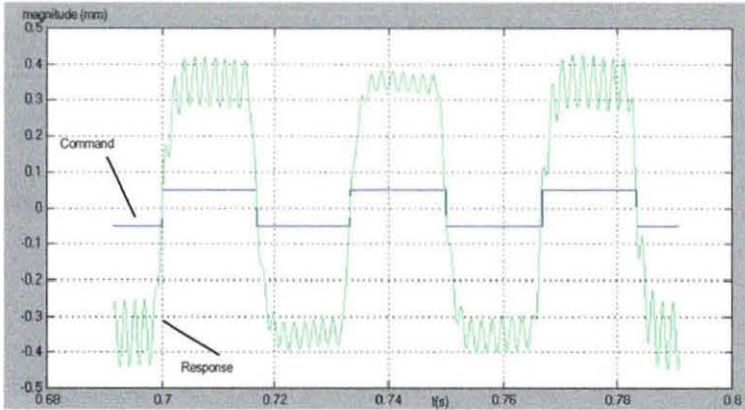
Figure 8.2.4.5 Hydraulic servo tracking performance.

Figure 8.2.4.6 shows the effect of doubling the maximum oscillation amplitude to 2x feed/rev is shown below, 5 tests are taken, starting at 0% of 2x feed/rev to 100% of 2x feed/rev, standard colourmap.
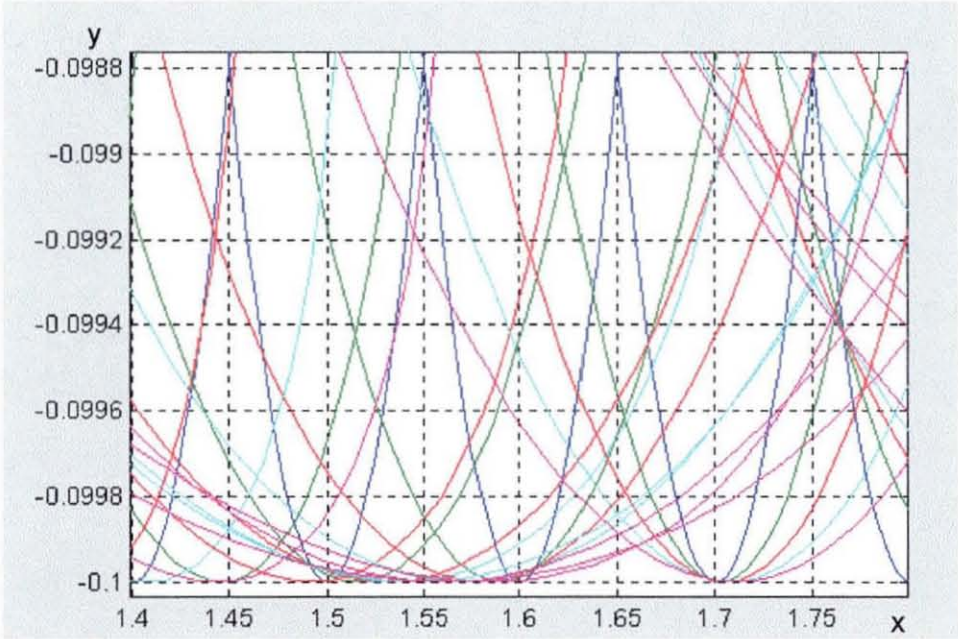
Figure 8.2.4.6, Effect of doubling oscillation amplitude.

162

8.3 Scanned images from test rig

8.3.1 Setup and repeatability tests

The scanned images included in this thesis are shown in this section, and can be organised into three groups.

The first group of results was taken in order to assess the repeatability of the experiments. Phase shift between the actuation signal and cutter position is irrelevant, since the oscillation crank was set to zero amplitude. Cutter diameter remains constant, and no machine parameters (such as feed/rev) were altered within each batch of three tests. In order to reduce quantisation noise, providing easier visualisation of waveform shape, a filter was applied to the output waveform. A raw waveform is shown in figure 8.3.1.1. Wave shape is not altered, but the signal becomes clearer. Group numbers start at 4 because previous result groupings applied to tests which were carried out in order to set up the machine and obtain a clean, backlash free, output signal, as shown in figure 8.3.1.2.

The filter is a sixth order lowpass elliptical filter, with 0.5 dB ripple in the passband, and a stopband 15dB down. Cut-off frequency is 0.08, a frequency of 1.0 referring to half the sample rate.

The elliptical filter has been chosen because of its sharp cut-off compared to say, a Butterworth or Chebyshev filter, and because this particular design of filter, with the right parameters, does not alter phase or amplitude characteristics in the frequency of interest, where the wavelength is equal to the cutter wave pitch.

The state space representation of the filter in the form of matrices [a,b,c,d] is as follows:

$$
A = \begin{bmatrix}
0.7636 & -0.1963 & 0 & 0 & 0 & 0 \\
0.1963 & 0.9781 & 0 & 0 & 0 & 0 \\
-0.1330 & 0.7837 & 0.9430 & -0.2430 & 0 & 0 \\
-0.0166 & 0.0980 & 0.2430 & 0.9696 & 0 & 0 \\
-0.1331 & 0.7843 & -0.0217 & 0.0394 & 0.9662 & -0.2489 \\
-0.0168 & 0.0993 & -0.0027 & 0.0050 & 0.2489 & 0.9685
\end{bmatrix}
$$

$$
B = 0.3151
$$

0.0351
0.3234
0.0405
0.3236
0.0410

C =   -0.0673   0.3968   -0.0110   0.0199   -0.0009   0.0019

D =   0.1637

Apart from a very slight DC shift, phase lag is zero as the data of interest is well within the passband. As can be seen from the following two diagrams, the cleaner processed signal has peaks and troughs of the same size and shape as those of the original, but visualisation of the wave shape is now made easier. This is particularly advantageous since the wave shape and cutter mark depth are only of interest, and not spurious HF components.
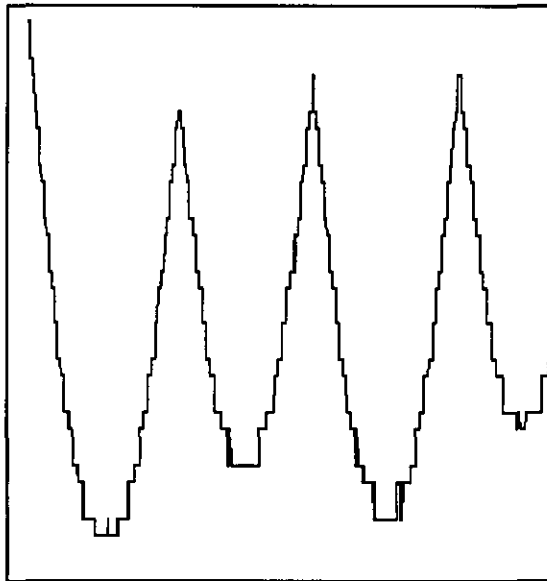
Figure 8.3.1.1 Cutter waveform before signal conditioning
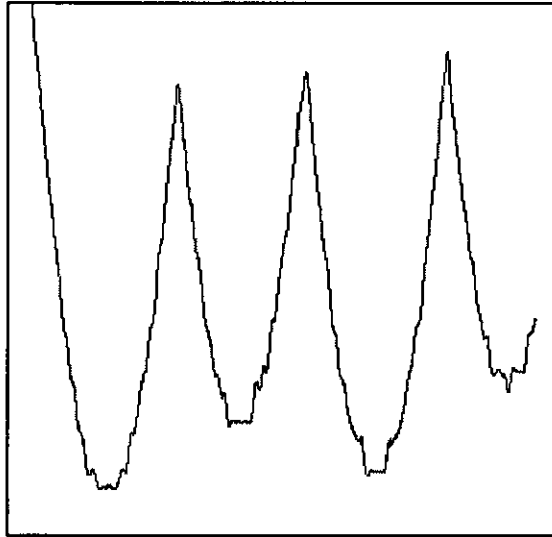
Figure 8.3.1.2 Cutter mark signal after conditioning.

Apart from the signal conditioning described above, scaling applied to all waveforms is equal, and no unevenness of horizontal stretching is applied. The following images were not of the highest quality achieved, being taken prior to the undertaking of machine modifications which produced a cleaner output signal.

File number = 1   Image name = G4_1a.raw   Image size = 4452,352

Phase angle (degrees) = 0   Feed / rev (mm) = 20.55

Oscillation (mm) = 0

This image was the fist of this batch of tests, and typically of these early plots, a degree of low frequency drift can be seen as a hump in the centre of the plot.   ·
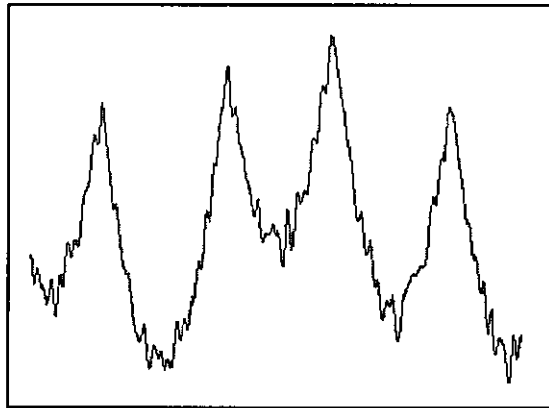
Figure 8.3.1.3 Setup waveform #1

File number = 2   Image name = G4_1b.raw   Image size = 4452,352

Phase angle (degrees) = 0   Feed / rev (mm) = 20.55

Oscillation (mm) = 0

The following image, figure 8.3.1.4 and the subsequent plot, figure 8.3.1.5, were taken under the same machine conditions as the first image. Steps were later taken to improve machine design.

Figure 8.3.1.4 Setup waveform #2

166
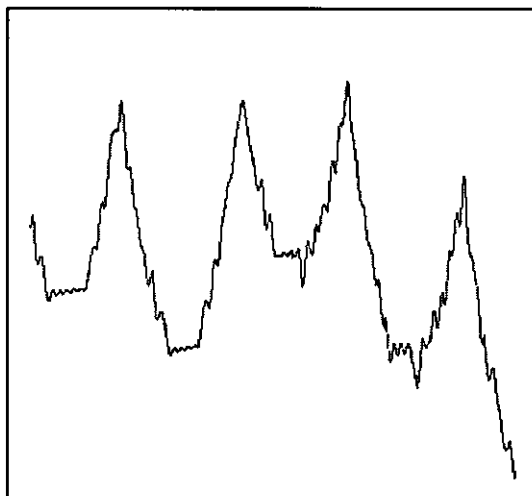
File number = 3   Image name = G4_1c.raw   Image size = 4452,352

Phase angle (degrees) = 0   Feed / rev (mm) = 20.55
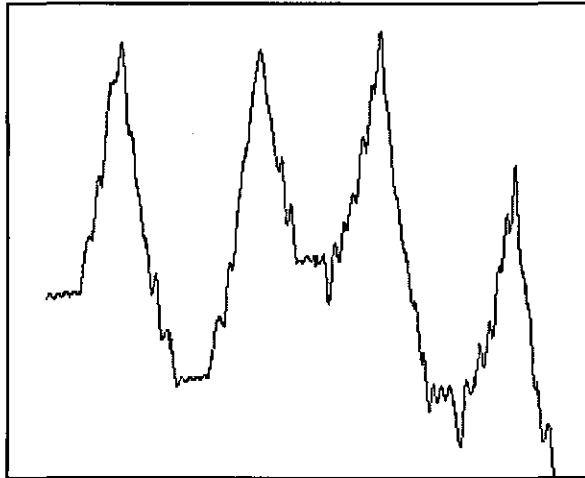
Oscillation (mm) = 0

Figure 8.3.1.5 Setup waveform #3

File number = 4   Image name = G4_2a.raw   Image size = 4452,352

Phase angle (degrees) = 0   Feed / rev (mm) = 23.30

Oscillation (mm) = 0

Machine design modifications produced the image shown below, in figure 8.3.1.6, improving surface worm wave plot quality. Magnification was increased to 50x.

Figure 8.3.1.6 Setup waveform #4

167
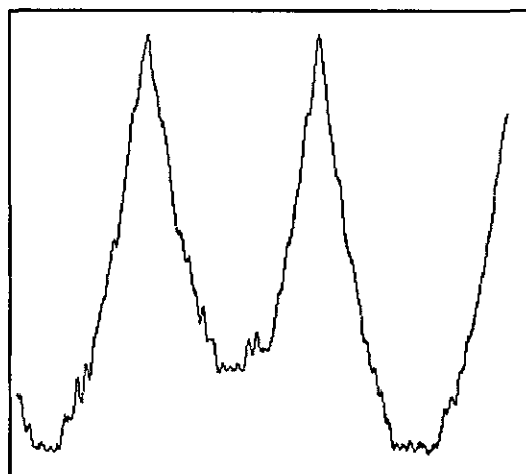
File number = 5   Image name = G4_2b.raw   Image size = 4452,352
                       Phase angle (degrees) = 0   Feed / rev (mm) = 23.30
                       Oscillation (mm) = 0

Similar in quality to the previous plot, figure 8.3.1.6, this image, figure 8.3.1.7, and figure 8.3.1.8, show that the process was now beginning to become slightly more repeatable.
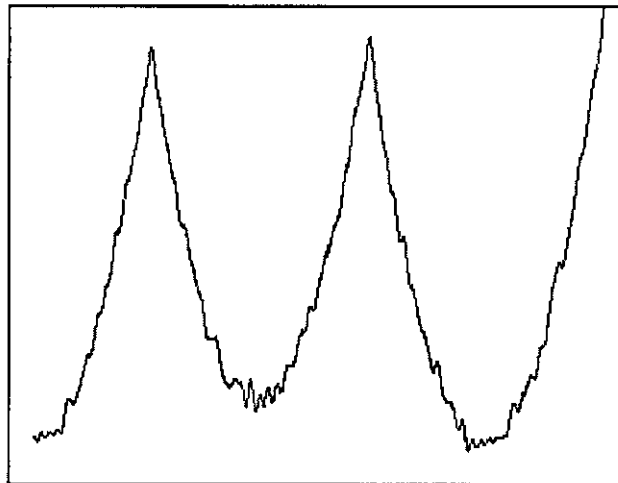
Figure 8.3.1.7 Setup waveform #5

File number = 6   Image name = G4_2c.raw   Image size = 4452,352
                       Phase angle (degrees) = 0   Feed / rev (mm) = 23.30
                       Oscillation (mm) = 0

Figure 8.3.1.8 Setup waveform #6

168
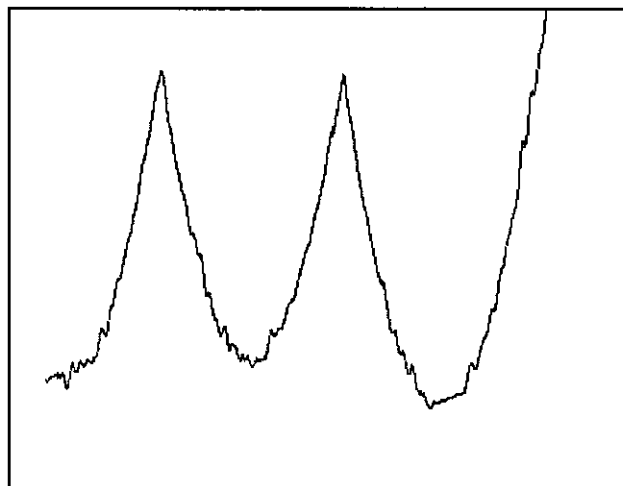
File number = 7   Image name = G4_3a.raw   Image size = 4452,352

                        Phase angle (degrees) = 0   Feed / rev (mm) = 10.9

                        Oscillation (mm) = 0

Increased surface noise may be seen in this and the following plot, figure 8.3.1.9, which resulted in a change in plotting speed, as discussed fully in section 9.6.2. Figure 8.3.1.10 shows a plot produced using the same machine parameters.
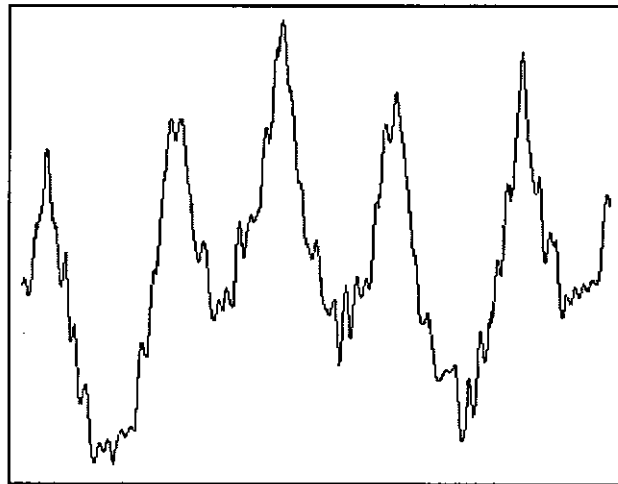
Figure 8.3.1.9 Setup waveform #7

File number = 8   Image name = G4_3b.raw   Image size = 4452,352

                        Phase angle (degrees) = 0   Feed / rev (mm) = 10.9
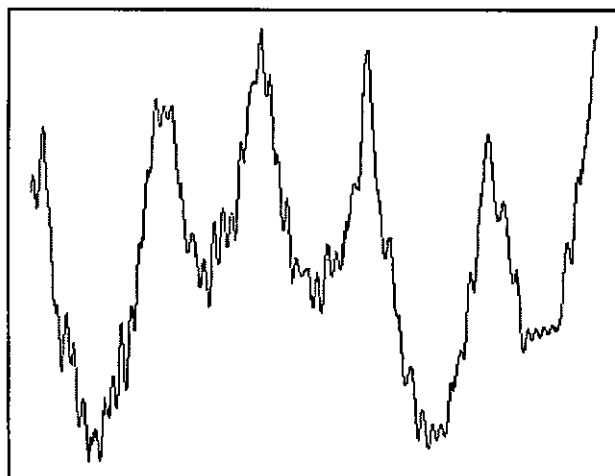
                        Oscillation (mm) = 0

Figure 8.3.1.10 Setup waveform #8

File number = 9   Image name = G4_3c.raw   Image size = 4452,352
Phase angle (degrees) = 0   Feed / rev (mm) = 10.9
Oscillation (mm) = 0

A reduction in surface noise achieved by refining the plotting parameters may be seen in the following image, figure 8.3.1.11.
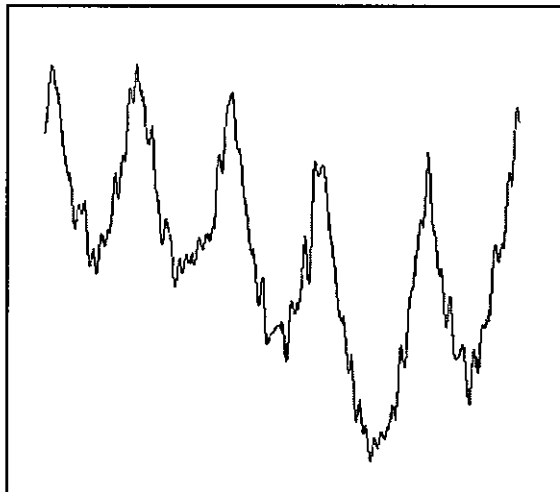
Figure 8.3.1.11 Setup waveform #9

8.3.2 Tests Following machine modifications

Machine modifications were carried out as described in section 7.2. Repeatability of the experiments was improved, and due to a lesser degree of drift in the scanned magnified images, magnified scanned images required no adjustment for 'tilted' waveforms produced by tracking errors. Prior to this it had been necessary to tilt images by as much as 4 degrees to achieve the correct orientation. The improved surface forms produced by the second batch of repeatability tests is shown in the following diagrams. The waveforms are measured in X and Y axes in pixels, and therefore displayed as such. The following plots were magnified during scanning such that 5 pixels = 1mm.
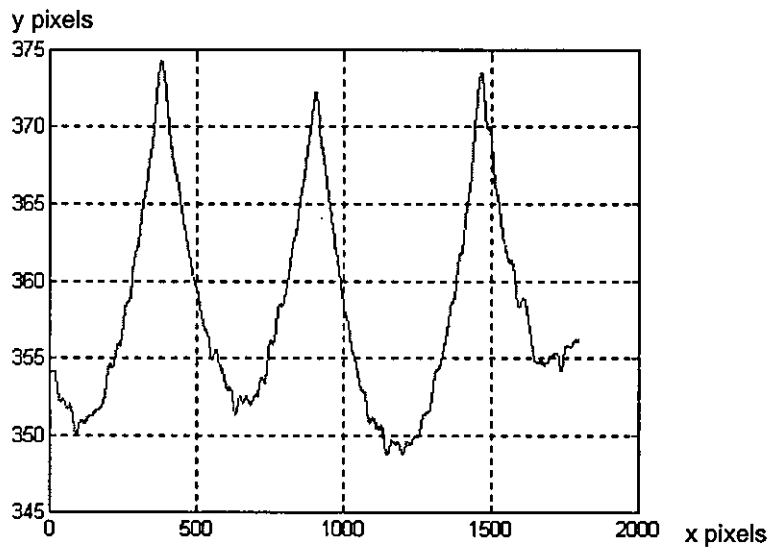
Figure 8.3.2.1 Setup waveform following machine modifications #1

171
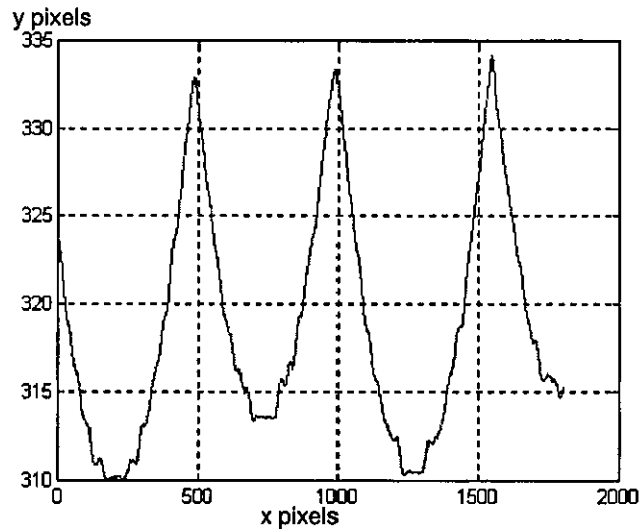
Figure 8.3.2.2 Setup waveform following machine modifications #2

An additional machine adjustment was undertaken to produce the plots shown in figure 8.3.2.3, 8.3.2.4, 8.3.2.5, and 8.3.2.6, whereby a 0.5N preloading of the main bevel gear was applied in order to try to reduce low frequency drift.
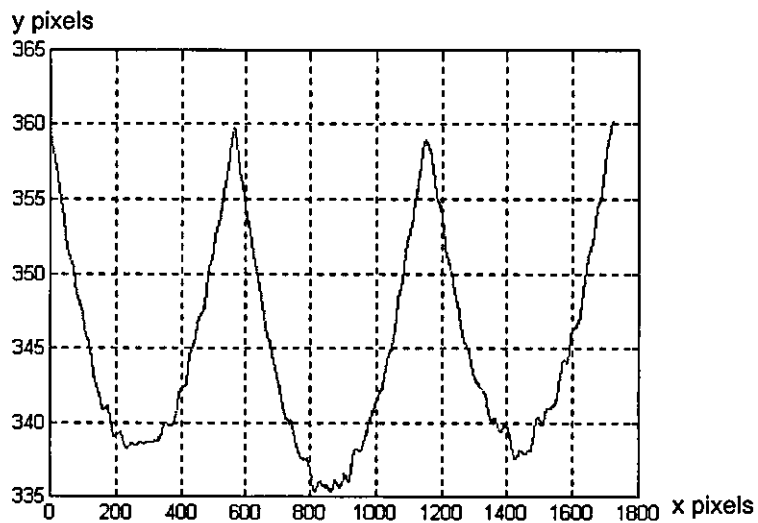
Figure 8.3.2.3 Setup waveform following machine modifications #3

172
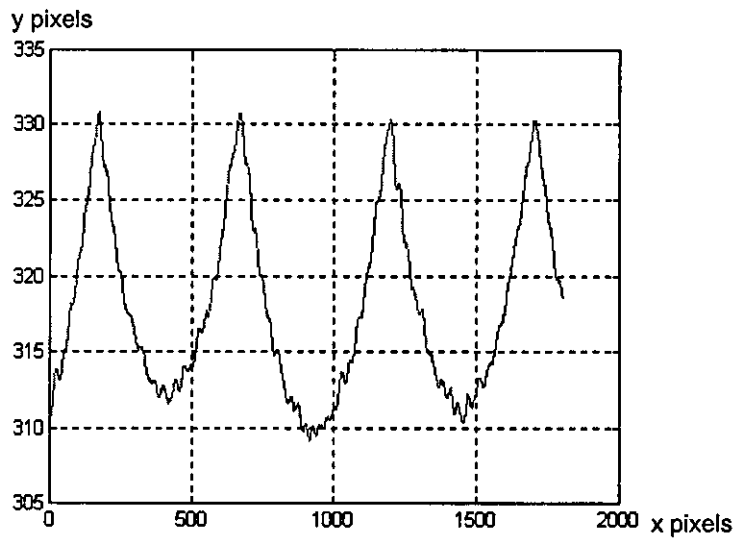
Figure 8.3.2.4 Setup waveform following machine modifications #4

Figure 8.3.2.5 Setup waveform following machine modifications #5

173
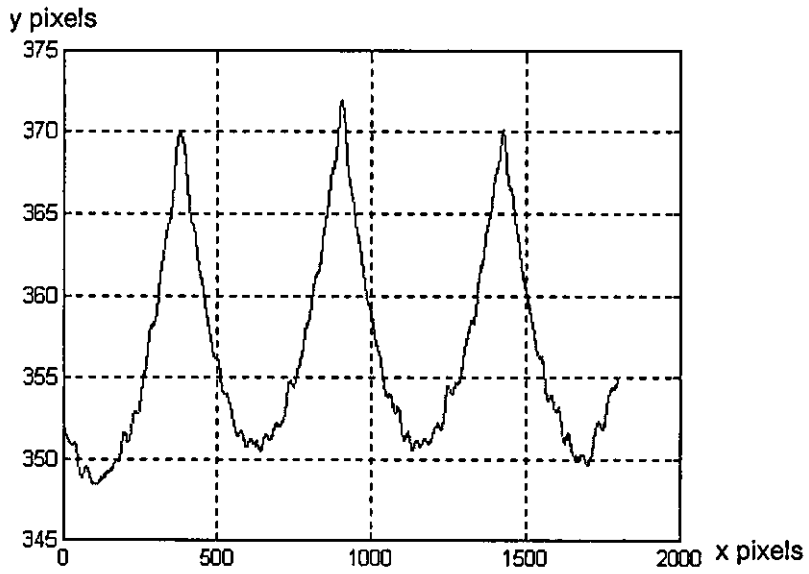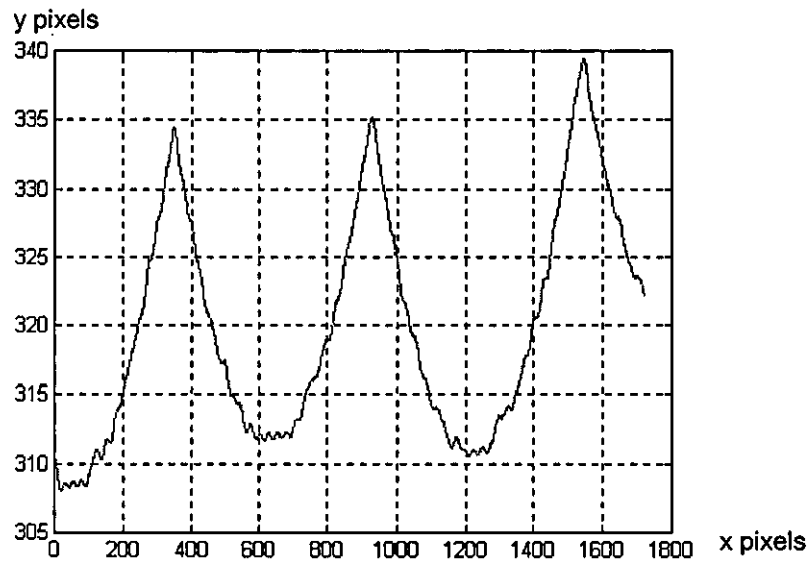
Figure 8.3.2.6 Setup waveform following machine modifications #6

Some low frequency drift can still be seen in the following two plots, figure 8.3.2.7, and 8.3.2.8, and this was eventually compensated for by better alignment of the plotted image during scanning.
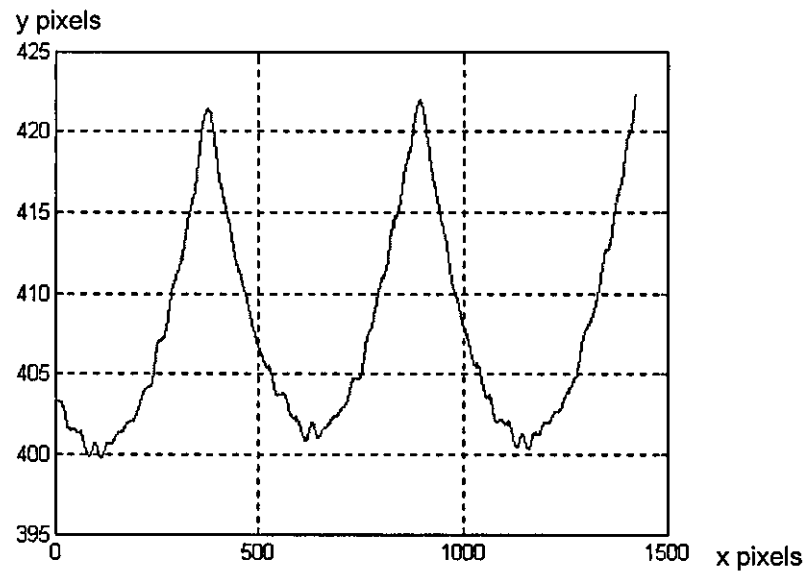
Figure 8.3.2.7 Setup waveform following machine modifications #7

174
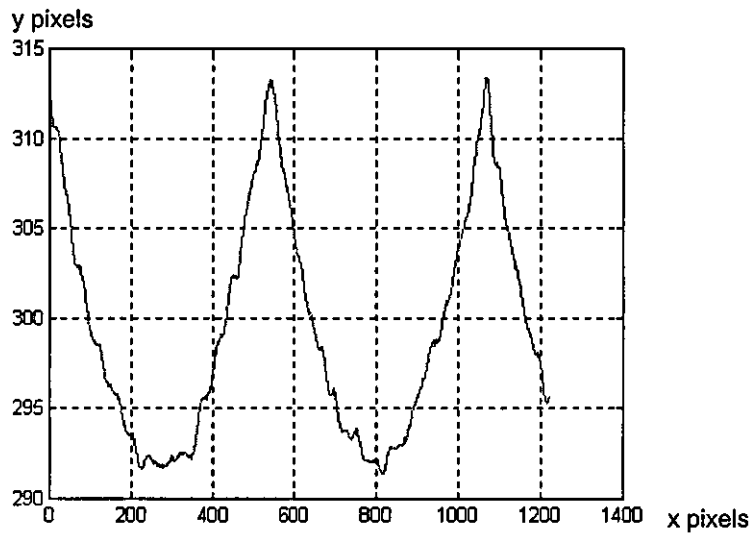
Figure 8.3.2.8 Setup waveform following machine modifications #8

Figure 8.3.2.9 Setup waveform following machine modifications #9

175
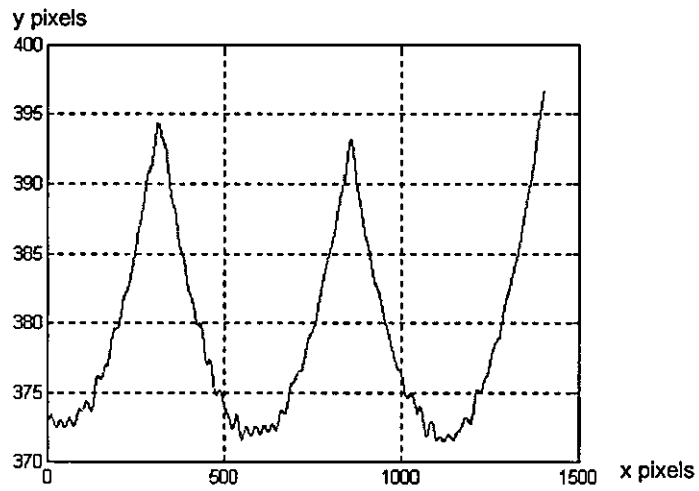
The following plots, figures 8.3.2.9, and 8.3.2.10, were undertaken with all machine modifications finalised, and subsequent plots were deemed to be of acceptable repeatability.
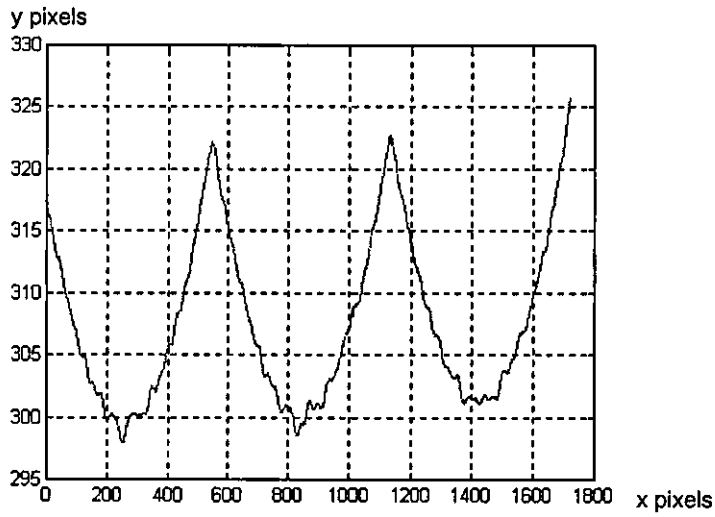
Figure 8.3.2.10 Setup waveform following machine modifications #10

Figure 8.3.2.11 Setup waveform following machine modifications #11

176
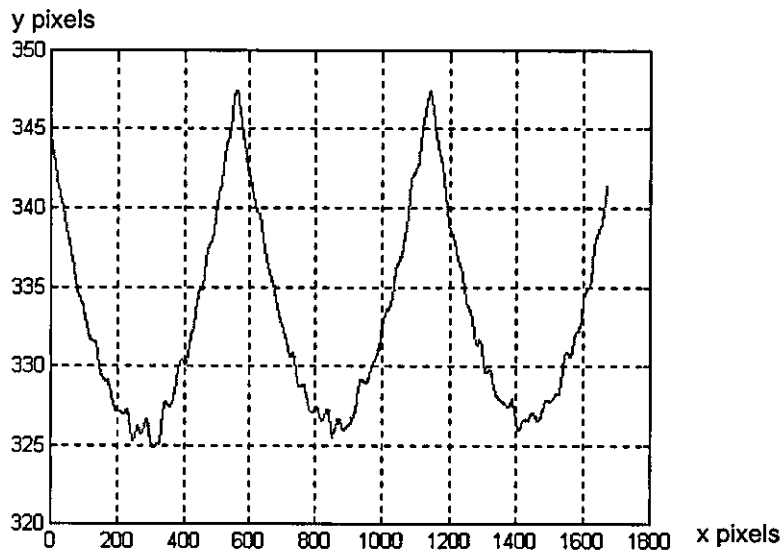
Waveform number	Mean peak height (pixels)	Mean trough height (pixels)	Mean surface wave height
1	372.5	351	21.5
2	333.5	312.5	21
3	360	337	23
4	330	311	19
5	370	351	19
6	335	314	20
7	322	300	22
8	312.5	292	20.5
9	394	373	21
10	422	400	22
11	347	325	22

Figure 8.3.2.12 Repeatability table for surface waveforms
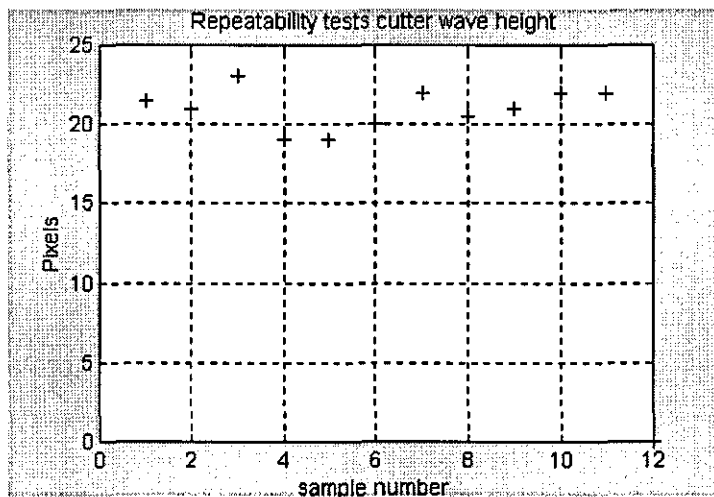
Figure 8.3.2.13 Repeatability plots for surface waveforms

177

8.3.3 Comparison between conventional surface form and surface form produced with cutterblock oscillation.

Repeatability of the un oscillated surface waveform having been established, a smaller number of surface waveform plots was taken in order to establish the surface wave height without oscillation. These plots were taken as a control to establish a reference point for the oscillated plots. No conditioning of the surface waveform was undertaken since the primary purpose of these tests was to asses the reduction in cutter wave height through oscillation of the cutterblock, rather than to visualise the surface form. Consequently a small degree of quantisation is visible. The degree of cutterblock oscillation used is 30% of the feed per revolution.

The mean surface wave height was taken by comparing each peak with the surrounding troughs, and taking a mean value for each plot. The magnification during scanning of the following plots was such that 200 pixels = 1mm.

The first batch of plots shown are taken without cutterblock oscillation.
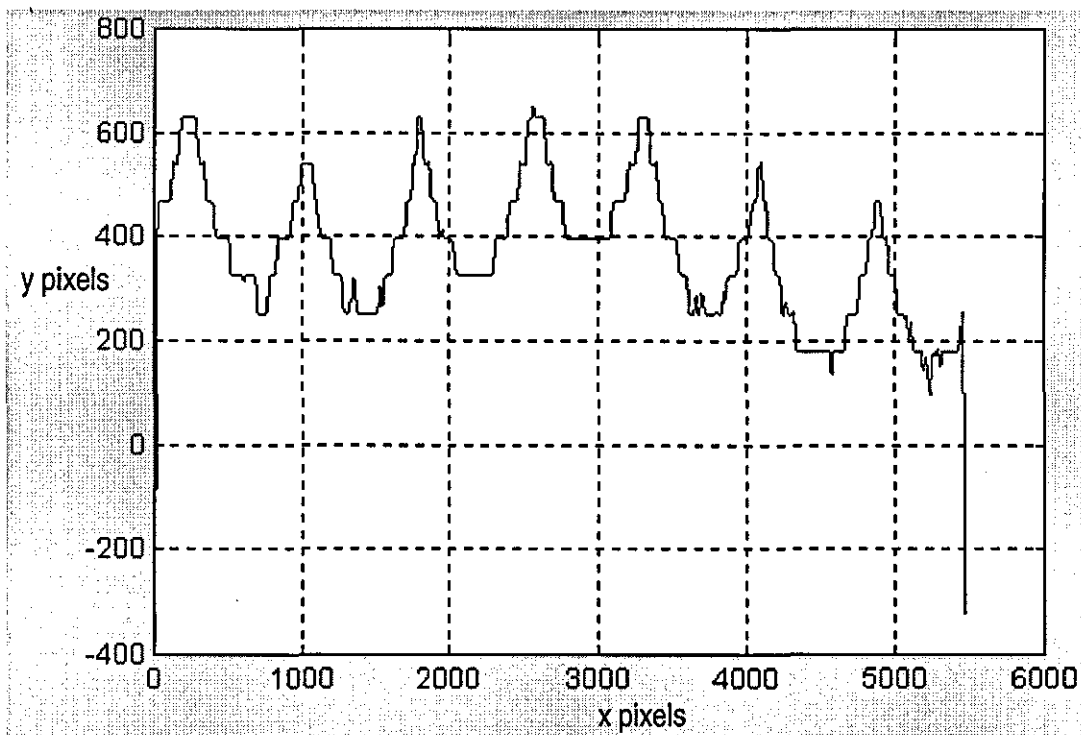
Figure 8.3.3.1 Surface waveform plot taken without oscillation #1
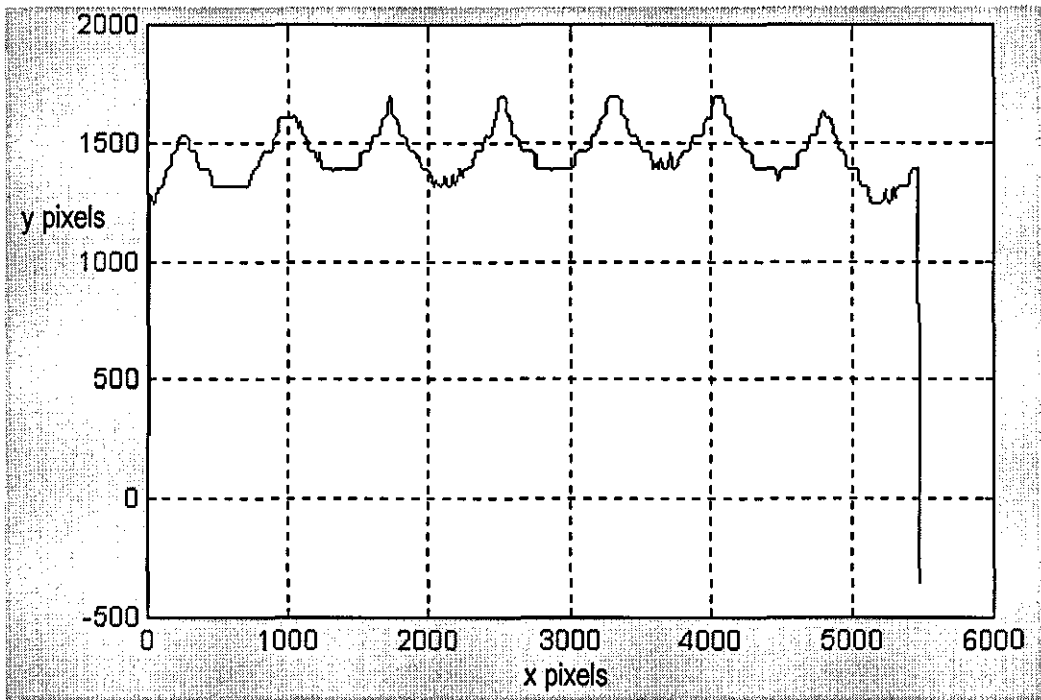
178

Figure 8.3.3.2 Surface waveform plot taken without oscillation #2

Figure 8.3.3.3 Surface waveform plot taken without oscillation #3

179
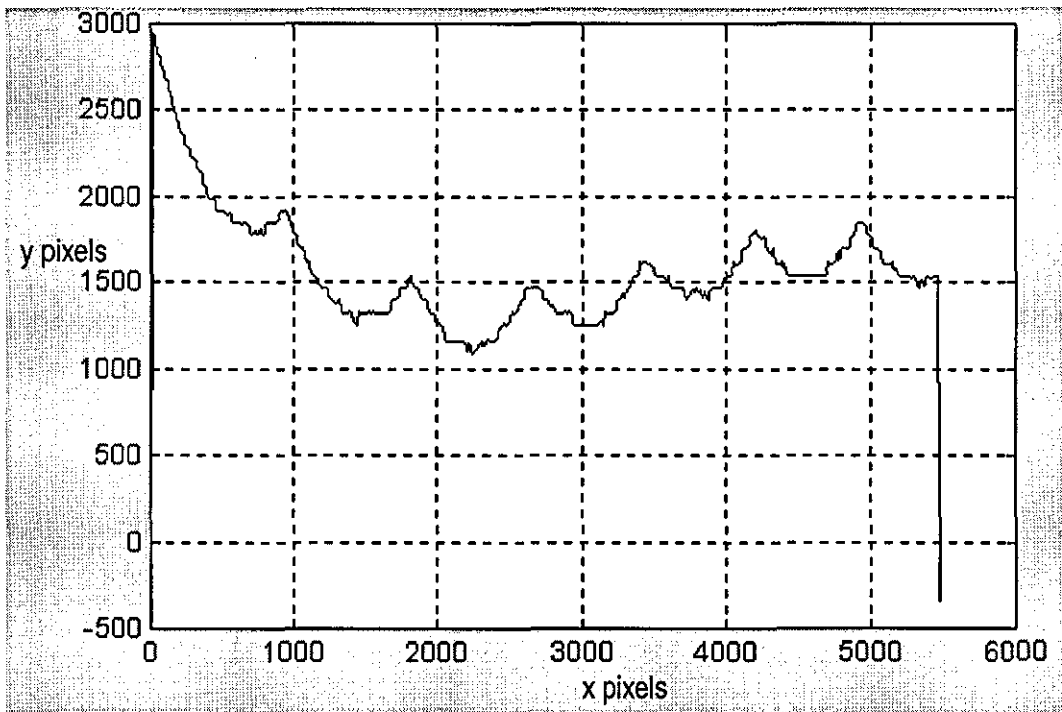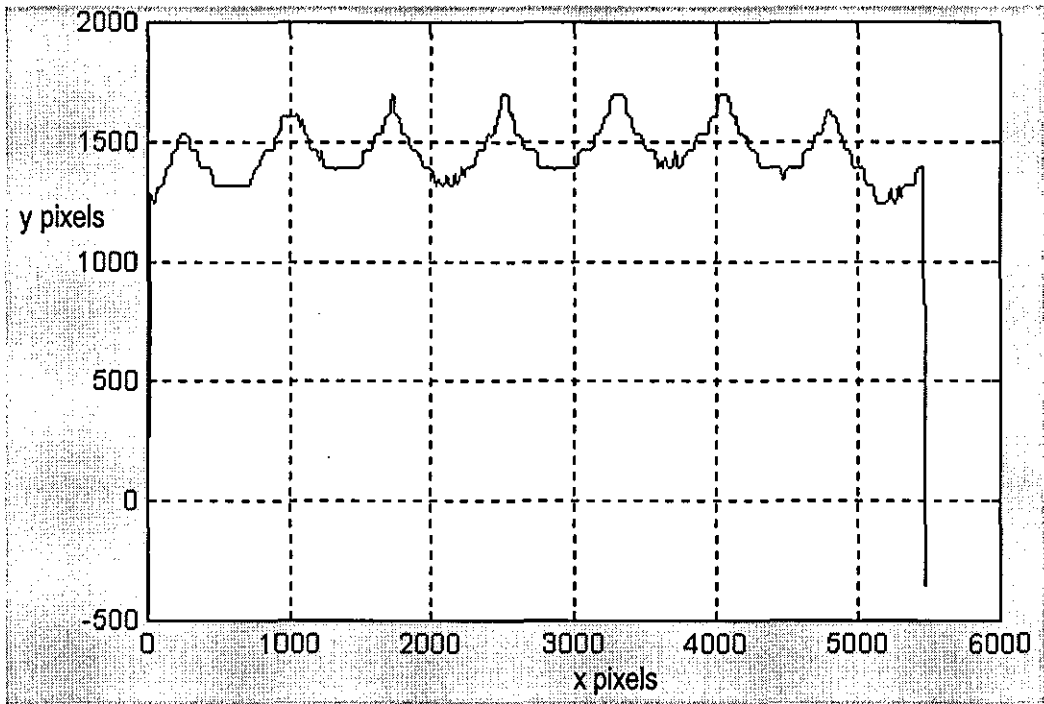
Figure 8.3.3.4 Surface waveform plot taken without oscillation #4

Figure 8.3.3.5 Surface waveform plot taken without oscillation #5

180
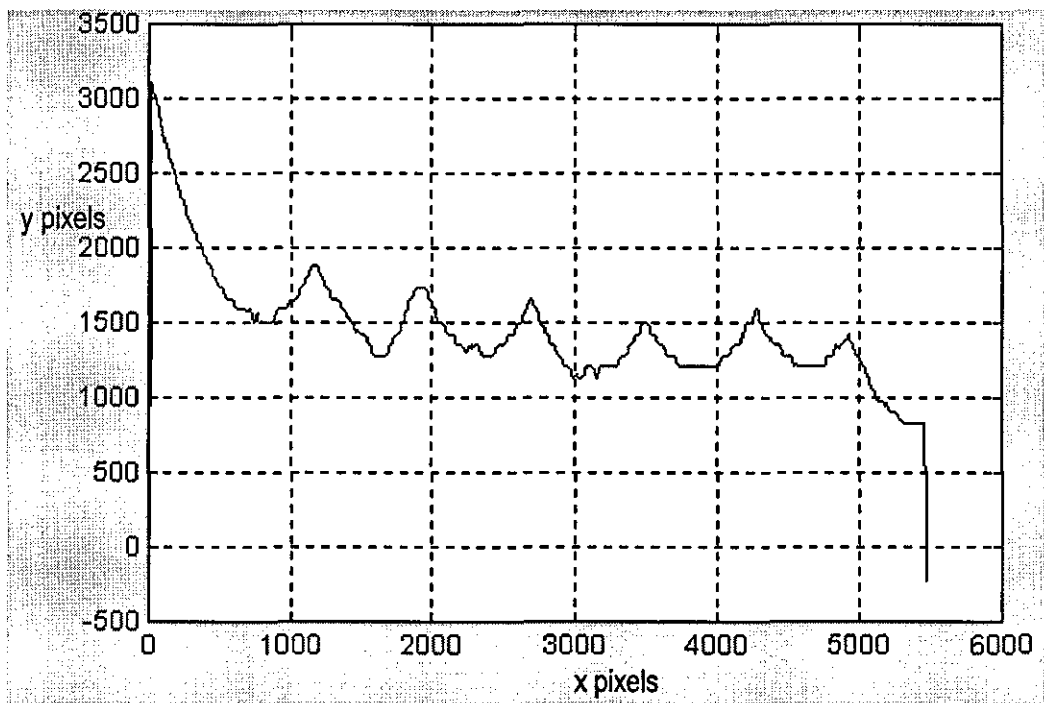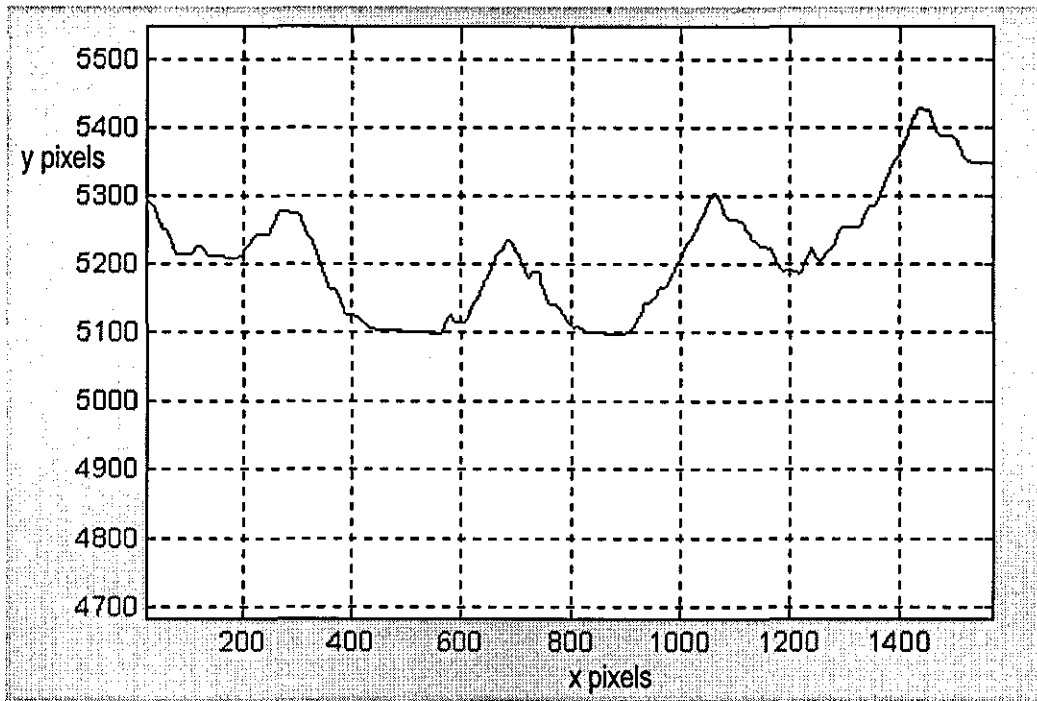
Figure 8.3.3.6 Surface waveform plot taken without oscillation #6

Some low frequency drift made the reduction of the horizontal range necessary, as can be seen in figure 8.3.3.7, though the drift experienced was not as great as that shown to have occurred prior to the machine modifications described in section 7.2, whose results are shown first in section 8.3.2.
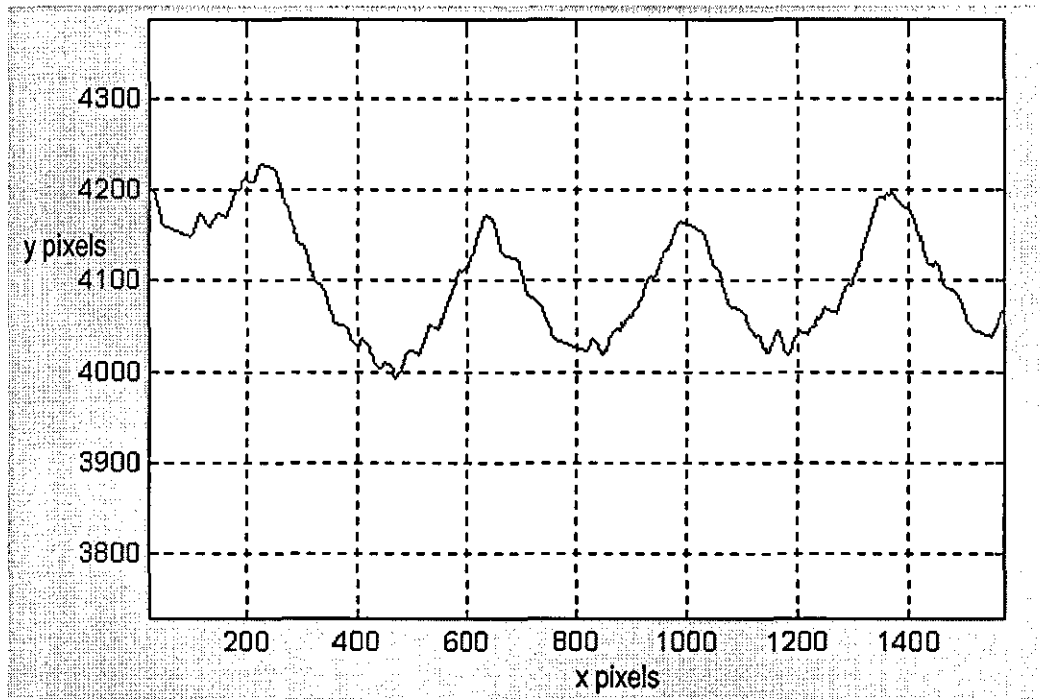
Figure 8.3.3.7 Surface waveform plot taken without oscillation #7
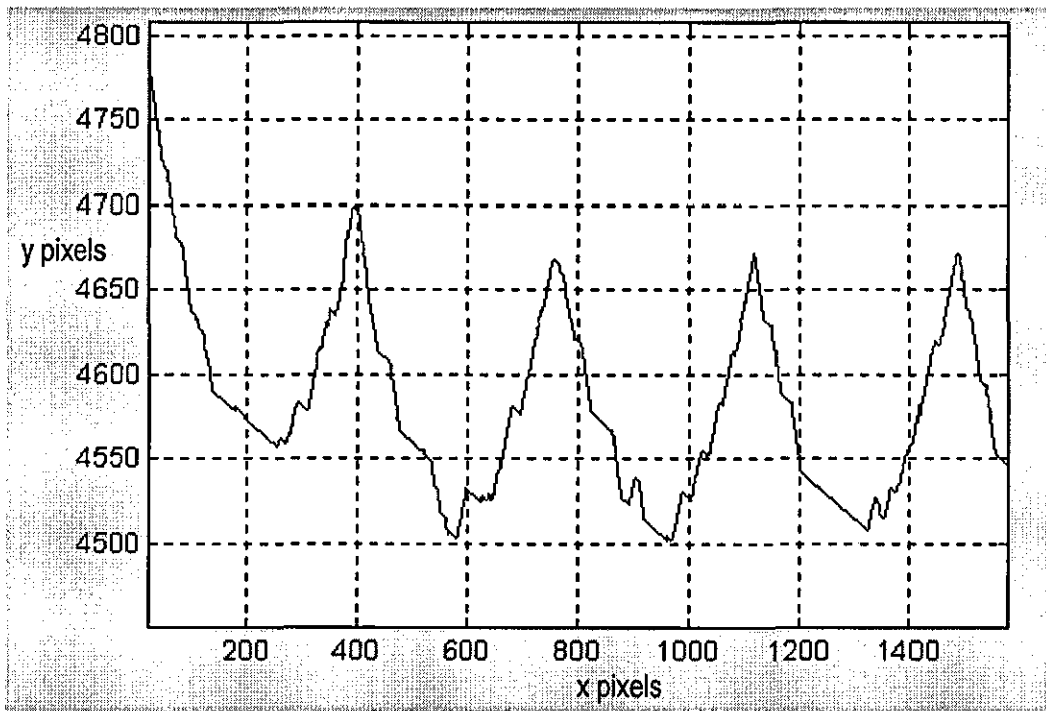
Figure 8.3.3.8 Surface waveform plot taken without oscillation #8

183

The images shown in figures 8.3.3.8 to 8.3.3.16 were exported as screen dumps from a computer with differing video, and consequently appear slightly differently on paper. Nevertheless, the process was still repeatable enough to formulate a judgement on the effectiveness of cutterblock oscillation, as is discussed in full in section 9.6.5.
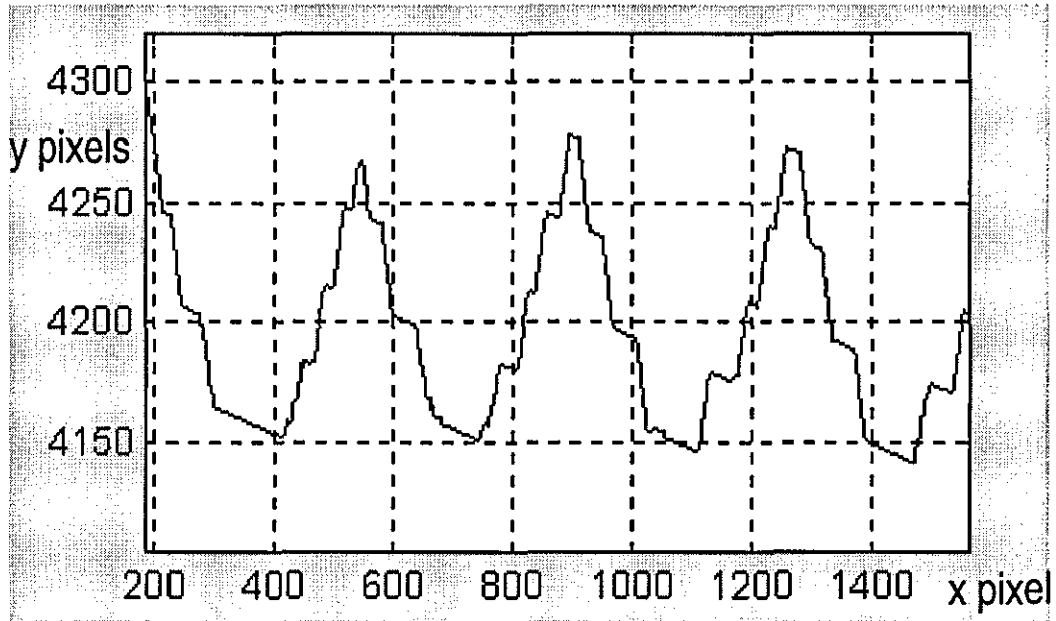
Figure 8.3.3.9 Surface waveform plot taken with oscillation #1
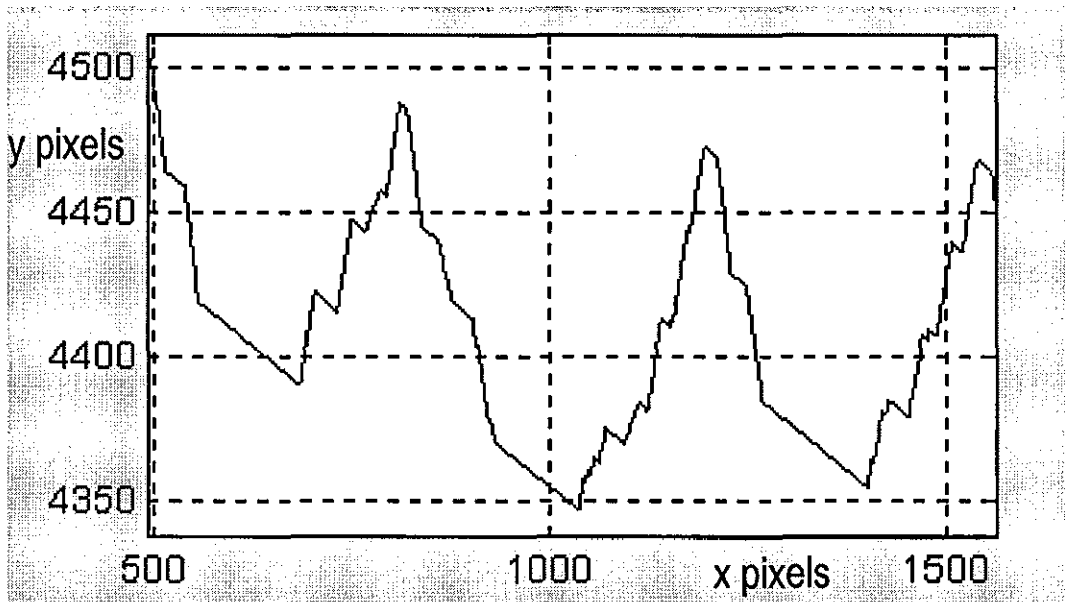
Figure 8.3.3.10 Surface waveform plot taken with oscillation #2

184
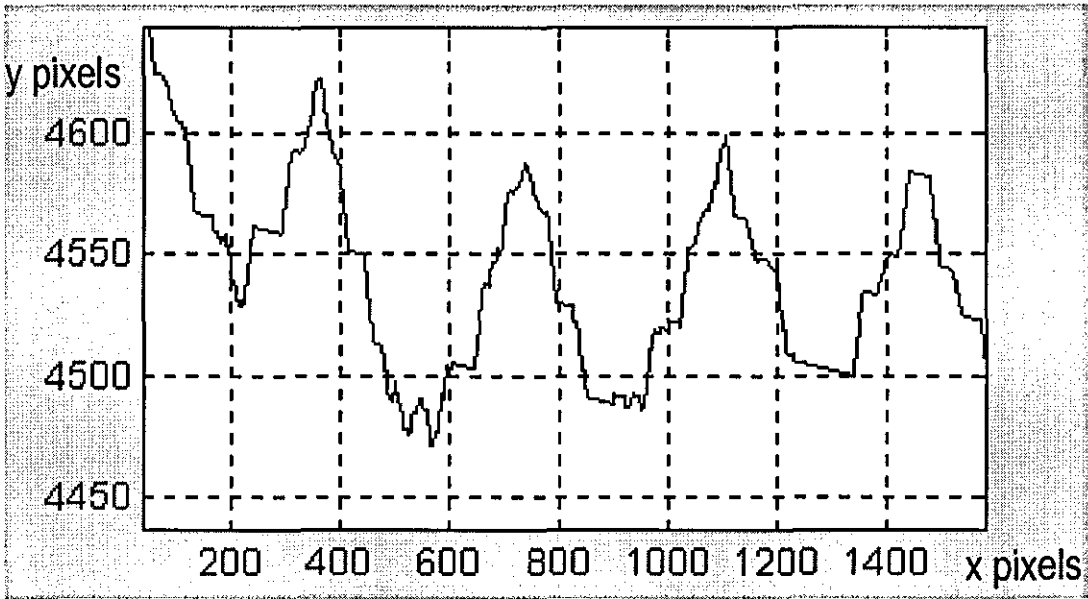
Figure 8.3.3.11 Surface waveform plot taken with oscillation #3

Figure 8.3.3.12 Surface waveform plot taken with oscillation #4

185
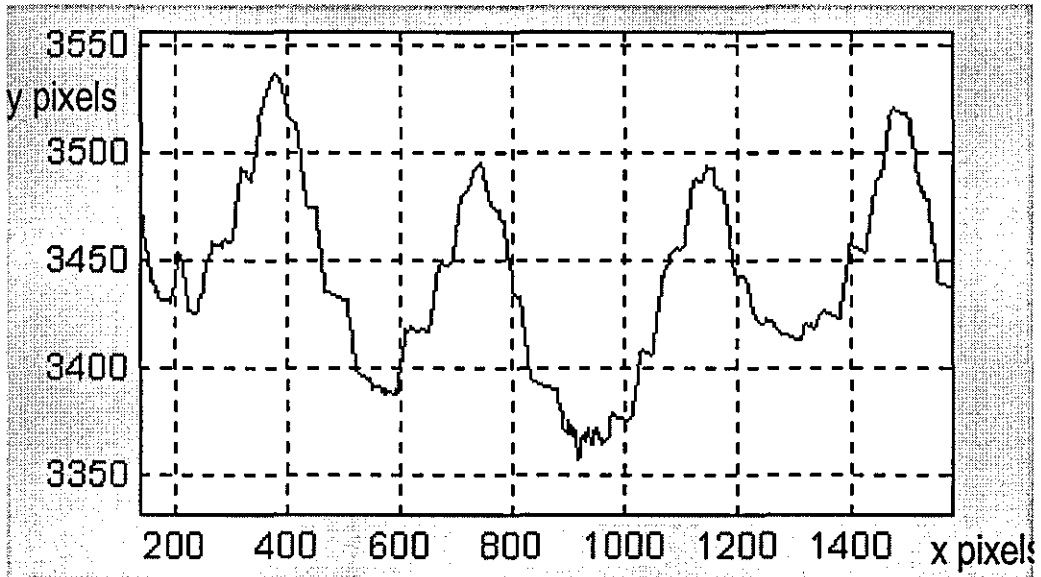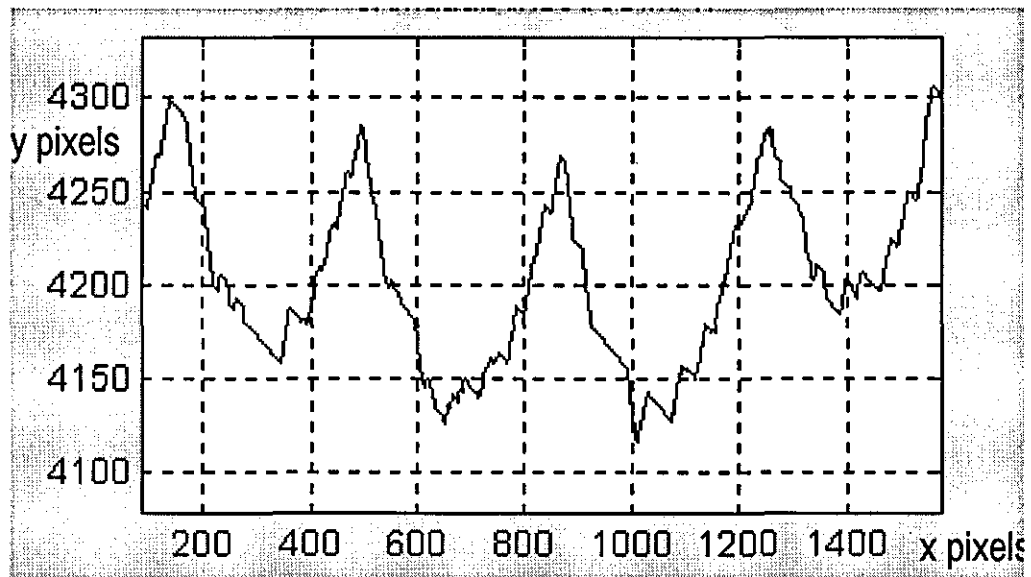
Figure 8.3.3.13 Surface waveform plot taken with oscillation #5
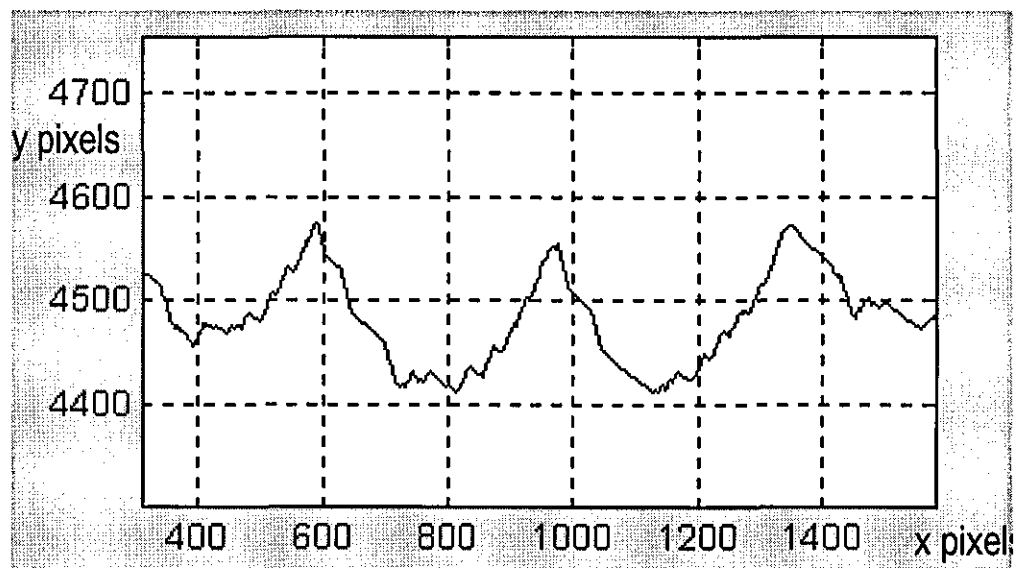
Figure 8.3.3.14 Surface waveform plot taken with oscillation #6
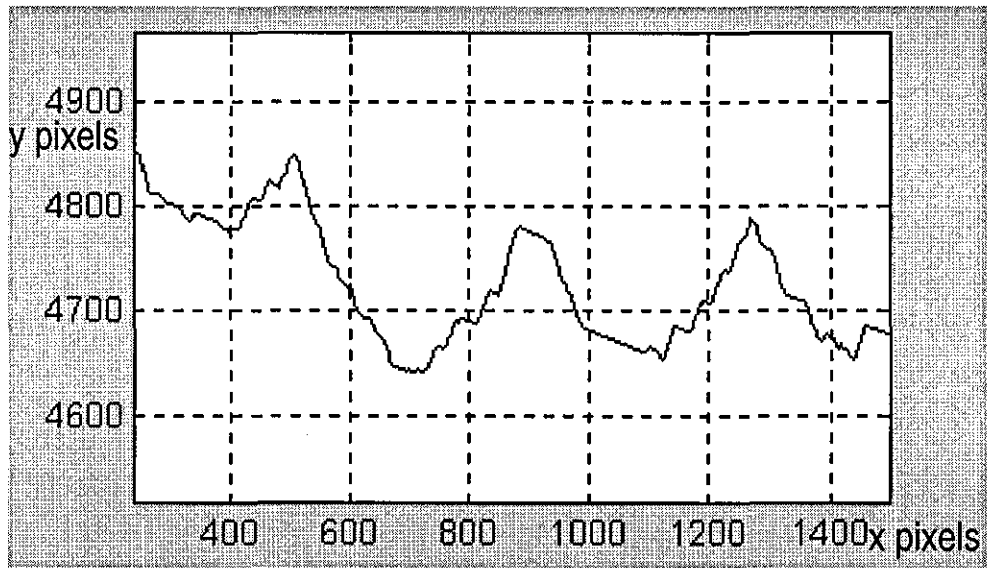
Figure 8.3.3.15 Surface waveform plot taken with oscillation #7
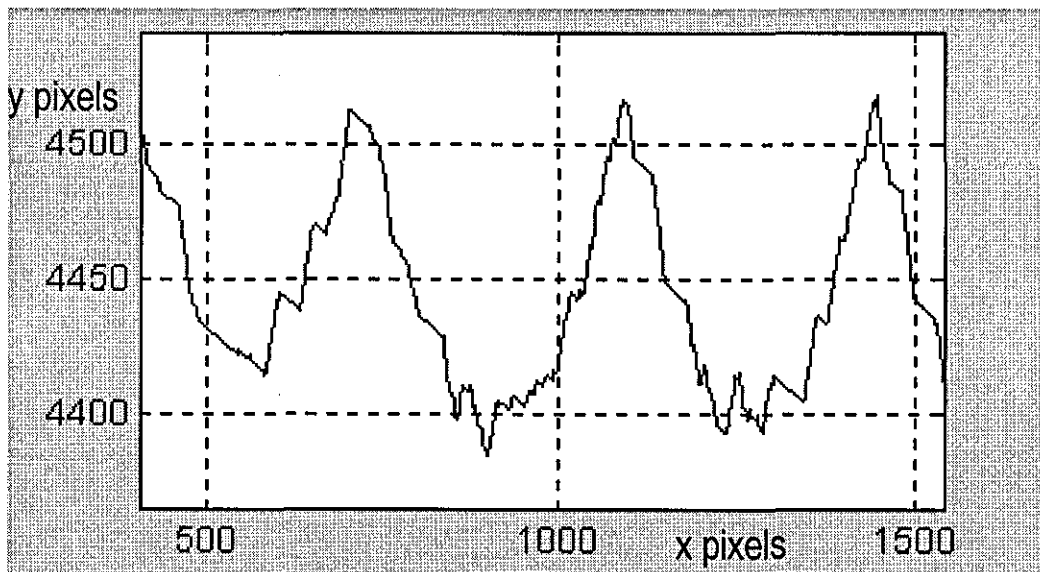
Figure 8.3.3.16 Surface waveform plot taken with oscillation #8

Sample (un oscillated)	Cutter wave height (pixels)	Sample (oscillated)	Cutter wave height (pixels)
1u	175	1o	100
2u	185	2o	108
3u	177	3o	93
4u	205	4o	94
5u	184	5o	90
6u	220	6o	128
7u	190	7o	120
8u	177	8o	119

Mean cutter wave height reduction = 47.6%

This compares with the simulated results for 30% feed per revolution for a pure sine wave oscillated system, whereby cutter wave height reduction is expected to be 50%.

9. Discussion - General

9.1. Performance of simulation software

9.1.1. Operating environment Saber™ basics

Saber™ primarily provides a component level modelling environment, which would appear to particularly suited to industry. 'Off the shelf' components may be assembled into circuits with ease, and highly complex simulations may be carried out. The simulation system utilises 'through' and 'across' variables (e.g. current and voltage, flow and pressure') running along the same lines, such that circuit design may be based upon a 'real world' model, as opposed to simulation using a standard block diagram approach, where for example, elements would need to be included for voltage drop and pressure feedback. This makes the initial design of the simulation rapid. The modelling language, MAST, may be used to design models and components which have not been included in the standard Saber™ library. Although very powerful as simulation code, the learning curve on MAST is very steep. A comprehensive knowledge of the syntax (which is by no means intuitive) is necessary to construct a model in MAST. An alternative is to write extra models in C which can then be compiled and interfaced to Saber™ as a foreign function. This process is time consuming, the process being not particularly well documented, a degree of trial and error must be employed to get the C code to interface with Saber™. However, the results are far more controllable and easily obtainable for anybody with a modicum of C programming experience, than with MAST. However, it must be mentioned that the MAST programming language, if used every day to overcome the learning curve, could become a far more powerful simulation tool than C. However, Saber™ was found to be lacking in some crucial areas with regard to this project, and the simulation was eventually ported to Simulink.

9.1.2. Template code in MAST

Two releases of Saber™ were used for this project, the first release being slightly less user friendly in use, the second using an enhanced GUI and better on-screen help facilities. Three disadvantages existed with the new version of Saber™ however, which influenced the transition to Simulink for modelling.

To begin with, the MAST templates provided in the Saber™ template library were viewable using a standard UNIX text editor. This enabled viewing of the syntax as an aid to learning the format of MAST based templates, and meant that the simulation algorithms could be viewed, in order to know how accurate the model would be, since the algorithm used to simulate a component could be thoroughly verified, and any generalisations in the model could be known. The following release used encrypted templates. Since only Saber™ is able to use the MAST language at present, the necessity for encryption is not clear. However, the primary upshot of the use of encryption was that no longer could the code representing the simulation be checked in the detail that was felt to be necessary. It can be argued that a simulation of a hydraulic circuit where the only information about the properties of, say, a hydraulic ram, is the graphic, which tells us only if it is single or double acting, and the properties window where ram surface area and end stop spring coefficients may be checked, does not provide a satisfactory picture of a hydraulic ram, since there are too many unknowns.

Another problem encountered was the use of a new file format for saved data. The first version of Saber™ used, saved simulation result files as binaries, which could be ported from SunOS (UNIX) to Windows(DOS) based software with ease. The following version, saved files in an unrecognised format. Unfortunately, Analogy, (providers of Saber™) representatives were unable to provide information regarding data export from the new version of Saber™, within the required time-frame.

9.1.3. Conversion to Simulink for simulation

Licence renewal problems followed, whereby the suability of Saber™ became erratic, with monthly licence renewal frequently occurring weeks late, the project was slipping rapidly behind schedule. Eventually, it was decided that Saber™ software was proving too unreliable to complete the research, and that time should be invested to extract as much work as possible from the Saber™ simulations, and to re implement the models using whichever simulation package could be found. A slow simulation was better than no simulation at all, so the simulations were thus ported to a far older version of Simulink (based on Matlab release 4.0), running on DOS based PC's. Simulation runs at this time were thus much slower, due to the then limited power of PC's (100MHz 486 processor. 16MB ram) compared to Sun Sparcstations (250 MHz 68008 processor., 48MB ram, plus UNIX OS with better memory management). Also, the amount of data that could be processed by a machine at a time was limited, due to licence limitations with the version of Matlab which was used (the Student version). Nevertheless, the reliability of the software licence was such that the advantages regarding the availability of this version of Simulink outweighed any performance penalties. Towards the very end of the project in month 35, a 32 bit fully featured version of Simulink became available. Bench mark checks indicated by this point, that Simulink running on a 200MHz pentium PC, possessed a 600% speed advantage over the Sun machines, and could handle 400% more data. From the point of view of simulation performance, the transition to Simulink and PC's reduced computation time required for the project to a point where overall simulation of the system, became a possibility.

9.1.4. GUI

After the simulation has been designed in DSCAP, which is the graphical design tool which is used to develop models for simulation using Saber™. the program graphical model is compiled as a further set of code, called a netlist, which is a text based representation of the model. This code is used in the Saber™ simulator. As can be seen, the process is sequential, with system design, netlist generation, and system simulation forming the three definable stages.

The GUI for Saber™ is written in C, and is the front end for it's FORTRAN based core code. The I/O characteristics of FORTRAN are limited, particularly with respect to graphics, and it is easy to gauge which parts of the software are written in FORTRAN,

and these parts may need accessing from time to time, for example when debugging the netlist, it may be necessary to port the simulation code to a UNIX text editor such as vi or emacs for debugging. This reduces the ease of use of the software somewhat.

The overwhelming impression gained from the use of Saber™ software from a user's point of view is that it is possibly the most rapid for development for standard components. The use of non-standard components would either require external coding with consequent time penalties, or construction of models in block diagram form.

Porting the simulation to a windows type environment gave additional benefits, for example, cutting and pasting of model blocks became a possibility, as did rapid connection of components. Previously, these operations had been menu driven and were slow and unwieldy.

9.1.5. Simulink simulation environment

The Simulink simulation environment used in version 4.0 was lacking in one major respect when compared to Saber™, that being the simulation library being based entirely on block diagram models. For the simulation of models based upon standard components, this would mean that the design of the simulation would require extensive re thinking, due to the non availability of a simulation front end based upon through and across variables. One distinct advantage existed with regard to data flow within the software, that being the fact that the simulation time could be tapped as a global variable, anywhere in the simulation. This meant that the timber surface simulation could be integrated into the model, and that the hydraulic side of the simulation could still be made to run with a variable time step.

Simulink enables alteration of variables during a simulation run, a distinct advantage over Saber™, with it's sequential simulation. This means that simulations may be optimised on line, with pseudo real time viewing of output waveforms.

User library functions may be written in Matlab code, C code, or may be assembled from the large number of low level diagram blocks which are available.

194

9.1.6. Real time adjustment of simulation parameters

Since the Simulink modelling and simulation environment allows adjustment of model parameters during a simulation run, the development time and debugging time for each model has been greatly reduced. It is also possible to look at the response of a hydraulic system over a range of frequencies during each simulation run.

9.1.7. In terms of simulation performance

Algorithm oscillation is automatically detected during a Saber™ simulation run, though the simulation will halt when oscillation is detected. Adjustment of simulation maximum step size along with maximum permissible error is necessary in order to avoid oscillation. More parameters are adjustable using Simulink than with Saber™, such as the choice of simulation algorithm, but greater attention must be paid to the simulation results since algorithm oscillation is not detected automatically by Simulink and therefore may produce misleading results.

9.1.8. Ability to interface with non standard components

The supplied template library for Saber™ is more extensive than that supplied with Simulink, though addition of custom components with Saber™ proved more difficult. It was found that using a block diagram modelling approach was the most flexible method of developing new non-standard components for simulation. Use of C code was necessary to construct the valve spool lookup table for the Saber™ model, since the MAST language entailed a longer development time for the code, mostly due to the un intuitive nature of it's syntax.

9.1.9. Overall system simulation - complete design for simulation

At the beginning of the project, it was envisaged that simulation of the hydraulic system would form a separate piece of work to the simulation of the timber cutting process. Waveforms produced by the Saber™ simulations would be ported to either Matlab or C based timber machining simulations to show the effect of cutterblock oscillation upon the timber surface form. Total simulation of the system became a possibility due to the rapidity with which the work was progressing towards the beginning of month 30. In addition, tentative steps could be made into the investigation of a suitable controller for

the hydraulic servo. The simulation described in section 6.0, not only fulfils the initial perceived purpose of the project, but has taken the intended simulation one step further, producing a fully tested, validated, complete model of the modified machining process. This model could form a keystone in work by carried out by future researchers in the construction of an industrial prototype.

9.1.10. Forwards compatibility

In addition to the writing of this thesis to describe the work undertaken during this project, it was decided that the software and methods developed herein should be of use to future researchers intending to continue with this work. To that end, the Simulink models developed are not system specific, and are readily exportable to many other simulation environments. The huge increase in the use of Matlab and Simulink in technical computing applications, to the point that it is deemed to be an industry standard, suggests that the model will be usable in its parent environment for many years to come.

9.1.11. Controller for hydraulic servo

The controller for the hydraulic system is readily implementable in software, and is a derivation of the traditionally applied phase locked loop. However, instead of using the phase difference to control a VCO, the phase difference is used to control a variable time lag. Some inroads were made into the design of a suitable PID controller for the hydraulic servo system, but the range of stable frequencies using this type of controller were somewhat limited. Since it was not envisaged that it would be possible to design a suitable controller during the project, due to the time required in developing other parts of the model, the controller can be seen to be an unexpected bonus. Design of the PLL controller is a necessity since full system simulation became possible, since it was found that even small phase lags within the hydraulic servo could actually have a detrimental effect upon surface finish.

9.1.12. Single knife finish

Although it was not necessary to simulate a multi knife finish in order to determine the effectiveness of cutterblock oscillation, a facility has been included within the Matlab surface simulation software in order to provide a simulation of multi knife finish, should it be required in the future. The Simulink model may be readily adapted to produce a multi knife finish, by using the multi knife cutter locus generation software (loci.m, listed in appendix 1), as a foreign function.

Horizontal cutterblock oscillation was deemed to require lower servo actuation speeds than for vertical cutterblock oscillation. However, the piezo actuation models developed as a spin-off to this project, and the Simulink based timber surface generator, with a little modification, could be used to gauge the effectiveness of small degrees of vertical cutterblock oscillation, which could be used to negate the effects of machine vibration and spindle runout. Such a method of cutterblock oscillation would require much tighter tolerances for phase angle matching were it to be used for cutter wave height reduction, but could be useful in removal of surface waviness defects for multi knife finish.

9.2. Performance of experimental apparatus

9.2.1. Mechanical design considerations

The experimental apparatus fulfilled two prime objectives, firstly increasing the speed of surface form generation, and secondly to validate the theory of cutterblock oscillation.

Initially, when simulations were being developed for the timber surface form model, generation of the timber surface waveform was slow, with a 1000 sample point waveform taking up to 45 minutes to process, with further time required for post processing and data extraction and plotting. The experimental apparatus provided a faster solution, taking around three minutes to perform each surface plot. Subsequent processing time was longer, but could be carried out automatically after scanning in large batches, using purpose written code to handle the scanned images. The use of a mechanical model which was constructed in month 12, at the time produced a more rapid and controllable surface form generator than was available using software at the time.

The Simulink based timber surface form generator, running on a faster platform, proved to be more effective when carrying out experiments with varying amounts of cutterblock oscillation, and when carrying out experiments to determine the effect of varying amounts of phase lag between command signal and servo output on the timber surface form. In addition, the Simulink model, as well as enabling parallel processing of waveforms with 5 different sets of initial conditions at once, was able to produce oscillated results with a variety of oscillation waveforms. Only sinusoidal oscillation was really practical with the experimental apparatus without the production of cams to generate waveforms equivalent to that produced by the hydraulic servo. Even in the short space of this project, computing technology has improved in performance at a pace which has radically improved the way in which these simulations have been carried out.

The validation of the cutterblock oscillation theory has nonetheless proven the effectiveness of the experimental apparatus. The predicted results for reduction in cutter wave height are very close to those produced by the machine. The purely mechanical nature of the waveform generator removes any presence of doubt that internal gains and software patches are needed to produce an accurate simulation. Some previous research has required the use of arbitrary constants within code to 'tweak' the output surface form in order to produce a result that closely resembles that produced in the real world. These

198

constants are not used in the model described here, since the output is found to be an accurate representation of the physically derived waveform. The surface waveform apparatus shows that the pure model, when thoroughly tested and designed rigorously, produces a simulation which is to all intents and purposes, a true and accurate representation.

9.2.2. Availability of Simulink requiring less results from machine, ease of parallel processing

The parallel processing of results has enabled the generation of larger amounts of simulated surface data than initially would have been thought possible. The software has produced a set of results which in depth and scope, are more satisfactory than the predicted data set at the project outset.

9.2.3. Post processing

The method of post processing results produced by the experimental apparatus, whilst effective in validating the theory of cutterblock oscillation, shows that variables are introduced for alignment of the plotting paper during plotting and scanning which are difficult to control. The magnification process greatly enhances any slope in the surface waveform, and rotation of raw images was sometimes necessary after scanning, in order to properly view the plotted waveform. A better solution would be to use a continuous strip of plotting material, with direct input of the surface waveform to a computer via a linescan camera and image grabber board. Although such equipment was not available during this project, it should be noted that there is scope for improvement of the method of cutterblock oscillation validation, as well as further study of the effects of vertical vibration upon the cutter surface waveform.

9.3. Discussion of experimental results for hydraulic simulations

9.3.1. Hydraulic servo simulations

The hydraulic servo simulations described here were primarily carried out in order to see if a hydraulic servo could operate under the required conditions, at frequencies such that a modified planing head utilising cutterblock oscillation, would be able to run at typical machine speeds. Thus, were cutterblock oscillation to be taken up as part of a wood machining line, it would not create a bottleneck. Servo simulations were carried initially at 100Hz, over distances in the order 0.5 - 3.0 mm. The simulations were carried out using the Saber™ simulation described in figure 4.4.5.1. References to hydraulic servo systems operating at such speeds, as described in the literature survey in chapter 3.0, show a speed / displacement trade-off, such that the work carried out here describes the development of a hydraulic servo with hitherto unobtained performance. The later availability of Simulink simulation code allowed the simulation of the servo using steeper transients, i.e. smaller time steps, and when this code became available, it was used to explore the servo lag properties in the sub 210 Hz region.

9.3.2. Servo under ideal conditions

Many set-up simulations were carried out in order to design the model used in simulation for the hydraulic servo, initially as a high level model, moving to a low level block diagram model in order to establish transient pressure characteristics, and moving back eventually to a higher level model with attributes such as fluid cavitation. A mass of data has been produced and some 'pruning' of the dataset has been necessary to produce a set of results which is succinct enough to be meaningful. Thus only the results which are essential to the description of the ultimate performance of the system designed are included.

9.3.3. Servo under ideal conditions, triangular wave control signal - 1

The simulation output waveform is shown in figure 8.1.1.1 after a simulation period of 4 seconds, this simulation taken to examine the effect of a simulation run of 400 oscillations on the servo in order to see if any low frequency components or instability are present. Tracking is poor because we are looking at an open loop system, with

200

inherent lags. A small degree of overshoot can be seen, as is a feature of such a non-stiff system, producing a rounded edge to the peaks and troughs of the cutterblock actuation waveform. The main criteria for the cutterblock actuation waveform was deemed to be that the acceleration characteristics matched those of the control signal over a broad area, such that the cutting stroke could be carried out with sufficient speed during the small time that the knife is in contact with the workpiece. Pressure was deliberately kept low for these simulations, due to the corruptive effect of high pressure transients in earlier simulations. The supply pressure for this model was 5MPa.

9.3.4. Servo under ideal conditions, triangular wave control signal - 2

This simulation, shown in figure 8.1.1.2, was carried out with an increased servo gain. Pressure supply was 5.5MPA. Cutterblock displacement achieved was 0.7mm. The system was still stable under simulation, and drift of the hydraulic servo at this frequency was negligible. Lag between command and response signals was 0.003s.

9.3.5. Servo under ideal conditions, triangular wave control signal - 3

An increased supply pressure of 6MPa is used in this simulation, shown in figure 8.1.1.3, with an achieved cutterblock displacement of 1.5mm. The majority of the output signal follows the slope of the input signal, over the most important area, the crossover point. Acceleration characteristics at the end stops do not affect the predicted surface finish, since this part of the oscillation cycle would occur when the cutter knife is no longer in contact with the workpiece.

9.3.6. Servo under ideal conditions, triangular wave control signal - 4

The single-acting servo is shown in this simulation, and as can be seen, the output is more symmetrical around the y axis than for previous plots. The servo output is seen in figure 8.1.1.4. This is due to adjustment of end stop spring coefficients as shown in section 4.4.5. Supply pressure is 7Mpa. The amplitude of oscillation produced here outperforms the minimum requirement by a factor of 2. This builds a degree of contingency into the design. When presenting these simulations, smaller intermittent steps in the development of the model are excluded. The net effect is that the results section often presents a simulation result whereby more than one variable has been altered since the preceeding model. This presentation method takes place for two reasons. Firstly, the inclusion of

every simulation result would not add extra clarity to the overall presentation of results, and secondly, because a degree of familarity had been achieved with the operation of the model such that sometimes more than one variable could be altered between simulations with confidence that the result would be predictable, i.e. the simulation would run without difficulty.

9.3.7. Output signals at start-up for varying frequencies

These simulations shown in figure 8.1.1.5 show that the amplitude of the hydraulic output signal increases slightly as the frequency decreases. from 100Hz down to 90Hz in 4 steps. This is to be expected since a greater flow of hydraulic fluid is achieved through the valve spool during the time that the ports allow fluid flow.

9.3.8. Square wave response

Figure 8.1.1.6 shows that a square wave provides an output signal closer to the ideal. Running at 100 Hz, it can be seen that the hydraulic servo is operating close to the maximum frequency with regard to rise time, since servo response is roughly triangular. Some low frequency effects may be seen as a low frequency drift superimposed upon the signal. Although a suitable controller could help to alleviate this, it is interesting to note that these effects are due to odd harmonics within the square wave actuation signal, affecting low frequency resonances within the servo model.

9.3.9. Servo lag for high level system developed using Saber™

The high level model was then adapted to include cavitation, which introduced nonlinearities within the system and a degree of increase in the compliance of the hydraulic servo. The first few cycles of the servo are at reduced amplitude since the ram is running towards the spring stops, until a balance is achieved.
This simulation's output plot is shown in figure 8.1.2.1 Servo lag 1 - Saber™ model. Pressure fluctuations at start-up do not affect the overall shape of the servo output response, and are an internal problem , alleviated by the use of the accumulator. The simulation shown in this figure was carried out with a supply pressure of 5MPa.

9.3.10. Servo lag 2 - Saber™ model

This plot shown in figure 8.1.2.2 shows the same simulation as in figure 8.1.2.1, 4 seconds later, using the servo with specifications as laid out in section 4.4.5, only continuing with a supply pressure of 5MPa.. Amplitude of the output waveform has stabilised, as has servo lag. This shows that the model is still stable after a 4 second period.

9.3.11. Servo lag 3 - Saber™ model

Referring to Figure 8.1.2.3, this simulation was carried out using the full specification supply pressure of 7MPa., and shows the start-up fluctuations of the servo under the same conditions as that which produced the simulation at T = 4.0s as shown in figure 8.1.1.4. As expected, the output amplitude ramp from initial to maximum is quicker, due to the increased supply pressure.

9.3.12. Servo lags for Simulink based model

When the hydraulic servo simulation was ported to Simulink, it was deemed necessary to establish servo lag around the intended operating region from transient simulations, in order to determine the amount of lag compensation required. Since the hydraulic servo would not be expected to operate far outside the specified frequency of operation (+ / - 10 %), a full scale system analysis within the frequency domain is not necessary, and the group of 7 transient plots which are described below, taken under stable operating conditions provides enough information to build a simple lag compensator which is used in the overall system simulation.

In order to examine the upper limits of the system performance further, the frequency of operation for the Simulink model was initially doubled, since the simulation code could allow for the reduced time step required, which had not been practicable using Saber™. A sine wave was used to drive the hydraulic servo model in these cases.

Figure 8.1.3.1: shows the tracking of the system running at 150Hz, with a 0.00175 second delay. Increase of the control frequency to 160Hz, as shown in figure 8.1.3.2, produces little difference, and for all practical purposes, we can assume a 0.001754 second delay. As expected however, servo lag will increase slightly with frequency, and the plot shown

in figure 8.1.3.3: shows the output response for the system running at 170 Hz, with an increased 0.0018s delay. Figure 8.1.3.4: shows a further increase in servo lag with the actuation control signal running at 180 Hz, the output response exhibits a 0.002s delay. We see the simulation output plots shown in figure 8.1.3.5, running at 190Hz producing a 0.0019s delay, the simulation shown in figure 8.1.3.6 200 Hz, 0.002s delay, and Figure 8.1.3.7: 210 Hz 0.00225s delay.

9.3.13. Secondary effects

Further investigations were carried out using the hydraulic servo model in order to examine the higher order effects of system components, and to examine more closely the effects of reduced system stiffness, due to reduction in fluid bulk modulus.

Reduction in the cylinder effective ram area by 50% for the system produces a marked reduction in system stiffness as shown in figures 8.1.4.1 Low frequency superimposition - 1, where marked low frequency effects may be seen, as well as some inconsistency in the symmetry of the output wave form.

Figure 8.1.4.2 Low frequency superimposition - 2, shows the start-up response of the same simulation. Many similar simulations of this nature had to be carried out during the initial design of the hydraulic servo, and show markedly the effects of reducing servo force gain in this manner.

9.3.14. Operating near to the resonant peak

During simulations at varying frequencies, it became apparent that the system was exhibiting resonance around $1.0e3$ rad.s^{-1}. A frequency sweep produced the bode plot shown in figure 8.1.5.1, which confirmed the theory, and produced a more accurate figure for system resonance at $1.25e3$ rad.s^{-1} Ten transient simulations carried out for a system running close to the resonant peak were taken. The simulation results shown in figure 8.1.5.2 and 8.1.5.3 show output waveform plots for the system operating close to the resonant peak. As can be seen, the output waveform shape for the system is assymetric and of poor quality, with the resonant frequency manifesting itself as a clearly visible component.

9.3.15. Stiffness reduction

Through reduction in bulk modulus of the hydraulic fluid it is possible to examine the effects of an increase in system compliance. (Viersima 1980) states that a reduction of fluid bulk modulus as great as 10% may be typical of a hydraulic installation towards the end of an 8 hour machine run. To this end, these simulations show the effect of reducing hydraulic fluid stiffness by 20% and show that proper maintenance of the hydraulic fluid during a machine run is critical in order to avoid low stiffness effects, when running at such high speeds.

Fluid maintenance measures recommended are:

Active oil cooling. The reduction in fluid temperature helps to maintain fluid viscosity, and in particular bulk modulus. Forced oil cooling using a radiator/ air draught system would be instrumental in maintaining oil stiffness.

Large reservoir size. In order to reduce the effects of air ingress and oil foaming, it is necessary to use a large volume settling tank to allow for air to naturally bubble from the hydraulic fluid. The use of oversized reservoirs in machine tools, much larger than those used for systems of similar capacity in plant with less critical operating parameters, is fairly common practice amongst machine tool manufacturers.

The effects of a large reduction in fluid bulk modulus may be seen initially in figure 8.1.6.1, showing a low stiffness system with square wave actuation. The output waveform can be seen to be largely random, with none of the required performance characteristics.

Figure 8.1.7.1 shows a low stiffness system with triangular wave actuation. Although less odd harmonics are present in the triangular actuation control wave, the effect of reduced stiffness means that the systems natural resonance becomes prevalent in the output waveform.

9.4. Discussion of results for timber surface simulations

9.4.1. Timber surface simulations

Early timber surface simulations were carried out using the timber surface simulation code developed using Matlab software. Simulation run times were long using the hardware available at the time, taking 60 minutes to produce each plot. The first results were carried out using a pure sine wave as a cutterblock actuation waveform, in order to provide a set of results which could be cross-correlated with the results produced by the test rig.

9.4.2. Pure sine wave oscillation

The first set of results shown are taken using 0% to 100% of the feed per revolution as an amplitude controller for the actuation waveform. These simulations were taken in 10% steps. The reduction in cutter wave height can be seen to be linear. The use of a large number of loci points (10000) for surface form extraction produces a surface form plot of high quality.

Since a sine wave does not produce ideal results for cutterblock oscillation, i.e. complete removal of cuttermarks is an impossibility, the most significant tests were carried out using a square wave for cutterblock oscillation, which is later used to drive the hydraulic servo in the overall simulation.

Figure 8.2.1.1 shows the pure timber surface waveform with no oscillation, and following simulations were carried out until the simulation shown in figure 8.2.1.11 - 100% of feed/rev pure sine oscillation

A typical output timber surface waveform produced using the Simulink timber surface model for pure sine wave cutterblock oscillation is shown in figure 8.2.1.12. A large amount of the cutter loci are visible in this plot, since the Simulink model does not perform surface wave extraction in the same way as the Matlab models. The larger amounts of cutter loci visible give a better indication of the surface form and the path of the cutterblock, particularly when viewing the results from several simulations at once.

206

In order to more closely examine the surface waveform simulations produced in parallel as shown in figure 8.2.1.12, successive magnifications of the surface image are made, showing in figure 8.2.1.13, an enhanced picture of the cutter loci, and the resultant surface finish. Although these plots give a good indication of the surface wave form, it was necessary to examine them in more detail to find correlation between experimental and simulated results, and so, higher magnification is used to produce the plot shown in figure 8.2.1.13, where the Simulink model is shown to produce the same results for surface wave height reduction as the earlier Matlab models.

Mapping physical quantities on to the cutter wave height figures in pixels has been avoided, because the system for assessing cutter wave height reduction was intended to be independent of knife tip radius, in order to be applicable to any machining scenario. However, it is interesting to state one typical set of machining parameters, and to predict what the reduction in cutter wave height would be through cutterblock oscillation. For example, a 180mm diameter cutterblock rotating at 6000 rev.min^{-1}, undergoes sine wave oscillation of equal amplitude to the feed per revolution. Timber feed is 10 m.min^{-1}. Two knives are producing a cut on the workpiece.

Applying equation 2.2.2.1, pitch of knife markings in mm is:

$$P = \left(\frac{10 \times 1000}{6000 \times 2} \right) \times 2\pi = 5.23mm \qquad 9.4.2.1$$

Cutter wave height using the conventional machining method may be found by applying equation 2.2.1.2:

$$h = 90 - \left(90^2 - \frac{5.23^2}{4} \right)^{0.5} = 37\mu m \qquad 9.4.2.2$$

Consider figure 8.2.1.14. Applying sine wave cutterblock oscillation, at 100% of feed per revolution amplitude, wave height may be reduced by a factor of 4. Thus cutter wave height becomes 9.4 microns.

9.4.3. Pure square wave oscillation

Pure square wave oscillation of the cutterblock was first simulated using the Matlab based surface simulation code, in order to view the ideal effects of cutterblock oscillation on surface wave height reduction. Output waveform plots are as follows:

Figure 8.2.2.1   0% of feed/rev pure square oscillation
Figure 8.2.2.2   25% of feed/rev pure square oscillation
Figure 8.2.2.3   50% of feed/rev pure square oscillation
Figure 8.2.2.4   75% of feed/rev pure square oscillation
Figure 8.2.2.5   98% of feed/rev pure square oscillation

100% of feed per revolution cutterblock oscillation produces a flat finish, and so has not been included in the results. The reduction in cutter wave height is more dramatic using a square wave oscillation waveform, with a 25% oscillation amplitude using square wave actuation producing the same height reduction as a 75% oscillation amplitude using a sine wave. For amplitude of 75% for square wave oscillation, we can see that the height of the cutter wave is -0.09988 units, where -0.1 units represents a flat surface, and the cutting circle follows a path of maximum amplitude in the y plane from -0.1 to 0.1. This computes to a cutter wave height reduction of 85% when compared with the un - oscillated system. As described in the previous section, the validation of the Simulink model of the timber surface generator was carried out by producing results correspondent to those produced by the Matlab surface simulation code.

Figure 8.2.2.6 shows a cutterblock oscillation simulation under ideal conditions using a square wave actuation waveform. Oscillation amplitude ranges from 0 to 100% in 25% steps. The surface wave height amplitudes produced by the Simulink model are the same as those produced by the Matlab model for square wave actuation of the cutterblock, whilst shown in figure 8.2.2.7 is a zooming in of figure 8.2.2.6 showing the change in width of the flat section at the bottom of each scallop mark produced by the cutter, for each successive increment in oscillation amplitude.

9.4.4. Effect of phase shift

Effects of the phase lag inherent to the hydraulic servo are outlined in section 8.2. Before the simulation of the total system, an investigation was made into the effects of phase lag between the cutterblock. Typical servo system phase lag for an open loop system is 0.002 ms. The simulations shown for pure square wave oscillation show that a greater tolerance is allowable for phase angle correction which may still provide surface height wave reduction of significant magnitude. Figure 8.2.3.2 shows the output surface waveform for a cutterblock oscillated with a pure square wave, with the maximum phase lag used being one order of magnitude greater than hydraulic servo phase lag, running to a maximum delay of 0.02ms. As can be seen, the increase in surface wave height is very small, producing a 1% increase in cutter wave height for a 0.02ms delay. A zoom in of the plot shown in figure 8.2.3.2 can be seen in figure 8.2.3.3, where the cutter wave shape with varying amounts of oscillation phase lag may be seen in more detail.

9.4.5. Further experimentation with cutterblock oscillation phase shift angle

A smaller amount of cutterblock oscillation phase lag more in keeping with the maximum 'worst case scenario' servo phase lag can be seen in 8.2.3.4. As can be seen, even for the maximum amount of phase lag, the difference between the 'lagged' waveform for the timber surface and the 'unlagged' waveform is very small. Figure 8.2.3.5 shows this figure in more detail, and it must be borne in mind that to the human eye, although cutter wave height is still low, the effect of light scatter upon the sharper peaks of the surface waveform may be such that the product is of unacceptable quality.

9.4.6. Hydraulic servo design for phase lag compensation

The hydraulic servo for the total system oscillation and it's corresponding lag compensator are designed with the consideration outlined in section in mind, and the PLL phase lag controller is tuned to produce a delay within an 0.005ms tolerance for a system running at 200Hz.

Figures 8.2.3.6, 8.2.3.7, and 8.2.3.8 show the effects of exaggerated phase lag upon the timber surface form. Note also that although a square wave actuation wave is used, the actual hydraulic servo output will have a finite slew rate, and consequently some rounding of the hydraulic servo output wave would lessen the effects of the sharp edges which are produced here on the cutter wave peaks.

9.5. Overall simulation of hydraulic system and timber surface form

9.5.1. Colour mapping for plots produced by parallel simulations

Ideal servo conditions (specifications as for actuator system described in section 4.4.4), using a square wave generated as shown in figure 6.5.1.1, produce successive reductions in cutter wave height as shown in figure 8.2.4.1. 5 simulations are shown here, the oscillation amplitude is stepping in 5 steps from 0 to 100%, ranging from blue (0%) through green (25%), red (50%), grey (75%), purple (100%). This colour progression uses the standard Matlab colour map and subsequent plots may be assumed to follow the same progression.

9.5.2. Discussion of results for overall system simulations

The overall system simulations revealed interesting results. As has already been stated, the hydraulic servo suffers from some small variations in phase lag, and due to the finite slew rate of the hydraulic servo when controlled by a square wave, a small degree of low frequency components are introduced into the servo output waveform. When used to control the timber surface form generator however, the reduction in cutter wave height is still significant. The standard actuation wave is generated using the cutter loci. Figure 8.2.4.1 shows an overall system simulation output timber surface waveform, 5 simulations being contained on this image. Reference to the colour map as depicted in figure 8.1.1.12 shows which colours refer to varying amounts of cutterblock oscillation amplitude. The simulations range in cutterblock oscillation amplitude in steps from 0% to 100% in 5 steps, as depicted in the previous Simulink based simulations shown in figure 8.2.1.14. Some 'bunching' of the cutter waves may be seen, as the hydraulic servo phase lag varies slightly from one loci to the next, but the overall result is a reduction in cutter wave height. Figure 8.2.4.2 shows a reduction in cutter wave height of 75% for 100% feed / rev oscillation amplitude for the overall system.

9.5.3. Improvement of controller parameters

Figure 8.2.4.3 shows another 5 simulations after optimisation of the PLL phase lag compensator, and shows a cutter wave height reduction of 89% when compared with the timber surface wave produced by the un- oscillated system.

9.5.4. Hydraulic servo low frequency drift

Low frequency drift was still present in the hydraulic servo, and further experimentation was carried out as described in section 8.2.4. Figure 8.2.4.4 shows that a low frequency phase angle drift is still present, though cutter wave height reduction is still significant. This points to a need for future research to develop a controller with improved phase characteristics in order to produce a surface form comparable in quality to that produced by the ideal (square) wave. However, the results are very encouraging, since a full simulation of the overall process has been produced, which was not previously thought to be possible within the available time, and inroads have been made into the design of a controller, which was also previously thought to be a subject for future work.

9.5.5. Enhanced machine performance visualised through simulation

It can be seen that although the performance of the system needs to be optimised to produce a surface simulation form which is closer to the ideal, the reduction in surface wave height gained (at least 75%) corresponds to the use of a cutterblock of a diameter 4 times than those used conventionally. Consequently the reduction in surface wave height achieved is generally only possible with an oscillated system, since most planing machines may not be fitted with cutterblocks of such size.

9.5.6. Hydraulic servo tracking performance

The figure 8.2.4.5 shows the current tracking performance of the hydraulic servo. Small degrees of phase lag variation may be seen in the plot, but performance is pleasing, since the literature survey in chapter 3.0 shows that a hydraulic servo has not yet been designed which continuously operates at frequencies greater than 100Hz, with an accurately tracked output of more than 1mm. The regions where the positive going slopes of the controlling square wave corresponds to the output signal are of greatest interest, since these areas represent where the knife will be in contact with the timber during the cut cycle.

9.5.7. Further experiments with increased oscillation amplitude

Since the hydraulic servo is capable of operating over displacements in the order of 4mm with no significant loss in tracking performance, a further 5 simulations have been carried out to examine the effect of increasing the amplitude of oscillation to double that of the feed per revolution. This computes to an oscillation amplitude of 4mm for the machining of timber with a conventional system producing a 2mm cutter wave pitch. As can be seen from figure 8.2.4.6, the cutter wave height reduction can be seen from the purple locus represents 200% oscillation, and minimum cutter wave height reduction is around 76%. The effects of the pseudo random nature of the effect of servo phase drift are reduced, such that over the majority of the timber surface, cutter wave height reduction (for the loci to the left of the highest) is in the order of 95%.

9.6. Discussion of scanned results from test rig

The test rig initially provided a rapid method of experimentation with varying amounts of cutterblock oscillation amplitude, and differing feedrates. Eventually, as the Simulink based timber surface model was found to outperform the test rig for speed in terms of data extraction, the primary purpose of the test rig became to validate the theory of cutterblock oscillation for a sinusoidal cutterblock actuation wave.

9.6.1. Scanned images from test rig - Set-up and repeatability tests

Set-up and repeatability tests carried out have produced promising results, producing a surface waveform plot which is of similar appearance to that produced using a stylus measuring instrument on an actual machined timber surface. The waveform plots are similar in form to those produced using a Talyrond 200 stylus measuring instrument, to examine machined timber samples, by (Maycock, 1993).

Figure 8.3.1.1 shows the timber surface waveform before signal conditioning. Visualisation of the actual timber surface form is rather difficult, due to stepping introduced by a degree of quantisation in the scanning process. This quantisation was necessary in order to limit scanned file size, and files were generally limited to less than 1MB. An image scanned at a full resolution of 1440 dpi would produce a cutter waveform plot of 30MB, and files of this size were too large to handle using the generation of hardware in use at the time. In order to partly overcome the problem of visualisation with the early setup signals, conditioning of the signals provided a smoother typical surface form plot, an example of which may be seen in figure 8.3.1.2. After the set-up waveform tests, the filtering process was discontinued, since the machine improvements outlined in section 7.2 enabled the production of surface form plots whiereby the surface form could be easily visualised with no further post processing.

9.6.2. Timber surface waveforms plotted during machine set-up and modification

Although many more tests were carried out during the construction of the machine, these images represent the first batch of formal tests carried out. Set-up waveform #1 , figure 8.3.1.3, shows the generated surface form for a single knife plot, i.e. one plotter pen is used to generate the predicted surface waveform. The image shown is typical of early

plots carried out using the test rig, whereby a degree of low frequency drift is seen as a hump in the centre of the plot. Magnification factor is 40x, so small unevenness in machine operation such as backlash, flexure of the machine frame, and bearing slack are contributory factors to an uneven base line for the timber surface form plots.

Figure 8.3.1.4 Set-up waveform #2, shows that a degree of low frequency drift can be compensated for by re alignment of the image during scanning. The Cutter wave marks shown in this image are sloping to one side due to a slight misalignment of the plotting paper, in this case 0.5 degrees, or +/- 0.8mm at the extreme edges of the paper. Greater attention was paid to the alignment of subsequent plots. Referring to figure 8.3.1.5 Set-up waveform #3, A degree of drift may still be seen in this plot, and attention was paid to the parts of the machine which may be causing such irregularities. The machine modifications which were carried out are described in full in section 7.2.

Referring to figure 8.3.1.6 Set-up waveform #4, a 50x magnification was used on this plot, and but for the low frequency drift, a surface waveform of high quality is visible. The images shown in Figure 8.3.1.7 Set-up waveform #5, and figure 8.3.1.8 Set-up waveform #6, show that the process was becoming more consistent between small numbers of successive peaks, using two different feedrates of 23.30 mm/rev and 10.9 mm/rev respectively. These feedrates are around 10 x those used in industry, in order to exaggerate cutter wave height to facilitate scanning. The effects on the surface geometry when applying cutterblock oscillation in terms of altering the cutter wave height, remain the same, independent of feedrate.

The timber surface waveform plots shown in figure 8.3.1.9 Set-up waveform #7, and Figure 8.3.1.10 Set-up waveform #8, are closer in quality to those produced using a stylus measuring instrument, and are quite noisy. Although any judgement of cutter wave height can be seen to be arbitrary, the effect of cutter wave height upon surface energy is still visible. However, surface quality could still be seen to be variable. Re-seating of some gears provided an improvement in low frequency drift as seen in these two plots.

Some surface noise could be attributed to bleeding of the plotting pen. In order to reduce 'wetting' of the ink into the surrounding paper fibres, the plotting speed was doubled to 12 rev/min, which produced a cleaner result.

Similar in nature to the previous two plots in terms of drift, the plot shown in Figure 8.3.1.11 Set-up waveform #9, was carried out using a finer plotting pen, 0.5mm as opposed to 0.8, and a higher plotting speed. Although low frequency drift was still quite

visible, since the main machine modifications had yet to be undertaken, the degree of high frequency surface noise could be seen to have been reduced by these measures.

9.6.3. Tests Following machine modifications

Machine modifications as outlined in section 7.2 greatly improved the repeatability of the process, and the problems of low frequency drift and overall slew were overcome.

The image in Figure 8.3.2.1 (Set-up waveform following machine modifications #1) shows the improved type of surface waveform which was produced after the machine modifications. As can be seen, the surface wave peaks were now of a high enough quality to make some judgements about the effect of the oscillation of the cutterblock upon surface wave height. The repeatability of the process was reinforced with subsequent tests, as can be seen in Figure 8.3.2.2 (Set-up waveform following machine modifications #2), and 8.3.2.3 (Set-up waveform following machine modifications #3), after improvement of the machine design. Although some low frequency drift is still present in the plot shown in figure 8.3.2.2, this is not of a magnitude great enough to affect an average cutter wave height measurement.

A further modification was made to produce the plots shown in Figure 8.3.2.4 (Set-up waveform following machine modifications #4), and Figure 8.3.2.5 (Set-up waveform following machine modifications #5), whereby 0.5N of preloading of the main bevel gear used for plotter head drive, in conjunction with a newer main bevel gear reduced the last vestiges of low frequency drift as shown in these two plots, to further improve the repeatability of the surface waveform plots.

The images shown in Figure 8.3.2.6 (Set-up waveform following machine modifications #6), and Figure 8.3.2.7 (Set-up waveform following machine modifications #7), and Figure 8.3.2.8 (Set-up waveform following machine modifications #8) highlight still that close attention needed to be paid to the alignment of plotter paper. Whilst the surface form image is still pleasing, showing good definition, temporary adhesive bonding of the plotted image to the scanner plate using 'post it' notes was used in subsequent plots to reduce any likelihood of the image drifting during the closure of the scanner lid, prior to scanning. The fixing of the plotted image positively to the scanner plate worked well, as shown in the two images Figure 8.3.2.9 (Set-up waveform following machine modifications #9), and Figure 8.3.2.10 (Set-up waveform following machine

216

modifications #10), and any drift in the image with regard to alignment could be gauged by a horizontal alignment mark taken during potting. This mark showed that alignment of the image was now within 1 degree for the un magnified image.

Surface waveform plots were now deemed to be of sufficient quality to carry out a batch of tests in order to validate the theory of cutterblock oscillation. The image shown in Figure 8.3.2.11 (Set-up waveform following machine modifications #11), is typical of the quality of surface waveform plots which was now achievable. Figure 8.3.2.12 shows the improvement in repeatability of the surface waveform plots in terms of surface wave height during this batch of tests, with the convergence shown graphically in figure 8.3.2.13.

9.6.4. Comparison between conventional surface form and surface form produced with cutterblock oscillation.

One final set of results taken using the cutterblock oscillation test rig has been included in this report, which shows that the predicted amount of cutterblock oscillation produces actual results very close to those predicted by the simulations. These results were taken using a lower feedrate of 5mm / rev, and scanning was carried out with no further filtering of the surface waveform. The results are very pleasing, and show that the theory of cutterblock oscillation for sinusoidal oscillation is valid, with a direct relationship between cutter wave height reduction and the oscillation of the cutterblock is existent.

Considering at first the three figures Figure 8.3.3.1 (Surface waveform plot taken without oscillation #1), figure 8.3.3.2 (Surface waveform plot taken without oscillation #2), figure 8.3.3.3 (Surface waveform plot taken without oscillation #3), These plots show the surface waveform output from the machine as a control, with no oscillation. A small degree of low frequency drift can be seen in the third plot, but is not considered significant since for the other plots taken, machine repeatability is good. Image quality is improved further with the next plot as can be seen in Figure 8.3.3.4 (Surface waveform plot taken without oscillation #4) Low frequency drift is not as prominent in this plot as previous plots. At this point, the mean cutter wave height for cutter waves with no cutterblock oscillation was beginning to be established at around 190 pixels.

217

The final three cutter wave plots taken without oscillation, Figure 8.3.3.5 (Surface waveform plot taken without oscillation #5), figure 8.3.3.6 (Surface waveform plot taken without oscillation #6), and figure 8.3.3.7 (Surface waveform plot taken without oscillation #7) show a repeatable surface wave plot, free from low frequency noise, and produce a good picture of cutter wave shape and height for timber surface form without cutterblock oscillation. Following these tests are the surface waveform plots taken with cutterblock (plotting head) oscillation.

The reduction in cutter wave height was noticeable throughout the following plots, and repeatability of the process was still of acceptable standard. Figure 8.3.3.11 (Surface waveform plot taken with oscillation #1) shows one of the better results, a small degree of quantisation still visible due to the scanning process, but the overall cutter wave height reduction is consistent.

A degree of alignment was necessary for the plot shown in Figure 8.3.3.12 (Surface waveform plot taken with oscillation #2), as can be seen from the slight sloping of cutter wave troughs. This was the exception rather than the rule however, and alignment properties of preceding plots was good. The plots shown in Figure 8.3.3.13 (Surface waveform plot taken with oscillation #3), figure 8.3.3.14 (Surface waveform plot taken with oscillation #4), figure 8.3.3.15 (Surface waveform plot taken with oscillation #5) show a consistent reduction in cutter wave height, as predicted by the simulations depicted in chapter 8.

The plots shown in Figure 8.3.3.16 (Surface waveform plot taken with oscillation #6), and figure 8.3.3.17 (Surface waveform plot taken with oscillation #7) complete the dataset for the timber surface wave forms produced by the cutterblock oscillation test rig. All plots produced a surface form image of good quality, with noticeable reduction in cutter wave height.

9.6.6. Overall cutter wave height reduction.

The mean cutter wave height reduction produced by the apparatus is very close (within 3%) to that predicted by the timber surface simulations. Allowing for a 1% quantisation error, and deviations in plotter line width of 2%, both of which were unavoidable, the results are very pleasing. The overall results suggest strongly that the construction of a purpose built machine, from purpose machined components, could produce a result even closer to the ideal.

10. Conclusions

10.1. Objectives realised

10.1.1. Hydraulic servo simulation

The hydraulic servo simulations carried out as part of this research show that the hydraulic servo model can be made to function at frequencies and amplitudes which have previously not been applicable to a hydraulic servo. Performance parameters are tight, and the maintenance of a system with low compliance is critical. The hydraulic servo simulation produced herein is robust, and can be used to explore the effects of high frequency running on the hydraulic servo. The simulations carried out show that in theory, the hydraulic servo model developed can be used to oscillate a cutterblock effectively at frequencies up to 200Hz, over a displacement of at least 3mm, which makes the hydraulic servo suitable for cutterblock oscillation at production speeds comparable to those currently used in the industry. The servo simulation produced can be used also in the further development of a controller which can compensate for low frequency drift in the phase lag properties of a hydraulic servo.

10.1.2. Cutterblock oscillation

Cutterblock oscillation has been validated in practice for a basic cutterblock actuation waveform, and the experimental results are promising, showing a reduction in cutter wave height through adoption of the modified machining method. The simulations carried out show that a sinusoidal cutterblock oscillation waveform can greatly reduce the amplitude of the cutter wave marks. The use of a perfect actuation waveform, i.e. a square wave, shows that complete removal of cutter wave marks is possible in theory. The output waveform from the hydraulic servo simulation produces a compromise between the two. Cutter wave height reduction is significant, and produces results which would not be achievable with conventional tooling.

221

10.1.3. Overall simulation

The overall simulation which has been produced, is a fully documented, fully functional, complete model of the modified machining process and its principal elements therein. The simulation has been used to explore the effects of altering various machining parameters, and has been used to carry out the groundwork with regard to system design for a prototype for a planing machine using the modified cutting method. The simulation is portable to other software packages which support graphical programming, and provides a solution to the simulation of the modified machining method, and the high speed hydraulic servo, which are in a form which will be useful in further research in this field.

10.1.4 Aims and objectives are fully realised

This project has researched the modification of the rotary machining process, in order to improve surface form. The research sought to demonstrate the effectiveness of modification of the cutting path to achieve this aim, and to develop a practical method of implementing it, which has resulted in a complete system design. All of the aims and objectives stipulated at the project outset have been met.

10.2. Future work

10.2.1. Controller

The further development of a controller for the hydraulic servo model could form an important basis for future research, and the exact matching of hydraulic servo output signal phase with that of the control signal, along with experimental validation, could even form a three year project in itself. The use of novel controllers such as neural network based controllers and fuzzy control methods could be explored, which at the time of writing are finding favour to a large extent over classical control methods, such as lag compensation. The design of an H- infinity controller as a regulator for the hydraulic plant model could provide an effective means of low frequency phase regulation, this type of controller being adept at coping with unforeseen plant variability. The excellent performance of neural network based controllers with non linear systems could provide an effective means of control for the hydraulic servo, which contains many non-linearities which have proven to be difficult to control with classical control methods. Effects such as cavitation, and the non linear porting of hydraulic fluid through all but overlapped square ported valves, could be therefore provided with an effective control solution.

The hydraulic servo system would need to be constructed as a prototype in order to continue with the design of a prototype machine, and long term effects, such as fluid degradation over several hours, and hydraulic component wear, could be examined. At the time of writing, these effects may not be effectively simulated.

10.2.2. Prototype technology demonstrator

When the hydraulic servo design has been validated, a suitable next step would be the construction of a prototype machine using the modified machining method. A standard planer head could be modified to allow for motion of the cutterhead in a horizontal plane, and power could be transmitted to the cutterhead via a cardan shaft. The technology developed herein could be put to two applications. These are visualised as follows:

223

Conventional tooling could be modified in order to produce a surface finish which is closer to the ideal. A best case scenario would be the removal of noticeable cuttermarks, in which case the production of timber components using the modified machining process could eliminate the need for sanding, and consequently remove a whole machining operation from the timber production process.

Since the modified machining process when using a cutterhead of far smaller size than with conventional tooling, would produce a surface finish of equal quality to the currently acceptable industry standard, a second proposal is the construction of a machine with smaller heads than are currently used, who's net effect would be a reduced balance requirement. Effects of cutterhead imbalance would be reduced, as well as the effects of proud knives. Tooling such as Cubic Boron Nitride, which may not be jointed, may be used in the modified machine to produce results of a quality which are currently only achievable with tungsten carbide tooling.

10.2.3. Closing the loop

The overall control of the cutting process could form the next step for future research, whereby a non-contact method of timber surface form assessment could be used to implement on-line control of the whole machining process. Vertical, as well as horizontal actuators could be used to compensate for cutterhead imbalance, providing on line compensation for deviations from a common cutting circle. In addition, the vision system used could flag faults in the machining process to an operator, before they became severe. This could reduce wastage, improve product quality, and extend machine and tooling life.

10.2.4. Impact on machine design

Whilst this project has concentrated on conceptual design of a system for cutterblock oscillation, a clear picture has emerged of the principal characteristics of a planing or moulding machine which would use cutterblock oscillation as part of the production process, with regard to machine design, and the outward appearance. The modified machining process would require a new approach to the design of the planer or moulder head, but would not necessarily involve a complete revision of current thinking with regard to the way in which a planer / moulder is put together.

Conventional planer / moulders are built up from a number of standard blocks, each of which carries the power unit, bearing assembly and cutterhead for a particular operation. The main casting from which each of these blocks is made is therefore located depending on where the cutterhead is to be located with respect to the timber. For instance, a block may be constructed to hold the cutterhead such that it cuts the bottom face of the timber, the top, or the sides. Universal heads may also be mounted which may carry a cutterhead with an adjustable spindle angle, useful for cutting bevel edges and other angled features. Some blocks may be designed to carry two cutterheads, such as for the top and bottom faces of the timber. These blocks are bolted together, and infeed and outfeed tables are bolted to the ends of the machine. Feed rollers are attatched to the machine, and may be carried on a horizontal gantry, for example, which is mounted over the outfeed table. The whole machine usually is surrounded by an acoustic enclosure.

This modular construction enables a machine to be built up using any combination of cutterhead types, enabling the construction of machines ranging from a simple single head planer, to a multi head moulding machine.
The modular construction also enables the straightforward addition of a machine block which may carry a cutterhead which utilises cutterblock oscillation, or several such blocks. The oscillating cutterhead could be offered as a single unit, which could be retro fitted to older machines, either as an additional cutterhead, or in place of an existing cutterhead.

The general appearance of a cutterhead would be similar to the current design, only the main bearing carrying the spindle would no longer be part of the main machine casting.
The cutterhead would be capable of oscillation because the spindle bearing housing would be mounted on ball slides, which would be no longer than the width of the spindle housing, since only a short throw of less than around 3mm would be required. In practice, ball slides with a throw of around 30mm may be used, in order that wear is not concentrated on one area.

The spindle could be mounted in bearings at each end of the cutterblock, and in order to remove cutterblock, end bearing would be removable but securely located when in position in a manner similar to the fixing of the end bearing in a horizontal milling machine. Alternatively, a suitable design could be produced which would free the spindle end, whereby only the main bearing housing is oscillated, though greater

attention would have to be paid to hydraulic and linear bearing design, since a greater moment would be produced by the cutterblock mass during oscillation.

The overall size of a cutterhead built to enable cutterblock oscillation would not necessarily be any greater than that of a conventional cutterhead. The hydraulic rams required would be of a short stroke, around 30mm, and consequently no larger than 100 mm length x 100 mm diameter.

Power transmission to the cutterhead could be via a belt drive, as for conventional cutterheads. Since the oscillation is of a relatively low amplitude, and would be perpendicular to the direction of the belt drive, fluctuations in belt tension would be unlikely to adversely affect machine performance. Should a belt drive prove insufficiently robust however, a constant velocity drive to the cutterhead could be provided by means of a Cardan Shaft.

The largest single addition to a planer/moulder would be the hydraulic power pack, though in order to oscillate a single cutterhead, a power pack capable of producing around 3 - 4 kW need occupy a space no larger than 400 x 400 x 400 mm. Should more than one cutterhead be fitted to a machine, a larger hydraulic power supply could be provided in order to supply hydraulic power to the machine.

The designer of a machine utilising cutterblock oscillation is faced with a choice with regard to tooling size. The designer could keep the cutterblock the same size, in order to produce a 'virtual cutterblock', through cutterblock oscillation which would have equivalent performance to a cutterblock of greater diameter. A 180mm diameter cutterblock, when oscillated with a sine wave, would have the same net effect as a cutterblock of over 600mm diameter, but with a massively lower balance requirement.
The designer could as an alternative opt for smaller and lighter tooling than is conventionally used, with less balancing difficulties than for conventional tooling. Smaller tooling would result in reduced power consumption, and a reduced overall machine size.

11.0 References

Allan, A. R.   Servoactuator Oscillates High Speed, Hydraulics and Pneumatics, 1962.

Altintas, Y.
Spence, A.D.   Solid modellers based milling process simulation and planning system. Winter annual general meeting of the American Society of Mechanical Engineers, Anaheim, CA, USA, 1992.

Analogy Inc.   Calling Foreign Subroutines, Saber™ MAST Reference Manual, Analogy inc. Saber™
User Guide. Analogy Inc. Aldwych House, Aldwych, London WC2B 4JP, 1995.

Aronson, R.A   Looking for Better Simulation and Sensing. Manufacturing Engineering, Vol. 113, Part 1, 1994.

Astrand, E.
Ronnqvist, M.   Crosscut Optimization of Boards Given Complete Defect Information. Forest Products Journal, 1994.

Avellaneda, M.   Magnetoelectric Effect in Piezoelectric/ Magnetorestrictive Multilayer (2-2) Composites. Journal of Intelligent Material Systems and Structures. Vol. 5, Part 4, 1994.

Bangert, H.   Update on Proportional Valve Performance. Hydraulics and Pneumatics, 1992.

Bishop, R. H.   Modern Control Systems Analysis and Design Using Matlab. Addison - Wesley Publishing Company, ISBN 0201596751, 1993.

Bobrow, J.E,
Lum, K.

Adaptive, High Bandwidth Control of A Hydraulic Actuator.
American Control Conf. Seattle, Part 1, June 1995.

Bolton, B.

Electromagnetism and it's Applications. Von. Nostrand
Publishing Co. Ltd, ISBN 0442302436, 1980.

Bosch (a)

Hydraulic Servo Cylinders 160 SV, 160 SVP, 160 SVU.
Ref: HP/VHI - BEY 015/2 DE, En, Fr (4.96) Robert Bosch
Gmbh, Stuttgart. 1997.

Bosch (b)

Bosch Hydraulics Short Catalogue Edition 2. Robert Bosch
Gmbh, Stuttgart. 1997.

Bracewell, R.
Sharpe, J.E.E

A Computer Aided Methodology For The Development of
Conceptual Schemes For Mixed Energy Transforming and
Real Time Information Systems.
http://www.comp.lancs.ac.uk/edc/papers/paper5/paper5.html
1996

Brown, N.

Development of Reliability Software, M.Sc. Thesis,
University of Leicester, Department of Engineering, 1994.

Brown, N.
Parkin, R. M.

Computer Simulation of a Hydraulic Servo Valve,
International Conference on Recent advances in
Mechatronics, ICRAM '95, 1995.

Brown, N.
Parkin, R. M.

A Design Model For A Mechatronic Approach To Novel
Woodworking Machinery, Mechatronics '96 5th UK
Mechatronics Forum International Conference, Guimarães,
Portugal. September 1996.

Burrows, C. R.
Tomlinson, S. P.
Hogan, P.A ,

Use of Computer Simulation in the Design and Selection of
Critical Components in Fluid Power Systems. The Fluid
Power Centre, University of Bath. Paper no. 911865, 1991.

Burton, R.T. Xu, P. Ramden, T. Krus, P. Sargent, C.	Feasibility of Training a Neural Network Based Hydraulic Component Simulator Using The Complex Method. Innovations in Fluid Power. The 7th Bath International Fluid Power Workshop, September 1994.
Carling, A.	Introducing Neural Networks, Sigma Press, Wilmslow, U.K, ISBN 1950581746, 1992.
Cheng, Y. De Moor, B. L. R.	Robustness and Control System Design for a Hydraulic Servo System. IEEE Transactions on Control Systems Technology, Vol. 2, No. 3, September 1994.
Clark, I.E Jennings, M.P	Syndite Cuts Wood. Industrial Diamond Review, Vol. 54, Part 561, 1994.
Compton, A. J.	Basic Electromagnetism and it's Applications. Von. Nostrand Publishing Co. Ltd, ISBN 0442317441, 1986.
Corinez, J. A.	Tooling; Cutting Edge Takes on New Shape. Tooling and Production, Vol. 57, Part 10, 1992.
Cui, P. Burton, R.T Ukrainetz, P.R.	Development of a High Speed On/Off valve. SAE Transactions, Vol.100, Part 2, 1991.
Cullman, J.	Servo Performance in Proportional Valves. Machine Design, June 25th, 1993.
Cyra, G. Tanaka, C.	On-Line Control of Router Feed Speed Using Acoustic Emission. 12th International Wood Machining Seminar, Kyoto, Japan, October 1995.
Dalay, B.S.	Enhanced Integration in the Woodworking Industry Through a Mechatronic Approach to Profile Grinding. Ph.D. Thesis. DeMontfort University. 1995.

Davalo, E. Naim, P.
(Translated by A
Rawesthorne)

Neural Networks, Department of Computer Science,
University of Manchester, 1992. 0333549961

DeVries, W. R.
Lemaster R.L.

Processing Methods and Potential Applications of Wood
Surface Roughness Measurement. 10th International Wood
Machining Seminar, Berkeley, CA. Oct 1991.

Dunn, P. H.

Piezo Actuators Used To Damp Tool Vibrations.Solid State
Technology, Vol. 37, Part 9, 1994.

Funakubo, T.
Tsubata, T.
Taniguchi, Y.
Kumel, K.
Fujimura, T.
Abe, C.

Ultrasonic Linear Motor Using Multilayer Piezoelectric
Actuators, Jpn J. Appl. Phys., Vol.34, Part 1, No. 5B, 1995.

Hagood, N. W.
Chung,
Von-Flowtow, A.

Modelling of Piezoelectric Actuator Dynamics for Active
Structural Control, AIAA 90 1097 CP, 1990.

Halstead, J.

Letter to N.Brown, Re: High Frequency Hydraulic Actuators,
J2 Mechatronics Ltd, Swindon, Wiltshire, SN6 7AG, 1995.

Harrison, M.

Practical C. Sigma Press, 1850580359, 1995.

Heisel, U,
Krondorfer, H.

Surface Method for Vibration Analysis in Peripheral Milling
of Solid Wood. 12th International Wood Machining
Seminar, Kyoto, Japan, October 1995.

Heisel, U.

New Tools and Machining Processes for Improved Surface
Finish during Woodworking. 12th International Wood
Machining Seminar, Kyoto, Japan, October 1995.

Hitchcox, A. (a)

Fluid Power Enters the Computer Age. Hydraulics and
Pneumatics, June 1993.

Hitchcox, A. (b)   P.L.C's Continue Thier Move Into Fluid Power Control.
                    Hydraulics and Pneumatics, May 1993.

Hodgson, P.G.   Computer Simulation of a variable Fill Hydraulic
Raine, J.K.   Dynamometer, Journal of Mechanical Engineering Science,
                    Part C, vol 206, pp 327 - 336, 1992.

Ikebe, Y,   On a Piezoelectric Flapper Type Servovalves Operated by a
Nakada, T.   Pulse Width Operated Signal, Trans ASME, Journal of
                    Dynamic Systems, Measurement and Control, Vol. 96, No.1,
                    1974

Hwang, C.L.   The Position Control of Electrohydraulic Servomechanism via
Lan, C.H.   a Novel Variable Structure Control. Mechatronics, Vol. 4, No.
                    4, 1994.

Ishida, M.   Principle And Operation of a New Type Motor Consisting of
Hori, T.   Piezoelectric Device And Strain Wave Gearing . Electrical
Hamaguchi, J.   Engineering in Japan, Vol. 112, No. 3, 1992.

Ismail, F.   Generation of Milled Surfaces Including Tool Dynamics and
Elbestawi, M. A.   Wear. . Journal of Engineering for Industry, Vol. 115, August
Du, R.   1993.
Urbasik, R.

Jackson, M.R.   Some Effects of Machine Characteristics on The Surface
                    Quality of Planed and Spindle Moulded Wooden Products.
                    Ph.D. thesis, Leicester Polytechnic, 1986.

Jung, C. Y.   Improvement of Surface Waviness by Cutting Force Control
Oh, J. H.   in Milling. International Journal of Machine Tools and
                    Manufacture, Vol. 31, No.1, 1991.

Kim, B. H.   Effect of Cutter Mark on Surface Roughness and Scallop
Chu, C. N.   Height in Sculptured Surface Machining. Computer Aided
                    Design, Vol. 26, Number 3, March 1994.

Kim, C. W.   Hierarchical Classification of Surface Defects on Dusty Wood
Koviro, A. J.   Boards. Pattern Recognition Letters, Vol. 15, Part 7, 1994.

Kim, J.D.   Study on the Modelling of Tool Motion and High Accuracy
Lee, E.B.   Surface Generation by the Use of Cutting Force Signals.
Hyun, D.H.   Journal of Materials Processing Technology, Vol. 47, Part 1 -
                     2, 1994.

Krus, P.   Fast Pipeline Models for Simulation of Hydraulic Systems.
Weddfelt, K.   Transactions of the ASME, Vol. 116, March, 1994.
Palmberg, J.O.

Kwong, A.H.M.   Design of Hydraulic Spatial Layout to minimise Noise and
                     Vibration. Project Description.
                     http://www.bath.ac.uk/Departments/Eng/edc/home.html

Lallement, J.   Hydropneumatic Accumulators, Fluid Power Components and
                     Systems - Second Bath International Fluid Power Workshop,
                     Mechanical Engineering Dept, University of Bath, U K. 1989.

Lampinen, J.   Self Organizing Feature Extraction in Recognition of Wood
Smolander, S.   Surface Defects and Colour Images.
                     International Journal of Pattern Recognition and Artificial
                     Intelligence, Vol. 10, Part 2, 1996.

Leaney, P. G. J.   The Modelling and Computer Aided Design of Hydraulic
                     Servosystems. L.U.T Ph.D Thesis, 1986.

Lebow, P.   Classification of Wood Surface Features By Spectral
Brunner, C.   Reflectance. Wood and Fiber Science, vol 28, part 1, 1996.
Maristany, A.G.
Butler, D.A.

Lee, Y. N.
Kim, T. W.
Suh, I. H.

A Look Up Table Self Organizing Fuzzy Plus Linear Controller. Mechatronics, Vol. 4, No. 1, 1994.

Lee, T. H.
Wang, Q. G.
Tan, W. K.

A Framework for Robust Neural Network Control of Non-linear Servomechanisms. Mechatronics, Vol. 4, No. 7, 1994.

Lee, B.Y.
Tryg, Y.S

Use of Model Based Cutting Simulation System for Tool breakage Monitoring in Milling. International Journal of Machine Tools and Manufacture, Vol. 32, No 5, 1991.

Lemaster, R.L.
Stewart, J.S

Progress in Evaluating Surface Quality Using Optical Profilometer Techniques. 12th International Wood Machining Seminar, Kyoto, Japan, October 1995.

Lemaster R.L.
Dornfeld D.A

Monitoring a Circular Sawing Process With Acoustic Emission. 19th International Wood Machining Seminar, Richmond, Canada, August 1988.

Lin, W.
Earl-Kline, D.
Araman, P.A.
Wiedenbeck, J.K

Design and Evaluation of Log to Dimension Manufacturing Systems using System Simulation. Forest Products Journal, 1994.

Lin, Z.C.
Liu, C.C.

A Finished Machining Simulation With A Pseudo Friction Coefficient. Journal of The Chinese Society Of Mechanical Engineers, Vol 16, Part 3, 1995.

Lorincz, J.A.

Tooling: Cutting Edge takes on New Shape. Tooling and Production, Vol 57, Part 10, January 1992.

Martin, H. A.
McCloy, D.

Pressure Transients Generated During the Rapid Braking of Asymmetric Hydraulic Actuators, IMechE Journal of Mechanical Engineering Science, Vol 21, No.2 1979.

233

Martin, K. F.   Pressure Transients in a Hydraulic Servo having Unequal Oil
                       Volumes. Measurement and Control, Vol. 5, June 1972.

Martin, K.F.   Stability and Step Response of a Hydraulic Servo with Special
                       Reference to Unsymmetrical oil Volume Conditions. Journal
                       of Mechanical Engineering Science, Vol. 12, No. 5, 1970.

Marusich, T.D   Simulation of Chip Formation in High Speed Machining.
Ortiz, M.   Applied Mechanics and Materials ASME Joint Conference, ,
                       Los Angeles. Vol. 208, 1995

Mathworks inc.   Matlab Neural Network Toolbox User Guide, Mathworks
                       inc., 24 Prime Park Way, Natik, MA 01760 U.S.A., 1993.

Maursich, T.D   Simulation of Chip Formation in High Speed
Oritz, M.   Machining.ASME Joint Conf. Los Angeles, Vol. 208, June
                       1995.

Maycock, K.M.   The Assesment of Surface Quality in Planed and Spindle
                       Moulded Products. Ph.D Thesis, DeMontfort University,
                       1993.

Melkote, S. N.   Enhanced Surface Texture Model For End Milling. Winter
Thangaraj, A.R.   annual general meeting of the American Society of
                       Mechanical Engineers, Anaheim, CA, USA, 08 - 13/11/92.

Mishanaevsky, L.L.   Mathematical Modelling of Cemented Carbide Tools in
                       Cutting Brittle Materials. International Journal of Machine
                       Tools and Manufacture, Vol. 35, No.5, 1995.

Molianen, H.   Piezoelectric Micromovement Actuator and Force Sensor
Lappalainen, J.   Hybridization Method Using a Thick - Film Double - Paste
Latinen, L.   Printing Method. Sensors and Actuators, Vol. 42 Part 1-3,
Leppavouri, S.   1994.

Moog Controls Limited, (a).	Proportional Control Valves with Integrated Electronics - D 660 Series. Moog Technical Catalogue No. D660 E10.93. Ahchurch, Tewkesbury, Gloucestershire, GL20 8NA, 1995.
Moog Controls Limited, (b).	Direct Drive Servo Valves with Integrated Electronics - D 633, D 634 Series. Moog Technical Catalogue No. D633/ 634 E01.94. Ashchurch, Tewkesbury, Gloucestershire, GL20 8NA, 1995.
Moog Controls Limited, (c).	Servovalves series E760. Moog Technical Catalogue No. E760 E-05.94. Ashchurch, Tewkesbury, Gloucestershire, GL20 8NA, 1995.
Morgan Matroc Limited, (a).	Piezoelectric Multilayer Actuators. Technical data for types 7111/03031/030, 7111/05051/030. Unilator Division. Vauxhall Industrial Estate, Ruabon, Wrexham, Clwyd, LL14 6HY, 1996.
Morgan Matroc Limited, (b).	Piezoelectric Bimorphs. Technical data for type PC5K. Unilator Division. Vauxhall Industrial Estate, Ruabon, Wrexham, Clwyd, LL14 6HY, 1996.
Morita, T Banshoya, M. Tsutsmoto, T. Murase, Y.	Cutting Performance of Diamond Coated Cemented Carbide Tools. 12th International Wood Machining Seminar, Kyoto, Japan, October 1995.
Ohta, M. Kawasaki, B.	The Effect of Cutting Speed on the Surface Quality in Wood Cutting. - Model Experiments and Simulations By the Distinct Element Method. 12th International Wood Machining Seminar, Kyoto, Japan, October 1995.
Park, S.	A Fine Linear Micromovement Actuator Using a Solid State Technology. Industrial Applications Society IEEE Annual Meeting, 1991.

Parmeko Ltd

1995 Catalogue. Parmeko Ltd. Percy Rd. Works, Aylestone, Leicester LE2, 1995.

Porankiewicz, B.
Ziomek-Moroz, M.
Wagner, K.

Study of Wearing Process of Cemented Carbide Cutting Edge when Milling Secondary Wood Products. 12th International Wood Machining Seminar, Kyoto, Japan, October 1995.

Rabie, M. G.

Improvement of Performance of an Electrohydraulic Servo Actuator by Developing a Pseudo Derivative Controller. . Modelling, Measurement and Control, ASME Press, Vol. 54, No.3, 1994.

Robotics World

Motion Control Software for Electromechanical Applications. Robotics World Vol. 11. Part 3. 1993.

Sansui, M.T.

The Computer Integrated Manufacture of Planed and Moulded Timber Products. M.Phil. thesis. Leicester Polytechnic, 1991.

Scheidl, R.
Garstenauer, M.
Grammer, S.

The Resonance Converter - A Novel Method for Hydraulic Fluid Power Control. Mechatronics '96 5th U.K Mechatronics Forum International Conference, Guimarães, Portugal. September 1996.

Scholliers, J.
Yli-Pietila, T.

Simulation of Mechatronic Systems Using Analog Circuit Simulation Tools. Robotics and Automation, IEEE conference, Nagoya, Vol. 3, 1995.

Sepehri, N.
Wan, F.L.K.
Dumont, G.A.M.

Hydraulic Compliance Identification Using a Parallel Genetic Algorithm. Mechatronics, Vol. 4, No. 6, 1994.

Sharpe, J.E.E (a)　　Integrated Platform for AI Support of Complex Design - (Part 1): Rapid Development of Schemes From First Principles. http://www.comp.lancs.ac.uk/edc/papers/part1/part1.html, 1995.

Sharpe, J.E.E (b)　　Integrated Platform for AI Support of Complex Design - (Part 2): Supporting The Embodiement Process. http://www.comp.lancs.ac.uk/edc/papers/part2/part2.html, 1995.

Shih, M.C.
Sheu, Y-R.　　The Adaptive Position Control of an Electro Hydraulic Servo Cylinder. JSME International Journal, Series III, Vol. 34, No. 3, 1991.

Silven, O.
Kauppinen, H.　　Recent Developments in Wood Inspection, International Journal of Pattern Recognition and Artificial Intelligence, Vol 10, Part 1, pp 83 - 95, 1996.

Simpson, P.K.　　Artificial Neural Systems: Foundations, Paradigms, Applications and Implementations. Pergamon Press Inc., ISBN 0080378951, 1980

Sims, W.L.　　200 Years of History and Evolution in The Woodworking Machinery Industry. Walders Press, Burton Lazars, Leicestershire. ISBN 0951117602, 1985.

Smith, C.C.
Jacobsen, S.C.
Allen-Robbins, L.
Wilcox, D.W.
Bohn, S.J.　　Design and Control of Electromechanical Actuation Systems. DSC - Volume 31, Modelling and Control of Compliant and Rigid Motion Systems. Transactions of the ASME, 1991.

Smits, J. G.　　Design considerations of a Piezoelectric on Silicon Microrobot.. Sensors and Actuators, Vol. 35, Part 2, 1992.

Sosa, H.Pourki, F.	Modelling of Piezoelectric Multilayer Structures. Proceedings of the SPIE, vol 1916, 1993.
Stewart, D.B.	A Novel Hydraulic Powered Vibrator Seismic Source. . International Mechanical Engineering Congress, Sydney. July 1991.
Stroud, K. A.	Engineering Mathematics.Macmillan, ISBN 0333620224, 1987.
Suematsu, Y. Yamada, H. Tsukamoto, T. Muto, T.	Differential Control of Electrohydraulic Servo System Operated by Differential Pulse Width Modulation. JSME International Journal, Series c, Vol. 36, No.1, 1993
Takata, S.	Generation of a Machining Scenario and It's Applications to Intelligent Machining Operations. Annals of the CIRP, Vol. 42, January 1993.
Tarng, Y.S. Shyur, Y.Y.	Identification of Radial Depth of Cut in Numerical Control Pocketing Routines. Journal of Machine Tools and Manufacture, 1992, Vol. 3 No 1.
Taylor, D.G.	Pulse - Width Modulated Control of Electromechanical Systems. IEEE Transactions on Automatic Control, Vol. 37, No. 4, April 1992.
Taylor, J.G	The promise of Neural Networks , Springer Verlag, ISBN 3540197737, 1993.
Thayler, W. J.	Transfer Functions for Moog Servovalves, January 1963. Moog Technical Bulletin 103. Moog Inc. Controls Division, East Aurora, N.Y. 14052, U.S.A.

Tran, H. D. DeBra, D. B.   Design of a Fast Short Stroke Hydraulic Actuator. . Annals of the CIRP, Vol. 43, Jan. 1994.

Tsao, T-C. Tomizuka, M.   Robust Adaptive and Repetitive Digital Tracking Control and Application to a Hydraulic Servo for Noncircular Machining. Transactions of the ASME, Vol. 116, March 1994.

Tunay, I. Kaynak, O.   Provident Control of an Electro Hydraulic-Servo System. IECON 93, 19th Conference, Hawaii, Vol. 1, 1993.

Uchiki, T. Nakazawa, T. Nakamura, K. Kurosawa, M. Ueha. S.   Ultrasonic Motor using Elastic Fin Rotor. Japanese Journal of Applied Physics. Vol. 38, No. 9B, September 1991.

Various.   British - United States Standard Units. Hydraulic Handbook, 2nd ed., Modern Trade and Technical Press Ltd, ISBN w7216157, 1968.

Viersma, T.J.   Analysis, Synthesis and Design of Hydraulic Servosystems and Pipelines. Elsevier, ISBN 0444418695, 1980.

Virvalo, T. Puusarri, P.   New Solution of Servo Control Problem in Mechatronic System. Computers and Electrical Engineering, Vol. 18, Part 1, 1992.

Wang, H.Z.   Surface Simulation Software. Software produced within the Mechatronics Research Group, Department of Mechanical Engineering, Loughborough University, 1995/6.

Watton, J.   Fluid Power Systems: Modelling, Simulation, Analog and Microcomputer Control.Prentice Hall, 1989. 0133231796

Weidenbeck, J.K.   Simulation for Rough Mill Options. Wood and Wood
                        Products, November 1992.

Weidenbeck, J.K.   Rough Mill Simulations Reveal That Productivity When
Araman, P.A.   Processing Short Lumber Can Be High.   Forest Products
                        Journal, January 1995.

Wilson, N.   Lotus Active Valve Train Research System. Ref: 1794/92,
Dopson, C.   Lotus Group p.l.c, 1992.
Muddell, G.

Wood Machinery   Wood Machinery Manufacturers of America: On The Move.
Manufacturers of   Wood and Wood Products, Vol.95, 1990.
America

Yokota, S.   A fast Acting Electro Hydraulic Digital Transducer, JSME
Akutu, K.   International Journal, Series 2, Vol 34, No.4, 1991.

Young, E   The Use of Linescan Cameras and a DSP Processing System
                        for High Speed Wood Inspection. . Proceedings of the SPIE,
                        Vol 2597, 1995.

Yun, J. S.   Application of an Adaptive Model Following Control
Cho, H. S.   Technique to a Hydraulic Servo System Subjected to
                        Unknown Disturbances.   Journal of Dynamic Systems,
                        Measurement and Control. Vol 113, September 1991.

Zhao, T.   Fuzzy Control of a Hydraulic Position Servo with Unknown
Virvalo, T.   Load. . 2nd IEEE International Conference on Fuzzy Systems,
                        San Francisco 1993.

12.1. Setup script for initial variable conditions

This function initialises process variables for one off simulations of the timber machining process. Larger batch runs are handled directly from the command line.

```
function [init_horiz_sampleo,feedo,imbalanceo,min_deptho,kniveso] =
setvar(feedi,imbalancei,knivesi)
ok = ['n']
ok = input('change init_horiz_sample? ','s');
if(abs(ok)==121)                              %Ascii code for x_reference
        init_horiz_sampleo = input('init_horiz_sample = ');
else
        init_horiz_sampleo = 0:0.001:20;
```

```
end
ok = ['n']
ok = input('change rev/min, feedrate? ','s');
if(abs(ok)==121)
        feed_per_min = input('feed / min? ');
        rev_per_min = input('rev / min? ');
        feed_per_rev = feed_per_min/rev_per_min;
        feedo = feed_per_rev.*init_horiz_sampleo;
else
        feedo = feedi;
end
ok = ['n']
ok = input('change imbalance? ','s');
if(abs(ok)==121)
        imbalanceo = input('cutterhead imbalance = ');
else
        imbalanceo = imbalancei;
end
ok = ['n']
ok = input('change no. of knives? ','s');
if(abs(ok)==121)
        kniveso = input('knives = ');
else
        kniveso = knivesi;
end
%feedo = feedo*init_horiz_sampleo;
feed_per_knife = feed_per_rev/2;
 min_deptho = 0-(sqrt(1- ((feed_per_knife/2)^2) ) )          %minimum depth of
cut from spindle centre
```

12.2. Cutter Tip Loci generator

Cutter tip loci are generated using the equations described in section 5.1. Shown below is the implementation of these equations in Matlab code.

```
% Neil Brown, Mechatronics Research Group, Dept. of Mech. Eng.
% Loughborough University
% Cutter Simulation  multi-knife surface finish for 2, 4, 6 knife cutters
% input vars are knives and feed, offsets to be applied to loci

function[rot_vert1,rot_vert2,rot_hori1,rot_hori2] =
loci(init_horiz_sample,feed,knives)

if knives == 2
    rot_vert1 = sin(2*pi*init_horiz_sample);
    rot_hori1 = feed+cos(2*pi*init_horiz_sample);
    rot_vert2 = sin((2*pi*init_horiz_sample)+pi);
    rot_hori2 = feed+cos((2*pi*init_horiz_sample)+pi);
    loc_hori = [rot_hori1,rot_hori2];
    loc_vert = [rot_vert1,rot_vert2];

elseif knives == 4
    rot_vert1 = sin(2*pi*init_horiz_sample);
    rot_hori1 = feed+cos(2*pi*init_horiz_sample);
    rot_vert2 = sin((2*pi*init_horiz_sample)+(pi/2));
    rot_hori2 = feed+cos((2*pi*init_horiz_sample)+(pi/2));
        rot_vert3 = sin((2*pi*init_horiz_sample)+pi);
    rot_hori3 = feed+cos((2*pi*init_horiz_sample)+pi);
    rot_vert4 = sin((2*pi*init_horiz_sample)+(3*(pi/2)));
    rot_hori4 = feed+cos((2*pi*init_horiz_sample)+(3*(pi/2)));
    loc_hori = [rot_hori1,rot_hori2,rot_hori3,rot_hori4];
    loc_vert = [rot_vert1,rot_vert2,rot_vert3,rot_vert4];
else
    rot_vert1 = sin(2*pi*init_horiz_sample);
```

```
rot_hori1 = feed+cos(2*pi*init_horiz_sample);
rot_vert2 = sin((2*pi*init_horiz_sample)+(pi/3));
rot_hori2 = feed+cos((2*pi*init_horiz_sample)+(pi/3));
       rot_vert3 = sin((2*pi*init_horiz_sample)+(2*(pi/3)));
rot_hori3 = feed+cos((2*pi*init_horiz_sample)+(2*(pi/3)));
rot_vert4 = sin((2*pi*init_horiz_sample)+pi);
rot_hori4 = feed+cos((2*pi*init_horiz_sample)+pi);
rot_vert5 = sin((2*pi*init_horiz_sample)+(4*(pi/3)));
rot_hori5 = feed+cos((2*pi*init_horiz_sample)+(4*(pi/3)));
rot_vert6 = sin((2*pi*init_horiz_sample)+(5*(pi/3)));
rot_hori6 = feed+cos((2*pi*init_horiz_sample)+(5*(pi/3)));

loc_hori = [rot_hori1,rot_hori2,rot_hori3,rot_hori4,rot_hori5,rot_hori6];
loc_vert = [rot_vert1,rot_vert2,rot_vert3,rot_vert4,rot_vert5,rot_vert6];
end
```

12.3. Cutter Simulation Routine

This section of the surface finish simulation controls and calls the filtering process described in section 5.2.1, in order to produce a surface wave from the cutter tip locus.

```
% Neil Brown, Mechatronics Research Group, Dept. of Mech. Eng.
% Loughborough University of Technology
% Cutter Simulation
%combine feedrates and oscillation

hori_fdrt = rot_hori+(1*x_reference);          %horiz. motion with feed _and_
                                               %rotation
ct_locus_vert = rot_vert;
[surface1] = finish((rot_hori+(1*x_reference)),ct_locus_vert); %call surface filter -
no actuation
for i = 1:20
    count = i;
    actuation_wave = rot_hori*(i/10);
    ct_locus_hori = rot_hori+(1*x_reference)+actuation_wave;
    %call actuation wave generator acwv
    [surface2] = finish(ct_locus_hori,ct_locus_vert);%call surface filter - actuation
    act_var_sf(i) = surface2(i);
    act_wv_ipt(i) = actuation_wave
end
surface_horiz = 0:0.01:5;
```

12.4. Main Surface finish function

This section of the simulation process contains the kernel code fopr surface wave extraction.

```
function [surface] = finish(ct_locus_hori,ct_locus_vert)

% Neil Brown, Mechatronics Research Group, Dept. of Mech. Eng.
% Loughborough University of Technology
% Cutter Simulation - surface filter

%filter - save some time by removing all parts of vert. locus greater than -0.6

[ascend,where_is] = sort(ct_locus_vert);   %verticals in ascending order
where_is = where_is(1:1000);          %take out largest 4 fifths by
locus_vert = ascend(1:1000);          %cutting indexes above 1000
locus_hori = ct_locus_hori(where_is);      %pull out corresponding horiz. pos.

%post processing - getting the surface waveform from the cutter tip locus

near_to = zeros(1,1000);where_is = zeros(1,1000);lowest =
zeros(1,1000);surface = zeros(1,251);

i = 1;
dist_horiz = abs((i/100)-locus_hori);      %distance of each locus point from feed
pos (spindle)
[near_to,where_in] = sort(dist_horiz);      %nearest ones first, and where in
matrix to look
lowest = where_in(1:10);         %get the nearest 10 to x_reference
verticals = locus_vert(lowest);         %get thier vertical positions
surface_local = min(verticals);         %the lowest one is where the wood is
surface(i) = surface_local;         %extraction complete
spread = 20;
```

%The unreadable but much faster version used for the main loop:

```
for i = 2:1:251;
    lasti = i-1;
    [near_to,where_in] = sort((abs((i/100)-locus_hori)));
    surface(i) = min(locus_vert((where_in(1:spread))));
    spreadless = spread;

    while (surface(i)==surface(lasti))&(spreadless>1)
        spreadless=spreadless-1;
        surface(i) = min(locus_vert((where_in(1:spreadless))));
    end
end
```

12.5. Algorithm used to get cutter wave peaks using y = mx + c::

This code has been included for the sake of completeness, and offers, on paper, a more elegant solution to the problem of surface wave extraction than the code described in section 12.4. Run time for this code however, was far greater using interpreted Matlab code, and therefore the code was used for performance evaluation purposes.

```
% Neil Brown, Mechatronics Research Group, Dept. of Mech. Eng.
% Loughborough University of Technology
% cutter wave peak filter


loop_limit = floor(length(newa)/5);


for i = 1:loop_limit
    Av = y(i);
    Ah = x(i);
    Bv = y(i+1);
    Bh = x(i+1);


    slopeAB = (Bv-Av)/(Bh-Ah);
    cAB = Av - (slopeAB*Ah);         %equation of line AB


    if Av>-0.9994


        for j = 2:loop_limit
            Cv = y(j);
            Ch = x(j);
            Dv = y(j+1);
            Dh = x(j+1);


            slopeCD = (Dv-Cv)/(Dh-Ch);
            cCD = Cv - (slopeCD*Ch); %equation of line CD
            testminhAC = min(Ah,Ch); %define the space in which
```

```
testminhBD = min(Bh,Dh); %to search for intersection
hmin = min(testminhAC,testminhBD);
testmaxhAC = min(Ah,Ch);
testmaxhBD = min(Bh,Dh);
hmax = max(testmaxhAC,testmaxhBD);

kstep = (hmax-hmin)/100;  %search ABCD quadrilateral for
                %xpoint
for k = hmin:kstep:hmax
    yAB = (slopeAB*Ah)+cAB; %using line eqns
    yCD = (slopeCD*Ch)+cCD;

    if yAB == yCD
        xpoint
        bk = 1;
        break
    else
        bk = 0;
    end
    end
    end
    end
end
```

12.6. De duplicate loci

This section of code was included in the data flow between the cutter loci generator and the surface wave filter. It offers a parallel implementation of a loci de duplicator, removing spurious loci points with the same displacement in x, only keeping the ones close to the timber surface. The speed advantage over a loop based method is significant, and the output dataset may be up to 15% smaller than the raw data output from the loci generator, with no loss of information in the timber surface region.

```
%Lcheck de duplicates loci with the same vertical position, pulling out the lowest
%and thus saving computation time::

function [lowest,aexceedb,bexceeda,same] = lcheck(a,b)


aexceedb = sign(sign(abs(a-b))+sign(a-b));  % 1 when a>b else 0
bexceeda = sign(sign(abs(b-a))+sign(b-a));  % 1 when b>a else 0
lowesta = bexceeda.*a;          % pull out low a components
lowestb = aexceedb.*b;          % pull out low b components
lowest = lowesta+lowestb;       % lowest a & b components
same = ~aexceedb&~bexceeda;       % apply NAND gate; trap same a,b's
```

12.7. Image loading for test rig output images::

When this code was developed, the version of Matlab used had no inherent function to load in 8 bit greyscale images, so this function was developed. The code shown below was simple and robust, and was used for the duration of the project.

```
function [picture] = loadimg(path_and_file,size)

file_name = [path_and_file,'.raw']   %set up file and path and extension
fid = fopen(file_name,'r');          %open binary file to read
fread(fid,size);                     %read it in
fclose(fid)                          %close it down
clear fid;
```

12.8. Image scanning for test rig output images::

This code is an edge detector for the 8 bit greyscale images pulled in from the code described in the previous section. The level check is embedded straightforward nested loop, and is used to detect any pixel with light intensity below a predetermined threshold of 50 (on a scale 0 to 255, black = 0, white = 255).

```
% Neil Brown, Mechatronics Research Group, Dept. of Mech. Eng.
% Loughborough University of Technology
% run through image and pull out the bottom part of the cutter tip locus

function [hist] = histo(picture,sizepic)

x_pixels = sizepic(1)
y_pixels = sizepic(2)

for j = 1:y_pixels
j;
    i = x_pixels;
    while (picture(i,j)>50&i>1)
        i;
        i = i-1;
    end
hist(j) = i;
end
```

12.9. Filtering for noisy surface form:: Top level::

This code calls the elliptical filter code which is included in the Matlab signal processing toolbox, filter design following the specifications described in section 8.3.1.

```
[b,a] = ellip(6,0.5,15,0.08);
h2 = filter(b,a,fliplr(histogram));
size h2
h2 = rotate(h2,start,finish);
```

12.10. Rotate function

This function corrects for any skew in the image which has occured during the scanning process. Since the image is greatly magnified, skew only becomes apparent after the raw image has been scanned and the surface wave image extracted using the scanning code listed in section 12.8.

```
function[rotated] = rotate(rtway,start,finish)


size(rtway)
rtway = 500-rtway(start:(finish));
continue = 1;
coeffs = polyfit(1:length(rtway),rtway,1);
plot(1:length(rtway),rtway,'k.',1:length(rtway),polyval(coeffs,1:length(rtway)),'r');
slope=polyval(coeffs,1:length(rtway));   %1st order polynomial=best line
diff = max(slope)-min(slope);
disp('diff = ')
disp(diff)
chd = input('change diff? 0 or 1 ?')
if chd == 1
    while continue == 1;
        diff =   input('new diff?')
        correct = (1:length(slope))./length(slope).*diff;
        plot(1:length(rtway),rtway+correct)
        continue = input('continue? 0 or 1')
    end
    else
        diff = diff;
end
pause
correct = (1:length(slope))./length(slope).*diff;
plot(1:length(rtway),rtway+correct)
grid
rotated=rtway+correct;
```

254

12.11. Text/binary data load::

This is a general purpose function which was developed in year 1, and used throughout the project to pull in ASCII text based data files. Whilst tha Matlab and Saber™ standards for data archiving are binary, they are not readily portable. Conversion of simulation results from binary to ASCII text ensures portability to future applications, as well as allowing visualisation of the results directly from file.

```
%load in data

function [data_back] = loaddat(path_name,file)

file_no = int2str(file);
file_name = [path_name,file_no,'.txt']

% try to read it in again to check for corrupted data
fid = fopen(file_name,'r');
[data_back] = fscanf(fid,'%f,%f');


fclose(fid)


%a2 is the returned variable from disk for error checking
```

12.12. Text/Binary data save::

This is the file output version of the code described in section 12.11, and was used to port binaries in the short term, with eventual data archiving in ASCII text format to ensure portability.

```
%save and return - saves something and returns it

function [a2] = savedat(data,path,name,file)
a = data;
file_no = int2str(file);
file_name = [path,name,file_no,'.txt']
[fid,error] = fopen(file_name,'w');
for i = 1:length(a)
    fprintf(fid,'%f\n',a(i));
end
fclose(fid);


% try to read it in again to check for corrupted data

fid = fopen(file_name,'r');
a2 = fscanf(fid,'%f');
fclose(fid)


%a2 is the returned variable from disk for error checking
```

12.13. Actuator power consumption::

As outlined in section 4.4.6, the code shown below was used to predict the power consumption of the hydraulic system in a broad sense.

```
function [force1,power1,force2,power2,power] = actpwr(mass,time,cut,disp)

% Neil Brown, Mechatronics Research Group, Dept. of Mech. Eng.
% Loughborough University of Technology
% Force, work done and power for cutterblock cut and retract cycles
% basic model, not taking viscous friction into account.

%force1, power1 are for cut, f2, p2 are for retract. disp is proportion of cycle for
%advance cut/ret cycle times

time_cut = (cut*time);
time_retract = time- time_cut;


%cut & retract cycle force & power for triangular wave input

force1 = (2*disp*mass)/time_cut^2;
power1 = (force1*disp)/time_cut;
force2 = (2*disp*mass)/time_retract^2;
power2 = (force2*disp)/time_retract;

work1 = force1*disp;
work2 = force2*disp;


power = (work1+work2)/time;
```

12.14. Linear motor template for servovalve actuator in MAST

This template was written as part of a range of building blocks for servo valve simulation in Saber™ at the beginning of the project, and was used in early simulation experiments as the prime mover for the valve spool model.

```
#Neil Brown, Mechatronics Research Group, Dept. of Mech. Eng., L.U.T. 1995.

element template linear_motor v_in v_gnd  shaft sh_ref = ke, kt, j, d, L, r

                        #  Declarations of the pins in the template header
electrical v_in,v_gnd           # electrical connections  (in volts and amps)
translational_pos shaft,sh_ref    # mechanical connections

# Argument declarations and their default values, if not passed in from netlist
number  ke=5m,           # motor electrical constant in  V/m/s
        kt=10,           # force constant in          N/A
        j=200u,          # armature mass in           kg
        d=3m,            # viscous losses in          N/m/s
        L=20m,           # armature inductance in        henries
        r=5              # terminal resistance in      ohms

{                       #  Start the internal definition of the motor:
                        #  Define some terms that will be used later
VAL h mom               # momentum
VAL frc_N visc,Tgen     # viscous losses force
VAL f flux              # magnetic flux in webers
VAL v vgen,vres,vin         # electrical potentials      volts
VAL pos_m w                 #  position of the shaft
                            #  (back EMF,resistance drop,input)
VAR i i                     # electrical flow in amps
values {                    # Describe the motor in terms of template
variables
    vin  = v(v_in) - v(v_gnd)       # electrical input voltage
    w    = pos_m(shaft) - pos_m(sh_ref)         # displacement output
    vgen = ke * w                   # voltage generated
    Tgen = kt * i                   # torque generated
    mom  = j * w                    # momentum
    visc = d * w                    # viscous losses of disp/t
    flux = L * i                    # magnetic flux in armature coil
    vres = r * i                    # voltage drop in coil resistance
    }
equations {                 #  Define the through variables for simulator
```

258

```
computations
  i:     vin = vres + vgen + d_by_dt(flux)
  i(v_in)    += i                     # current through electrical
  i(v_gnd)   -= i                     #  nodes
  frc_N(shaft)   += Tgen - d_by_dt(mom) - visc      # usable force
  frc_N(sh_ref)  -= Tgen - d_by_dt(mom) - visc      # reference flow
  }
}
```

12.15. General purpose MAST i/f for external C code

This code provides an interface between Saber™, and compiled external code.

```
#Neil Brown, Mechatronics Research Group, Dept. of Mech. Eng., L.U.T. 1995.

template table control pressure flow
output nu flow
input nu pressure,control

{
foreign number tablecode()
flow = tablecode(pressure,control)
}
```

12.16. Experimental external C code listing for valve spool

```c
#include <stdio.h>
#include <math.h>
#include <stdlib.h>

/*Neil Brown, Mechatronics Research Group, Dept. of Mech. Eng., L.U.T. 1995.
*/

/* Foreign function to model valve spool dynamics using a lookup table    */
/* in/out = arrays of inputs/outputs, nin/nout = number of array elements */
/* aundef = constant indicating undefined quantities in "in" array        */
/* ignore other arguements, they're used for releases of Saber™ beyond v3.4 */

/* use "int tablecode_(e.t.c)" for SunOS5.4 */

int tablecode_(in,nin,ifl,nifl,out,nout,ofl,nofl,aundef,ier)
int *nin,*nifl,*nout,*ofl,*nofl,*ier;
double *in, *out, *aundef;

{
double result;
double pressure = 0;
int pressure_local_datum,spool_local_datum,loop,i,j = 0;
double
flow_horiz,flow_vert,flow_out,pressure_local,spool_local,spool_positive_negative
= 0.0f;        /* ditto */

       /*table for Moog D760 series */

double flow_table [7][6] = {
          { 0, 0, 0, 0, 0,  0},
          { 0,10,20,30,40, 40},
          { 0,15,30,45,58, 58},
          { 0,19,40,55,66, 66},
          { 0,20,45,65,90, 90},
          { 0,22,50,70,100,100},
          { 0,22,50,70,100,100},
                   };
pressure_local = 0.0f;
spool_local = 0.0f;
spool_positive_negative = 1.0f;
pressure_local = in[0];
spool_local = in [1];
```

261

```c
if (spool_local<0.0)
{
spool_positive_negative = -1.0f;
}
else
{
spool_positive_negative = 1.0f;
}

pressure_local = (100-(fabs(pressure_local)))/100;      /* convert from
percentage for testing */
spool_local = fabs((spool_local)/100);
pressure_local_datum = floor(pressure_local*5);
spool_local_datum = floor(spool_local*4);

flow_horiz = ((pressure_local)-(pressure_local_datum/5))*
((flow_table[(pressure_local_datum+1)][spool_local_datum])-
(flow_table[(pressure_local_datum)][spool_local_datum]));
flow_vert = ((spool_local)-(spool_local_datum/4))*
((flow_table[(pressure_local_datum)][spool_local_datum+1])-
(flow_table[(pressure_local_datum)][spool_local_datum]));

flow_out = ((flow_table[(pressure_local_datum)][spool_local_datum])+
sqrt((pow(flow_horiz,2))+pow(flow_vert,2)))*spool_positive_negative;

*out = flow_out;

return 0;

}
```

13.0 Appendices: Publications

13.1 Appendix 2 - Paper: Computer simulation of a hydraulic servo valve.

This paper was presented at the International Conference on Recent Advances in Mechatronics, Istanbul, Turkey, August 14 - 16, 1995

Computer Simulation of a Hydraulic Servo Valve

N. Brown B.Eng. M.Sc., RM. Parkin B.Sc. Ph.D. C.Eng. MIEEE MIEE F.I.Mech E
Mechatronics Research Group, Department of Mechanical Engineering, University of Loughborough, LE11 3TU, UK
email N.Brown@lut.ac.uk

Abstract

An application within a research project into novel machining methods for the woodworking industry, has produced a need for a single stage spool type servo valve capable of operating in the region 80 - 100 Hz. It was necessary to know how well a valve would perform, and whether such high frequency running would adversely affect the other parts of the hydraulic circuit.

A simulation was undertaken using a powerful mechatronic modelling package, Saber ™, produced by Analogy inc..

The end result is a valve simulation which is comprehensive and flexible, yet straightforward to use. By using a combination of the methodology developed herein, along with manufacturers technical data, the suitability of a servo valve for a particular purpose may be more rapidly determined than was previously possible.

1.0 Nonclemature

	deflection of piezo actuator (mm)
d	charge constant ($\times 10^{-12} CN^{-1}$)
	length (mm)
	thickness (mm)
	applied voltage (V)

1 Introduction

Servo valves are either single stage, two stage, or three stage where high flow rates are encountered. In a single stage spool type servo valve, the main valve spool is actuated directly by an electric torque motor, linear motor, or more frequently a solenoid. Figure 1 shows a cross section of a typical servo valve, in this case the spool is driven directly by a linear motor. The control circuitry is used to generate a pulse width modulated voltage which is fed to the linear motor. A linear variable differential transformer is used as a position sensor which provides feedback to the control circuitry.

The spool is ported in a standard 4 way configuration. Flow in most single stage valves is limited by the power of the torque motor, since the motor shifts the spool directly. In

the two stage servo valve, the pilot or first stage receives an electromechanical input, amplifies it, and controls the movement of the second (main) stage. In a typical 2 stage spool type servo valve the low force torque or linear motor actuates the pilot spool which in turn ports high pressure fluid to shift the second stage. Most servo valves are two stage.
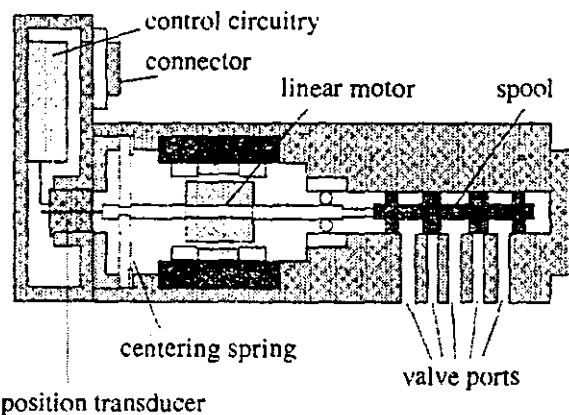

Figure 1: Cross section of direct drive servo valve

2.1 Modular Construction of Servo Valve

It could be seen that although many different configurations of servo valves exist, all of which perform much the same purpose, the primary components are always an actuator, and one or more spools [1]. One spool only need be created for the purposes of modelling, since spools may then be cascaded to produce extra stages.

It was therefore decided to produce a range of building blocks from which a valve model could be assembled.

Figure 2(a,b,c) show the block diagrams for a two stage torque motor actuated valve, a direct drive single stage linear motor actuated valve, and a piezoelectric stack operated valve as described in [2] respectively. The following circuits were designed in order to simulate a range of servo valves.

1) A linear motor model, which may also be used to simulate a solenoid with linear force/stroke characteristics. Linear force/stroke solenoids are increasingly used in hydraulic servo valves in place of torque motors [3], [4].

2) A torque motor model. In this case it was discovered that the DC permanent magnet motor model produced by Analogy inc. could be used, though a method of converting the output from the motor from rotational to linear had to be found, in order to connect the output to the valve spool input.

3) A valve spool model. This was the most complex part to model, so effects of the spool upon the actuators such as friction and viscous damping were added to the actuator models in order to simplify the spool model. This also facilitated straightforward connection between spools in multi-stage valves.

4) An interface was produced so that spools could be cascaded for simulation of multi-stage valves.

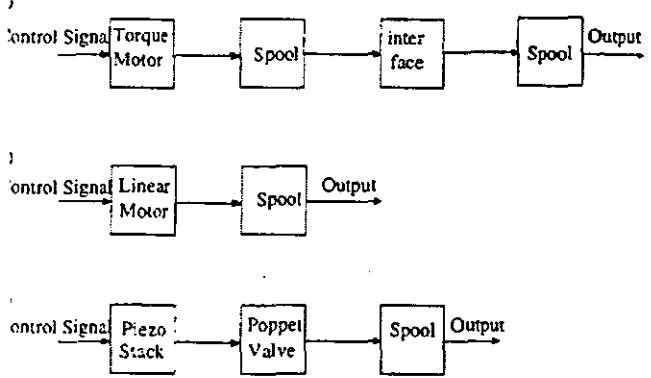5) A model for a hydraulic load was produced to aid testing of the model.

Figure 2: Simulation of servo valves using standard blocks

4.0 Use of Saber™ and Related Software

Analogy inc. produce a range of simulation software products. Figure 3 is a flow diagram showing the simulation process and the relationships between these products.

Component models are called templates. Templates are written in MAST, the Saber™ modelling language, which is similar in structure to C. [5]. These templates have associated symbols which are used to represent the templates on screen. An extensive library of standard components is available for modelling mechatronic systems, components being available for mechanical, electronic (digital and analogue), hydraulic, magnetic and optical systems.

Custom templates may be written by the user to describe components not included in the library produced by Analogy inc. [5].

MAST code can be interfaced with external code such as C, or Fortran, so that existing simulation code may be incorporated into the design.
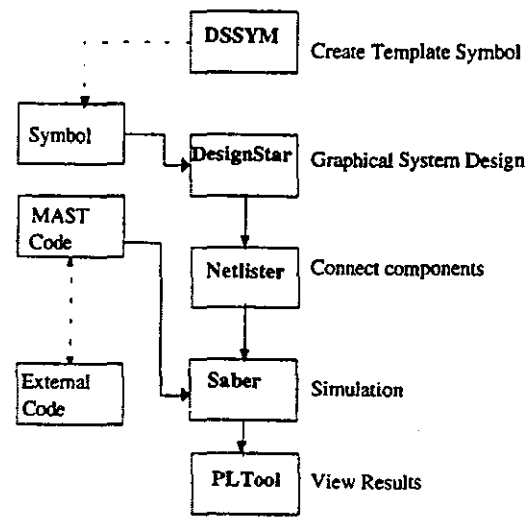

Figure 3: Simulation process using Saber™

3.1 DesignStar™

DesignStar™ is the graphical editor which enables the user to connect components together on screen in order to build up a complete circuit. The other software packages in the group may all be accessed from Designstar™.

3.2 DSSYM™

When a new component is to be designed from scratch, a symbol for the component template is drawn in DSSYM™, the designstar symbol editor. A symbol contains three main types of information.

1) Text and graphics used to identify the symbol in Designstar™.

2) Ports which are used for connecting the symbols together.

3) Properties. These are used to define the symbol characteristics, for example, the stiffness of a spring.

3.3 Netlister™

The first step in running a simulation is to generate a netlist of the design. A netlist is a list of parts in the design circuit, property values which have been assigned to them, and a description of their connections to each other [5]. The

ıftware also searches for, and reports on errors in the
ısign such as missing properties.

4 Saber™

4.1 Variable Step Length

ıber™ is the core of the simulation package, and contains
e algorithms which carry out the simulation.

correct step length used when solving differential
uations using numerical methods, can be a major cause of
rors in computer simulation [1], [6], [7], [8]. In all
nulation software there consequently exists a
eed/accuracy trade-off [6].

ber™ features a variable step length whereby the user
lects the required accuracy of the simulation, and the
nimum step length. The software automatically selects a
ıger step length when the accuracy of the simulation is
thin the required range, though it will backtrack and
rform a smaller step length otherwise. The saving in
mputation time using this method is considerable.

predictor-corrector algorithm is used to set the time step.
:ond order polynomial extrapolation is used to predict the
ıswer at dT in the future. The simulator then solves the
item at that point.

..2 On Running a Simulation

was generally found that simulations requiring a very
all step size in order to produce results within the
uired limits of accuracy, were in some way faulty.
ually errors in the schematic are picked up by the
lister.

wever when working on a hypothetical valve model,
itrary constants are inserted in order to test the model
ich may not be completely realistic.

en a simulation is aborted for this reason, error messages
y be viewed in the .out file generated by saber. These
ır messages should point the user to the faulty
ıponent.

quare wave was used to actuate the valve model for a
:ar motor actuated servo valve. At low frequencies,
0Hz), results were good, with computation times rarely
eeding 15s for a 1s transient analysis with a step size of
:-3.
vever, shorter step sizes were required for higher
uencies such that large files were often generated. This
 also the case when increasing the length of the transient
ıysis such that particular attention must be paid to
ing up enough hard disk space for the software to
:tion correctly. 80Mb of hard disk space was found to be
ıuate.

It is useful to note which algorithms are used by saber in
order to carry out a simulation. The following sections will
describe which analyses are used, and the algorithms which
are used within.

Saber utilises automatic algorithm selection, ALGSTEPping
such that if one algorithm does not produce convergence,
the code will try the next.

For further information on the use of these simulation
processes, the reader should consult [5].

3.4.3 DC Operating point Analysis

The DC operating point at time=0 is found by this analysis.

ALGSTEPping uses one of the following methods to
converge the solution:

1) Simple D C, using Newton-Raphson with no ramping.

2) Dynamic Supply Ramping, which uses Newton-Raphson
with dynamic supply ramping.
Dynamic ramping ramps the supply voltages in real time
whilst applying the fully the transient solution technique.
All dynamic effects are taken into account.

3) Conductance Ramping, using Newton Raphson with
Gmin ramping and no supply ramping.
Gmin ramping applies small leakage conductances to
certain nodes of the circuit, then removes them successively.

4) Density Ramping, using static supply ramping but no
Gmin ramping.
Density ramping uses successive approximation to find the
values and derivatives in non - linear models, whilst static
ramping slowly increments all of the sources in the circuit to
their steady state values.

5) Katznelson with density ramping, with no supply or
Gmin ramping.

3.4.4 Fourier Analysis

The fourier analysis uses discrete fourier transforms, DFT's
to obtain the magnitude versus frequency characteristics of
the system.

3.4.5 AC Analysis

The AC analysis determines the frequency domain
characteristics of a system using a small sine wave as the
input. The assumption is made that the signal is sufficiently
small to keep the system linear.

4.6 Noise analysis

his analysis identifies sources of noise in an electrical rcuit. The effects of thermal, shot, and flicker noise are :termined.

4.7 Distortion analysis

oduces harmonic distortion results with respect to :quency.

4.8 Monte Carlo Analysis

Monte Carlo analysis of a system is possible through .ber, which is particularly useful for determining the obability of failure (pfail) for a system, and to optimise the iability of the system. Uniform and normal distributions ‹ included as standard, though custom distributions, (e.g. :normal for fatigue life calculations) can be introduced.

; PLTOOL™

hen the simulation has run, results may be viewed using .TOOL™. PLTOOL™ allows the user to view, inipulate and plot wave forms. Further information can extracted from simulation results using the PLTOOL™ st processing code.

though progress with this software is rapid, a considerable rning curve still exists such that a thorough knowledge of : software, the system being modelled, and the hardware iitations is required, particularly for the modelling of chatronic systems Nevertheless, the simulation has 'eral advantages over physical modelling.

ta collection is most straightforward, since the Saber™ :kage contains some very powerful data processing code.

: simulation is completely repeatable, allowing the user nplete control over the development of the model [6].

iighly realistic model can be produced, yet the simulation free from the physical limitations of the system being lied [7].

Modelling of Valve components

Actuators

outlined in section 2.1, it was decided that a template uld be produced for a DC linear motor [1], [5]. The iplete schematic for the linear motor actuator is shown in ure 5, and the schematic for the dc torque motor iator, as described in [3], is shown in Figure 5.

: gain of -1 for the extend control signal within the iator templates, produces the signal zinv. The two ials are later used to simulate the effect of switching

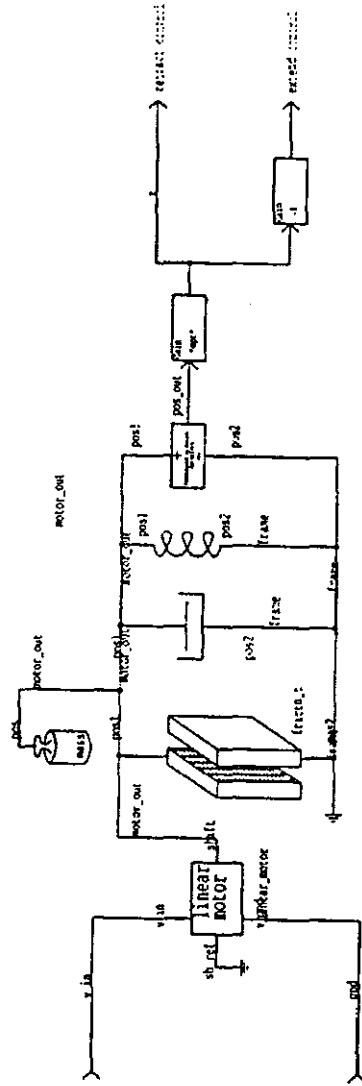between extend pressure, retract drain, and retract pressure, extend drain.

Figure 4: Linear Motor Actuator

A piezo stack operated servo valve, as described in [1], has been shown to offer a particularly good response. Therefore a template was written for a piezoelectric bimorph using equations obtained from manufacturers data [11], to describe tip deflection (1), and blocking force (2), for a bimorph.

$$x(L,V) := 2.\frac{3}{2}d_{31}.\frac{L^2}{t^2}.V \qquad (1)$$

$$F_b(L,w,V) := 2.\frac{3}{8}d_{31}.V.w.\frac{t}{L.SD_{11}} \qquad (2)$$

me experimentation was then undertaken using a mulation of a piezoelectric bimorph as part of a flapper lve, though with little alteration to the template code a ezoelectric stack could be simulated.
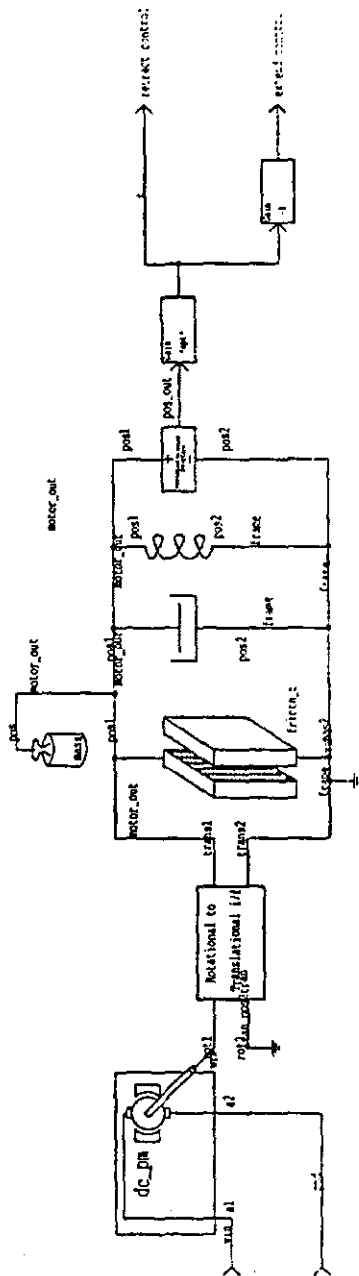

Figure 5: Torque Motor Actuator

pool

matic diagrams are included at the end of this paper. e 6 shows the spool schematic. The spool was built control blocks contained in the DesignStar™ control n template library, and was interfaced with the anical and hydraulic parts of the circuit using the

Trnl2var and Var2Q templates. These templates convert a translational position into a unitless variable, and a unitless variable to a hydraulic flow rate respectively.

The input gain is used to match the output of the actuator to the input of the spool, and is generally used where a linkage will exist between a torque motor and the valve spool [3].
The signal is then split in order to produce the correct 4 way characteristics. The constraints are used to set the opening positions of the ports, all dimensions being in mm.
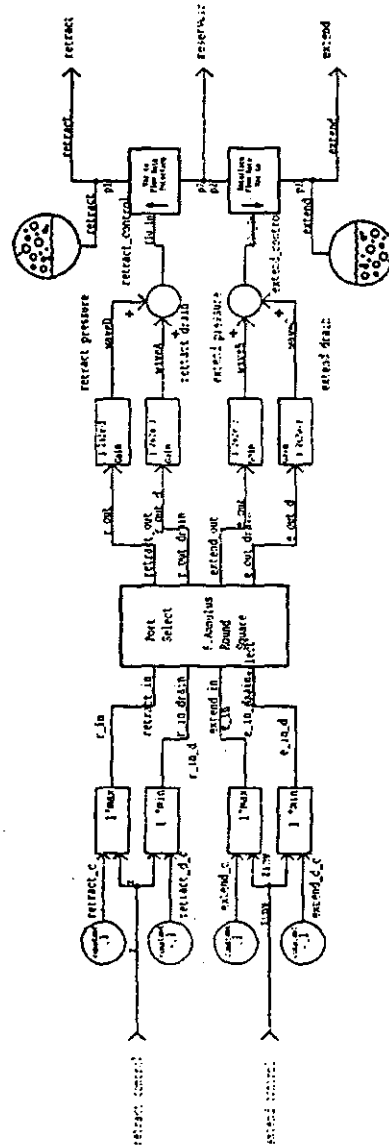

Figure 6: Valve Spool

Figure 7 shows the hydraulic load which was used to test the spool circuit, and Figure 8 shows the cascade interface used for multiple stage valves.
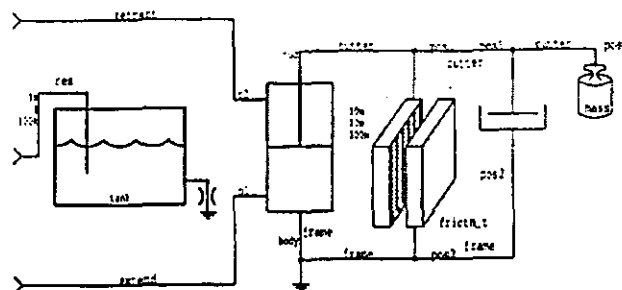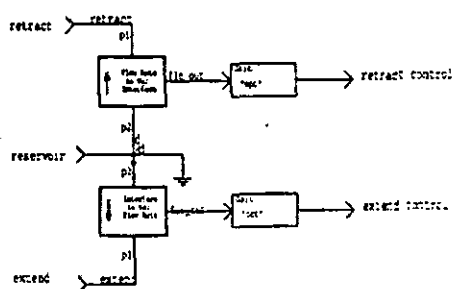
Figure 7: Hydraulic Load

Figure 8: Cascade Interface

2.1 Valve Lap

ap is the physical relationship between spool metering
nds and port openings. An open centre servo valve refers
an underlapped condition in which the lands are slightly
rrower than the porting area of the body or sleeve. When
e valve is centred, this arrangement allows a constant flow
oil from the pressure side of the pump to flow across the
rts to the reservoir [3]. The pressure drop across these
strictions produces an intermediate pressure at the
linder ports. This pressure is normally 40 - 60% of the
pply pressure [3]. A closed centre valve has an outer
pped arrangement in which the lands are slightly larger
an the porting area. This construction is not so common
servo valves, because it creates a dead zone and therefore
akes the valve unresponsive to small signals. A slight
erlap may be used however, in conjunction with dither.
igh frequency, low amplitude vibration of the spool
ercomes stiction effects) to ensure a dynamic line to line
ndition. A line to line servo valve features spool metering
nds which just co-incide with the port openings. With this
nfiguration, leakage provides enough flow to establish the
termediate cylinders port pressures, and the valve is ready
respond to very small movements.

nsequently open centre, closed centre, and line to line
ool cylinder arrangements may be modelled simply by
tering these constraints.

Friction and stiction of the spool as well as spool mass may
be incorporated. Viscous damping of the linear motor and
solenoid cores due to immersion in the hydraulic fluid may
be modelled using the viscous damper attatched to the motor
output.

4.2.2 Port type

Typical non linear flow/position characteristics of the spool
due to orifice shape, derived from [2], are shown in figure 9.
These characteristics must be included in the valve model
for maximum accuracy [1], [12].

A custom template was written in MAST in order to
produce the effect of round, square or full annulus ports. A
function representing the flow rate/valve spool position
characteristics of the valve may then be inserted into the
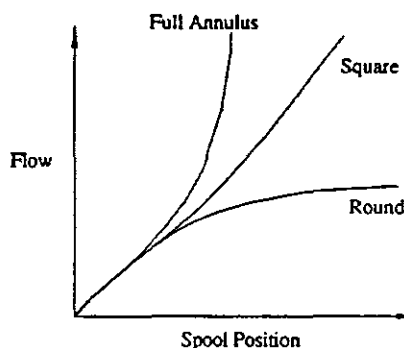template.

Figure 9: Spool position versus flow characteristics for
different port shapes.

Separate gains are used for all port positions to allow for
unusual spool designs, spool and seal wear [1].
The retract and drain signals are then combined using the
summing blocks before being passed to the var2q interfaces.

4.2.3 Cavitation

As stated in the Saber^{TM} user guide: "Cav template models
an ideal cavitation effect with one hydraulic pin. Its
behaviour is such that when pressure at the pin is
maintained, the pressure is maintained at that level until
the system recovers" [5].

Therefore, the effects of over-running hydraulic cylinders
and motors on the valves performance may be taken into
account.

5.0 Conclusions

A range of building blocks for the simulation of hydraulic
servo valve components has been produced.

sub circuit for a complete valve spool now exists, as well templates for a linear motor. a piezoelectric actuator, and emplate has been written which can be adapted to include rt shape in the model.

can be said in conclusion therefore, that for this plication the speed and ease with which a simulation can produced with this software has proven most satisfactory.

Acknowledgements

e authors would like to thank Analogy inc. for their ›port. Saber, DSSYM, DesignStar, and Netlister are demarks of Analogy inc.

References

- P G J Leaney, The Modelling and Computer Aided sign of Hydraulic Servosystems, Ph.D Thesis, ughborough University of Technology, 1986.

S Yokota and K Akutu, A fast Acting Electro Hydraulic gital Transducer, JSME International Journal, Series 2, ıl 34, No.4, 1991.

- James E Johnson, Electrohydraulic Servo Systems, blished by the editors of Hydraulics and Pneumatics ıgazine, 1977.
- E W Reed and I S Larman, Fluid Power with croprocessor Control, Prentice Hall International, 1985.

5 - Analogy inc. Saber^{TM} User Guide, Analogy Inc. Aldwych House. Aldwych, London.

6 - R J Ord - Smith and J Stephenson. Computer Simulation of Continuous Systems, Cambridge University Press, 1975.

7 - E Wallace and S Sutherland, Simulation Using Digital Computers, Prentice Hall International, 1967.

8 - N Brown, Development of Reliability Software, M.Sc. Thesis, University of Leicester, 1994.

9 - Moog Controls Limited, Ashchurch, Tewkesbury, Gloucsestershire, GL20 8NA, U.K. catalogue: D660 E 10.93

10 - Moog Controls Limited, Ashchurch, Tewkesbury, Gloucsestershire, GL20 8NA. U.K. catalogue: D633 / 634 E - 01.94

11 - Morgan Matroc Limited, Unilator Division, Vauxhall Industrial Estate Ruabon, Wrexham, Clwyd LL14 6HY, U.K., Piezoelectric Ceramic Products Catalogue MML - UR 9001 2M

12 - P G Hodgson and J K Raine, Computer Simulation of a Variable Fill Hydraulic Dynamometer, Journal of Mechanical Engineering Science, Part C. 1992 vol 206 pp 327 - 336.

13.2 Appendix 3 - Paper: A Design Model for a Mechatronic Approach to Novel Woodworking Machinery

This paper was presented at the Mechatronics '96 5th U.K Mechatronics Forum International Conference, September 1996, University of Minho, Guimares, Portugal.

A DESIGN MODEL FOR A MECHATRONIC APPROACH TO NOVEL WOODWORKING MACHINERY

N.Brown B.Eng M.Sc, RM Parkin B.Sc Ph.D C.Eng MIEEE MIEE F.I.Mech E
Mechatronics Research Group, Department of Mechanical Engineering, University of Loughborough LE11 3TU, U.K.
email N.Brown@lut.ac.uk

ABSTRACT

Rotary machining is extensively used for planing and moulding operations within the woodworking industry. Although the surface finish produced by these machining methods is good, the rotary machining action produces cutter marks on the wood surface such that further finishing operations, such as sanding, are often required to produce a product of suitable standard. It has been theorised that the surface finish of planed and moulded timber products may be improved by oscillation of the cutter block to a larger degree in either a vertical or horizontal plane. This paper describes the computer simulation of the cutting process and the system used to oscillate the cutterblock in order to determine the effect on surface finish, and as a tool for effective design and optimisation design of the actuators.

1 NONCLEMATURE

C	= Capacitance
d	= Strain developed / applied field
D	= Dielectric displacement
E	= field
f_m	= Resonant frequency
f_n	= Antiresonant frequency
g	= Strain developed / applied charge density
k_a	= Drive amplifier constant (mA/V)
Q_m	= Energy supplied / dissipated per cycle
S	= Strain
T	= Stress
v_m	= Valve actuator time constant
V_v	= Valve voltage
X_s	= Valve spool displacement
Z_m	= Minimum impedance
ε_o	= Relative permitivity
ε_r	= Permitivity of free space
ω_v	= Valve natural frequency
ζ_v	= Valve spool damping
$I(t)$	= Instantaneous knife position
r_{ct}	= Cutter tip radius
F_d	= Feedrate
ω_{ct}	= Cutterblock angular velocity

2 INTRODUCTION

In order to produce an acceptable surface finish yet maintain high throughput, larger numbers of cutters on each cutterblock have been employed. This requires a larger cutterblock in order to accommodate the extra blades, which exaggerates vibration problems when running the machine at high speeds.
The use of a smaller cutterblock enables a high spindle speed since vibration problems are reduced to some extent, though the smaller number of knives used will reduce useful cutter life.
Fixed knife planing has been shown to produce an excellent surface finish whereby none of the defects produced by rotary machining are present (figure 1). The high feed forces and feed methods used however mark at least one surface of the product.
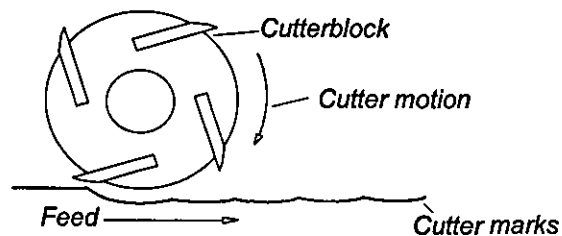

Figure 1: Effect of rotary machining on timber surface

3 APPROACH TAKEN TO WORK

3.1 Modified cutterblock motion
The cutter advances producing a clean cut (figure 2 - displacements are exaggerated for clarity), then retracts in order to begin the next cut (figure 3).
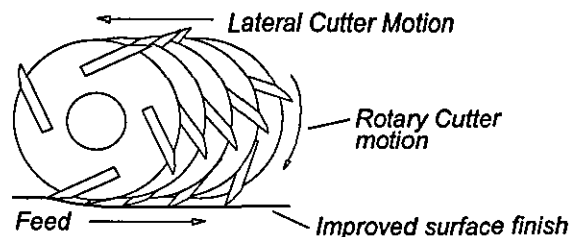

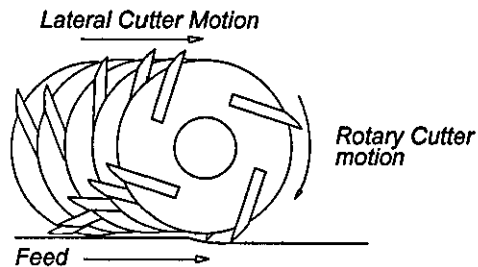Figure 2: Improved surface due to horizontal cutter motion.

273

Figure 3: Retraction of cutter prior to cycle re-commencement

Figure 4: Hydraulic system schematic

3.2 Actuator performance requirements

High frequencies of actuation are required, for example a 4 knife cutter rotating at 6000 r.p.m requires 8 oscillations of the cutter head per revolution, or 12000 oscillations/min.

3.3.1 Vertical Oscillation

Small variations in cutter position have been used to improve surface finish in machining of metals, [1-2], using piezoelectric actuators, though at lower feedrates and cutter speeds than for wood machining.

Vertical oscillation of the cutter block would need to be of a similar amplitude ($\approx 5\mu m$) in order to produce a uniform depth of cut.

Piezoelectric multilayer actuators are highly suited to this purpose, since they posses the required force/stroke characteristics.

3.3.2 Horizontal Oscillation

Horizontal oscillation of the cutterblock would require amplitudes in the order of a 2-4 mm.

Hydraulics were seen as the best choice of horizontal actuator, whereby hydraulic cylinders would be controlled by valves capable of operating at high frequencies, such as servo valves. Therefore a hydraulic system would have to have good response up to at least 200 Hz. (This figure takes into account the effects of wear of the hydraulic system and hydraulic fluid degradation, such that a degree of contingency is built into the design.)

A 500 Hz hydraulic actuator has been developed [3], though the maximum amplitude achieved is only 0.2mm. [5] Describes a system with a greater amplitude of ≈ 12.5 mm, though output frequency is limited to 20 Hz.

4. ACTUATOR SYSTEM SIMULATION

4.1 Hydraulic circuit simulation

The complete hydraulic circuit is simulated, including the hydraulic source, servo valve and hydraulic load (Figure 4). Effects peculiar to a hydraulic system are included such as fluid bulk modulus, oil column stiffness, and pressure dependent friction, in order to produce a comprehensive model. [5-6].
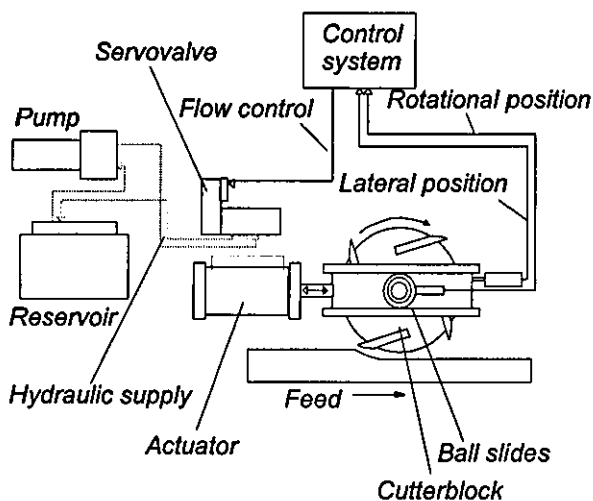
4.1.1 Servo valve simulation

Two methods for simulating the hydraulic servo valve are employed. Where manufactures data is available [5], transfer functions of the valves are utilised, (1). The transfer function shown in (2) is used to model the hydraulic ram and slideway.

$$\frac{X_{ram}(s)}{V_v(s)} = \frac{k_a}{1+v_m \cdot s} \cdot \frac{k_s}{\frac{s^2}{w_v^2} + \frac{2z_v}{w_v} \cdot s + 1} \quad (1)$$

$$\frac{X(s)}{Q(s)} = \frac{\frac{1}{A} \cdot \frac{k_B A^2}{M_v}}{s^3 + \frac{\mu}{M} s^2 + \frac{k_B}{Mv} A^2 s} \quad (2)$$

The non linear flow/position characteristics of valve spools are modelled using a look-up table system developed in C when data is available.

For hypothetical valve designs, and where less manufacturers data is available, a modular model has been produced. The modular valve simulation (Figure 5), takes into account all aspects of servo valve design, and an be used to model a torque motor actuated servo valve as described in [7], or a direct drive servo valve utilising a linear motor. The modular approach is such that valve spools may be cascaded in order to produce a multi stage valve.

Alternative designs of proportional valve are evaluated, such as the piezoelectric operated servo valve described in [8].
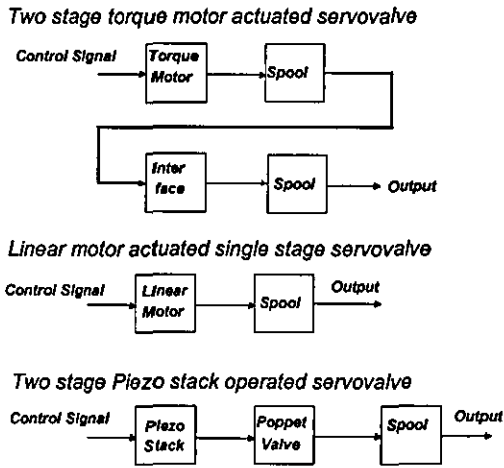
Figure 5: Simulation of servo valve components using standard blocks.

4.1.2 Ram - slideway model
Servo valve models are used in conjunction with the ram - slideway model to form a complete hydraulic circuit model (figure 6).

4.2 Piezoelectric actuator simulation
A model of a piezoelectric multilayer actuator has been produced using proven methods outlined in [9-11], in conjunction with manufacturers data [12]. Equations (3 - 7) are used to describe the behaviour of the actuator.

$$S = s^E T + dE \qquad (3)$$

$$D = dT + \varepsilon^T E \qquad (4)$$

$$E = -gT + (\varepsilon^T)^{-1} D \qquad (5)$$

$$S = s^D T + gD \qquad (6)$$

$$Q_m = \frac{f_n^2}{2\pi . f_m Z_m C(f_n^2 - f_m^2)} \qquad (7)$$

$$d = \varepsilon_r \varepsilon_o g \qquad (8)$$

4.3 Simulation software
Computer simulation of the system is undertaken using Saber™ [13] - a powerful mechatronic simulation package produced by Analogy Inc. Component models are called templates. An extensive template library already exists for modelling mixed technology systems, though custom templates have been written in order to describe extra components.

Templates are written in Mast - the Saber™ modelling language. Functions describing complex component behaviour have been developed in C, which are then interfaced with Saber™ as foreign subroutines (Figure 7). Short routines are written in MAST, and longer code is developed on P.C's running DOS in ANSI standard C. This code is then fully compatible with the sun OS5.1 compiler used on the Sun Sparcstation running Saber™.
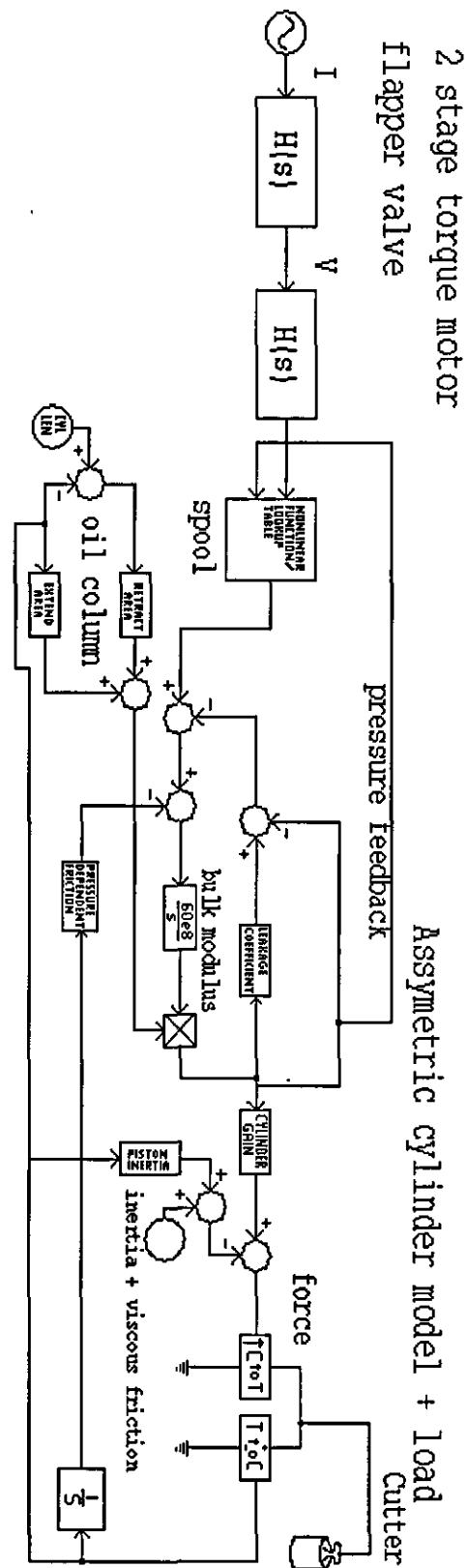

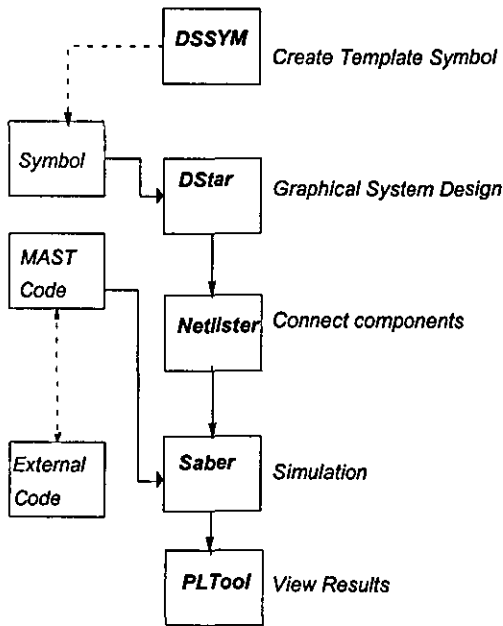Figure 6: Hydraulic system schematic for simulation.

Figure 7: Simulation process using Saber™

These foreign functions are used to model valve spool characteristics, and the surface finish produced by the cutting tool.

The code used to model the cutter takes into account cutter head imbalance, accuracy of knife setting, and machine vibration. Varying degrees of cutter head oscillation may then be applied.

5.0 SURFACE FINISH SIMULATION

The simulation of the cutting process is carried out using Matlab software. An ideal cutter tip locus is first described using equations (9,10). Horizontal and vertical components are then superimposed upon a matrix representing this locus, in order to produce a model which takes into account cutterhead imbalance, the effect of a proud cutter knife, and machine vibration.

The effect of horizontal cutterblock actuation is included in the prototype model, whereby the actuation waveform is generated using the model described in section 4.1.

$$I(t)_x = r_{ct}.\cos(F_d + \omega_{ct}) - r_{ct}\cos(F_d) \qquad (9)$$

$$I(t)_y = r_{ct}.\sin(F_d + \omega_{ct}) - r_{ct}\sin(F_d) \qquad (10)$$

An algorithm has been developed and optimised for rapid processing within Matlab in order to filter the data produced from the cutter tip locus algorithm, in order to produce the cutter wave height. This algorithm is independent of the basic cutter tip locus geometry, consequently allowing more rapid experimentation with different actuator control waveforms.

6.0 RESULTS

6.1 Hydraulic system

The behaviour of the hydraulic oil as a second order mass-spring system can be observed, whereby it's natural

frequency limits the bandwidth of the system considerably (figure 8). Coupled with the natural response times of various servovalves, it becomes apparent that a particularly fine trade-off exists between the maximum possible speed of oscillation, and the maximum permissible cutter mass.
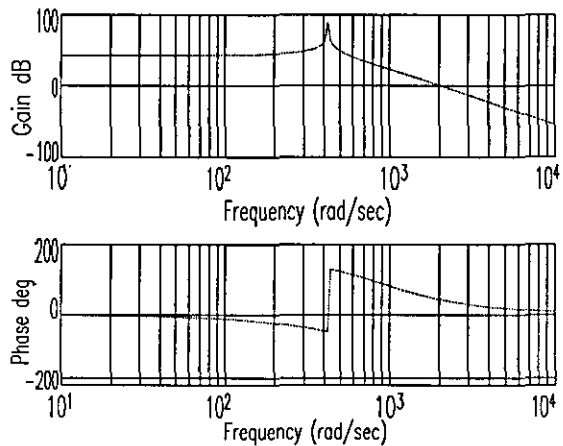

Figure 8: Bode plot for hydraulic servo - ram - slideway model.

The mesh shown in figure 9 was generated using Matlab software using transfer functions derived during the modelling of a slideway with differing masses of cutterblock propelled by 100mm diameter ram. It can clearly be seen that changes in fluid bulk modulus (due to ingress of air or change in temperature for example) have a pronounced effect upon system natural frequency for lower cutterblock masses.
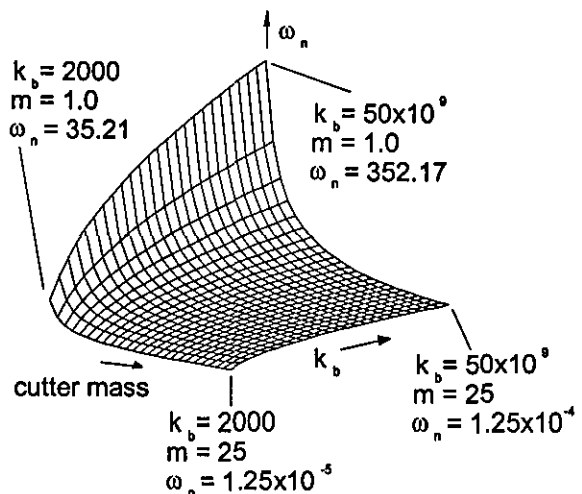

Figure 9: Mesh plot showing effect of altering cutter mass and fluid bulk modulus upon system natural frequency.

Sharp pressure spikes (figure 10) observed when applying a step input to the hydraulic model which are discussed in [14,15] had made necessary very small time steps in the original system simulation. The addition of an accumulator connected to the pump - servo valve line was found not only to greatly reduce the effect of these

spikes, but also greatly reduced the calculated power consumption. The effect of the horizontal control signal upon cutterblock horizontal position may be seen in figure 11.
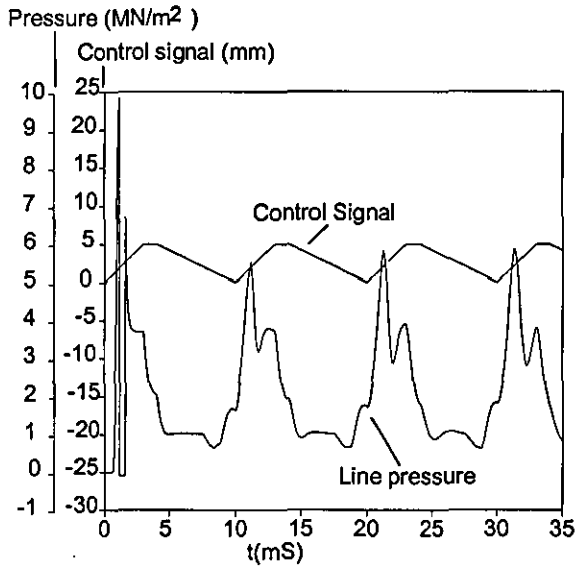
Pressure (MN/m²)

Figure 10: Hydraulic pressure transients during system start-up
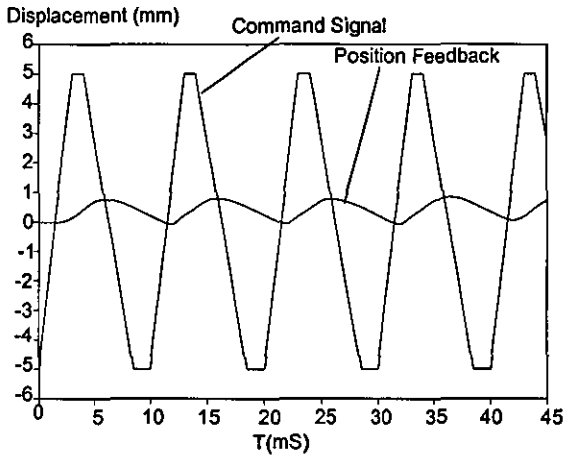

Figure 11: Cutterblock horizontal position transient response

6.2 Piezoelectric System

The simulation of complex non-linear system components including the valve spool, piezo stack, and the cutter has proved particularly successful. A step response for 2 typical piezo actuators driving a 15kg cutterblock is shown in figure 12.
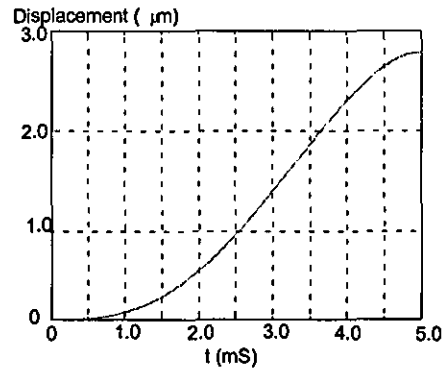

Figure 12: Step response for piezoelectric actuator.

6.3 Surface Finish

The effect of horizontal cutterblock actuation upon the cutter tip locus can be seen in figure 13 (A single knife cutter locus has been shown here for clarity). The waveform used for actuation here comes from a 200 Hz hydraulic system simulation with low fluid bulk modulus, and is virtually sinusoidal. Further shaping of the actuation wave towards a triangular wave through the implementation of a suitable controller in the feedback loop will produce a surface finish closer to the ideal.
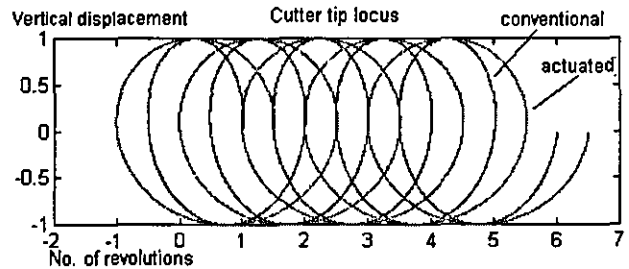
Figure 13: Effect of cutterblock oscillation upon cutter tip locus

A reduction of cutter mark height greater than 50% is achieved with an actuation amplitude of 0.5 x (feed/rev), (Figure 14), (around 2.3 mm peak - peak), using the same actuation waveform as described above. It is clear that even at high speeds the achievable improvement in surface finish is considerable.

Figure 14: Effect of cutterblock oscillation on planed surface wave height

7.0 CONCLUSIONS

A complete model of the cutting process using either piezo-electric or hydraulic actuators has been produced,

277

and two methods of hydraulic servo valve modelling have been developed.

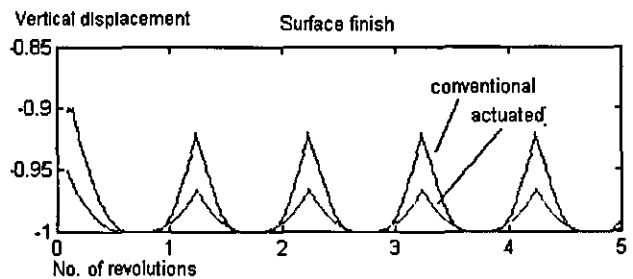The usefulness of simulating the system has been proven, computer modelling having highlighted certain aspects of the hydraulic system to which particular attention must be paid as the design process continues. It has been decided that a hydraulic system will provide the better means of cutter block actuation, and the suitability of hydraulics for such a high - speed system has been proven.

The simulation of the cutting process proves that the modified machining method can be made to work. Accurate sequencing of the actuation wave with cutter rotational position is necessary to ensure improvements in surface finish with further refinements of the system.

REFERENCES:

1 - C Y Jung, J H Oh, *Improvement of Surface Waviness by Cutting Force Control in Milling.* Int. J. Mach. Tools Manufact., Vol 31, No.1, pp 9 - 21, 1991.

2 - P H Dunn, *Piezo Actuators Used to Damp Tool Vibrations,* Solid State Technology, Vol 37, part 9, pp34- , 1994.

3 - D B Stewart, *A Novel Hydraulic Powered Vibrator Seismic Source,* pp35 - 40,
International Mechanical Engineering Congress, Sydney, 8 - 12 July 1991.

4 - A R Allan, *Servoactuator Oscillates High Speed,* Hydraulics and Pneumatics, pp 98 - 102, December 1962.

5 - P G J Leaney, *The Modelling and Computer Aided design of Hydraulic Servosystems,* Ph.D Thesis, Loughborough University of Technology, 1986

6 - P G Hodgson and J K Raine, *Computer Simulation of a variable Fill Hydraulic Dynamometer,* Journal of Mechanical Engineering Science, Part C, vol 206, pp 327 - 336, 1992.

7 - James E Johnson, *Electrohydraulic Servo Systems,* Published by the editors of Hydraulics and Pneumatics Magazine, 1977.

8 - S Yokota and K Akutu, *A fast Acting Electro Hydraulic Digital Transducer,* JSME International Journal, Series 2, Vol 34, No.4, 1991.

9 - H Sosa, F Pourki, *Modelling of Piezoelectric Mulitlayer Structures,* Proc. of the SPIE, vol. 1916, pp 222-230, 1993.

10 - T Funakubo, T Tsubata, Y Taniguchi, K Kumel, T Fujimura, C Abe, *Ultrasonic Linear Motor Using Multilayer Piezoelectric Actuators,* Jpn J. Appl. Phys., Vol.34, Part 1, No. 5B, 1995.

11 - N W Hagood, W H Chung, A Von Flowtow, *Modelling of Piezoelectric Actuator Dynamics for Active Structural Control,* AIAA 90 1097 CP, 1990.

12 - Morgan Matroc Limited, Unilator Division, Vauxhall Industrial Estate Ruabon, Wrexham, Clwyd LL14 6HY, U.K. *Piezoelectric Ceramic Products Catalogue* MML - UR 9001 2M.

13 - Analogy inc. Aldwych Ho., London U.K. WC2B 4JP *Saber^TM User Guide.*

14 - H A Martin D McCloy, *Pressure Transients Generated During the Rapid Braking of Asymmetric Hydraulic Actuators,* IMechE Journal of Mechanical Engineering Science, Vol 21, No.2 1979.

15 - K. F. Martin. *Pressure Transients in a Hydraulic Servo having Unequal Oil Volumes.* Measurement and Control, Vol. 5, June 1972.

13.3 Appendix 4 - Paper: Modification of the Rotary Machining Process to Improve Surface Form

This paper was presented at the Configuration And Control Aspects of Mechatronics Conference, Ilmenau, Germany, September 1997.

MODIFICATION OF THE ROTARY MACHINING PROCESS TO IMPROVE SURFACE FORM

N.Brown B.Eng M.Sc, RM Parkin B.Sc Ph.D FRSA C.Eng MIEEE FIEE F.I.Mech E
Mechatronics Research Group, Department of Mechanical Engineering, Loughborough University, LE11 3TU, U.K..
email N.Brown@lboro.ac.uk

Abstract

Rotary machining is extensively used for planing and moulding operations within the woodworking industry. Although the surface form produced by this machining method is acceptable, the rotary machining action produces cutter marks on the wood surface such that further finishing operations, such as sanding are often required to generate a product of acceptable standard. It has been theorised that the surface finish of planed and moulded timber products may be improved by oscillation of the cutter block. This paper describes the use of a rapid surface simulation algorithm to predict surface finish, and simulation and testing of the effectiveness of cutterblock oscillation. The results show the effectiveness of both the simulation algorithm and the use of cutterblock oscillation

1 Introduction

The rotary wood machining process is similar in nature to the upcut milling of metals. There are however, marked differences between the two applications, the primary one being cutting speed, which lies in the range 30m.sec^{-1} - 80m.sec^{-1} compared with typically 0.5m.sec^{-1} - 1.5m.sec^{-1} for the milling of metals. The feed speed in wood machining is correspondingly high ranging from 5m.min^{-1} - 100m.min^{-1}. Figure 1 shows the general layout of a 2 head planing machine. Timber lengths are fed into the machine by hand, and are taken up by powered rollers. Machining is carried out by knives mounted on cutterblocks.
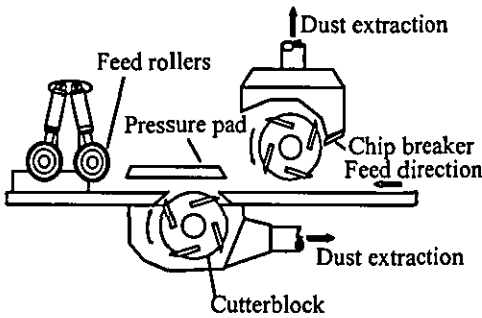

Figure 1: Machine general layout

Planed and moulded surfaces appear, when viewed closely, as a series of waves whose peaks are perpendicular to the passage of the product through the machine. Machining errors may exist which affect surface finish, these being error of form, and surface waviness which is the component of texture upon which the undulating knife traces are superimposed, and can result from cutterhead imbalance(the principal cause of waviness [1,2]), flexure of the machine frame, and machine vibrations.

Cutter wave pitch and height are given by equations (1) and (2), assuming a common cutting circle.

$$pitch(P) = f_d.10^3 / n.N \qquad (1)$$
$$Height(h) = r_{ct} - (r_{ct}^2 - P^2 / 4)^{0.5} \qquad (2)$$

where: f_d = feedrate (m.min^{-1}), n = spindle speed (rev.min^{-1}), N = number of knives in the cutterhead producing a wave on the workpiece, and r_{ct} = radius of cutting circle (m)

2 Novel cutterblock motion

It was intended that through simulation and eventual testing, that the effectiveness of a modified form of cutterblock motion could be verified. Figures 2 and 3 show how a cutterblock with two degrees of freedom may reduce cutter wave height. The cutter advances producing a clean cut (figure 2 - displacements are exaggerated for clarity), then retracts in order to begin the next cut (figure 3). Of course, achieving a perfectly flat surface would only be possible if cutterblock rotation could be halted, but it was also envisaged that the novel cutterblock motion could be used to compensate for inaccurate knife grinding and cutterhead imbalance.

2.1 Actuator performance requirements

The stroke of the actuator system is determined by the cutter wave pitch for horizontal oscillation, and cutter wave height for vertical oscillation.
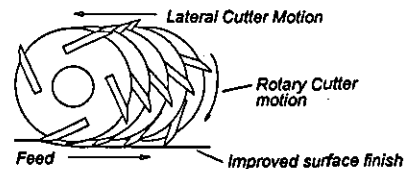For average quality material cutter wave pitch figures in excess of 2.5mm are
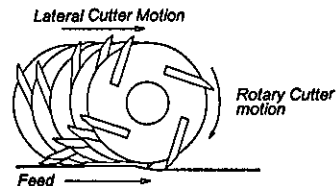

Figure 2: Cutter advance

Figure 3: Cutter retract

commonplace, though for high quality products, wave pitch should be 1.0mm or less [1]. Assuming a knife tip radius of 70 mm therefore, a wave pitch of 2.5mm, and 1.0mm, will possess heights of 1.8 and 3.6 microns respectively. High frequencies of actuation are required, for example a 4 knife cutter rotating at 6000 rev/min requires 4 oscillations of the cutter head per revolution, or 24000 oscillations/min.

Hydraulics were seen as the best choice of horizontal actuator, whereby hydraulic cylinders would be controlled by valves capable of operating at high frequencies, such as servo valves. A hydraulic system for the proposed prototype running speed of 6000 rev.min^{-1}, using a 2 knife cutterblock would require good response up to at least 250 Hz.

3 Actuator system simulation

3.1 Hydraulic circuit simulation

The complete hydraulic circuit is simulated, including the hydraulic source, servo valve and hydraulic load (Figure 4). Effects peculiar to a hydraulic system are included such as fluid bulk modulus, oil column stiffness, and pressure dependent friction, which are needed to produce a comprehensive model. [3,4,5].

Two methods for simulating the hydraulic servo valve are employed. Where manufactures data is available (e.g. [6]), valve transfer functions are utilised, (3). The transfer function shown in (4) is used to model the hydraulic ram and slideway.
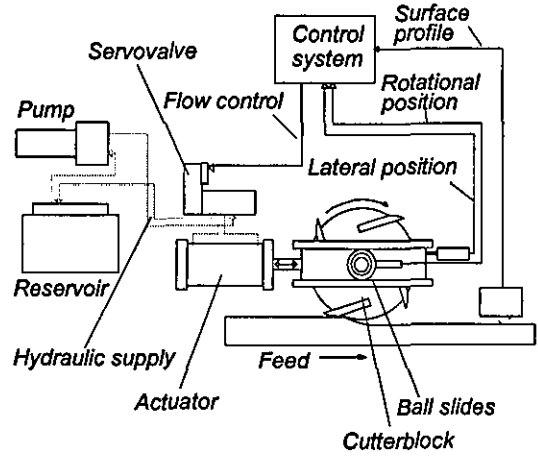

Figure 4: Hydraulic system schematic

$$\frac{X_{ram}(s)}{V_v(s)} = \frac{k_a}{1+v_m.s} \cdot \frac{k_s}{\frac{s^2}{w_v^2}+\frac{2\zeta_v}{w_v}.s+1} \quad (3)$$

$$\frac{X(s)}{Q(s)} = \frac{\frac{1}{A} \cdot \frac{k_B A^2}{M_v}}{s^3 + \frac{\mu}{M}s^2 + \frac{k_B}{Mv}A^2 s} \quad (4)$$

where: A = hydraulic ram area (m^2), k_s = Spool displacement gain (mm.mA^{-1}), k_A = Drive amplifier constant (mA.V^{-1}), M = Total ram, slideway and cutterblock mass (kg), μ = coefficient of viscous friction, S = laplace operator, v_m = valve actuator time constant, V = volume of oil column (m^3), V_v = valve voltage (V), ω_v = valve natural frequency (rad/s), X_{ram} = hydraulic ram displacement (m), X_s = valve spool displacement (m), ζ_v = valve spool damping

Hydraulic valve ports may be round, square or fully annular (i.e. a groove in the housing surrounding the valve spool). Only a square ported valve possesses a linear flow/pressure relationship. The majority of valves are round ported. The simplest and most effective method of modelling the servo valve spool flow/pressure relationship for given spool displacements, was to use a look up table based subroutine developed in C. Manufacturers data was used to produce a table of flow rates, input variables to the function being pressure feedback and spool displacement, the output variable was flow.

For hypothetical valve designs, a modular model has been produced. The modular valve simulation (Figure 7), takes into account all aspects of servo valve design, and an be used to model a torque motor actuated servo valve as described in [3,4], or a direct drive servo valve utilising a linear motor. The modular approach is such that valve spools may be cascaded in order to produce a multi stage valve. Manufacturers transfer functions [6] are used as an extra check of the models accuracy. Using this method alternative designs of proportional valve are evaluated, such as the piezoelectric operated servo valve described in [7].

3.2 Simulation software

Computer simulation of the hydraulic system is undertaken using Saber^{TM} [8] - a powerful mechatronic simulation package produced by Analogy Inc. Component models are called templates. An extensive template library already exists for modelling mixed technology systems, though custom templates have been written in order to describe extra components. These models have been developed in C, which are then interfaced with Saber^{TM} as foreign subroutines and are used to model valve spool characteristics, and the surface finish produced by the cutting tool.

4...Surface Finish Simulation

Modelling of milling has taken place in some depth, particularly with respect to end milling [9] An SSA (surface simulation algorithm) is described in [10] which is flexible enough to take into account spindle runout, cutterhead imbalance, and the effect of a proud knife. However surface form is not considered to be as important by the authors as a mean value for surface roughness (R_A). The simulation of the cutting process is carried out using Matlab software (figure 5). An ideal cutter tip locus is first described. Horizontal components are added to the model, after which a filter algorithm produces a partially complete surface finish taking out loci data from above the maximum cutter wave height as described in equation (1), using pitch data obtained from equation (2). vertical components are then superimposed upon the filter output. This produces a model which takes into account cutterhead imbalance, the effect of a proud cutter knife, and machine vibration.

Recently, methods of processing timber surface data using artificial neural networks (ANN's) have been proven whereby data throughput is rapid enough for use with woodworking machinery [11,12]. Surface form data has been obtained using a laser based system [13], and it is intended that surface data be obtained for system control using this method, which will subsequently be fed into an ANN used in the control loop in order to provide the required performance for real time system control. It is therefore sensible to provide an algorithm which can produce a dataset of sufficient size and variation for network training from the outset.
Previous surface simulations produced excellent surface finish results [2] and were used to check the performance of Matlab code, but would have required extensive rewriting to include the effect of cutterblock oscillation.
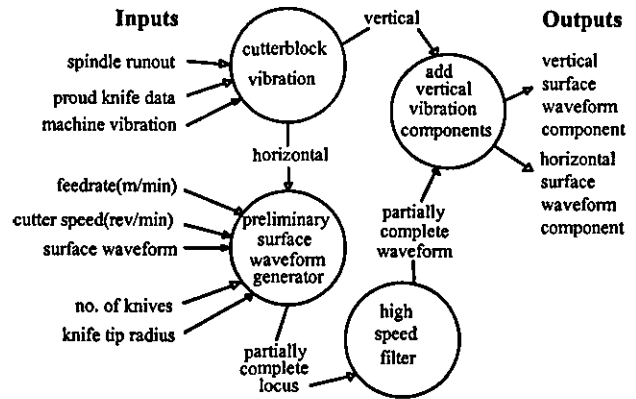

Figure 5: data flows within surface simulation software

A test rig has been constructed in order to validate the theory of cutterblock oscillation (Figure 6) Drive is transmitted to the cutter wheel and the oscillating mechanism via a norton gearbox (1), and to the feed mechanism via a variable speed drive (2), which are powered by a low speed D.C motor (3). A cardan shaft (4) transmits power to the cutter wheel (5). Test pieces or transducers may be mounted to the traversing table (6).

5 Results

5.1 Hydraulic system

Sharp pressure spikes (figure 7) observed when applying a step input to the hydraulic model which are discussed by Martin [14], had made necessary very small time steps (1.0×10^{-8}s) in the original system simulation. The addition of an accumulator connected to the pump - servo valve line was found not only to greatly reduce the effect of these spikes, but also greatly reduced the calculated power consumption to that of equal cut and retract times. Figure 8 shows power requirements for the un modified system.
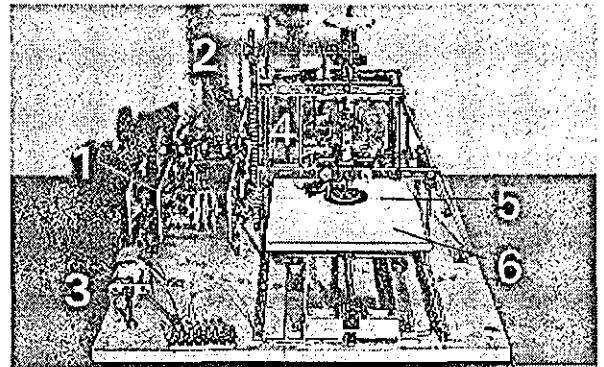

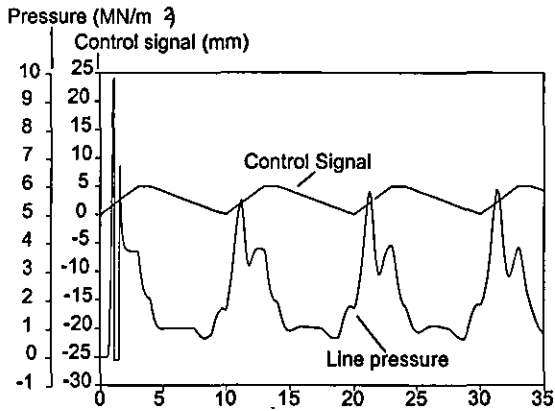Figure 6: Cutterblock oscillation test rig

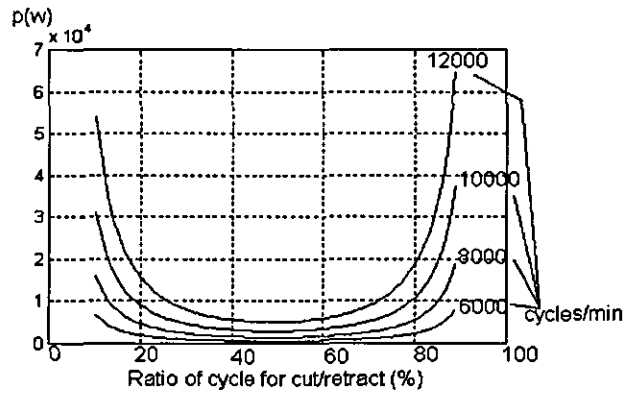Figure 7: Hydraulic pressure transients during system start-up

Figure 8: hydraulic system maximum power consumption

5.2 Surface Finish

The effect of horizontal cutterblock actuation upon the cutter tip locus can be seen in figure 9 (A single knife cutter locus has been shown here for clarity). The waveform used for actuation here comes from a 200 Hz hydraulic system simulation. A sine wave is used to control the servo valve. A reduction of cutter mark height greater than 50% is achieved with an actuation amplitude of 0.5 x (feed/rev), (around 2.3 mm peak - peak which is within the capabilities of a hydraulic actuator), using the same actuation waveform as described above, and a single knife cutter model.

The effect of cutterblock oscillation on surface wave height as shown by the test rig can be seen in figure 10. An LVDT was used to measure depth of cut, such that 1v = 0.989mm depth of cut. The example shown here uses an exaggerated feed rate of 8.6 mm/rev in order to show the effect of cutterblock oscillation more clearly. A reduction in cutter wave height of ≈ 50% is achieved with an oscillation wave of 4.3 mm peak - peak.

Further experiments were carried out to determine the effect of a shift in phase angle between the actuation wave and the cutterblock angle, which would happen if, for example, a change in hydraulic fluid bulk modulus occured due to ingress of air. It was found that too great a drift in phase angle (the extent of which depending of course upon the actuation waveform used), could in fact prove detrimental to the surface finish.
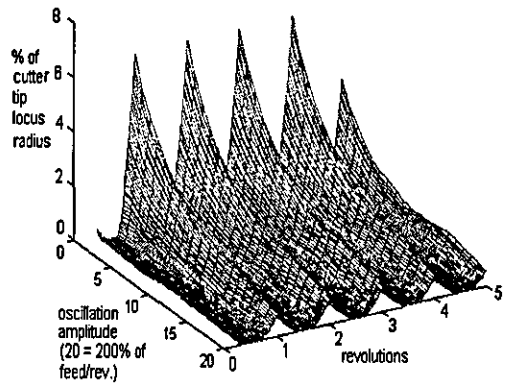

Figure 9: Effect of cutterblock oscillation on surface wave (simulated)

6 Conclusions

A complete model of the cutterblock actuation system using either piezo-electric or hydraulic actuators has been produced, and two methods of hydraulic servo valve modelling have been developed. The hydraulic simulations prove that while conventional servo valves provide adequate flow rates for actuation frequencies less than 250 hz, novel valves will be required for higher frequencies.

A surface simulation algorithm has been developed which may be used to model the effect of cutterblock oscillation, and unintended vibration. This SSA offers a fourfold improvement in run-time performance over previous versions. The usefulness of simulating the system has been proven, computer modelling having highlighted certain aspects of the hydraulic system to which particular attention must be paid as the design process continues. It has been decided that a hydraulic system will provide the better means of cutter block actuation, and the suitability of hydraulics for such a high - speed system has been proven.

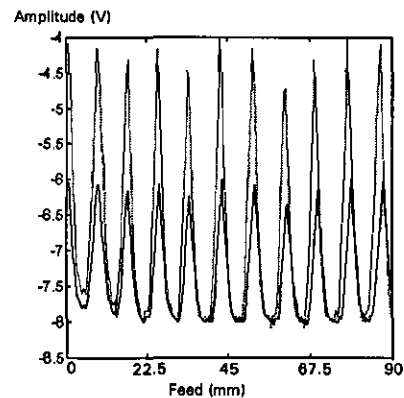The simulation of the cutting process proves that the modified

Figure 10: Effect of cutterblock oscillation on surface wave height (actual).

machining method can be made to work, and this is borne out by the results obtained from the test rig. It is apparent that correct synchronisation of the actuation signal with cutterblock angle is critical in order to obtain an improved surface finish.

References

1. M.R Jackson, "Some effects of machine characteristics on the surface quality of planed and spindle moulded wooden products." *Ph. D. Thesis, Leicester Polytechnic and Wadkin Plc.* June 1986.

2. K.M Maycock. "The Assessment of Surface Quality in Planed and Spindle Moulded Products." *Ph.D Thesis, DeMontfort University,* 1993.

3. C. R. Burrows, S. P. Tomlinson and P.A Hogan. "Use of Computer Simulation in the Design and Selection of Critical Components in Fluid Power Systems." *The Fluid Power Centre, University of Bath.* Paper no. 911865.

4. P G J Leaney, "The Modelling and Computer Aided design of Hydraulic Servosystems." *Ph.D Thesis,* Loughborough University of Technology, 1986

5. T.J Viersma, "Analysis, Synthesis and Design of Hydraulic Servosystems and Pipelines." , *Elsevier,* 1980.

6. W.J. Thayler, "Transfer Functions for Moog Servovalves", *Moog Technical Bulletin 103.* Moog Inc. Controls Division, East Aurora, N.Y. 14052, U.S.A., January 1963.

7. S Yokota and K Akutu, "A fast Acting Electro Hydraulic Digital Transducer," *JSME International Journal,* Series 2, Vol 34, No.4, 1991.

8. Analogy inc. Aldwych Ho., London U.K. WC2B 4JP "Saber^{TM} User Guide".

9. F. Ismail, M. A. Elbestawi, R. Du, R. Urbasik. "Generation of Milled Surfaces Including Tool Dynamics and Wear." *Journal of Engineering for Industry,* Vol. 115, August 1993.

10. S N Mezzelkote, AR Thangaraj, "Enhanced Surface Texture Model For End Milling". *Winter annual general meeting of the American Society of Mechanical Engineers,* Anaheim, CA, USA, 08 - 13/11/92.

11. O Silven, H Kauppinen. "Recent Developments in Wood Inspection". *International Journal of Pattern Recognition and Artificial Intelligence,* Vol 10, Part 1, pp 83 - 95, 1996.

12. J. Lampinen, S.Smolander, "Self Organizing Feature Extraction in Recognition of Wood Surface Defects and Colour Images." *International Journal of Pattern Recognition and Artificial Intelligence,* Vol. 10, Part 2, pp 97 - 113, 1996.

13. P.Lebow, C.Brunner, A.G Maristany, D.A Butler. "Classification of Wood Surface Features By Spectral Reflectance." *Wood and Fiber Science,* vol 28, part 1, pp 79 - 90, 1996.

13.4 Appendix 5: Paper: Improving wood surface form by modification of the rotary machining process - a mechatronic approach

IMPROVING WOOD SURFACE FORM BY MODIFICATION OF THE ROTARY MACHINING PROCESS - A MECHATRONIC APPROACH

N.Brown B.Eng M.Sc, RM Parkin B.Sc Ph.D FRSA C.Eng MIEEE FIEE F.I.Mech E

Mechatronics Research Group, Department of Mechanical Engineering, University of Loughborough LE11 3TU, U.K.

email N.Brown@lboro.ac.uk

ABSTRACT

Rotary machining is extensively used for planing and moulding operations within the woodworking industry. Although the surface form produced by this machining method is acceptable, the rotary machining action produces cutter marks on the wood surface so that further finishing operations, such as sanding are often required to generate a product of acceptable standard. It has been theorised that the surface finish of planed and moulded timber products may be improved by oscillation of the cutter block in either a vertical or horizontal plane. This paper describes the use of a rapid surface simulation algorithm to predict surface finish, and the use of computer simulation to model cutterblock oscillation. The result is a tool for effective design and optimisation of a hydraulic oscillation system in order to improve surface form.

KEYWORDS

Hydraulic, Machining, Modelling Servo, Simulation, Surface, Wood.

1. NOMENCLATURE

ANN   Artificial Neural Network

SSA   Surface Simulation Algorithm

A Hydraulic ram area (m^2)

B Bulk modulus ($N.m^{-2}$)

C Capacitance (F)

C_{cv} Coefficient of viscous friction

d Strain developed / applied field ($C.N^{-1}$)

D	Dielectric displacement (C.m^{-2})
E	field (V.m^{-1})
ε_o	Permitivity of free space (F.m^{-1})
ε_r	Relative permitivity (F.m^{-1})
ε^T	Relative permitivity (constant stress)
f_k	Feed per knife (m)
f_m	Resonant frequency (Hz)
f_d	Feedrate of workpiece (m.s^{-1})
f_n	Antiresonant frequency (Hz)
F	Force (N)
g	Strain developed / applied charge density (m^{2}C^{-1})
H	Original horizontal sample array
h	Depth of knife marking (m)
$I(t)_x$	Instantaneous cutter tip locus position (x axis)
$I(t)_y$	Instantaneous cutter tip locus position (y axis)
k_A	Drive amplifier constant (mA.V^{-1})
k_{LE}	Leakage coefficient (cm^3/N.m^{-2})
k_s	Spool displacement gain (mm.mA^{-1})
M	Total ram, slideway and cutterblock mass (kg)
μ	Coefficient of viscous friction
N	Number of knives in the cutterhead producing a wave on the workpiece
n	Cutterhead rotational speed (rad.s^{-1})
p	Hydraulic fluid pressure (N.m^{-2})
P	Pitch of knife marking (mm)
P_f	Pressure required to overcome viscous friction
q	Hydraulic fluid flow, single acting ram input (cm^3.s^{-1})
Q	General hydraulic fluid flow (cm^3.s^{-1})
Q_m	Energy supplied / dissipated per cycle
r_{ct}	Radius of cutting circle (m)
S	Laplace operator

s^E	Mechanical Compliance (m^2.N^{-1})
S_d	Scallop depth: Depth of knife marking (mm)
S	Strain
t	Time (s)
T	Stress (N.m^{-2})
v_m	Valve actuator time constant
V	Volume of oil column (m^3)
V_v	Valve voltage (V)
ω_v	Valve natural frequency (rad.s^{-1})
x	Hydraulic ram displacement (m)
X_s	Valve spool displacement (m)
ζ_v	Valve spool damping
Z_m	Minimum impedance (Ω)
Z_v	Valve actuator coil impedance (Ω)

2. INTRODUCTION

The rotary wood machining process is similar in nature to the upcut milling of metals. There are however, marked differences between the two applications, the primary one being cutting speed, which lies in the range 30m.s^{-1} - 80m.s^{-1} compared with typically 0.5m.s^{-1} - 1.5m.s^{-1} for the milling of metals [1]. The feed speed in wood machining is correspondingly high ranging from 0.08m.s^{-1} - 1.6m.s^{-1}. Figure 1 shows the general layout of a 2 head (top and bottom) planing / moulding machine.

Timber lengths are initially fed into the machine by hand. Feed is then taken up by powered rollers, tyred with a soft material, in order not to damage the product. Machining is carried out by knives mounted on cutterblocks. Cutterblocks may be removed from machine spindles for regrinding and balancing.

Planed and moulded surfaces appear, when viewed closely, as a series of waves whose peaks are perpendicular to the passage of the product through the machine (figure 2). Machining errors may exist which affect surface finish, these being surface waviness and error of form. Waviness is the component of texture upon which the undulating knife traces (roughness) are superimposed, and can result from cutterhead imbalance, the flexure of the machine frame, and machine vibrations.

Cutterhead imbalance is the principal cause of surface waviness in planed and moulded timber components. [1,2]. Cutter wave height and pitch are given by equations (1) and (2), assuming a common cutting circle.

$$Height(h) = r_{ct} - (r_{ct}^2 - P^2 / 4)^{0.5} \qquad (1)$$

where:

$$pitch(P) = \left(\frac{f_d \cdot 10^3}{n.N} \right) 2\pi \qquad (2)$$

Fixed knife planing has been shown to produce an excellent surface finish whereby none of the defects produced by rotary machining are present. Figure 3 shows the arrangement of a fixed knife planing machine.

The high feed forces required to draw the timber across a stationary knife, and feed methods used (such as toothed wheels) however may mark the product, and the length of fixed knife machines may prohibit their use. Only a small amount of material may be removed using a fixed knife, around 0.2mm [1], hence fixed knife machining is not suitable for moulding.

3. NOVEL CUTTERBLOCK MOTION

It was intended that, through simulation and eventual testing, the effectiveness of a modified form of cutterblock motion could be verified. The idea behind cutterblock oscillation is that when each knife contacts the wood surface, the cutter is advanced in a horizontal plane in order to produce a trough like cuttermark instead of the conventional scallop shaped cuttermark. This is followed by a retraction of the cutterhead prior to the next knife contacting the workpiece. This results in a reduction in cutter wave height to an extent that the finished surface bears no visible cuttermarks to the naked eye. Figures 4 ,5,6 and 7 show how a cutterblock with two degrees of freedom may reduce cutter wave height. The

cutter advances producing a clean cut (figure 4 - displacements are exaggerated for clarity). Cutter motion detail is shown in figure 5. Displacements have been further exaggerated for clarity, and only one (of 4) cutter knives on each cutterblock is shown, also for clarity. The numbered cutterblocks refer to the same cutterhead, shown in different parts of the oscillation cycle. The knife contacts the surface at the beginning of the cycle as shown by the cutter numbered 1. As the cycle progresses, the knife is advanced across the timber surface as shown by cutters 2,3 and 4. The knife is moving further away from maximum depth of cut by position 5. The cutter is then retracted. Figure 6 shows an overview of the retraction part of the cutterblock actuation cycle. Referring to figure 7, where displacements have been exaggerated further to show this part of the cycle more clearly, the cutter begins the retraction cycle with a knife cut having just been completed (position 6). Retraction is rapid, whilst the cutterblock continues to rotate, as shown by cutterblock positions 7, 8 and 9. The beginning of the next actuation cycle begins with the following cutter knife beginning to contact the timber surface, as shown in position 10.

Achieving a perfectly flat surface would only be possible if cutterblock rotation could be halted, and inertia due to cutterblock mass in the range 20 - 80 kg at rotational speeds in the range 62 - 1800 rad.s^{-1} would make this impracticable, though it was envisaged that a considerable reduction in cutter wave height could be achieved through cutterblock oscillation.

It was also envisaged that the novel cutterblock motion could be used to compensate for inaccuracies in the cutting circle (i.e. proud knife) and cutterhead imbalance, thereby improving surface form. For vertical oscillation it was envisaged that the spindle be oscillated to compensate for surface waviness [3], though reduction of cutter marks may also be possible at lower speeds [4].

3.1 Actuator performance requirements

The stroke of the actuator system is determined by the cutter wave pitch. In order to remove or reduce the effects of cuttermarks, actuator stroke must be equal to or greater than surface wave pitch, as shown in equation 2.

For average quality material cutter wave pitch figures in excess of 2.5mm are commonplace, though for high quality products, wave pitch should be 1.0mm or less [1].

It can be seen through application of equations (1) and (2), that when assuming a knife tip radius of 70 mm, that a wave pitch of 2.5mm, and 1.0mm, will possess heights of 3.6 and 1.8 microns respectively.

High frequencies of actuation are required, for example a 4 knife cutter rotating at 6000 rev/min, or 628 rad.s^{-1} requires 4 oscillations of the cutter head per revolution, or an actuator capable of operating at 400 Hz..

3.2 Actuator for Cutterblock Oscillation

Hydraulics were seen as the best choice of horizontal actuator. Pneumatic actuators would not offer significant actuation forces and a purely mechanical system would not allow as much experimentation with differing actuation waveforms. In the hydraulic system, hydraulic cylinders would be controlled by valves capable of operating at high frequencies, such as servo valves. Therefore a hydraulic system for the proposed prototype running speed of 314 rad.s^{-1}, using a 2 knife cutterblock would require good response up to at least 250 Hz. (This figure takes into account the effects of wear of the hydraulic system and hydraulic fluid degradation, such that a degree of contingency is built into the design). While the majority of cutterblocks in industry use 4 or more knives, a two knife cutter was chosen for initial design in order to simplify the design process, nonetheless the principle remains the same.

Where high operating frequencies are required, the trade-off between flow rate and speed of response, have placed large constraints on the hydraulic servo designer.

A 500 Hz hydraulic actuator has been developed [6], though the maximum amplitude achieved is only 0.2mm, which is stated to limit system performance. Allan [7] describes a system with a greater amplitude of $\approx$ 12.5 mm, though output frequency is limited to 20 Hz. Although high actuation forces are achieved, this is achieved by using multiple servovalves in parallel. Such a solution should be avoided for cutterblock oscillation if possible, in order to keep manufacturing costs down.

4. ACTUATOR SYSTEM SIMULATION

4.1 Hydraulic circuit simulation

The complete hydraulic circuit is simulated, including the hydraulic source, servo valve and hydraulic load (Figure 8). Effects peculiar to a hydraulic system are included such as fluid bulk modulus, oil column stiffness, and pressure dependent friction, which are needed to produce a comprehensive model. [8,9,10].

4.2 Servo valve simulation

Two methods for modelling the hydraulic servo valve are employed. The first method uses manufactures transfer functions when they are available (e.g. [11]), transfer functions of the valves are, determined by the manufacturer's practical testing of the servo valves. (3). The transfer function shown in (4) is used to model the hydraulic ram and slideway, a derivation of which is given in Appendix A.

$$\frac{Q(s)}{V_v(s)} = \frac{k_a}{1 + v_m \cdot s} \cdot \frac{k_s}{\frac{s^2}{w_v^2} + \frac{2z_v}{w_v} \cdot s + 1} \quad (3)$$

$$\frac{X(s)}{Q(s)} = \frac{1}{\frac{MV}{BA}s^3 + \left(\frac{k_{LE}M}{A} + \frac{\mu V}{BA}\right)s^2 + \left(\frac{k_{LE}\mu}{A} + A\right)s} \quad (4)$$

Hydraulic valve ports may be round, square or fully annular (i.e. a groove in the housing surrounding the valve spool). Only a square ported valve possesses a linear flow/pressure relationship. The majority of valves are round ported. The simplest and most effective method of modelling the servo valve spool flow/pressure relationship for given spool displacements, was to use a look up table based subroutine developed in C. Manufacturers data was used to produce a table of flow rates, input variables to the function being pressure feedback and spool displacement, the output variable being flow.

The second method of modelling has been produced for manufactured servo valves, but primarily for hypothetical designs. The modular valve simulation (Figure 9), can be used to model the majority of configurations of currently available servo valves, and can be used to model a torque motor actuated servo valve as described in [8,9], or a direct

drive servo valve utilising a linear motor. The modular approach is particularly useful in that valve spools may be cascaded in order to produce a multi stage valve.

This model is more flexible in use than one based entirely on manufacturers transfer functions, as a more comprehensive model of the valve spool may be produced, and of course alternative servo valve designs may be considered at a later date. It is also much more straightforward to alter parameters within the model during simulation than with a transfer function based model, since the software used enables the altering of model parameters within a block diagram based model whilst a simulation is running.

Manufacturers transfer functions [11] are used as an extra check of the models accuracy. Using this method, novel designs of proportional valve may be evaluated, such as the piezoelectric operated servo valve described in [12].

4.3 Piezoelectric actuator simulation

A model of a piezoelectric multilayer actuator has been produced using proven methods outlined in [13,14], in conjunction with manufacturers data [5]. Equations (5 - 10) are used to describe the behaviour of the actuator.

Equation 9 depicts a general case for the ratio of energy supplied / dissipated per cycle. Manufacturers data for resonant and anti resonant frequency is derived through experimentation and is the most variable factor when determining efficiency, but will not actually directly affect the timber surface waveform. For the purposes of the simulations described here however, greater importance may be placed on the force / displacement characteristics of the piezo actuators.

$$S = s^E T + dE \qquad (5)$$

$$D = dT + \varepsilon^T E \qquad (6)$$

$$E = -gT + (\varepsilon^T)^{-1} D \qquad (7)$$

$$S = s^E T + gD \qquad (8)$$

$$Q_m = \frac{f_n^2}{2\pi . f_m Z_m C(f_n^2 - f_m^2)} \qquad (9)$$

$$d = \varepsilon_r \varepsilon_o g \qquad (10)$$

4.4 Ram - slideway model

Servo valve models are used in conjunction with the ram - slideway model to form a complete hydraulic circuit model. The hydraulic servo valve and control signal waveform generator model may be seen in figure 10, and the hydraulic ram and slideway model in figure 11. Transfer functions G1(s) (Equation 11) and G2(s) (Equation 12) are obtained from manufacturers data.

$$G1(s) = \frac{I(s)}{V(s)} = \frac{k_a}{1 + v_m \cdot s} \qquad (11)$$

$$G2(s) = \frac{X_{spool}(s)}{I(s)} = \frac{k_s}{\frac{s^2}{w_v^2} + \frac{2z_v}{w_v} \cdot s + 1} \qquad (12)$$

4.5 Simulation software

Computer simulation of the hydraulic system is undertaken using Saber™ [15] - a powerful mechatronic simulation package produced by Analogy Inc. Component models are called templates. An extensive template library already exists for modelling mixed technology systems, though custom templates have been written in order to describe extra components. The use of Saber™ enabled a higher level system using standard hydraulic components to be designed, which is the next logical design step following the research outlined in this paper. At the time of writing the model used only specially developed, new component models due to their non standard nature, no existing component models being available which could be adapted. Oscillation of simulation algorithms is automatically detected by the software, thereby removing a potential source of misleading results.

Templates are written in MAST - the Saber™ modelling language. Functions describing complex component behaviour have been developed in C, which are then interfaced with Saber™ as foreign subroutines (Figure 12). Short routines are written in MAST, and longer code is developed on P.C's running DOS in ANSI standard C. This code is then fully compatible with the sun OS5.1 compiler used on a Sun Sparcstation running Saber™.

These foreign functions are used to model valve spool characteristics, and the surface finish produced by the cutting tool.

5. SURFACE FINISH SIMULATION

Matlab is essentially an environment based upon a fourth generation interpreted language, and as such is most suitable for applications such as the prediction of surface geometry where software development is rapid. The choice of two different environments for simulation has been made to keep programming as straightforward as possible.

The simulation algorithms that are part of the Saber™ package, lend themselves most readily to the simulation of hydraulic components, but a far greater amount of software would be required to perform a timber surface simulation using Saber™ than with Matlab. .

Modelling of milling has taken place in some depth, particularly with respect to end milling [16] Of particular interest is [17] where an SSA is described which is flexible enough to take into account spindle runout, cutterhead imbalance, and the effect of a proud knife. However surface form is not considered to be as important by the authors as a mean value for surface roughness (R_A). The simulation of the cutting process is carried out using Matlab software. The development of a surface simulation algorithm in Matlab proved more rapid than with MAST, the Matlab environment lending itself more readily to simulation of surface geometry, and a more flexible graphical output using Matlab enabling more rapid surface visualisation than with Saber™.

Taking an initial horizontal sample array, *H,* upon which to base the simulation, we can chose to determine knife tip position based upon time with an external clock overseeing the simulation, or by putting *H* equal to the instantaneous position of the spindle centre, assuming zero runout. This allows a simplification of the model from the beginning which makes it more straightforward to add a signal for cutterblock oscillation. Since the cutterblock oscillation waveform is likely to be complex, it will be difficult to model. It is prudent therefore, to keep the cutterblock model open to this waveform.

Two output arrays are therefore produced, taking unit cutterblock diameter rather than including a separate variable for this, since the wave shape is of primary interest. It should be noted that unity cutterblock diameter, i.e. the physical size, should have no effect on the performance of the hydraulic servo, only on the cutter wave height as explained in equation 1.

Only the cutterblock mass may have an effect on servo performance. Cutterblock mass of course, does not affect the surface finish. The only connecting variable between the servo simulation and the timber surface simulation therefore is the horizontal position of the cutterblock spindle.

Results can be scaled following computation to show results for differing cutterblock sizes if necessary, but the primary aim is to verify the effectiveness of cutterblock oscillation for a given cutterblock diameter, and corresponding knife tip radius.

$$I(t)_x = \cos(2\pi H_i) + F_d H_i \qquad\qquad I(t)_y = \sin(2\pi H_i)$$

Horizontal components are added to the model, after which a filter algorithm produces a partially complete surface finish taking out loci data from above the maximum cutter wave height as described in equation (1), using pitch data obtained from equation (2). vertical components are then superimposed upon the filter output. This produces a model which takes into account cutterhead imbalance, the effect of a proud cutter knife, and machine vibration. Data flows within the surface simulation code are shown in figure 13.

Previously, analysis of wood surface defects and features using machine vision has been carried out primarily to check for inherent timber defects, using either CCD's [18] or spectral reflectance [19]. Recently however, methods of processing timber surface data using artificial neural networks (ANN's) have been proven whereby data throughput is rapid enough for use with woodworking machinery [20]. Surface form data has been obtained using a laser based system [2], and it is intended that surface data be obtained for system control using this method, which will subsequently be fed into an ANN used in the control loop in order to provide the performance necessary for real time control of the system. ANN's are highly suited to the control of hydraulic servomechanisms since they feature rapid response and the ability to cope with nonlinearities [21] and time variant properties inherent to hydraulic servos [22]. e.g. oil column stiffness will drop over a period of several hours of run time due to increased temperature and ingress of air into the system. This would naturally increase the lag between the command signal to the servo valve and the response of the actuator.

It is therefore sensible to provide an algorithm which can not only evaluate the effects of cutterblock oscillation, (figure 10) but which is also powerful enough to produce a dataset of sufficient size and variation for network training

Previous surface simulations produced excellent surface finish results [2] and were used extensively to check the performance of Matlab code, but would have required extensive rewriting to include the effect of cutterblock oscillation using the waveform ported from the hydraulic simulation. Consequently the new filtering algorithm is independent of the basic cutter tip locus geometry. The cutter tip locus is stored as a two dimensional image. The image is then scanned in order to find the lowest vertical components of the cutter tip locus. Since the cutter loci overlap, and the horizontal spacing is irregular, a large part of run time is taken up by error checking for spurious results (seen on the simulated surface as irregular spikes). These spurious results are produced when taking the cutter tip locus data, and finding a corresponding timber surface plot from the lowest part of the cutter tip locus, i.e. the part of the locus corresponding to the interaction between the cutter knife and the timber surface. Because the timber surface plot takes an even horizontal spacing, and the horizontal spacing of the cutter tip locus is uneven, when the software takes a horizontal sample for surface form, it can easily pull down a stray sample from a point further away from the actual timber surface. The surface simulation software was developed with this in mind, and automatically finds the correct loci points in order to produce a plot of the timber surface form. Also, the graphical approach used to predict the surface finish has bought about a large increase in speed over previous simulations, which relied heavily on the mathematical model. The Matlab based SSA takes just under 2 minutes to produce 1024 samples, compared with 5 minutes for a previous SSA compiled from C.

Performance is also enhanced due to the realisation that regular increments in the horizontal output are not required for the training set. Whilst previous SSA's [2] were required to produce 1024 evenly spaced samples, the horizontal spacing is simply produced as a separate array. Surface visualisation in Matlab is achievable with irregular horizontal steps, as is training of ANN's. The actuation waveform is generated using the model described in section 4.1.

6. EXPERIMENTAL VALIDATION OF CUTTERBLOCK OSCILLATION

A test rig was constructed for three reasons. The first was to provide a physical illustration of the effectiveness of cutterblock oscillation, and the second was to use the results captured from the machine in order to check the validity of the data outputted from surface simulation software. The third reason for constructing the rig was one of speed - surface simulations can now be carried out using differing input parameters with greater ease than with a purely software based simulation. Also with a physical method of validating the theory of cutterblock oscillation, error checking is easier.

The test rig is shown in Figure 14. Drive is transmitted to the cutter wheel and the oscillating mechanism via a norton gearbox (1), and to the feed mechanism via a variable speed drive (2), which are powered by a low speed D.C motor. A cardan shaft (3) transmits power to the cutter wheel (4). Test pieces or transducers may be mounted to the traversing table (5).

7. RESULTS

7.1 Hydraulic system

The behaviour of the hydraulic oil as a second order mass-spring system can be observed, whereby it's natural frequency limits the bandwidth of the system considerably (figure 15). Coupled with the natural response times of various servovalves, it becomes apparent that a particularly fine trade-off exists between the maximum possible speed of oscillation, and the maximum permissible cutter mass.

The mesh shown in figure 16 was generated using Matlab software using transfer functions derived during the modelling of a slideway with differing masses of cutterblock propelled by 100mm diameter ram. It can clearly be seen that changes in fluid bulk modulus (due to ingress of air or change in temperature for example) have a pronounced effect upon system natural frequency for lower cutterblock masses.

Sharp pressure spikes (figure 17) observed when applying a step input to the hydraulic model which are discussed by Martin [23] and are noted for being problematic in the design of high performance servo systems, had made necessary very small time steps (1.0×10^{-8}s) in the original system simulation. The addition of an accumulator model connected to the pump - servo valve line model was found not only to greatly reduce the effect of these spikes, but also greatly reduced the calculated power consumption to that of equal cut and retract times, such that the accumulator could be used to store energy during parts of the oscillation cycle with a low power demand, and release it when high cutterblock accelerations are required. Figure 18 shows power requirements for the un-modified system. The effect of the horizontal control signal upon cutterblock horizontal position may be seen in figure 19. It must be borne in mind that running such a hydraulic servo at frequencies greater than 150Hz will produce a considerable amount of lag, though a simple transport delay may be included in the servo model to compensate for lag. The inherent lag is not a problem, since overall design of a controller for the cutterblock oscillation system and hydraulic servo, can be carried out in order to compensate. The

amplitude variation, or loss of gain, between input control signal and hydraulic servo output is not detrimental to the oscillation of the cutterblock, since even at high frequency the amplitude of the hydraulic servo is sufficient to reduce cutter wave height. The hydraulic servo must provide the most acceleration on the cutting stroke. Whilst the use of a triangular control wave would appear to make little difference to surface wave height , the geometry of the surface waveform is such that the use of a triangular actuation wave for the hydraulic servo produces a surface with a cutter wave height around 15% less than that produced using a sine wave of equal amplitude.

6.2 Surface Finish

The effect of horizontal cutterblock actuation upon the cutter tip locus can be seen in figure 20 (A single knife cutter locus has been shown here for clarity). The waveform used for actuation here comes from a 200 Hz hydraulic system simulation with low fluid bulk modulus. A sine wave is used to control the servo valve. Further shaping of the actuation wave towards a triangular wave through the implementation of a suitable controller in the feedback loop will produce a surface finish closer to the ideal.

A reduction of cutter mark height greater than 50% is achieved with an actuation amplitude of 0.5 x (feed/rev), (around 2.3 mm peak - peak which is within the capabilities of a hydraulic actuator), using the same actuation waveform as described above, and a single knife cutter model. A more general view of the effect of altering the degree of cutterblock oscillation on the surface form can be seen in figure 21.

The effect of cutterblock oscillation on surface wave height as shown by the test rig can be seen in figure 22. The example shown here uses an exaggerated feed rate of 8.6 mm/rev in order to show the effect of cutterblock oscillation more clearly. A reduction in cutter wave height of $\approx$ 50% is achieved with an oscillation wave of 4.3 mm peak - peak. The oscillation waveform used in these tests is a pure sine, and the results correlate well with those produced by the simulation.

7.0 CONCLUSIONS

A complete model of the cutterblock actuation system using either piezo-electric or hydraulic actuators has been produced, and two methods of hydraulic servo valve modelling have been developed. The hydraulic simulations prove that while conventional servo valves provide adequate flow rates for actuation frequencies less than 250 hz, novel valves will be required for higher frequencies. Although physical validation of the use of a hydraulic cutterblock actuation servo will eventually be necessary, it must be borne in mind that building a hydraulic servoactuator without simulation would have produced a faulty system with a short life. The use of an accumulator model in the hydraulic circuit simulation has shown that high pressure transient spikes in the hydraulic supply lines may be avoided, thus increasing the reliability of a physical system, and increasing the overall system life. The simulation of the system using the accumulator as an energy storage device, suggests that utilising an accumulator to reduce peak power consumption of the system will be highly effective.

A surface simulation algorithm has been developed which may be used to model the effect of cutterblock oscillation, and unintended vibration due to cutterblock imbalance. The algorithm is flexible enough to include the effects of the horizontal position data obtained from the ram - slideway simulation upon the surface finish.

The usefulness of simulating the system has been proven, computer modelling having highlighted certain aspects of the hydraulic system to which particular attention must be paid as the design process continues. It has been decided that a hydraulic system will provide the better means of cutter block actuation, and the simulation of the hydraulic servo has been successful, paving the way to a prototype machine.

The simulation of the cutting process strongly suggests that the modified machining method can be made to work. Accurate sequencing of the actuation wave with cutter rotational position is necessary to ensure improvements in surface finish with further refinements of the system.

REFERENCES:

1. M.R Jackson, *Some effects of machine characteristics on the surface quality of planed and spindle moulded wooden products*. Ph. D. Thesis, Leicester Polytechnic and Wadkin Plc. June 1986.

2. K.M Maycock. *The Assessment of Surface Quality in Planed and Spindle Moulded Products.* Ph.D Thesis, DeMontfort University, 1993.

3. P H Dunn, *Piezo Actuators Used to Damp Tool Vibrations,* Solid State Technology, vol 37, part 9, pp34-, 1994.

4. C Y Jung, J H Oh, *Improvement of Surface Waviness by Cutting Force Control in Milling.* Int. J. Mach. Tools Manufact., Vol 31, No.1, pp 9 - 21, 1991.

5. Morgan Matroc Limited, Unilator Division, Vauxhall Industrial Estate Ruabon, Wrexham, Clwyd LL14 6HY, U.K. *Piezoelectric Ceramic Products Catalogue* MML - UR 9001 2M.

6. D B Stewart, *A Novel Hydraulic Powered Vibrator Seismic Source,* pp35 - 40, International Mechanical Engineering Congress, Sydney, 8 - 12 July 1991.

7. A R Allan, *Servoactuator Oscillates High Speed,* Hydraulics and Pneumatics, pp 98 - 102, December 1962.

8. C. R. Burrows, S. P. Tomlinson and P.A Hogan. *Use of Computer Simulation in the Design and Selection of Critical Components in Fluid Power Systems.* The Fluid Power Centre, University of Bath. Paper no. 911865.

9. P G J Leaney, *The Modelling and Computer Aided design of Hydraulic Servosystems*, Ph.D Thesis, Loughborough University of Technology, 1986

10. T.J Viersma, *Analysis, Synthesis and Design of Hydraulic Servosystems and Pipelines.* , Elsevier, 1980.

11. W. J. Thayler, *Transfer Functions for Moog Servovalves*, January 1963. Moog Technical Bulletin 103. Moog Inc. Controls Division, East Aurora, N.Y. 14052, U.S.A.

12. S Yokota and K Akutu, *A fast Acting Electro Hydraulic Digital Transducer*, JSME International Journal, Series 2, Vol 34, No.4, 1991.

13. T Funakubo, T Tsubata, Y Taniguchi, K Kumel, T Fujimura, C Abe, *Ultrasonic Linear Motor Using Multilayer Piezoelectric Actuators*, Jpn J. Appl. Phys., Vol.34, Part 1, No. 5B, 1995.

14. N W Hagood, W H Chung, A Von Flowtow, *Modelling of Piezoelectric Actuator Dynamics for Active Structural Control*, AIAA 90 1097 CP, 1990.

15. Analogy inc. Aldwych Ho., London U.K. WC2B 4JP *Saber^{TM} User Guide.*

16. F. Ismail, M. A. Elbestawi, *Generation of Milled Surfaces Including Tool Dynamics and Wear*. R. Du, R. Urbasik. Journal of Engineering for Industry, Vol. 115, August 1993.

17. S N Mezzelkote, AR Thangaraj, *Enhanced Surface Texture Model For End Milling*. Winter annual general meeting of the American Society of Mechanical Engineers, Anaheim, CA, USA, 08 - 13/11/92.

18. O Silven, H Kauppinen. *Recent Developments in Wood Inspection*, International Journal of Pattern Recognition and Artificial Intelligence, Vol 10, Part 1, pp 83 - 95, 1996.

19. P.Lebow, C.Brunner, A.G Maristany, D.A Butler. *Classification of Wood Surface Features By Spectral Reflectance*. Wood and Fiber Science, vol 28, part 1, pp 79 - 90, 1996.

20. J. Lampinen, S.Smolander, *Self Organizing Feature Extraction in Recognition of Wood Surface Defects and Colour Images*. International Journal of Pattern Recognition and Artificial Intelligence, Vol. 10, Part 2, pp 97 - 113, 1996.

21 R.T Burton, P.Xu, T.Ramden, P.Krus, C.Sargent. *Feasibility of Training a Neural Network Based Hydraulic Component Simulator Using The Complex Method.* Innovations in Fluid Power. The 7th Bath International Fluid Power Workshop, September 1994.

22. T. H. Lee, Q. G. Wang, W. K. Tan. *A Framework for Robust Neural Network Control of Non-linear Servomechanisms.* Mechatronics, Vol. 4, No. 7, 1994.

23. K. F. Martin. *Pressure Transients in a Hydraulic Servo having Unequal Oil Volumes.* Measurement and Control, Vol. 5, June 1972.

APPENDIX A

In order to derive the ram - slideway transfer function, a hydraulic ram is considered as shown in figure (23). The piston cross sectional area is taken as A, the input fluid flow to the ram is given by q(t), p(t) is the fluid pressure and the ram position is given by x(t).

In order to provide a comprehensive model, it is necessary to consider the mass moved, (i.e. ram, slideway and cutterblock), any leakage which may exist between ram and cylinder wall, effects of viscous friction, and the compressibility of the fluid, i.e. the fluid bulk modulus.

The governing equation for a simple ram is given by:

$$q(t) = A\frac{dx(t)}{dt} \qquad (15)$$

Taking into account leakage, where a leakage flow of $k_{LE}p(t)$ exists, the flow continuity equation then becomes:

$$A\frac{dx(t)}{dt} + k_{LE}p(t) \qquad (16)$$

Calculation of $p(t)$ due to inertia is achievable through applying Newton's Second Law, i.e. *Force = Mass x Acceleration.*

$$p(t)A = M\frac{d^2x(t)}{dt^2} \qquad (17)$$

The ram will be subject to a viscous load, whereby the coefficient of viscous friction μ affects the force available from the ram. The pressure $p_f(t)$ required to overcome this frictional loss is therefore:

$$p_f(t) = \mu \frac{dx(t)}{dt} \qquad (18)$$

It is then necessary to consider the effects of fluid compressibility. Bulk modulus may be defined as change in fluid pressure divided by change in volume per unit volume, i.e.

$$B = \frac{\Delta p}{\Delta V} \qquad (19)$$

$$\therefore \frac{dV}{dt} = \frac{V}{B} \frac{dp}{dt} \qquad (20)$$

The complete flow continuity equation is therefore:

$$q_{in} = q_{vel} + q_{leakage} + q_{compressibility} \qquad (21)$$

$$\therefore q(t) = A \frac{dx(t)}{dt} + k_{LE} p(t) + \left(\frac{V}{B} \cdot \frac{dp(t)}{dt} \right) \qquad (22)$$

Viscous friction and inertia are used to calculate the pressure required to move the ram:

$$p(t)A - \mu \frac{dx(t)}{dt} = M \frac{d^2 x(t)}{dt^2} \qquad (23)$$

$$\therefore q(t) = A \frac{dx(t)}{dt} + k_{LE} \left(\frac{M}{A} \frac{d^2 x(t)}{dt^2} + \frac{\mu}{A} \frac{dx(t)}{dt} \right) + \frac{V}{B} \left(\frac{M}{A} \frac{d^3 x(t)}{dt^3} + \frac{\mu}{A} \frac{d^2 x(t)}{dt^2} \right) \qquad (24)$$

$$\therefore q(t) = \frac{VM}{BA} \frac{d^3 x(t)}{dt^3} + \left(\frac{k_{LE} M}{A} + \frac{\mu V}{BA} \right) \frac{d^2 x(t)}{dt^2} + \left(\frac{k_{LE} \mu}{A} + A \right) \frac{dx(t)}{dt} \qquad (25)$$

304

Taking Laplace transforms for zero initial conditions gives the ram - slideway transfer function:

$$\frac{X(s)}{Q(s)} = \frac{1}{\dfrac{MV}{BA}s^3 + \left(\dfrac{k_{LE}M}{A} + \dfrac{\mu V}{BA}\right)s^2 + \left(\dfrac{k_{LE}\mu}{A} + A\right)s} \quad (26)$$

305

13.4.1 List of Figures

Two head planing / moulding machine schematic

Effect of rotary machining on timber surface

Fixed knife planer

Lateral Cutter Motion

Rotary Cutter motion

Improved surface finish

Overview of cutter motion during cutter advance

Lateral Cutter Motion

5 4 3 2 1

Rotary Cutter motion

Feed

Improved surface finish

Detail of cutter motion during cutter advance

Lateral Cutter Motion

Rotary Cutter motion

Overview of retraction of cutter prior to cycle re-commencement

Lateral Cutter Motion

6 7 8 9 10

Rotary Cutter motion

Feed

Detail of cutterblock motion during retraction

Servovalve

Control system

Surface profile

Pump

Flow control

Rotational position

Lateral position

Reservoir

Hydraulic supply

Actuator

Feed

Ball slides

Cutterblock

Hydraulic system schematic

Two stage torque motor actuated servovalve

Control Signal → Torque Motor → Spool

inter face → Spool → Output

Linear motor actuated single stage servovalve

Control Signal → Linear Motor → Spool → Output

Two stage Piezo stack operated servovalve

Control Signal → Piezo Stack → Poppet Valve → Spool → Output

Sample modular valve model configurations
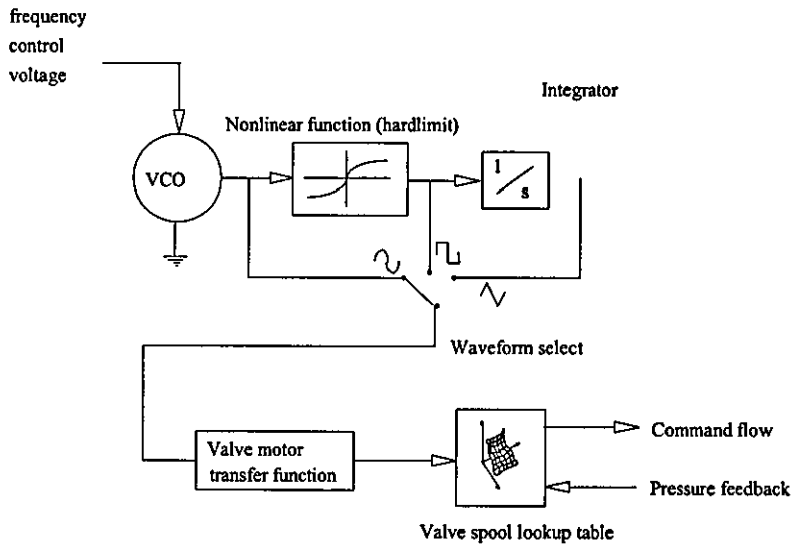
Hydraulic servo valve model and control signal waveform generator
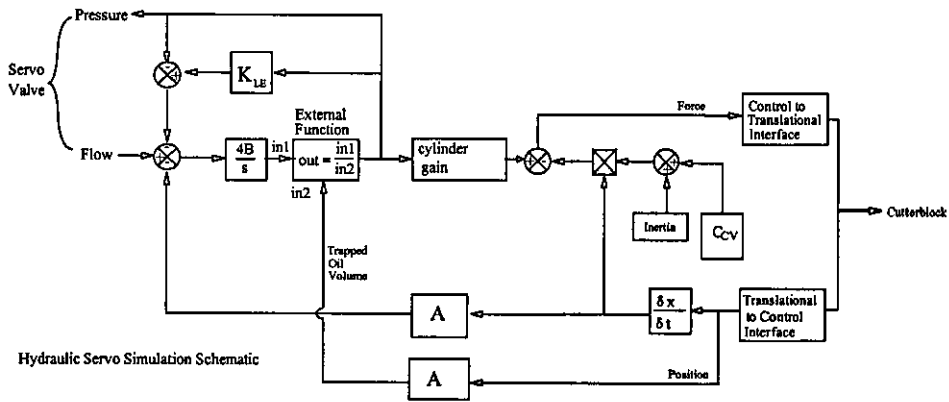
Hydraulic Servo Simulation Schematic
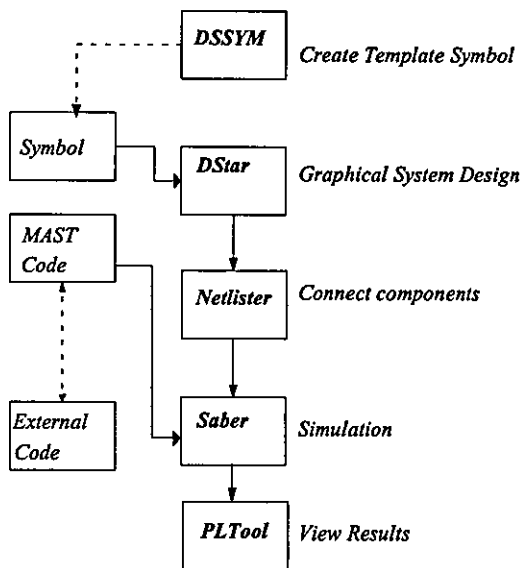
Saber Simulation Process
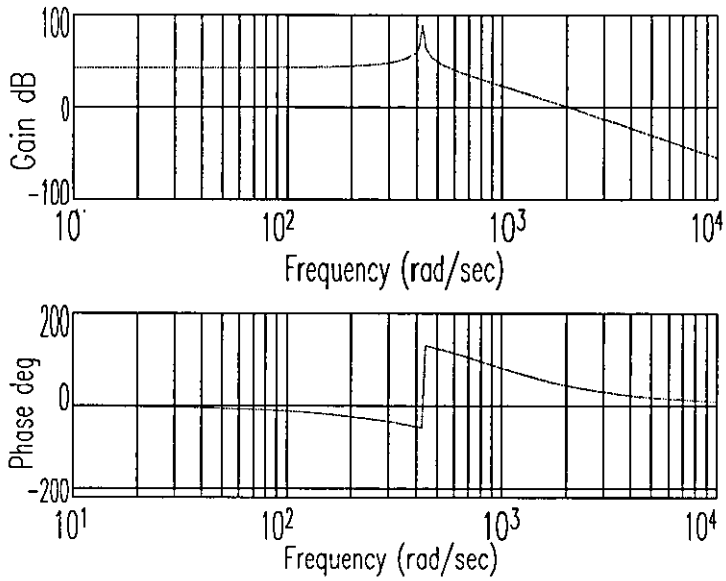
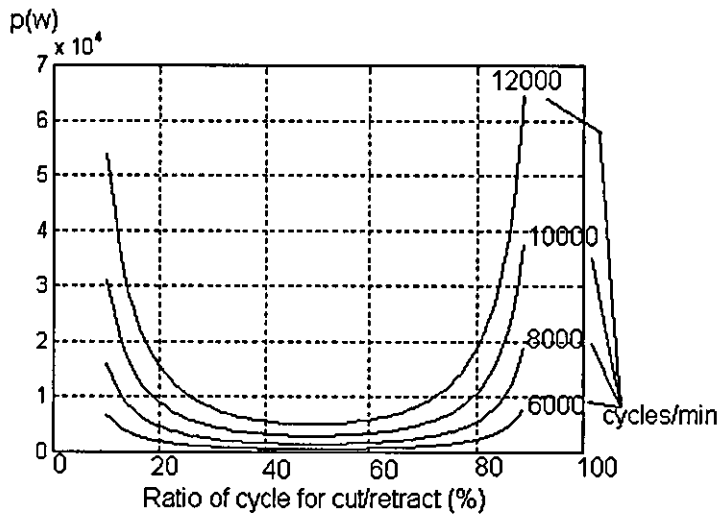Bode plot for hydraulic servo - ram - slideway model.
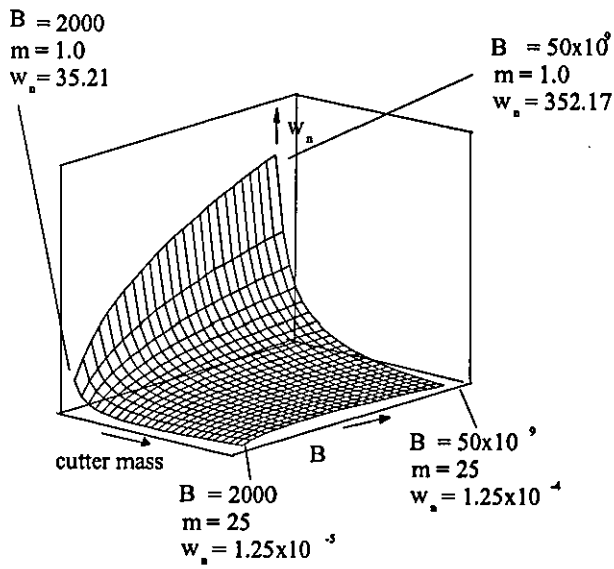
$B = 2000$
$m = 1.0$
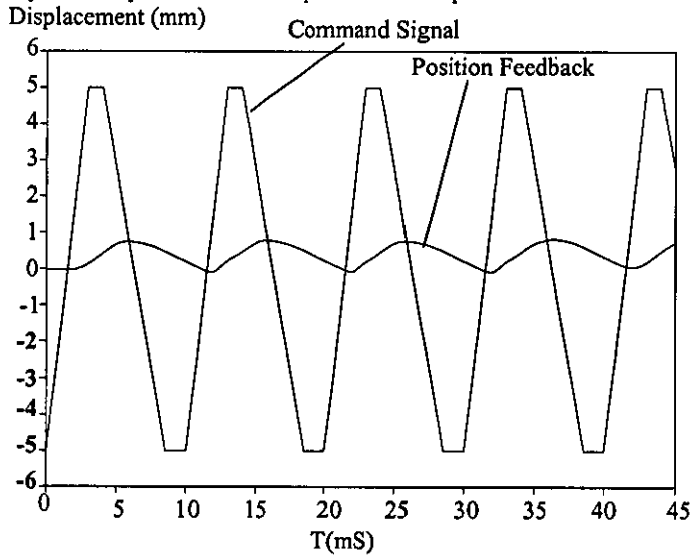$w_n = 35.21$

$B = 50 \times 10^9$
$m = 1.0$
$w_n = 352.17$

$B = 50 \times 10^9$
$m = 25$
$w_n = 1.25 \times 10^{-4}$

$B = 2000$
$m = 25$
$w_n = 1.25 \times 10^{-5}$

cutter mass

B

Mesh plot showing effect of altering cutter mass and fluid
bulk modulus upon system natural frequency.

Control Signal

Line pressure

Hydraulic pressure transients during system start up

311
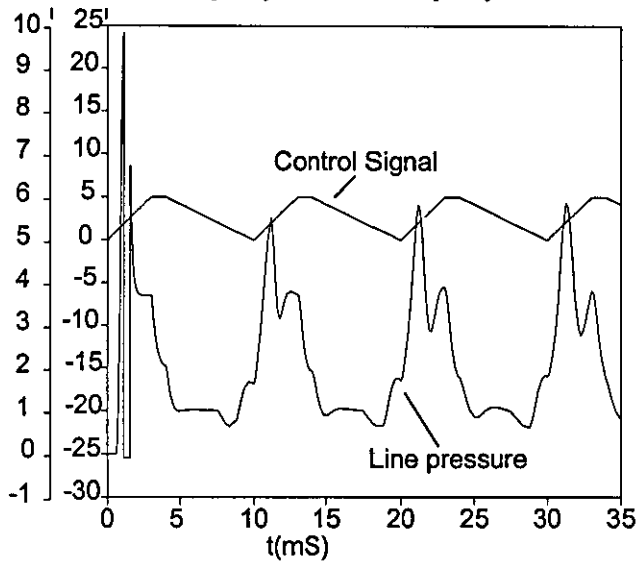
Hydraulic system maximum power consumption

Cutterblock horizontal position transient response
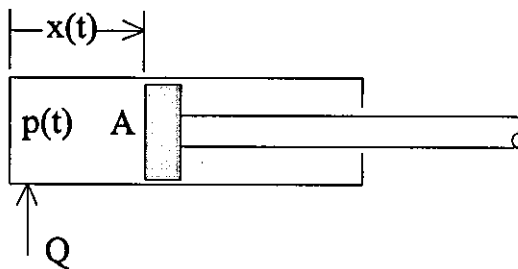

• = conventional cutterblock motion
+ = modified cutterblock motion

Simulated effect of cutterblock oscillation upon cutter tip locus.

% of cutter tip locus radius

oscillation amplitude (20 = 200% of feed/rev.)
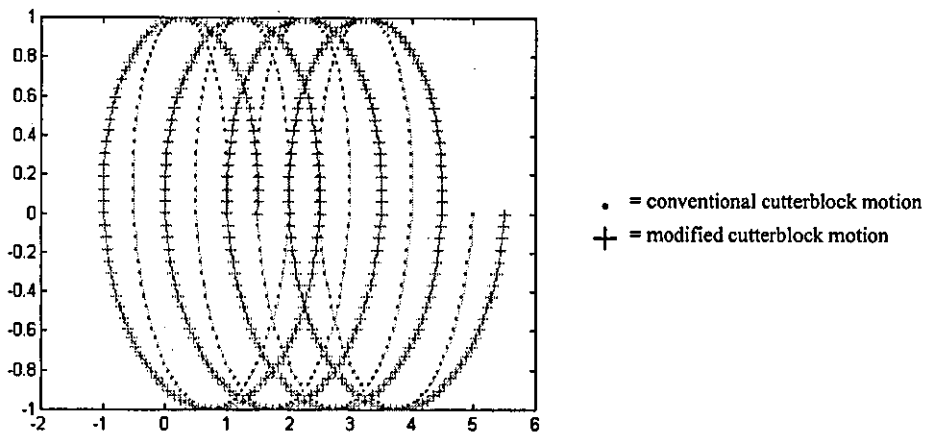
revolutions
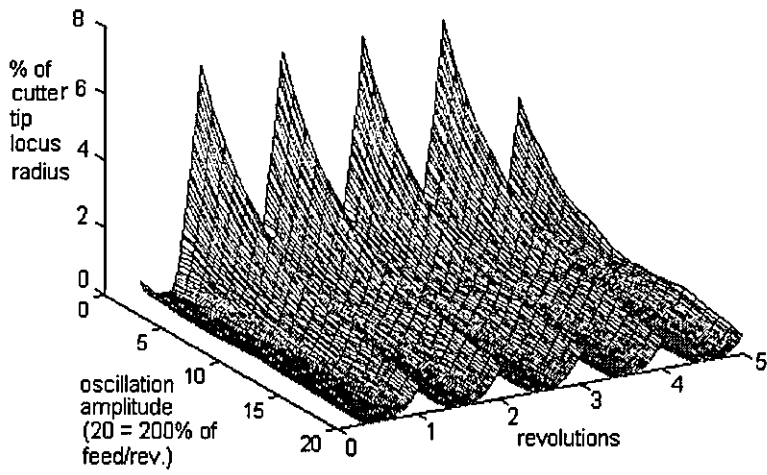
Simulated effect of modified cutterblock motion upon surface wave height

Cutter wave height (mm)

Higher peaks denote conventional cutter motion

Lower peaks denote surface produced with cutterblock actuation
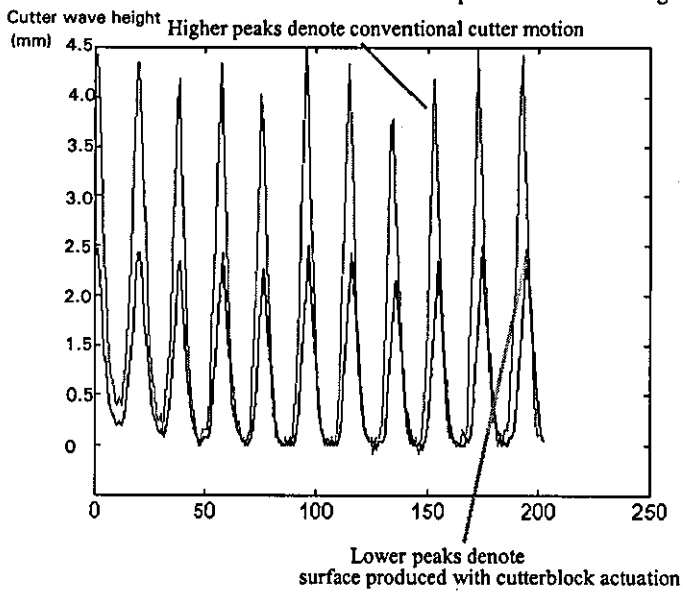
Experimentally obtained surface form using conventional and modified knife tip motion

x(t)

p(t)   A

Q

Hydraulic ram

13.5 Appendix 6: A mechatronic system for the Improvement of surface form in planed and moulded timber components

Presented at Mechatronics 98 conference, Skovde, Sweeden, 1998

A MECHATRONIC SYSTEM FOR THE IMPROVEMENT OF SURFACE FORM IN PLANED AND MOULDED TIMBER COMPONENTS

N Brown B.Eng M.Sc,
R M Parkin B.Sc Ph.D FRSA C.Eng MIEEE FIEE F.I.Mech E
Mechatronics Research Group, Systems Engineering Research Centre, Faculty of Engineering,
University of Loughborough LE11 3TU, U.K.
email N.Brown@lboro.ac.uk, telephone (44) 1509 263171

ABSTRACT

Planing and moulding operations carried out within the woodworking industry make extensive use of rotary machining. Cuttermarks are produced on the timber surface which are generally accepted as unavoidable. More noticeable surface defects may be produced by such factors as cutterhead imbalance, and until recently most research has concentrated on removing these defects. When a high quality finish is required however, a further machining operation, such as sanding, is often required to remove cuttermarks. It has been proposed that surface form of the timber surface may be improved by oscillation of the cutterblock in order to obviate the need for further machining. This paper describes the development of a system for cutterblock oscillation for this purpose. Results are promising, and show clearly the effectiveness of this method for improving surface quality.

Keywords: Mechatronic, Wood, Cutter, Simulation, Hydraulic.

NOMENCLATURE

A	Hydraulic ram area (m^2)
B	Bulk modulus (N.m^{-2})
f_d	Feedrate (m.min^{-2})
$I(t)_x$	Instantaneous cutter tip locus position (x axis)
$I(t)_y$	Instantaneous cutter tip locus position (y axis)
k_A	Drive amplifier constant (mA.V^{-1})
k_{LE}	Leakage coefficient (cm^3/N.m^{-2})
k_s	Spool displacement gain (mm.mA^{-1})
M	Total ram, slideway and cutterblock mass (kg)
p	Pressure (N.m^{-2})
μ	Coefficient of viscous friction
r_{ct}	Radius of cutting circle (m)
S	Laplace operator
v_m	Valve actuator time constant
V	Volume of oil column (m^3)
V_v	Valve voltage (V)
ω_v	Valve natural frequency (rad/s)
x	Hydraulic ram displacement (m)
X_s	Valve spool displacement (m)
ζ_v	Valve spool damping

INTRODUCTION

The rotary wood machining process is similar in nature to the upcut milling of metals. There are however, marked differences between the two applications, the primary one being cutting speed, which lies in the range 30m.sec^{-1} - 80m.sec^{-1} compared with typically 0.5m.sec^{-1} - 1.5m.sec^{-1} for the milling of metals [1]. The feed speed in wood machining is correspondingly high ranging from 5m.min^{-1} - 100m.min^{-1}. Figure 1 shows the general layout of a 2 head (top and bottom) planing / moulding machine.
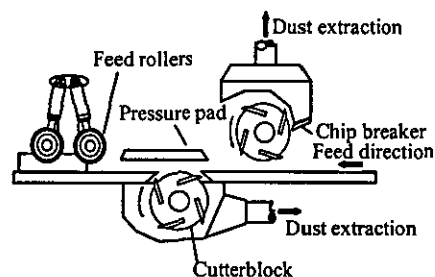

Figure 1: General layout of planing/ moulding machine

Planed and moulded surfaces appear, when viewed closely, as a series of waves whose peaks are perpendicular to the passage of the product through the machine (figure 2). Machining errors may exist which affect surface finish, these being surface waviness and error of form. Waviness is the component of texture upon which the undulating knife traces (roughness) are superimposed, and can result from cutterhead imbalance, the flexure of the machine frame, and machine vibrations.
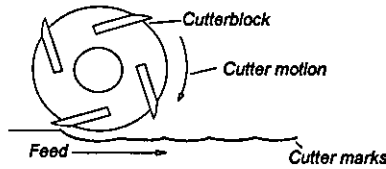
Figure 2: Effect of rotary machining on timber surface

Fixed knife planing has been shown to produce an excellent surface finish whereby none of these defects are present. The high feed forces and feed methods used however may mark the product, and only a small amount of material may be removed using a fixed knife, around 0.2mm [1], hence fixed knife machining is not suitable for moulding.

NOVEL CUTTERBLOCK MOTION

It was intended that the effectiveness of a modified form of cutterblock motion could be verified. Figures 4 and 5 show how a cutterblock with two degrees of freedom may reduce cutter wave height. The cutter advances producing a clean cut (figure 3 - displacements are exaggerated for clarity).
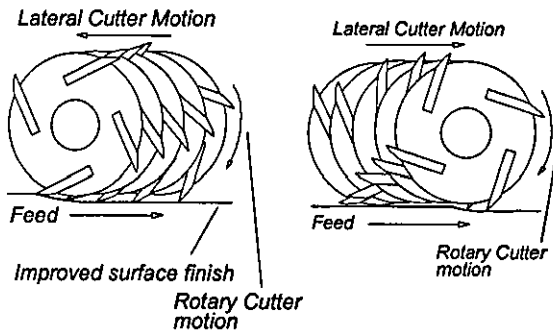

Figure 3: Improved surface due to horizontal cutter motion

Actuator performance requirements

The stroke of the actuator system is determined by the cutter wave pitch .For average quality material cutter wave pitch figures in excess of 2.5mm are commonplace, though for high quality products, wave pitch should be 1.0mm or less [1].

High frequencies of actuation are required, for example a 4 knife cutter rotating at 6000 rev/min requires 4 oscillations of the cutter head per revolution, or 24000 oscillations/min.

ACTUATOR SYSTEM SIMULATION

Hydraulics were seen as the best choice of actuator, whereby hydraulic cylinders would be controlled by valves capable of operating at high frequencies, such as servo valves.

The complete hydraulic circuit is simulated, including the hydraulic source, servo valve and hydraulic load (Figure 4). Effects peculiar to a hydraulic system are included such as fluid bulk modulus, oil column stiffness, and pressure dependent friction, which are needed to produce a comprehensive model. [8,9,10].
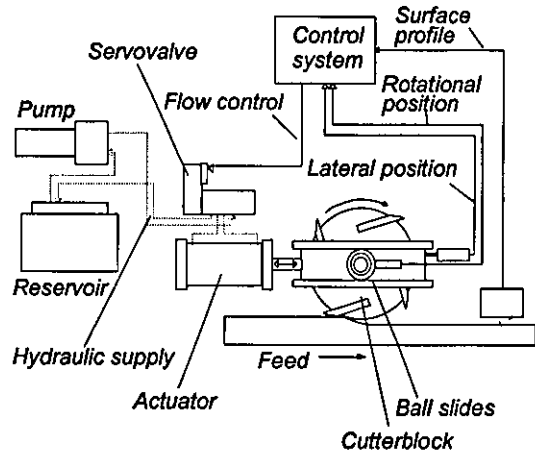

Figure 4: Hydraulic system schematic

Actuator Simulation

Two methods for simulating the hydraulic servo valve are employed. Where manufactures transfer functions are available (e.g. [4]), transfer functions of the valves are utilised, determined by manufacturer's practical testing of the servo valves. (eqn 1). The transfer function shown in (eqn 2) is used to model the hydraulic ram and slideway.

$$\frac{Q(s)}{V_v(s)} = \frac{k_a}{1+v_m \cdot s} \cdot \frac{k_s}{\frac{s^2}{w_v^2} + \frac{2z_v}{w_v} \cdot s + 1} \quad (1)$$

$$\frac{X(s)}{Q(s)} = \frac{1}{\frac{MV}{BA}s^3 + \left(\frac{k_{LE}M}{A} + \frac{\mu V}{BA}\right)s^2 + \left(\frac{k_{LE}\mu}{A} + A\right)s} \quad (2)$$

In order to derive the ram - slideway transfer function, a single acting hydraulic ram is considered as shown in figure 5. The piston cross sectional area is taken as A, the input fluid flow to the ram is given by q(t), p(t) is the fluid pressure and the ram position is given by x(t).
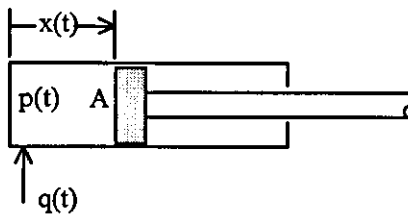

Figure 5: Hydraulic ram

In order to provide a comprehensive model, it is necessary to consider the mass moved, (i.e. ram, slideway and cutterblock), any leakage which may exist between

ram and cylinder wall, effects of viscous friction, and the compressibility of the fluid, i.e. the fluid bulk modulus.

The governing equation for a simple ram is given by:

$$q(t) = A\frac{dx(t)}{dt} \quad (3)$$

Taking into account leakage, where a leakage flow of $k_{LE}p(t)$ exists, the flow continuity equation then becomes:

$$A\frac{dx(t)}{dt} + k_{LE}p(t) \quad (4)$$

Calculation of $p(t)$ due to inertia is achievable through applying Newton's Second Law, i.e. *Force = Mass x Acceleration.*

$$p(t)A = M\frac{d^2x(t)}{dt^2} \quad (5)$$

The ram will be subject to a viscous load, whereby the coefficient of viscous friction μ affects the force available from the ram. The pressure $p_f(t)$ required to overcome this frictional loss is therefore:

$$p_f(t) = \mu\frac{dx(t)}{dt} \quad (6)$$

It is then necessary to consider the effects of fluid compressibility. Bulk modulus may be defined as change in fluid pressure divided by change in volume per unit volume, i.e.

$$B = \frac{\Delta p}{\Delta v} \quad (7)$$

$$\therefore \frac{dv}{dt} = \frac{V}{B}\frac{dp}{dt} \quad (8)$$

The complete flow continuity equation is therefore:

$$q_{in} = q_{vel} + q_{leakage} + q_{compressibility} \quad (9)$$

$$\therefore q(t) = A\frac{dx(t)}{dt} + k_{LE}p(t) + \left(\frac{V}{B}\cdot\frac{dp(t)}{dt}\right) \quad (10)$$

Viscous friction and inertia are used to calculate the pressure required to move the ram:

$$p(t)A - \mu\frac{dx(t)}{dt} = M\frac{d^2x(t)}{dt^2} \quad (11)$$

$$\therefore q(t) = A\frac{dx(t)}{dt} + k_{LE}\left(\frac{M}{A}\frac{d^2x(t)}{dt^2} + \frac{\mu}{A}\frac{dx(t)}{dt}\right)$$
$$+ \frac{V}{B}\left(\frac{M}{A}\frac{d^3x(t)}{dt^3} + \frac{\mu}{A}\frac{d^2x(t)}{dt^2}\right) \quad (12)$$

$$\therefore q(t) = \frac{VM}{BA} + \frac{d^3x(t)}{dt^3} + \left(\frac{k_{LE}M}{A} + \frac{\mu V}{BA}\right)\frac{d^2x(t)}{dt^2}$$
$$+ \left(\frac{k_{LE}\mu}{A} + A\right)\frac{dx(t)}{dt} \quad (13)$$

Taking Laplace transforms for zero initial conditions gives the ram - slideway transfer function:

$$\frac{X(s)}{Q(s)} = \frac{1}{\frac{MV}{BA}s^3 + \left(\frac{k_{LE}M}{A} + \frac{\mu V}{BA}\right)s^2 + \left(\frac{k_{LE}\mu}{A} + A\right)s} \quad (14)$$

For hypothetical valve designs, a modular model has been produced. The modular valve simulation takes into account all aspects of servo valve design, and enables differing valve configurations to be tested.

SURFACE FINISH SIMULATION

The simulation of the cutting process is carried out using Matlab software. An ideal cutter tip locus is first described using equations (15), and (16).

$$I(t)_x = r_{ct}.\cos f_d + \left(\frac{2\pi n}{60}\right) - r_{ct}\cos(f_d) \quad (15)$$

$$I(t)_y = r_{ct}.\sin f_d + \left(\frac{2\pi n}{60}\right) - r_{ct}\sin(f_d) \quad (16)$$

The cutter tip locus is then processed using software outlined in figure 5. This produces a model which takes into account cutterhead imbalance, the effect of a proud cutter knife, and machine vibration, but improves upon previous models [5,6,7] in that the effect of external vertical or horizontal waveforms may be predicted.

The high speed filter was designed to give the software developed in Matlab equivalent performance to software previously developed in C. The cutter tip locus is scanned to produce the waveform.
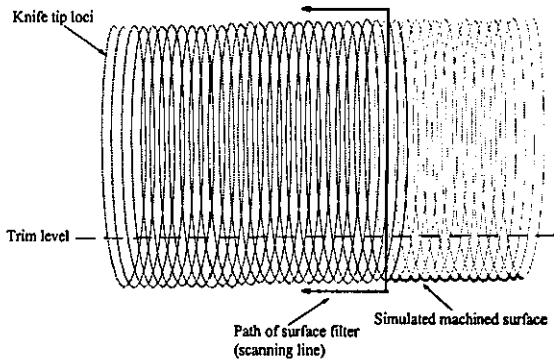
Figure 6 - Extraction of surface data from cutter tip loci.

The trim level shown in the figure is reached through using a sorting algorithm which forms a standard part of the Matlab command library. The vertical components of the entire locus are sorted in ascending order, with a separate array storing the locations of the corresponding horizontal components. The lowest 20% of the vertical components are then extracted, and the corresponding horizontal components are stored in a similar output array. The order of these components is not important since the sorting algorithm will still scan through the vertical components within a fragmented equivalent of a 2 dimensional variable space (i.e. not every location in the variable space is filled).

Figure 7 shows the effect of using a fixed sampling period to produce a waveform with regular horizontal steps. In practice such a method generates a particularly messy output waveform, often with spurious samples having vertical components from the upper curves of the cutter tip locus. The use of a large number of loci points appears to overcome this problem in part, but the appearance of spurious samples is of course not completely overcome, and the large arrays used to hold the cutter loci are too unwieldy for computation. An array of around one Mb in length for the cutter loci was found to be capable of producing a 1000 point regularly spaced horizontal sample with around 50 spurious samples. The time spent processing this data would be inordinate, unless manual cleaning up of the results was deemed acceptable.
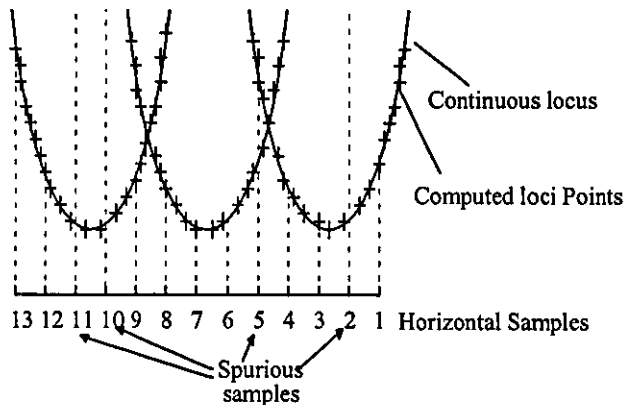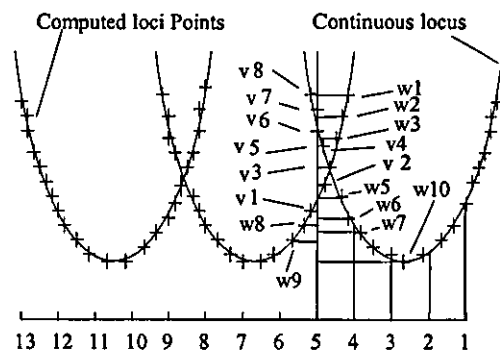

Figure 7 - Spurious data produced by uneven horizontal loci.

The main control loop of the filtering software initially specifies which output sample is to be taken. A scan is then made of which loci points are above the sample point. A small tolerance is built in such that a specified number of sample points which come nearest to the vertical sampling line are taken only. A high speed bubble sort algorithm is used to sort the surrounding area in order of distance from the sample line. A fixed number of the lowest sample points in the list are taken.

This list is then sorted using the same algorithm in order of vertical height. Ideally, the first sample point in the list would always be the lowest loci component, and therefore the appropriate point to be stored in the horizontal sample array. Unfortunately the same loci sample may be shared by one or more inputs to the horzontal sample, so it is necessary to sucessively pull in the spread of loci samples until it is clear that the lowest loci sample nearest to the sample line has been found.

For example, referring to figure 8, it is clear that sample point v1 is the closest, and therefore most appropriate sample to take in terms of accuracy at the vertical line marked by sample 5. Vertically spurious samples are easily produced by exixting software: a simpler algorithm may pick up the loci point closest to the sample line, which in this case would be v6, which would clearly be a spurious sample, giving an incorrect picture of the surface waveform. Horizontally spurious samples must be avoided by thaking succesively smaller pictures of the surrounding area to the sample line, e.g in the first wave of sampling, in general all v samples as well as w1 -7, and in particular samples w8 - 10 would be produced as candidates for the lowest sample point. The code contained in the while loop in the filtering software is able to home in on the sample point V1 in order to alleviate this. The final iteration may produce samples v1, v2, v6 and v7. It is then very straightford to pick the lowest of these samples.

This is achieved with a while loop, counting down the number of points taken near to the sample line with each loop. Code then re sorts the nearest loci points to the sample line and checks the lowest value against that found in the preceeding loop. When the value of the vertical loci component of the lowest percieved loci sample starts to rise in the following loop, it is clear that a minimum vertical loci point has been found with no 'smearing' of the results from one fixed horizontal point to the next. Consequently the sampling method is completely robust, and changes in the spacing of the loci

318

points will not affect the performance of the sampling code, which adjusts automatically. The complete code for the filter, whilst taking much desigh, is very compact at less than 30 lines of code. Processing of a 10 000 sample point loci to produce a 1024 sample point output waveform takes around 40 seconds on an 80 MHz 486 PC.

The majority of the Matlab code used has been included in the appendix, but any reader with a working knowledge of programming in a high level language should be able to appreciate the general working of the filtering software, such that it has been included on the following page to make the description of it's operation clearer.
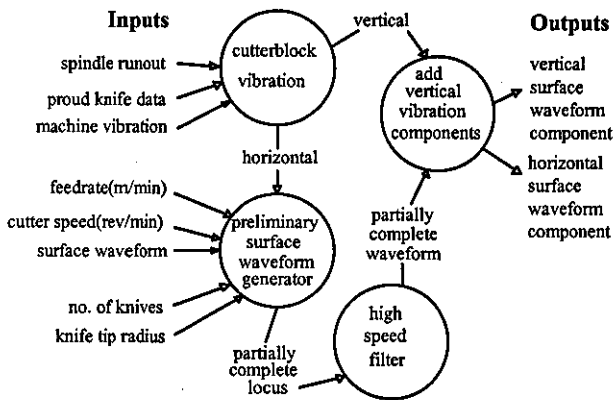
Figure 5: data flows within surface simulation software

RESULTS

Hydraulic system

The plot shown in figure 6 shows the simulated response of the (open loop) hydraulic servo to an actuation signal running at 200 Hz.

X = Typical servovalve response
+ = Computed servovalve response using 1st order transfer function
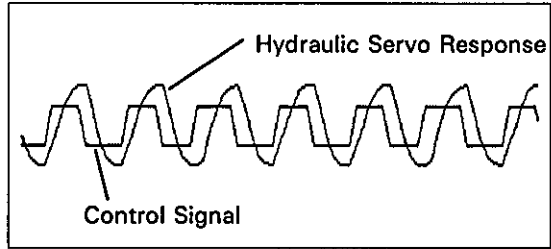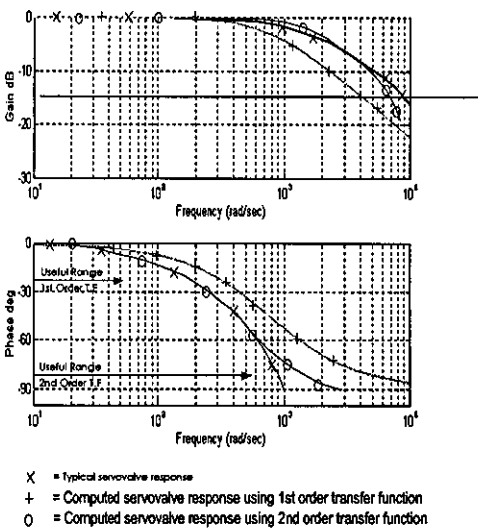O = Computed servovalve response using 2nd order transfer function

Figure 6: Hydraulic Servo Response

Further tests have revealed that the closed loop system is stable for gain values which place the magnitude of the servo response within the required limits for cutterblock oscillation. With the correct design of controller in place, the servo output should be stable and drift should be negligeable.

Surface Finish

The cutter tip locus is shown for a cutterblock with zero horizontal oscillation in figure 7. Stepping through figures 8,9,10, cutterblock is increased in steps of 25%, using a square wave actuation wave form with rise time equal to 5% of the wave period, an improvement in surface finish may be seen in figure 11 whereby an oscillation of equal magnitude to the feed per revolution produces a surface ripple reduction in excess of 98%. The actuation waveform comes from a clipped sinewave which is generated from the vertical component of the cutter tip locus.
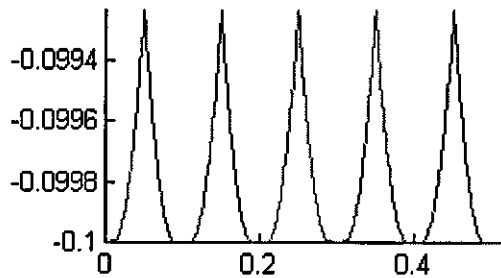

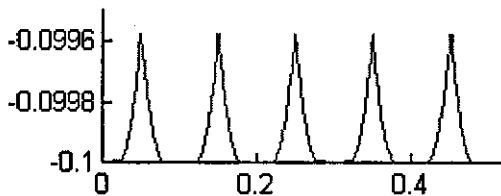Figure 7: Surface wave produced with 0% cutterblock oscillation

Figure 8: Surface wave produced with 25% cutterblock oscillation
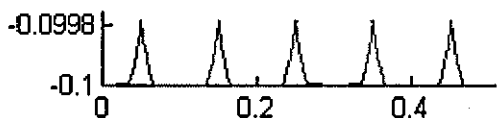

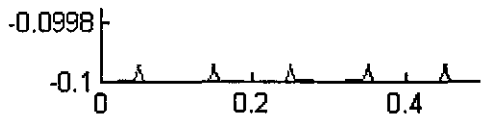Figure 9: Surface wave produced with 50% cutterblock oscillation

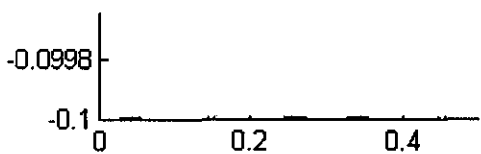Figure 10: Surface wave produced with 75% cutterblock oscillation

Figure 11: Surface wave produced with 100% cutterblock oscillation

CONCLUSIONS

A surface simulation algorithm has been developed which may be used to model the effect of cutterblock oscillation, and unintended vibration due to cutterblock imbalance. The algorithm is flexible enough to include the effects of the horizontal position data obtained from the ram - slideway simulation upon the surface finish.

The usefulness of simulating the system has been proven, computer modelling having highlighted certain aspects of the hydraulic system to which particular attention must be paid as the design process continues. It has been decided that a hydraulic system will provide the best means of cutter block actuation, and the suitability of hydraulics for such a high - speed system has been proven.

The simulation of the cutting process proves that the modified machining method can be made to work. Accurate sequencing of the actuation wave with cutter rotational position is necessary to ensure improvements in surface finish with further refinements of the system.

REFERENCES:

1. M.R Jackson, *Some effects of machine characteristics on the surface quality of planed and spindle moulded wooden products*. Ph. D. Thesis, Leicester Polytechnic and Wadkin Plc. June 1986.

2. P G J Leaney, *The Modelling and Computer Aided design of Hydraulic Servosystems*, Ph.D Thesis, Loughborough University of Technology, 1986

3. T.J Viersma, *Analysis, Synthesis and Design of Hydraulic Servosystems and Pipelines.* , Elsevier, 1980.

4. W. J. Thayler, *Transfer Functions for Moog Servovalves*, January 1963. Moog Technical Bulletin 103. Moog Inc. Controls Division, East Aurora, N.Y. 14052, U.S.A.

5. K.M Maycock. *The Assessment of Surface Quality in Planed and Spindle Moulded Products.* Ph.D. Thesis, DeMontfort University, 1993.

6. F. Ismail, M. A. Elbestawi, *Generation of Milled Surfaces Including Tool Dynamics and Wear.* R. Du, R. Urbasik. Journal of Engineering for Industry, Vol. 115, August 1993.

7. S N Mezzelkote, AR Thangaraj, *Enhanced Surface Texture Model For End Milling.* Winter annual general meeting of the American Society of Mechanical Engineers, Anaheim, CA, USA, 08 - 13/11/92.